ON THE APPLICATION OF SAFT TO MODEL FLUID-FLUID BEHAVIOR OF SOLVENT+ NON-ADSORBING POLYMER+NANOPARTICLE MIXTURES

by

Quentin C. J.-M. Remy

A thesis submitted in partial fulfillment of the requirements for the degree of

Master of Science

in

CHEMICAL ENGINEERING

Department of Chemical and Materials Engineering
University of Alberta

Abstract

Ternary mixtures comprising cyclohexane + polystyrene + silica nanoparticles were recently shown to exhibit a closed loop two-phase region comprising colloid-gas and colloid-liquid phases[1]. This two-phase region is surrounded by single-phase colloid-gas and colloid-liquid phase regions and there are two colloid-gas colloid-liquid critical points along the two-phase to one-phase boundary. One of the critical points, C1, is essentially temperature invariant. The other critical point, C2, is temperature dependent and its placement impacts the shape and size of the two-phase region significantly as temperature is varied. The presence and impact of this second critical point in these phase diagrams has yet to be modelled for this example or in general, and the need to discriminate depletion interaction and depletion flocculation is underscored. Engineering tools are needed for process design and process operation optimization that include such mixtures. In this work, the experimental results and their basis are rehearsed, and a Statistical Associating Fluid Theory (SAFT) based model comprising: spheres of different size to represent the solvent, and the nanoparticles, and chains of spheres to represent the polymer, is described and then evaluated for this application. Qualitative, and quantitative outcomes are presented, and model limitations and required future work are discussed.

Acknowledgments

I would like to express my sincere gratitude to my supervisor Dr. John M. Shaw, for all his help and all the very interesting conversations we had on many subjects. I am also very grateful to him for letting me work on everything that interested me so that I could satisfy my curiosity. I am also thankful to Mildred Becerra and all the other members of the group for their help and always kindly answering my questions. I thank Dr. Sergio Quiñones Cisneros for helping me with thermodynamic and numerical calculations. Several results presented in this thesis are due to his great help. I thank Tema Frank for proofreading Appendix A1, and Dr. Remco Tuinier for a detailed discussion about depletion flocculation. Finally, I am very grateful to my family and close friends for their support during these two years. Thank you very much for always being present.

Table of Contents

List of Tables

List of Figures

List of Symbols

a: Molar Helmholtz energy of the system

A: Helmholtz energy of the system

f^{α}: Mole fraction of phase α in the system

g: Molar Gibbs free energy of the system

G: Gibbs free energy of the system

h: Planck constant

k_B: Boltzmann constant

k_{ij}: Binary interaction parameter

m_i: Number of spheres in molecule i

M_i: Mass of one particle of component i

MW_i: Molar mass of component i

n: Total number of moles (of molecules) in the system

n_i: Number of moles of component i

n_{A_i}: Number of identical sites A_i

N_a: Avogadro constant

P^*: Pressure of the system (fixed)

P: Pressure as a function of molar density

R: Ideal gas constant

T: Temperature of the system

V: Volume of the system

$\boldsymbol{x} = (x_1, x_2, \dots)$: Mole fraction vector

x_i: Mole fraction of component i in the mixture

$\boldsymbol{x}^\alpha = (x_1^\alpha, x_2^\alpha, \dots)$: Mole fraction vector in phase α

x_i^α: Mole fraction of component i in phase α

X_{A_i}: Fraction of association sites A_i of molecules i that are not bonded

w_i: Mass fraction of component i

λ_i: Thermal de Broglie wavelength for component i

$\Delta_{A_i B_j}$: Association strength between association sites A_i and B_j

ε_i: Dispersion energy of interaction of component i

$\varepsilon_{A_i B_j}$: Association energy between association sites A_i and B_j

$\kappa_{A_i B_j}$: Bonding volume between association sites A_i and B_j

μ_i: Chemical potential of component i

$\eta = \zeta_3$: Packing fraction of the system

ρ: Molar density of the mixture

$\boldsymbol{\rho}$: Molar density vector of the mixture

ρ_i: Molar density of component i

$\boldsymbol{\rho}^\alpha$: Molar density vector in phase α

ρ_i^α: Molar density of component i in phase α

σ_i: Hard sphere diameter of component i

τ: Close packing fraction for spheres of equal size

Subscripts

assoc: Association contribution

chain: Chain contribution

disp: Dispersion contribution

ig: Ideal gas contribution

hs: Hard sphere contribution

Superscripts

$\alpha, \beta, \ldots$: Phase of interest

Chapter 1: Introduction

Colloidal dispersions have been studied for a long time and have many applications. The addition of polymers to colloidal dispersions introduces additional phenomena that are significant from industrial and theoretical perspectives[2]. For polymers that adsorb onto the surface of colloidal particles, bridging flocculation and steric stabilization can occur depending on the concentration of polymer. This behavior is shown in Figure 1.1 (a) for bridging flocculation and Figure 1.1 (b) for steric stabilization. At low polymer concentration, polymers create bridges between colloids that then aggregate. At high polymer concentration, aggregates break down in order to free up space for polymer. For polymers that do not adsorb onto the surface of the colloidal particles depletion interaction and depletion restabilization[2] can occur.   These latter phenomena, the focus of this work, are illustrated in Figure 1.1 (c) and (d), respectively. Because the polymer is not adsorbed, a layer depleted of polymers appears around the colloids. When these layers overlap, polymers are excluded and this creates an osmotic pressure difference leading to an effective attraction between colloids and coalescence of solvent + particle regions in the fluid. Depletion interaction may lead to particle flocculation adding to the complexity of the resulting phase behavior, as particle flocculation may or may not be reversible. Depletion stabilization is similar to steric stabilization but for non-adsorbing polymers.

At a macroscopic scale, depletion interaction causes phase separation. One of the phases has a high colloid concentration and is called the colloid-liquid phase (L). The other phase contains a low concentration of colloid and is then called the colloid-gas phase (G). The resulting critical point (L=G) appearing on the two-phase to one-phase boundary is called C1. At critical point C1 the composition and nanoparticle behaviors in the two phases are identical. For reversible interactions, one would expect the two-phase region (L+G) to close at a second critical point C2 with a higher polymer concentration such as in Figure 1.2 because of depletion stabilization. This type of behavior has been seen experimentally[1,3]. When the concentration of colloids is high, there can also be a solid phase called the colloid-crystal phase (C). The appearance and properties of colloid-crystal phases is beyond the scope of this study.

Several approaches have been used to model phase diagrams of such mixtures but none of them reproduce both critical points C1 and C2[4-7]. Statistical Associating Fluid Theory[8] (SAFT) does not discriminate between colloids and molecules and is a promising approach for phase diagram prediction. SAFT provides an equation of state which models many classes of mixtures including polymers + solvents[9-11] and has been applied to the modeling of the depletion flocculation effect[12,13], but not the fluid portion of polymer + solvent + colloidal particle phase diagrams over all. Further, the terms depletion interaction and depletion flocculation are not well discriminated in the literature. Is the difference an issue of degree or is it simply a question of reversibility?
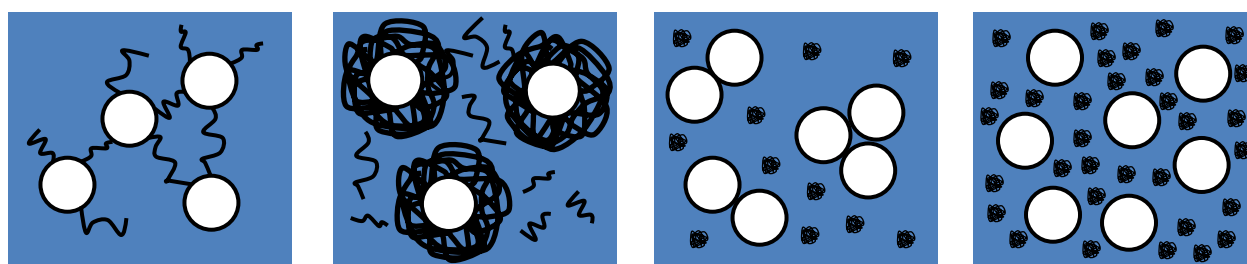
Figure 1.1 a) Bridging flocculation; b) Steric stabilization; c) Depletion flocculation; d) Depletion restabilization[2].

In this work, the main objective is to model the phase diagram shown in Figure 1.2 qualitatively using a simple SAFT approach. The hard sphere version of SAFT called SAFT HS seems appropriate. It models molecules as non-penetrating spheres or chain of spheres. It also allows the presence of association sites on the surface of each component to model short-range attractions with specific directions. It is especially appropriate to model aromatic rings on polymers and it could work to model a short-range attraction around colloids. However, any other kinds of attraction are simply modeled as mean fields and thus this model does not accurately take into account medium-range effects such as electrical double layers. The objectives of this work are to create a program that simulates phase diagrams of ternary mixtures (solvent + polymer + nanoparticles) using the SAFT HS equation of state and apply it to model liquid phase behaviours of the cyclohexane + polystyrene + silica nanoparticle mixtures qualitatively. The effects of association sites are also studied and results are compared to experiments.
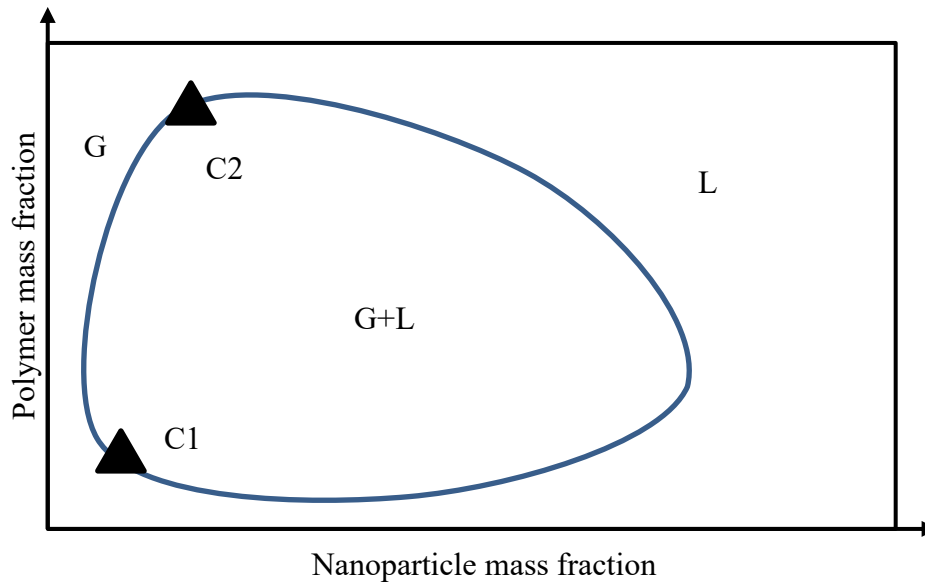
Figure 1.2 Sketch of the two-phase region observed experimentally. Black triangles represent critical points.

This thesis comprises five chapters and three appendices. In addition to the introduction these are:

- Chapter 2: Literature Review where previous works related to this study are presented. It includes overviews of depletion flocculation, a dominant phenomenon in the literature, thermodynamic perturbation theories and SAFT.

- Chapter 3: The SAFT equation of state chosen and the way it is used are explained. A computer code is presented and validated.

- Chapter 4: Phase diagram results obtained using different sets of parameters are presented and discussed. Where appropriate, parameters are taken from the literature. Other parameters are varied and their influence on qualitative aspects of the phase diagrams are reported.

- Chapter 5: Concluding remarks are presented and future works are suggested on the basis of the results obtained.

- Appendices:
  - A1 provides a detailed derivation of the SAFT HS model based on primary works. It provides a compact and sequential presentation of concepts and mathematical steps, not available elsewhere, and is intended for readers who want to understand

Statistical Association Fluid Theory. A modified chain term is also suggested based on a close reading of the literature.

- o A2 comprises the MATLAB[14] code prepared for this work.
- o A3 provides supplemental cyclohexane + polystyrene + silica nanoparticle ternary phase diagrams with diverse parameter sets that support the related discussion in Chapter 4.

Chapter 2: Literature Review

2.1 Ternary mixtures containing nanoparticles and non-adsorbing polymers

The study of mixtures with nanoparticles and non-adsorbing polymers began with the study of depletion flocculation[15]. Both nanoparticles and polymers were modeled as hard spheres in a continuous medium. Because polymers cannot adsorb onto the surface of nanoparticles, if the latter are close enough, a region depleted of polymers appears causing a difference of osmotic pressure and so an effective attraction. This attraction then causes the formation of nanoaggregates, which is the cause of a phase separation. De Hek and Vrij[16] theorized this behavior and later the Free Volume Theory[6] and the Generalized Free Volume Theory[7] were introduced. The temperature invariant phase diagrams given by these theories are shown in Figure 2.1. The characteristics of interest here are the presence of a colloid-gas colloid-liquid two-phase region (G+L) and critical point C1 that arises if the ratio of the polymer radius to the colloid size is large enough.
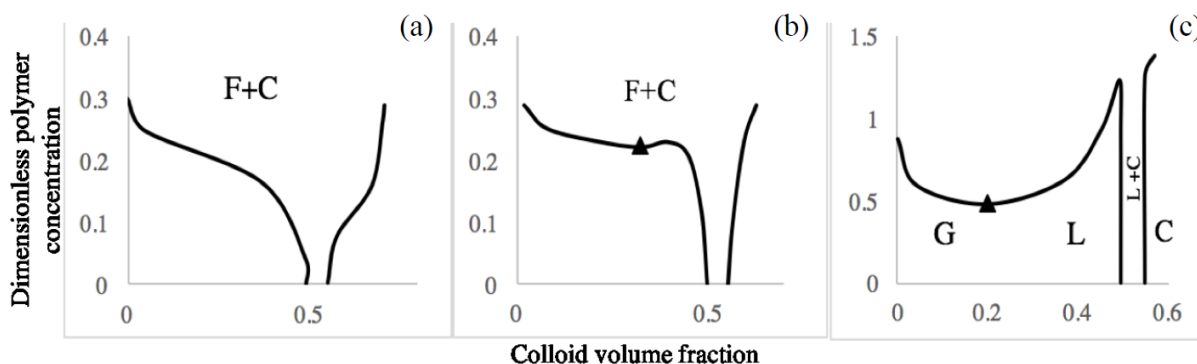
Figure 2.1 Phase diagrams obtained with Free Volume Theory and Generalized Free Volume Theory for different values of the ratio Rg/a = polymer radius of gyration/colloid size. (a) Rg/a = 0.08; (b) Rg/a = 0.33; (c) Rg/a = 0.57[16]. The critical point C1 is indicated with the solid triangle. F is the fluid phase.

Recent experiments[1,3] show that the two phase region (G+L) may form a closed loop and thus there may be two critical points (G=L) C1 and C2 in temperature invariant phase diagrams. The case of a cyclohexane + polystyrene + silica nanoparticles is shown in Figure 2.2 and the case of Athabasca pentane asphaltenes + polystyrene + toluene is shown in Figure 2.3. This behavior

appears because depletion stabilization[2] arises at high polymer concentration and this introduces a second critical point C2, and temperature variation in the phase boundary location in the resulting phase diagram. For these latter cases, the depletion interaction need not include particle flocculation.
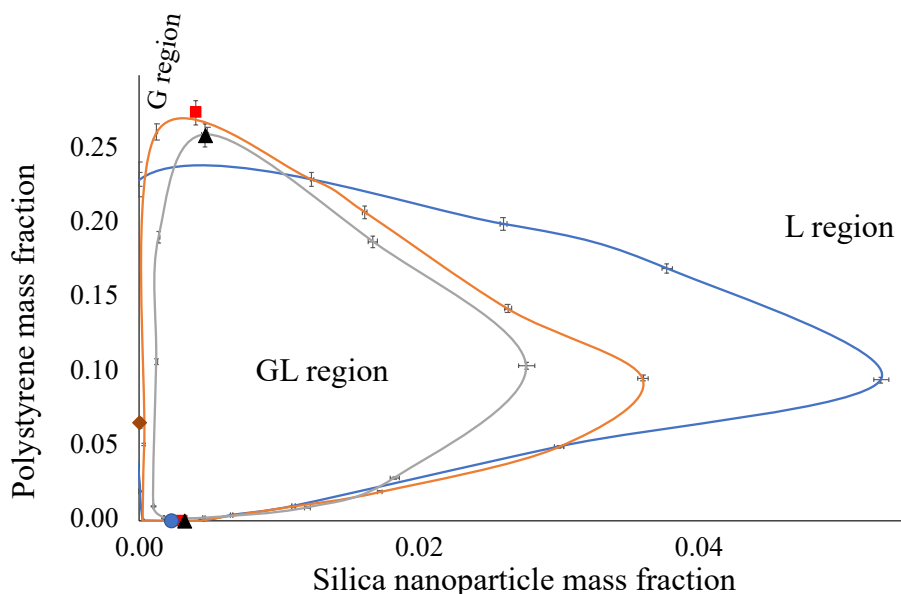
Figure 2.2 Superimposed phase diagrams for mixtures of cyclohexane + polystyrene (237 Kg/mole) + silica nanoparticles (7 nm diameter) showing two-phase to one phase boundaries at 296 K (——), 303 K (——) and 313 K (——). Symbols: G=L critical points at 296 K (●), 303 K (■) and 313 K (▲); (◆) UCEP for the polystyrene + cyclohexane binary (299 K)[17].

The temperature dependence arises in part because at low temperatures the G + L region intersects the polymer mass fraction axis, e.g.: at 296 K in Figure 2.2. This occurs because cyclohexane and polystyrene are not miscible at low temperatures. This transition to two-phase behavior arises at the upper critical end point (UCEP) temperature. The immiscibility effect is attributed to a conformational transition in the polymer from coil (below the UCEP) to globule[18] (above the UCEP). The radius of gyration of the polymer is thus temperature dependent in this temperature interval.

Critical point C1 is effectively temperature independent as expected from depletion interaction theories over temperature ranges where the radius of gyration of the polymer is temperature

independent, while critical point C2 is hypothesized to move along a critical locus starting at the UCEP as shown in Figure 2.4[17].
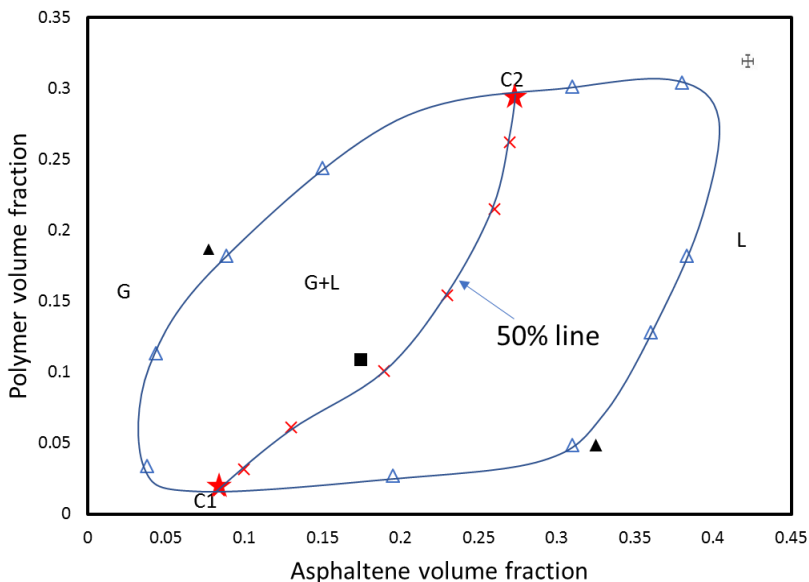
Figure 2.3 Experimental phase diagram for Athabasca pentane asphaltenes + polystyrene + toluene. (G) colloid gas like phase, (L) colloid liquid like phase, (G+L) coexisting colloid liquid like and gas like phases, (—) phase boundary, (x) 0.5 (volume fraction of L and G), (C1) first critical point, and (C2) second critical point, (■) two phase region, (▲) single phase region[3].
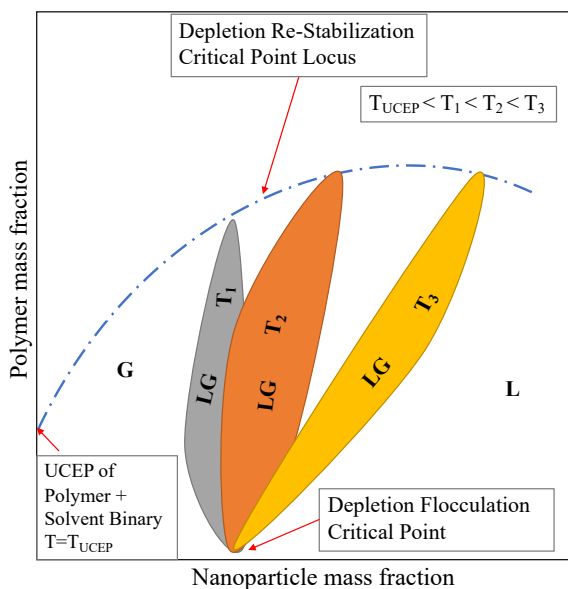
Figure 2.4 Movement of critical points as temperature increases above the UCEP temperature[17].

Cyclohexane and polystyrene are well-defined compounds. Their thermophysical properties are well known experimentally and are well-approximated using theoretical and empirical models. This is not the case for nanoparticles. From Derjaguin–Landau–Verwey–Overbeek (DLVO) theory[19,20], one can have a good understanding of the local behavior of individual nanoparticles in a solution, but the physics and chemistry become more complicated if related potentials are included rigorously in an equation of state. The question of how nanoparticles should be modeled thus arises. Poon[21,22] discussed how colloids can be treated as big atoms. While it might not be appropriate in general, the approach can be used to explain depletion flocculation effects. However, it is not well established whether the "big atom" point of view is applicable to other features of phase diagrams, such as depletion restabilization effects, or to special particle properties such as hygroscopy[1], and the modeling of poorly defined particles such as asphaltenes[3]. Further, Dr. Remco Tuinier, a founder of the field, asserted (during a discussion on July 17, 2018) that depletion interaction and depletion flocculation must be discriminated and that the phase behavior observed around critical point C1 in Figures 2.2, 2.3 and 2.4 is not depletion flocculation but depletion interaction, because two distinct phases are observed and the phase behaviors are reversible. However, it remains unclear, mechanistically whether or how, exactly, these two phenomena differ – one of degree or reversibility.

2.2 Thermodynamic Perturbation Theories

Perturbation theories are a set of methods that give approximate solutions to equations around a reference state that cannot be solved analytically, using Taylor series. If the perturbation is small enough, only a few terms in the Taylor series are needed. This type of method was first used for gravitational systems. For two planets, equations of motion can easily be solved but this is not possible once additional planets are added. For example, if the influence of a third planet is small enough (because it is small or far enough), its interaction energy can be seen as a perturbation and an approximate solution is obtained. These methods were first applied by Zwanzig in thermodynamics in 1954[23,24]. He developed the general formalism, with the hard sphere potential as a reference, but second order or higher terms were difficult to calculate, requiring radial distribution functions between more than two particles. Barker and Henderson[25,26] found

approximations to the second order terms where only the usual radial distribution function is required, and introduced an effective temperature dependent diameter for spheres. These equations have been combined with the depletion flocculation interaction[4,5] and provide phase diagrams that are qualitatively similar to those obtained from Free Volume Theory, i.e.: a second critical point C2 on the two-phase to one-phase boundary at higher polymer concentration is not obtained. Around the same time, Wertheim[27-30] developed a more elaborate Thermodynamic Perturbation Theory (TPT) for a specific kind of potential energy. The reference potential is still the hard sphere potential but perturbations are association sites so that short-range attractions in specific directions can be modeled. Wertheim's perturbation theory is applied in a specific way. Graph theory is reformulated in order to take different kinds of bonding into account (referred to as multidensity formalism) and steric effects corresponding to some of the neglected configurations when hard spheres are non-penetrating. The first order of this TPT is the basis of the Statistical Associating Fluid Theory (SAFT).

2.3 Statistical Associating Fluid Theory

With works from Boublík[31] and Mansoori et al.[32] to model hard spheres, SAFT[8,33,34] uses Wertheim's first order TPT to model chains of hard spheres and association sites. The hard sphere equation of state is thus modified to take short range attractions with specific directions into account. Dispersion interactions differ depending on the way actual spheres (also called segments) are modeled. For hard spheres, a simple mean field term is added to an equation of state[33,34]. If segments already include an attractive part in their potential energy, a different perturbation theory must be used. The perturbation theory and the Wertheim first order TPT should be applied sequentially and are not independent. However, this is a difficult process leading to complicated equations and in general the two are treated as if they are independent. Consequently there are numerous SAFT based equations of state that take different effects into account[35-42]. For example, for the perturbed chain variant PC-SAFT[36,37] Equation of State, segments are modeled with a square-well potential. A perturbation theory similar to Barker and Henderson perturbation theory[25,26] is applied, with the attractive part of the segment potential as a perturbation, once Wertheim first order TPT has been applied to model chains of spheres. PC-SAFT is both a rigorous and accurate model when association sites are not considered. The hard sphere variant SAFT HS

[10,11,43] (segments are simple hard spheres and dispersion is a mean field) has received limited practical as opposed to theoretical use. It is inaccurate but provides interesting qualitative results[10,11,43].

The main drawback of SAFT equations of state is their numerical difficulty[44,45], especially when association sites are used. Association requires solution of a system of non-linear equations to calculate Helmholtz free energy plus a linear system of equations for each derivative (pressure, chemical potentials, Hessian, etc). The other contributions, without association, are also significantly more complex than cubic equations of state (seventh order[45]). Overall, there can be more than three compressibility roots and computation times are significant. Despite this, SAFT EOS has already been used, in combination with Density Functional Theory, to model local depletion flocculation effects[13]. AlHammadi et al.[12] were the first to study ternary diagrams (comprising toluene + polystyrene + asphaltenes) where asphaltenes are modeled as a chain of spheres and without association sites. Their results agreed with available experimental results concerning depletion flocculation criticality and the adjacent two-phase to one-phase boundaries but show no indication of a second critical point C2, driven by depletion restabilization.

In this work, the goal is to model the two-phase region of solvent + polymer + nanoparticle mixtures including observed critical phenomena. The SAFT HS equation of state was chosen for its simplicity and its clear theoretical background, which allows three different types of attraction (association, chain formation and dispersion as a mean field) on top of the hard sphere reference state. The effects of these three attractive interactions is studied as a basis for more detailed evaluations including different potential energies. We are particularly interested in whether a simple form of SAFT models can mimic the existence and properties of the phase diagram exemplified by cyclohexane + polystyrene + silica nanoparticles mixtures in Figure 2.2 with the critical properties shown diagrammatically in Figure 2.4. This has not been demonstrated previously and it is not clear that available theories possess the required nanoscopic physics to explain observed macroscopic behaviors. Based on the current understanding of the depletion interaction phemonenon, an entropic effect, it should be modelable with the hard sphere term of the SAFT HS equation of state. However, it is not clear what the influence of molecular interactions is, and especially whether SAFT HS can model the coil/globule behavior of polymers.

Chapter 3: Model Development

In this chapter the method used to reach the objectives detailed in chapter 1 and 2 is elaborated. First, the SAFT HS equation of state is presented and explained in summary form. A complete derivation is provided in Appendix A1. Second, the phase equilibrium conditions and equations are rehearsed. Then a numerical model, presented as a MATLAB[14] code in Appendix A2, for generating ternary phase diagrams using SAFT HS is explained. Finally, the code is evaluated and validated against outcomes from previous works obtained using the same equation of state.

3.1 The SAFT HS model

The first SAFT model[33,34], known as SAFT HS, was chosen for its simplicity and because it can capture phase behavior effects that are expected to arise at a macroscopic scale. With SAFT HS, molecules are modeled as hard spheres and chains of hard spheres with some attractive interactions enabled among them. A complete derivation of this model is presented in appendix A1, except for the solution of the Percus-Yevick equation for the hard sphere potential. In the SAFT HS model, a system is described by its molar Helmholtz free energy a written as follow:

$$a = a_{ig} + a_{hs} + a_{chain} + a_{assoc} + a_{disp} \qquad (3.1)$$

Figure 3.1 provides a summary for the meaning of each term. In the case of an ideal gas, particles are points with a mass and a position. A hard sphere potential can be accurately accounted for with the hard sphere equation of state provided by Mansoori[32]. This is the reference potential for Wertheim first order TPT which enables the formation of chains and association i.e. attraction between different association sites. The latter type of attraction is only possible when association sites are overlapping (represented by blue circles in Figure 3.1). Only certain types of attractions are considered with these two forms of potential and thus a dispersion potential must be added. In the SAFT HS approach, this term is modeled as a simple mean field.
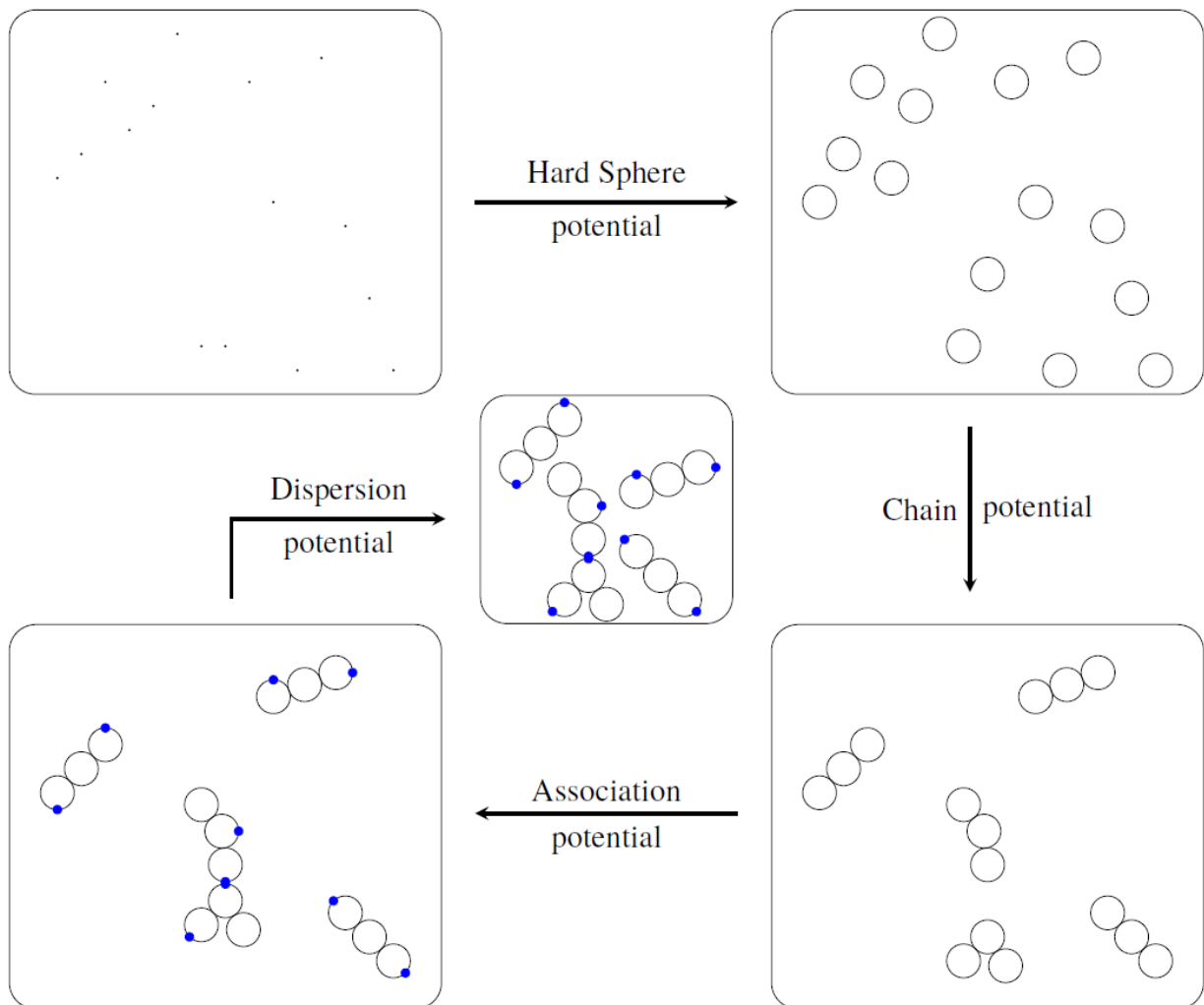
Figure 3.1 SAFT HS Equation of State physical meaning.

The molar quantities are defined as moles of molecules and not by moles of spheres. The ideal gas term a_{ig} is given by:

$$a_{ig}(T, \rho, x_i) = RT \sum_i x_i \left(\ln\left(N_a \rho x_i \lambda_i^3 \right) - 1 \right) \tag{3.2}$$

Where the sum means that it is carried out over each component. The thermal de Broglie wavelength λ_i of component i is :

$$\lambda_i = \frac{h}{\sqrt{2\pi M_i k_B T}} \tag{3.3}$$

With M_i the mass of component i. The hard sphere term is given with the following form[39]:

$$a_{hs}(T, \rho, x_i) = \frac{6RT}{\pi N_a \rho} \left(\frac{3\,\xi_1 \xi_2}{1 - \xi_3} + \frac{\xi_2^3}{\xi_3(1 - \xi_3)^2} + \ln(1 - \xi_3) \left(\frac{\xi_2^3}{\xi_3^2} - \xi_0 \right) \right) \tag{3.4}$$

Where:

$$\zeta_k = \frac{\pi}{6} N_a \rho \sum_i x_i m_i \sigma_i^k \; ; k = 0,1,2,3 \tag{3.5}$$

m_i is the number of spheres in molecule i. The packing fraction η of the mixture is exactly equal to ζ_3. This general form is preferred to the one chosen by Chapman[8] as the mixture can contain spheres with significantly different diameters (e.g.: nanoparticles and molecular segment). The chain term is[8]:

$$a_{chain}(T, \rho, x_i) = RT \sum_i (1 - m_i) \ln\left(g_{ii}(\sigma_i)^{hs} \right) \tag{3.6}$$

Where:

$$g_{ij}(\sigma_i, \sigma_j)^{hs} = \frac{1}{1 - \zeta_3} + \frac{3\sigma_i \sigma_j}{\sigma_i + \sigma_j} \frac{\zeta_2}{(1 - \zeta_3)^2} + 2 \left(\frac{\sigma_i \sigma_j}{\sigma_i + \sigma_j} \right)^2 \frac{\zeta_2^2}{(1 - \zeta_3)^3} \tag{3.7}$$

is the hard sphere radial distribution function between components i and j in a mixture. For the chain term where $i = j$, equation (3.7) becomes:

$$g_{ii}(\sigma_i)^{hs} = \frac{1}{1 - \zeta_3} + \frac{3\sigma_i}{2} \frac{\zeta_2}{(1 - \zeta_3)^2} + 2 \left(\frac{\sigma_i}{2} \right)^2 \frac{\zeta_2^2}{(1 - \zeta_3)^3} \tag{3.8}$$

The association term is[8]:

$$a_{\text{assoc}}(T, \rho, x_i) = RT \sum_i x_i \left(\sum_{A_i} \ln(X_{A_i}) - \frac{X_{A_i}}{2} + \frac{1}{2} \right) \tag{3.9}$$

The second sum is carried out over all the association sites on component i. It is written here in a slightly simplified form where the number of association sites per molecule is hidden inside the second sum. It comes from the fact that the number of association sites on a molecule i is $\sum_{A_i} 1$. X_{A_i} is implicitly given by:

$$X_{A_i} = \frac{1}{1 + N_a \rho \sum_j \sum_{B_j} x_j X_{B_j} \Delta_{A_i B_j}} \tag{3.10}$$

The association strength $\Delta_{A_i B_j}$ is given by:

$$\Delta_{A_i B_j} = \sigma_{ij}{}^3 g_{ij}(d_{ij})^{\text{hs}} \kappa_{A_i B_j} \left[\exp\left(\frac{\varepsilon_{A_i B_j}}{k_B T} \right) - 1 \right] \tag{3.11}$$

$$\sigma_{ij} = \frac{\sigma_i + \sigma_j}{2} \tag{3.12}$$

where $\kappa_{A_i B_j}$ is the bonding volume and $\varepsilon_{A_i B_j}$ is the association energy, between association sites A_i and B_j. More details about the meaning of $\kappa_{A_i B_j}$ are given in the appendix but it should be borne in mind that it corresponds to the overlapping volume between association site A_i and B_j (although it has no unit here). Finally, the dispersion term is[43]:

$$a_{\text{disp}}(\rho, x_i) = -N_a \left(\frac{\pi N_a \rho}{6} \right) \sum_{i,j} x_i x_j m_i m_j \sigma_{ij}^3 \varepsilon_{ij} \tag{3.13}$$

with:

$$\varepsilon_{ij} = (1 - k_{ij}) \sqrt{\varepsilon_i \varepsilon_j} \tag{3.14}$$

where k_{ij} is a binary interaction parameter and ε_i is the mean field value of the dispersion energy of interaction of component i.

The dispersion term in this model, while necessary, does not arise from a rigorously defined interaction potential and value of ε_i are often higher (by one or two orders of magnitude) than the values used in other SAFT equations of state, where it is better defined. The hard sphere and chain terms explain the basic shape of molecules and it is permissible to use non-integer values of m_i in order to fit data for molecules with known properties. The combination of the association and dispersion terms explains the attractive interactions. Association sites model oriented short-range attractions. Dispersion is used to model all other attractions. The main problem of the dispersion term is that it does not take local variations of potential energy into account.

In the first order theory used for association in SAFT, the association term, does not depend on the position of association sites as illustrated in equations (3.9), (3.10) and (3.11). Moreover, ring-like structures cannot be modeled as explained in Appendix A1. In SAFT, the radial distribution function only considers spheres that are touching. $\kappa_{A_i B_j}$ and $\varepsilon_{A_i B_j}$ lose a part of their physical sense because different pairs of these parameters can provide the same value for $\Delta_{A_i B_j}$. In this work, $\kappa_{A_i B_j}$ is estimated using equation (A.235) so that the impact of the one degree of freedom allowed by equation (3.11) is studied by changing $\varepsilon_{A_i B_j}$.

The Wertheim first order perturbation theory also considers some steric effects, as explained with more detail in the Appendix A1. These steric effects are represented in Figure 3.2. Steric effect I appears when three hard spheres are considered. If association sites are small enough compared to the radius of the hard spheres, it is not possible for three association sites to overlap. Steric effect II prevents one association site from bonding with two association sites of another hard sphere. This happens when association sites are small but also when association sites (on hard sphere 2) are not close enough to one another. Finally, steric effect III prevents one hard sphere from bonding to another hard sphere with two or more different association sites (on each hard sphere). Again, this happens when association sites are small and not close enough to one another.
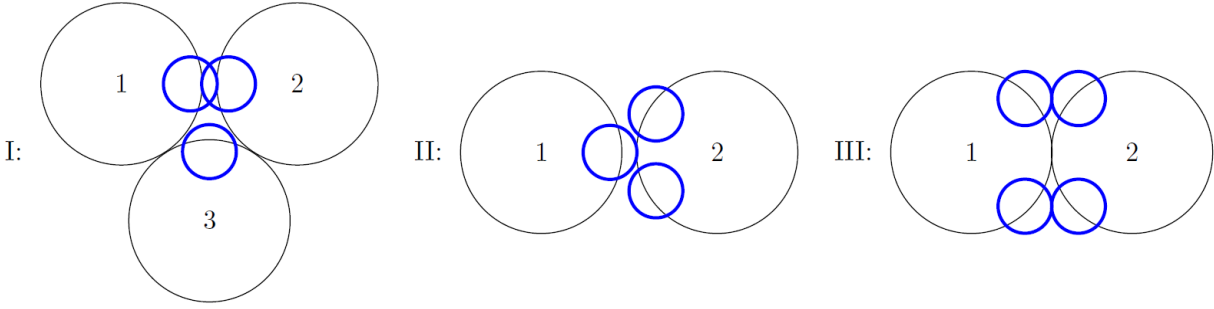
Figure 3.2 Steric effects considered in SAFT[8]. Black circles represent hard spheres and blue circles represent association sites.

3.2 Phase equilibria

For a set of parameters (temperature, pressure, interaction energies, size of the particles… and an overall composition), the number of phases, the fraction and the composition of each phase can be obtained from an equation of state. By repeating these "flash calculations" for many different conditions, PT (at fixed composition), Px (at fixed T), Tx (at fixed pressure) phase diagrams are obtained. For the most common isothermal flash calculation, the main physical principle to get this information is the minimization of the Gibbs free energy at constant pressure and temperature. In simplest terms, the Gibbs free energy, as a function of composition, is generated and then the tangent plane criterion developed by Michelsen[46] is applied.

The first step is to calculate a in equation (3.1). There is no difficulty except for the association term, equation (3.10), which is a non-linear system of as many equations as there are different association sites. From the form of this system of equations, one can see that all X_{A_i} are between 0 and 1. Xu et al.[44] showed that there can be only one solution for equation (3.10). Thus, successive iteration $X_{A_i} \rightarrow f_{A_i}$ with $f_{A_i} = \frac{1}{1 + N_a \rho \sum_j \sum_{B_j} x_j X_{B_j} \Delta_{A_i B_j}}$ is sufficient to find the solution and this iterative method was chosen here because it converges faster than the MATLAB solver routine.

The next step is to calculate chemical potentials μ_i of all components i:

$$\mu_i = \frac{\partial A}{\partial n_i}\Big|_{T,V,n_{j \neq i}} \quad ; A = na \qquad (3.15)$$

16

Chemical potentials obtained from equation (3.15) are derived in Appendix A1. From these, the Gibbs free energy G is obtained with:

$$G = \sum_i \mu_i n_i \tag{3.16.1}$$

Or the molar version:

$$g = \sum_i \mu_i x_i \tag{3.16.2}$$

From:

$$G = A + PV \tag{3.17}$$

It is directly shown that:

$$P(\rho) = \rho(g(\rho) - a(\rho)) \tag{3.18}$$

where the molar density dependence is written. Pressure can also be calculated as a partial derivative of a:

$$P(\rho) = \rho^2 \frac{\partial a}{\partial \rho}\bigg|_{T,n_i} \tag{3.19}$$

The fact that equation (3.18) and (3.19) give the same result is a consequence of Gibbs-Duhem equation. Pressure is fixed so the molar density must verify the following equation:

$$P^* = P(\rho) \tag{3.20}$$

Where P^* is the fixed pressure and P is the pressure given by equation (3.18) or (3.19). There are in general several solutions to this equation. The solution that minimizes Gibbs free energy must be kept. Once this is done, one can calculate Gibbs free energy and chemical potentials with equations (3.15) and (3.16).

For an overall composition of interest x_0, the tangent plane distance D^G at x_0 as a function of the composition vector $x = (x_1, x_2, \dots)$ is:

$$D_{x_0}^G(x) = \sum_i x_i\big(\mu_i(x) - \mu_i(x_0)\big) \tag{3.21}$$

According to Michelsen[46], this function must always be a positive function if one-phase is stable at composition x_0. This is the tangent plane criterion. The mole balance defines the composition space:

$$\sum_i x_i = 1 \; ; \; \forall\, i\, , 0 \le x_i \le 1 \tag{3.22}$$

If it happens that the tangent plane distance is not positive for a given composition, one-phase cannot be stable at composition x_0 and there must be a phase separation. Then two or more phases have to be present and each of them must satisfy the tangent plane criterion. In addition to that, chemical potentials in each given phase α and β (for each component) must be the same:

$$\forall\, i, \mu_i^\alpha = \mu_i^\beta \tag{3.23}$$

Introducing x_i^α which is the mole fraction of component i in phase α, all the equations needed in the case where multiple phases are present in the system can be written. The mole balance becomes:

$$\forall\, i, x_i = \sum_\alpha x_i^\alpha f^\alpha \tag{3.24}$$

$$\forall\, \alpha, \sum_i x_i^\alpha = 1 \tag{3.25}$$

Where in equation (23) f^α is the mole fraction of phase α in the system. Equation (3.23) becomes:

$$\forall\, i, \; \mu_i(\boldsymbol{x}^\alpha) = \mu_i(\boldsymbol{x}^\beta) \tag{3.26}$$

Where $\boldsymbol{x}^\alpha$ is the vector of all the x_i^α.

Minimizing Gibbs free energy can lead to numerical problems and thus one might prefer to minimize Helmholtz free energy[47]. Only temperature is then fixed. In this case, it is more convenient to work with molar density vectors instead of mole fraction vectors. These are defined as:

$$\boldsymbol{\rho} = \rho x \tag{3.27}$$

In component form:

$$\rho_i = \rho x_i \tag{3.28}$$

Therefore, $\boldsymbol{\rho}^\alpha$ is the molar density vector in phase α and ρ_i^α is the molar density of component i in phase α. In this case, the set of independent thermodynamic variables becomes $(T, \boldsymbol{\rho})$. In the previous section, this set had three variables $(T, \rho, \boldsymbol{x})$ but was subject to equation (3.22). The tangent plane distance D^A at $\boldsymbol{\rho}_0$ as a function of $\boldsymbol{\rho}$ is in this case:

$$D_{\boldsymbol{\rho}_0}^A(\boldsymbol{\rho}) = -\frac{P(\rho) - P^*}{\rho} + \sum_i \frac{\rho_i}{\rho}\left(\mu_i(\boldsymbol{\rho}) - \mu_i(\boldsymbol{\rho}_0)\right) \tag{3.29}$$

Note that ρ is the sum of each component of $\boldsymbol{\rho}$. This is one of the reasons molar density vectors are more convenient. One can get composition and molar density simultaneously. The same remarks as above apply to this case. The main difference is that with the Gibbs free energy approach, one has to find all the roots of equation (3.20) while with the Helmholtz free energy approach one has to deal with an additional dimension (pressure). Moreover, as pressure is still fixed:

$$P(\boldsymbol{\rho}^\alpha) = P(\boldsymbol{\rho}^\beta) \tag{3.30}$$

and pressure equality (3.20) must be verified on top of equations (3.26) in the Helmholtz free energy approach. How these equations are actually used is shown in section 3.3.

It is convenient to use the Helmholtz free energy approach to calculate critical points[47,48]. A critical point is a point where two or more phases become one. Thus, it must be on the one-phase/multi phase limit (i.e. the binodal in the case of the one-phase/two-phase limit). This implies that the minimum value of the tangent plane distance at a critical point must be exactly zero. For a point inside the multiphase region, this value is negative, and it is zero for points inside a one-phase region. When pressure and temperature are fixed in a ternary mixture, a critical point depends on two parameters, the mole fraction of two of the compounds (the other mole fraction is found so that equation (3.22) is verified). Thus, the condition that the minimum value of the tangent plane distance is zero is not sufficient to find a critical point. The fact that phases become identical means that around critical points, one-phase is only slightly unstable. It means that a critical point is also on the limit between the region where one-phase is unstable and the region where one-phase is not unstable (i.e. metastable or stable). This work focuses on critical points where only two-phases become identical. They are ordinary critical points and also are the intersection points between a

binodal and a spinodal in binary and ternary phase diagrams. One can show[47,48] that, in the Helmholtz free energy approach, an ordinary critical point verifies the two following equations:

$$\lambda_1 = 0 \tag{3.31}$$

$$\frac{d\lambda_1}{d\boldsymbol{\rho}} \cdot \boldsymbol{u_1} = 0 \tag{3.32}$$

Where λ_1 and $\boldsymbol{u_1}$ are the smallest eigenvalue of the Helmholtz free energy Hessian (at constant temperature) and the corresponding eigenvector respectively. The Helmholtz free energy Hessian is:

$$(\boldsymbol{H}^A(T,\boldsymbol{\rho}))_{i,j} = \frac{\partial^2 \rho a}{\partial \rho_i \partial \rho_j}\bigg|_{T,\rho_k} \tag{3.33}$$

The derivative in equation (3.32) is the gradient of λ_1 so that the entire left hand side is a directional derivative along $\boldsymbol{u_1}$. In the Helmholtz free energy approach, pressure is not fixed. Thus, equations equation (3.20) must be verified on top of equations (3.31) and (3.32). Note that the condition:

$$\boldsymbol{u_1^T} \cdot \frac{d^2\lambda_1}{d\boldsymbol{\rho}^2} \cdot \boldsymbol{u_1} > 0 \tag{3.34}$$

(gradient of the vector field $\frac{d\lambda_1}{d\boldsymbol{\rho}}$ in the direction $\boldsymbol{u_1}$) is also verified but is not necessary to find the critical point. Note that the instability region is determined by the sign of λ_1.

3.3 MATLAB program

The MATLAB[14] program embodying the concepts and equations noted above and used to generate the results presented in the next chapter is provided in Appendix A2. It is organized into three parts: functions that give values for the main equations (Helmholtz free energy, chemical potential, pressure and Helmholtz free energy Hessian), subroutines that solve equations introduced in the previous section and the main script for ternary mixtures. The script for binary mixtures is essentially the same as the one for ternary mixtures and is not included. However, subroutines that are specific to the binary mixtures case are included.

There is not much to say about the first part. Equation (3.1) to (3.14) plus similar equations for the other thermodynamic quantities (given in Appendix A1) are directly translated into MATLAB

code. The only difficulty is the association term. For Helmholtz free energy, a "while" loop is used in order to find the fixed point of equation (3.10). The criteria to stop this loop is determined by the parameter "error_assoc". It is possible to use the approximate forms of SAFT HR[38-40] as starting points for the loop but this is not applicable for the mixtures studied here and any starting point led to a solution with similar computation times. The other properties (chemical potential, pressure and Helmholtz free energy Hessian) require solving a linear system of equations as explained in Appendix A1. Also, in order to simplify the use of association sites, a parameter "n_Ai" is introduced. It is an array whose elements are the number of identical association sites A_i (i.e. sites with the exact same properties). Indeed, because the position of association sites does not matter in Wertheim's first order TPT, one can consider only one representative element for each different kind of site and accordingly multiply each $\Delta_{A_i B_j}$ (or identically $k_{A_i B_j}$) by the number of identical site of each kind. Equation (3.9) must also be changed accordingly to take this into account in the sum carried out over association sites. Each contribution (association, dispersion,...) are calculated separately and then combined in functions "helmholtz", "chempot", "pressure" and "hessian".

The other subroutines are presented following the main script. The first part of the code is dedicated to preparing the environment and defining all required parameters. The MATLAB function "addpath" is used to call subroutines from different subfolders and the following lines:

```
coresenv=str2num(getenv('SLURM_CPUS_PER_TASK'))
c = parcluster('local');
c.NumWorkers = coresenv;
parpool(c, c.NumWorkers);
```

are required to use more than twelve cores on clusters. The "parpool" function enables parallel computation on a given number of cores.

The next part of the code provides data for pure components.

Then, variables are created in order to store thermodynamic properties on a grid of points. This is done because the tangent plane criterion requires a global study of the Gibbs free energy. The Gibbs free energy approach is then used first as it easily provides a good idea of the entire phase diagram. The main idea is to calculate the Gibbs curve on this grid of points at fixed temperature and pressure and then apply the tangent plane criterion to each point on the grid. In order to calculate the Gibbs curve at constant pressure and temperature, one has to solve equation (3.20)

for each grid point. Then the tangent plane criterion is applied with a double "for" loop on all the elements of the grid to verify whether or not, for each grid point, there exists another grid point so that the tangent plane distance (given by equation (3.21)) is negative. The grid is characterized by three parameters (defined in the first part of the code). Parameter "n" gives the number of point on each row and column of the grid. Two other parameters "za" and "zb" are used to reduce the observed region of the composition space (explained below). Each point of the grid is a set of three numbers in the case of ternary mixtures, or two in the case of binary mixtures, that satisfy equation (3.22). In order to store these three numbers for each grid point, a cell structure is more convenient than arrays (arrays can only store numbers whereas cells can store any type of data). If the phase diagram is a function of mass fractions and not mole fractions, grid points have to be converted. Finally, the cell array is transformed into a cell vector in order to be usable with parallel computing (explained below).

The next part of the code focuses on solving equation (3.20) but with pressure given as a function of the packing fraction instead of molar density. For each point this is done via the subroutine "thermo_properties_p". Equation (3.20) is translated into an objective function called "obj_pressure" whose zeros are found using the MATLAB function "fzero". The difficulty is that "fzero" can only find one zero and only if the objective function has a different sign at the beginning and at the end of a starting interval. The starting packing fraction interval is specified by two parameters "eta_start_a" and "eta_start_b" so that to verify the latter condition and surround all possible zeros of equation (3.20). To find all zeros, the following simple algorithm is used: find one zero → bisect the starting interval around this point → repeat on the new starting intervals. If the objective function does not have different signs on a given starting interval, it is bisected. The algorithm stops when a given number of zeros "max_n_roots" has been found or when a given number of bisections (related to "max_counter") have been done. As this work focuses on liquids, it is possible to accelerate calculations by choosing a starting interval that does not include gas roots. While there is only one liquid root in the systems studied here and "max_n_roots" and "max_counter" can be set to 1, "max_n_roots = 5" and "max_counter = 6" are used first with a small resolution "n" to be certain that no zeros are missed in the computational space. The "for" loop used in this case is a "parfor" loop so that each available worker can work on a different part of the grid. That is why the grid is transformed into a vector, otherwise one

22

needs two "for" loops to cross the entire grid and it is not possible to use nested "parfor" loops. All subsequent parallel calculations are made with this "parfor" loop.

Once the Gibbs curve is calculated (and the corresponding chemical potentials), a phase stability test is applied to the grid with the subroutine "Stability". For each point of the grid (x_0), it calls another subroutine "TPD_x0" whose output is 1 if one-phase is stable at this point and 2 otherwise. In order to do this, the latter function calls another function "TPD_fast" for every point on the grid, which calculate the tangent plane distance $D_{x_0}^G$ at these other points. If it gives a negative number at some point, then one-phase cannot be stable at x_0. A parameter "threshold" is used to get rid of numerical noise that may give negative tangent plane distances inside the one-phase region. At the end of this process, two sets of points are created (single and non single phase points). This method needs to have a resolution parameter "n" high enough so that the resulting one-phase region/multiphase region boundary converges to the actual boundary. However, it provides good results when combined with appropriate value of "za" and "zb" (which depend on the size of the multiphase region) and more importantly, it is numerically reliable because only one (one dimensional) solver is used and otherwise only analytical derivatives values are compared. This provides a computational advantange compared to the part of the code that generates tie lines which is unreliable in certain cases (discussed in chapter 4).

A similar process is done to find the instability region on the grid. The molar density has already been fitted at each point of the grid to ensure that pressure is constant. Using these values of molar densities and corresponding compositions, one can calculate the Helmholtz free energy Hessian at constant pressure and temperature and then calculate its smallest eigenvalue with the MATLAB function "eig". Two sets of points are then generated depending on the sign of the eigenvalue. First, points inside the multiphase region and inside the instability region are stored in a vector. Then the MATLAB function "boundary" is used to create a polygon around the multiphase region and the instability region (separately) so that the two respective boundaries can be plotted. Multiphase behaviours including phases with high nanoparticle mass/mole fractions are excluded from consideration as colloid crystal behavior is not part of the model.

Compositions near the intersection of the single-phase instability curve (spinodal) with the two-phase to one phase boundary (binodal), provides good starting points for the determination of critical points. Equations (3.31) and (3.32) are implemented in the subroutine "critical_functions".

Eigenvectors and eigenvalues are found using the MATLAB function "eig" and the third order derivative of equation (3.32) is calculated numerically from the Helmholtz free energy gradient given by the subroutine "gradient". This is then combined with equation (3.20) as an objective function in the function "critical_obj_ternary". Finally, this objective function is minimized using the MATLAB function "lsqnonlin" in the subroutine "critical_point_ternary". A similar subroutine "critical_point_binary" is used to find critical points for binary mixtures. When using these subroutines with starting points found graphically, the solver does not converge well (by looking at the value of the objective function). However, using the solution provided by the subroutine as a new starting point for the calculation, one finds accurate values. There is a graphical way to verify that this solution corresponds to a critical point. Using the subroutine "Dsup", one can plot the tangent plane distance of the critical point $D_{\rho_c}^A$ (ρ_c is the molar density vector of the critical point of interest) in the direction u_1 corresponding to the minimum eigenvalue of the Helmholtz free energy Hessian λ_1. According to the previous discussion this tangent plane distance should be always positive outside the multiphase region and is sometimes negative inside it. So at the critical point, $D_{\rho_c}^A$ is also positive but equation (3.31) and (3.32) imply that it should be very flat around the critical point. Equation (3.34) implies that the function should also be convex. This is illustrated in the next section. The subroutine "Dsup" does not plot the tangent plane distance at constant pressure but this is not required here because one wants to see what happens locally, around the critical point.

Tie lines are calculated two different ways depending on whether the Gibbs or Helmholtz free energy approach is used. However, in the end, equations (3.20), (3.26) and (3.30) are always the ones that need to be solved, on top of mole the balance. In the Gibbs free energy approach, starting points are first guessed with the subroutine "min_TPD" which globally minimizes $D_{x_0}^G$ for a point x_0 inside the multiphase region. In this case, $D_{x_0}^G$ is given by the subroutine "TPD". This global minimization is done with the MATLAB Global Optimization Toolbox[14]. This provides a starting point for each phase. In this work, only two-phase equilibria are calculated. Three phase regions are not calculated. Thus, one can take two starting points that are graphically good compared to the previously plotted binodal and spinodal. When only tie lines are wanted (and not the amount of each phase), they are determined by four parameters and thus four equations are required. Three of them are provided by equations (3.26) and another one is given by equation (3.24) for a phase

mole fraction of 0.5 for instance. The subroutine "phase_split_t" solves these equations with "lsqnonlin". The objective function is given by "equi_pot_t". "phase_split_b" solves these equations in the binary case. In the Helmholtz free energy approach, one starts by calculating tie lines close to critical points. The function "pre_tielines" creates two molar density vectors slightly away from a critical point in a direction perpendicular to u_1. Using the one inside the two-phase region, one can plot the tangent plane distance of this composition in the direction u_1 (the subroutine "TPDA_u1", very similar to "Dsup", is used for that purpose). Being inside the two-phase region, the tangent plane distance should have two minima, which are used as starting points to find the tie lines. One needs five equations in this case because pressure is not fixed. Equations (3.20) and (3.30) provide two of them and equations (3.26) provide the remaining three. The objective function is given by "equi_cond" and solved by "tie_line_A" also with "lsqnonlin". Note that there are six components overall with the two molar density vectors for each phase so one of them must be fixed. Once one tie line is found, the same process is repeated but with the middle of the tie line instead of a critical point. This approach is not as convenient as the Gibbs free energy approach even if it converges faster. Indeed, one can only have tie lines step by step whereas with the Gibbs free energy approach, one can get any tie line first. It is not an issue in general but with the system studied here, starting points are difficult to get because the tangent plane distance $D_{\rho_0}^A$ does not have two minima for a composition too far from a critical point or the middle of a tie line.

Finally, one can plot a phase diagram combining the binodal, the spinodal, critical points and tie lines. Tie lines cannot always be calculated accurately and one can qualitatively know their trend once critical points are calculated, thus they are only plotted for the final results of chapter 4. Here in binary cases, tie lines do not bring any information thus they are not plotted neither, except for the next section to test the program.

3.4 Validation of the method

This program was tested for internal consistency during development, against different methods for the same calculations and was then tested against a prior work[11] that used the same equation but a different mixture. For example, one must ensure that all the equations are correctly implemented. Indeed, equations for derivatives of Helmholtz free energy are quite complex. These derivatives can be obtained numerically and these values must agree with analytical derivatives.

For pressure this can also be done by verifying that equations (3.18) and (3.19) give the same result. For chemical potentials, equations (3.16.1) and (3.17) should provide the same Gibbs free energy. Finally regarding the Hessian, it should provide a spinodal which remains inside the binodal and which touches it at a certain number of points (depending on the number of components and the number of phases). The binodal and the spinodal can be tested with a binary case at fixed pressure and temperature and one can see that the corresponding Gibbs curve agrees with the binodal and the spinodal. Critical points should be at the instersection of the spinodal and the binodal and the tangent plane distance (at these points) should be flat. Finally, one can test that tie lines are correct by verifying that the corresponding two-phases are located on the binodal and that tie lines shrink close to critical points. These internal checks were performed and verified for the temperature/composition phase diagram of water + 1-butanol at 200 MPa obtained by Garcia-Lisbona et al.[11] shown in Figure 3.3. Parameters used in the MATLAB program include[11]:

```
P = 2e8;
sigma_i = [3.6 3.86];
mw_sol = 18.0153;
mw_pol = 74.1216;
mw = [mw_sol mw_pol];
m_i = [1 2.2];

%Dispersion term parameters
e_i = kb * [4452 3135];
k_ij = [0 -0.035356978321922;-0.035356978321922 0];

%Identical association sites are counted as one here
e1 = kb*1558;
e2 = kb*3236;
e12 = kb*1803;
e_AiBj(1,1,:,:) = [0 0;e1 e12;0 e12];
e_AiBj(2,1,:,:) = [e1 e12;0 0;0 0];
e_AiBj(1,2,:,:) = [0 0;e12 e2;0 0];
e_AiBj(2,2,:,:) = [e12 e2;0 0;0 0];
e_AiBj(3,2,:,:) = [e12 0;0 0;0 0];

%Number of identical association sites
n_Ai = [2 1;2 1;0 1];
%Multiply each k_AiBj by the number of identical association site
k1 = 1.3578/(sigma_i(1)^3);
k2 = 0.3910/(sigma_i(2)^3);
k12 = 0.777/((sigma_i(1)+sigma_i(2))/2)^3;
k_AiBj(1,1,:,:) = [0 0;2*k1 k12;0 k12];
k_AiBj(2,1,:,:) = [2*k1 k12;0 0;0 0];
k_AiBj(1,2,:,:) = [0 0;2*k12 k2;0 0];
k_AiBj(2,2,:,:) = [2*k12 k2;0 0;0 0];
k_AiBj(3,2,:,:) = [2*k12 0;0 0;0 0];
```
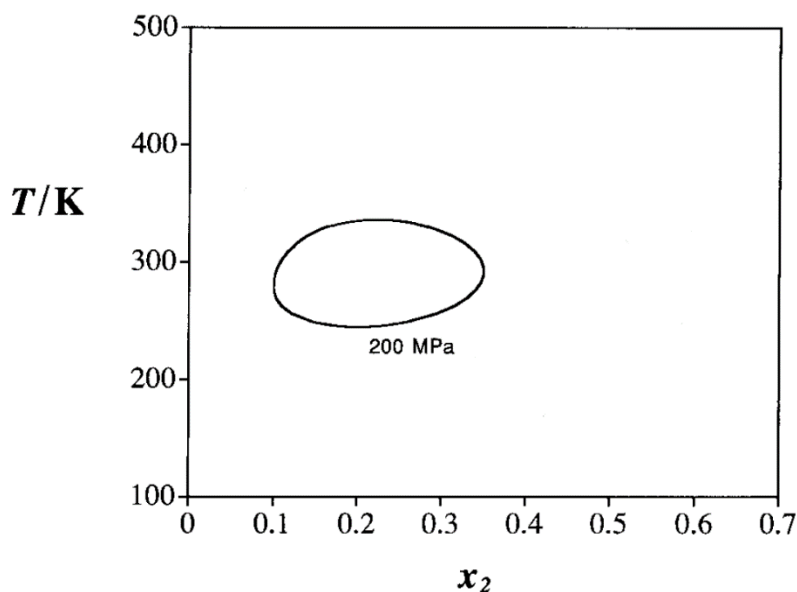
Figure 3.3 Water + 1-butanol temperature/composition phase diagram obtained by Garcia-Lisbona et al.[11]. x_2 is the 1-butanol mole fraction.
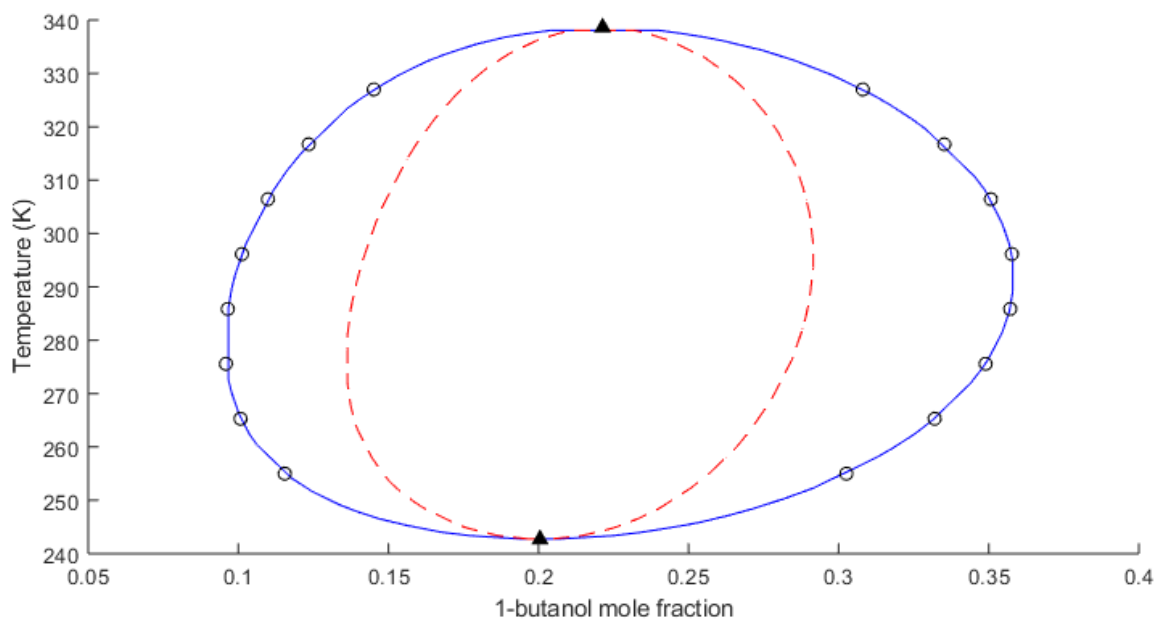
Figure 3.4 Water + 1-butanol temperature/composition phase diagram at 200 MPa obtained in this work with the MATLAB program. The blue solid line is the binodal and the red dashed line is the spinodal, both obtained using stability and instability criteria on a grid of points. Black circles are coexisting compositions obtained by solving equilibrium equations with "phase_split_b". Solid traingles are critical points obtained by solving critical conditions with "critical_point_binary".

27

Results obtained with the MATLAB program are in Figure 3.4. First, one can see that the binodal corresponds with the one on Figure 3.3. "max_n_roots" and "max_counter" were set to 1, "eta_start_a" to 0.4 and "eta_start_b" to 0.6 once it was verified that the code was able to find the compressibility root which minimizes the Gibbs free energy. The spinodal is inside the binodal and touches the binodal at the top and the bottom of the two-phase region, as it should when pressure is invariant. Tie lines (only represented by circles in Figure 3.4) do lie on the calculated binodal. The objective function "equi_pot_b" was found to be well-minimized for these temperatures. The sum of the residual functions squares is below 10^{-25} except near the critical points where the objective function was around 10^{-20}. The low temperature critical point is at (Tc1 = 242.69 K, 0.20053) and the high temperature critical point is at (Tc2 = 338.61 K, 0.22137). One can verify graphically that these points correspond to critical points. The tangent plane distance in the u_1 direction for these two points and for slightly different temperatures and around critical point compositions are shown in Figure 3.5.
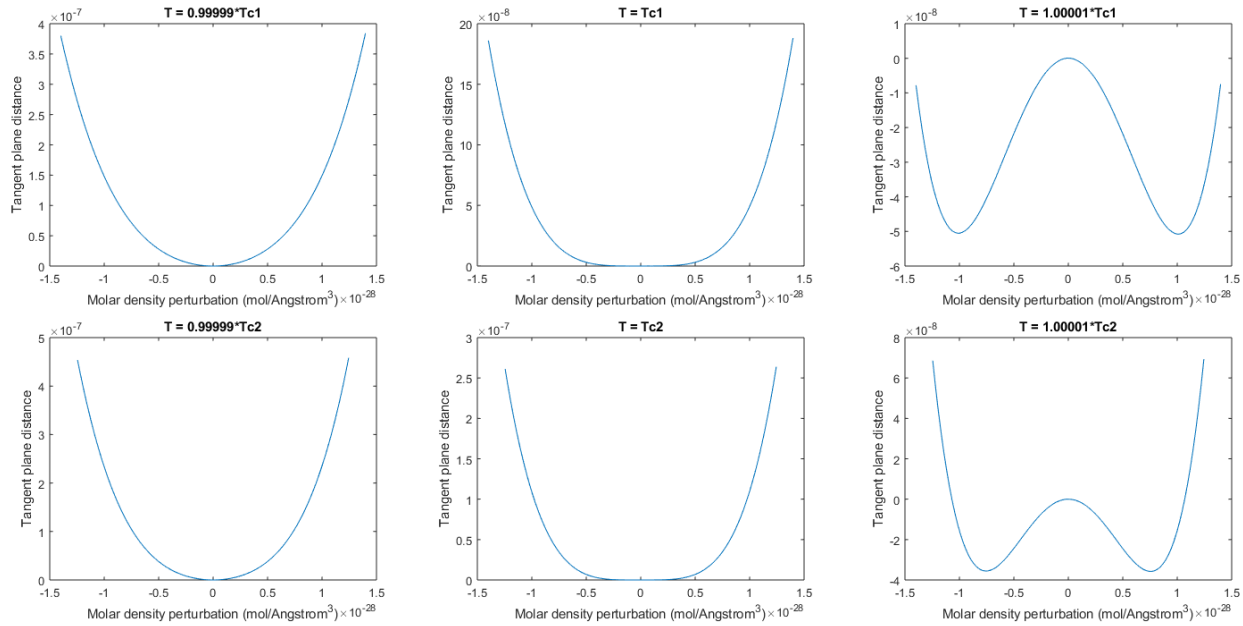
Figure 3.5 Tangent plane distance functions around the critical points (pressure is not fixed).

The abscisa represents the molar density variation around the molar density at the critical point, in the u_1 direction. One can see that at the critical points, equations (3.31), (3.32) and (3.34) are verified. Indeed, the curve is convex and flat around the critical point. For temperatures slightly

below the critical temperature, the curve is not flat anymore even if the slope is zero at the critical point composition. For temperatures above critical temperatures, one also looses the convexity because these temperatures are inside the two-phase region. Note that pressure is not fixed here, which is why, for the high temperature critical point, the system has two phases above and not below the critical temperature as one would expect from Figure 3.4. Overall, this example demonstrates that the MATLAB program simulates phase diagrams using the SAFT HS equation of state. Results provided by this code also agree with a code prepared independently by Dr. Sergio Quiñones Cisneros (April 2018).

Chapter 4: Results and Discussion

Phase behavior simulation for cyclohexane + polystyrene + silica nanoparticle provides a test case for the assessment of SAFT HS. Can realistic parameters for the qualitative study of solvent + polymer + nanoparticle mixtures that exhibit a closed loop phase boundary with two critical points be identified, and can a transition to a phase diagram where the two-phase region intersects the polymer composition axis be predicted? The literature fixes parameters for cyclohexane and polystyrene and Kumar[1] provides some fixed parameters for the silica nanoparticles. Pressure is also fixed at 0.1 MPa. Phase diagrams are presented in terms of mass fractions of polystyrene w_2 and nanoparticles w_3. The exposition in this chapter focuses on the case where the hard core of each component (size of hard spheres plus chain length) is fixed and energy parameters are constrained by the density of cyclohexane and polystyrene. The qualitative influence of other parameters is studied and only a configuration of parameters that has the simplest and best physical sense is kept. Other configurations and the corresponding phase diagrams are showed in Appendix A3.

4.1 Cyclohexane

It is convenient to start by modeling cyclohexane. It is a simple compound. Values for its sphere diameter, chain length and molar mass are shown in Table 4.1[38]. Cyclohexane is a non-associating compound so no association sites are used. However, the dispersion term only models the mean field. Association sites could be used to take into account the fact that close to individual molecules, the dispersion energy depends on orientation. Doing so provides better results for cyclohexane densities as a function of pressure but does not change the nature of the ternary phase diagram. Thus, the simplest model without association sites was retained. Adjusting the cyclohexane dispersion energy ε_1, one finds that the value $\varepsilon_1 = k_B 3100$ J provides qualitatively good results for density. At 298 Kelvin and 1 bar, the density it provides is 775.00 g/L which is in agreement with the 779 g/L density provided by Kumar[1]. A liquid-vapor transition is also observed at 0.003 MPa against a value of 0.013 MPa provided by NIST[49].

4.2 Cyclohexane + Polystyrene

Polystyrene has also been studied with the SAFT equations of state[50]. There are binary phase diagrams available for polystyrene + cyclohexane, as well[51]. Kumar used atatic polystyrene with a molar mass of 237 kg/mol[1], fixing the molar mass value in this work. The chain length is then the ratio of the molar mass of a polystyrene molecule to the molar mass of a styrene molecule. The molar mass of styrene is 104.152 g/mol[52]. The corresponding value for the chain length of polystyrene is given in Table 4.1. The radius of a sphere representing a monomer is also given in Table 4.1 and is obtained from a previous SAFT work[50]. The dispersion energy ε_2 is adjusted so that pure polystyrene has a density of 1.05 g/mL[1].

Experimental temperature/composition phase diagrams of this binary mixture are given in Figure 4.1. Polymer molar mass is a parameter. The importance of association sites on the polymer is easily demonstrated in the case of SAFT HS. One can try to get qualitatively similar phase diagrams, in their absence, by varying the binary interaction parameter k_{12}. Results for various values of this parameter are shown in Figure 4.2. One can clearly see that qualitative agreement is not possible. There is a UCEP for negative values of k_{12} and at high polystyrene mass fraction. From the experiments the UCEP is at low polystyrene mass fraction. Although it is possible to model this mixture without association sites using a different dispersion term[9,50], the dispersion term in SAFT HS is inadequate. One can then assume that there is a specific kind of attraction between cyclohexane and the aromatic rings of polystyrene as well as an attraction between aromatic rings on polystyrene themselves. However, according to Wertheim's first order TPT, attraction between aromatic rings in the same molecule cannot be accounted for. Considering the symmetry of cyclohexane and aromatic rings in the polystyrene monomer, two association sites are added to each cyclohexane molecule and two for each polystyrene monomer. A value for all the $\kappa_{A_i B_j}$ parameters is estimated using the function "kappa" in the MATLAB program. A cyclohexane molecule with an association site whose center is at the surface of a cyclohexane hard sphere and whose diameter is half the diameter of a cyclohexane hard sphere provides a value of 0.0873. For the association energy $\varepsilon_{A_i B_j}$, a value of $k_B 500$ J between cyclohexane and polystyrene association sites and a value of $k_B 230$ J for polystyrene self-association provides the temperature/composition phase diagram in Figure 4.3. The dispersion energy ε_2 is then $k_B 970$ J. The computed phase boundaries agree qualitatively with the experimental data (Figure 4.1). The

computed UCEP temperature 299.6 K and polystyrene mass fraction 0.0197 are also similar to the corresponding experimental values (298.7 K ± 0.2 K, 0.087 ± 0.005)[17].
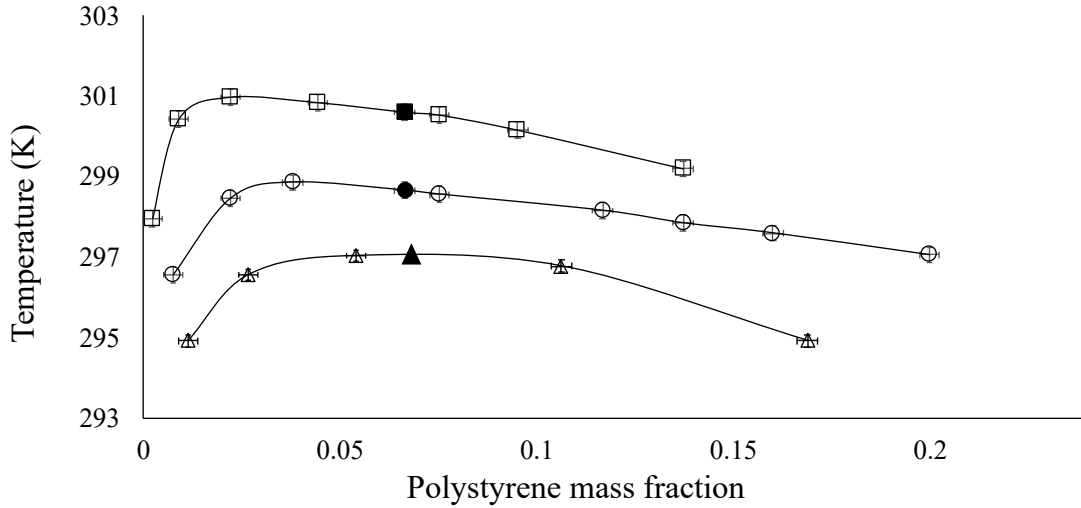
Figure 4.1 Liquid-liquid to liquid phase boundary experimental data for polystyrene + cyclohexane binary mixtures.[17] Open symbols: polystyrene molar mass 237 kg/mol (O)[1], 250 kg/mol (□)[53] and 200 kg/mol (△)[51]; Solid markers show UCEPs.

Table 4.1 Fixed parameters for the mixture considered

Component (i)	Cyclohexane (1)	Polystyrene (2)	Silica nanoparticles (3)
σ_i (Ångström)	3.165	4.1071	70
m_i	3.970	2 275.520	1
MW_i(g/mol)	84.162	237 000	248 754.810
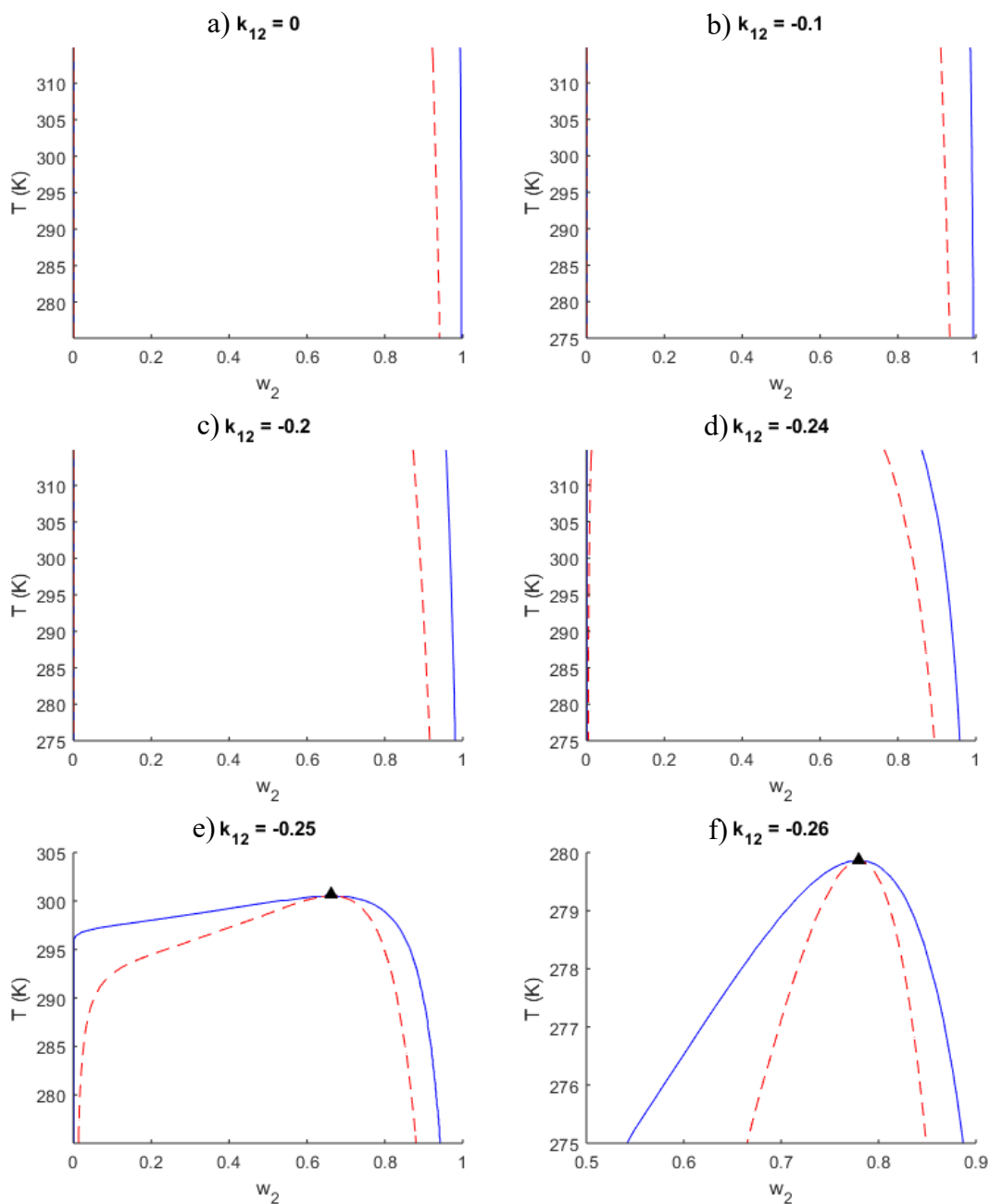
Figure 4.2 Temperature/composition phase diagram for polystyrene + cyclohexane binary mixtures with various values of k_{12}. The blue solid line is the binodal and the red dashed line is the spinodal. Solid triangles represent the UCEP. a) $k_{12} = 0$, b) $k_{12} = -0.1$, c) $k_{12} = -0.2$, d) $k_{12} = -0.24$, e) $k_{12} = -0.25$, f) $k_{12} = -0.26$.
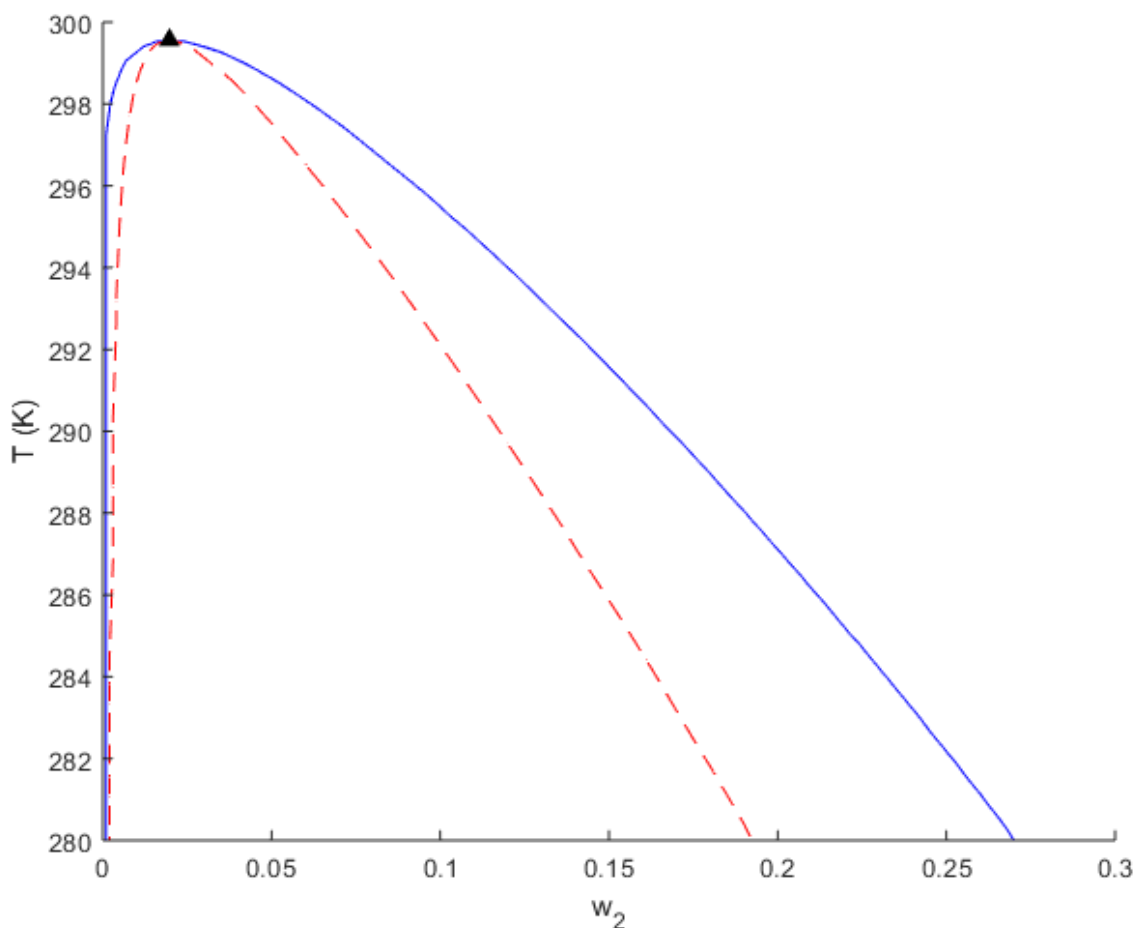
Figure 4.3 Temperature/composition phase diagram for polystyrene + cyclohexane binary mixtures with association sites and $k_{12} = 0$. The blue solid line is the binodal and the red dashed line is the spinodal. Solid triangles represent the UCEP.

4.3 Cyclohexane + Polystyrene + Silica Nanoparticles

Adding silica nanoparticles raises several issues. The only fixed parameters are the ones in Table 4.1. Kumar used 7 nm diameter, non-porous and amorphous nanoparticles[1]. It is assumed that these nanoparticles are perfectly spherical and monodispersed hard spheres here. The molar mass is calculated from the intrinsic density of silica (2.3 g/mL) and the diameter of the nanoparticles. Silica is well-known to be hygroscopic, so association sites can be used to model water particles at the surface of the nanoparticles, if desired. How nanoparticles interact with cyclohexane and polystyrene is not clearly defined. Polystyrene does not adsorb onto the surface of nanoparticles

34

so there cannot be any association interaction between polystyrene and nanoparticles. The only way interaction between the latter two components can be modeled is then through the dispersion term. This term can be varied but is constrained to be attractive within the model. Variation of this term has no qualitative effect as illustrated in Figure A3.4. For nanoparticles and cyclohexane, both dispersion attraction and association are possible.

Model Variant 1: No association sites on nanoparticles and $k_{ij} = 0$.

In a first set of calculations, no association sites are added to the nanoparticles and k_{ij} values are set to zero in the SAFT HS model. This calculation focuses on the role of density. One expects the silica particle packing fraction to be between 0.6 and 0.63[51]. This provides a first order estimate of the magnitude of the dispersion energy parameter ε_3. Before studying the influence of this parameter, another issue that arises for the ternary mixture must be considered. Even though only one part of the phase diagram is studied in this work, a global study of the phase diagram has to be done in order to be certain that additional multiphase regions are not missed. Then one can focus on the part of the phase diagram of interest. It is possible that the packing fraction exceeds the close-packing fraction for monodispersed spheres $\tau = \pi/(3\sqrt{2}) \approx 0.74$. This occurs if small diameter spheres occupy the free volume among closely packed large spheres. A larger upper limit for the packing fraction can then be approximated by considering the voids among close packed spheres of diameter σ_3. A fraction, τ, of the voids can be filled by spheres of radius $\sigma_2 \ll \sigma_3$, yielding a filled volume fraction of $\tau + (1 - \tau)\tau \approx 0.93$. This limit cannot be reached in this case, because the nanoparticles have a narrow size distribution, but clearly the limit τ is too restrictive. One can verify that, in this work, there is only one liquid compressibility root for packing fractions below this higher upper limit.

With this higher packing limit, ternary phase diagrams were generated over a broad range of values of ε_3. These phase diagrams are shown in Figure 4.4. (below the UCEP temperature) and in Figure 4.5 (above the UCEP temperature)[1]. The corresponding packing fraction of silica nanoparticles is also shown.

---

[1] For values of ε_3 of $k_B 15000$ J and higher, the subroutine "critical_point_ternary" is not able to provide a critical point accurately (the results do not pass the graphic test of section 3.4 as well). This comes from the way the derivative in equation (32) is calculated numerically. If this derivative

In these diagrams, only the silica nanoparticles dispersion energy parameter ε_3 is varied. Some ranges of ε_3 values generate phase diagrams similar to ones anticipated by Figures 2.1-2.3. Others generate phase diagrams that are inconsistent with known behaviors and which constrain the feasible range for this parameter. For example, ε_3 values less than or equal to $k_B 7000$ J lead to phase separation for cyclohexane + silica nanoparticle binary mixtures. For $k_B 7000$ J $< \varepsilon_3 <$ $\sim k_B 9000$ J, the two-phase region has two critical points below 280K. It is possible to increase the temperature for which the second critical point C2 appears by increasing the value of ε_3 which further constrains the minimum ε_3 value to $\sim k_B 9000$ J.

For values of ε_3 around $k_B 13000$ J there is no two-phase region for temperatures above the UCEP. For ε_3 values above $\sim k_B 15000$ J there are two critical points above the UCEP. However, for values of ε_3 from $\sim k_B 15000$ J (Figure 4.5) to $\sim k_B 18000$ J, there is a two-phase region above the UCEP temperature, but it quickly vanishes as temperature increases so this range of values of ε_3 is excluded. Consequently, the first range of ε_3 values which simulates an appropriate two-phase region above and below the UCEP (corresponding to the phase diagrams with $\varepsilon_3 = k_B 9000$ J and $k_B 10000$ J in Figures 4.4 and 4.5) is referred to as the low silica nanoparticle packing fraction range where the packing fraction of pure silica nanoparticles is roughly between 0.59 and 0.63 (corresponding to $\varepsilon_3 = k_B 12000$ J) at 280K. The other one (corresponding to the phase diagrams with $\varepsilon_3 = k_B 20000$ J and $k_B 30000$ J in Figures 4.4 and 4.5) is referred to as the high pure silica nanoparticle packing fraction range. In the latter range, an upper limit for ε_3 is set by the fact that the packing fraction of pure silica nanoparticles cannot exceed τ and thus the packing fraction is between ~ 0.67 and τ at 280K.

In the low silica nanoparticle packing fraction range, the critical point C1 is on the right side of the two-phase region and does not have the same relative location as experimental C1 critical points (Figure 2.2 and 2.3). Further, a critical point C2 appears below the UCEP temperature. This means that close to and below the UCEP temperature there is a three-phase region, which is not

---

is estimated too accurately, values for the objective function to be minimized it provides diverge. Otherwise, one must evaluate values of chemical potential for molar densities that return complex values. In these cases, critical points are shown with a white triangle and were found as the intersection points between the spinodal and the binodal.

observed experimentally. This is the case for the entire low silica nanoparticle packing fraction range (including $\varepsilon_3 = k_B 9000$ J and $k_B 10000$ J) but that three-phase region appears at lower temperatures for lower values of ε_3. For the high silica nanoparticle packing fraction range, the critical point C1 is also on the right side of the two-phase region but at a higher polymer mass fraction (this is especially visible at 305K in Figure 4.5). The critical point C2 appears exactly at the UCEP temperature and remains on the left side of the two-phase region. However, it is not present below the UCEP, an expected behavior from experiments. Quantitatively, the low silica nanoparticle packing fraction range gives better results than the higher packing fraction range with respect to the experimental phase diagram in Figure 2.2. Moreover, packing fractions of that range correspond better to what is expected for randomly packed spheres. Thus, the value $\varepsilon_3 = k_B 10$ 000 J is kept, corresponding to a silica nanoparticle packing fraction of ~ 0.6. With the latter value, the two-phases region exists on a broader range of temperatures above the UCEP temperature and the three-phase region appears only around 290K, which is convenient for this qualitative study. Values of all dispersion energies, when no association sites are present on the nanoparticles and when k_{ij} values are zero, are summarized in Table 4.2. This topic is explored in more detail in Appendix A3 where phase diagrams for $\varepsilon_3 = k_B 20\ 000$ J over a range of temperatures are presented. From a computational perspective, the choice of ε_3 parameter value is clear. Critical point C1 must exist above and below the UCEP temperature. Critical point C2 should arise close to the UCEP temperature. Irrespective of choice there is compromise with respect to behavior. In this case, the preferred choice of parameter indicates a three-phase region close to the UCEP. This is not an experimentally observed behavior but is feasible.
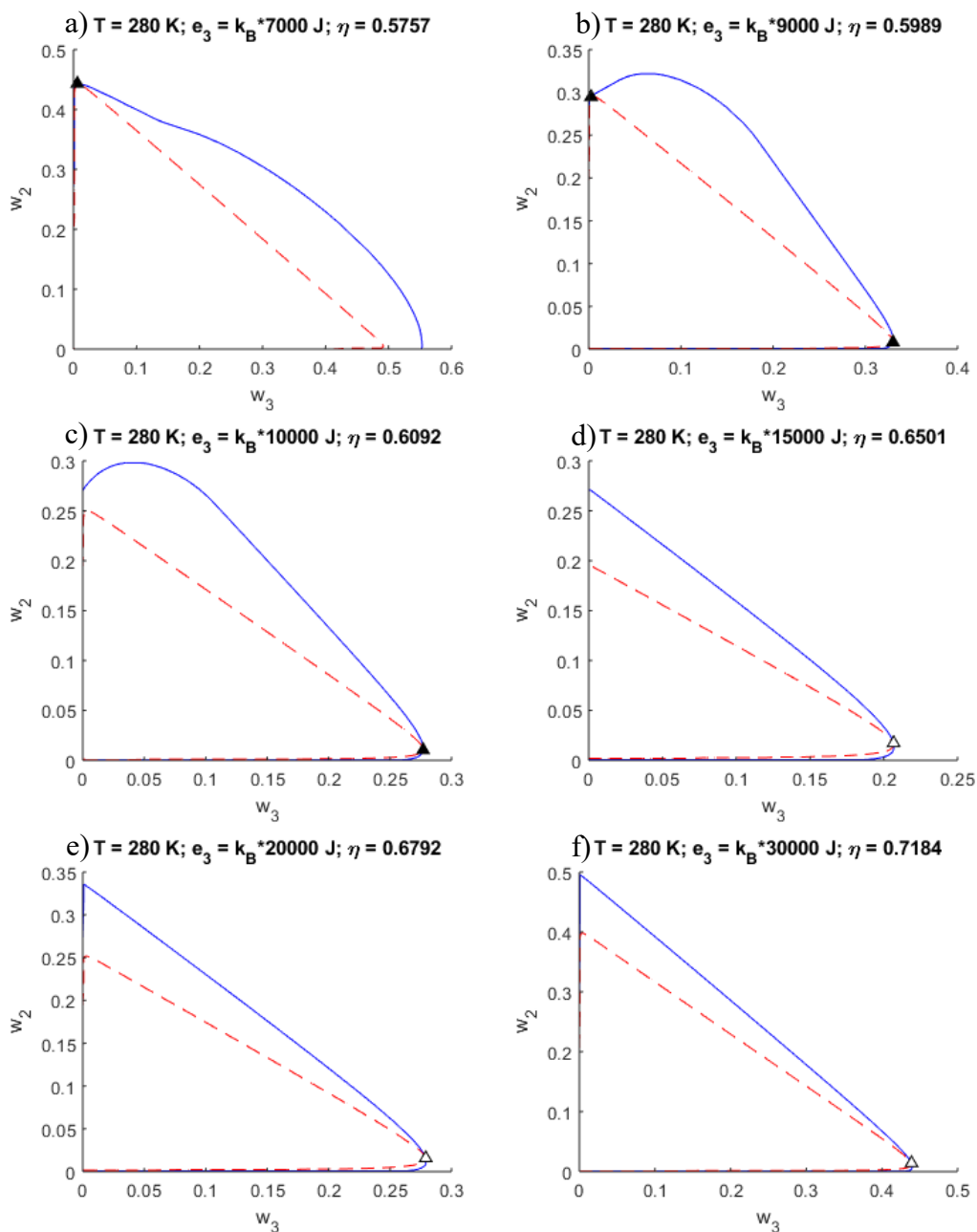
Figure 4.4 Ternary phase diagrams for cyclohexane + polystyrene + silica nanoparticles mixtures at 280K for different values of the nanoparticle dispersion energy. η designates the packing fraction of pure silica nanoparticles. The blue solid line is the binodal and the red dashed line is the spinodal. Solid triangles represent the critical points calculated with "critical_point_ ternary". Open triangles represent critical points for which the graphic test failed. a) $\varepsilon_3 = k_B 7000$ J, b) $\varepsilon_3 = k_B 9000$ J, c) $\varepsilon_3 = k_B 10000$ J, d) $\varepsilon_3 = k_B 15000$ J, e) $\varepsilon_3 = k_B 20000$ J, f) $\varepsilon_3 = k_B 30000$ J.
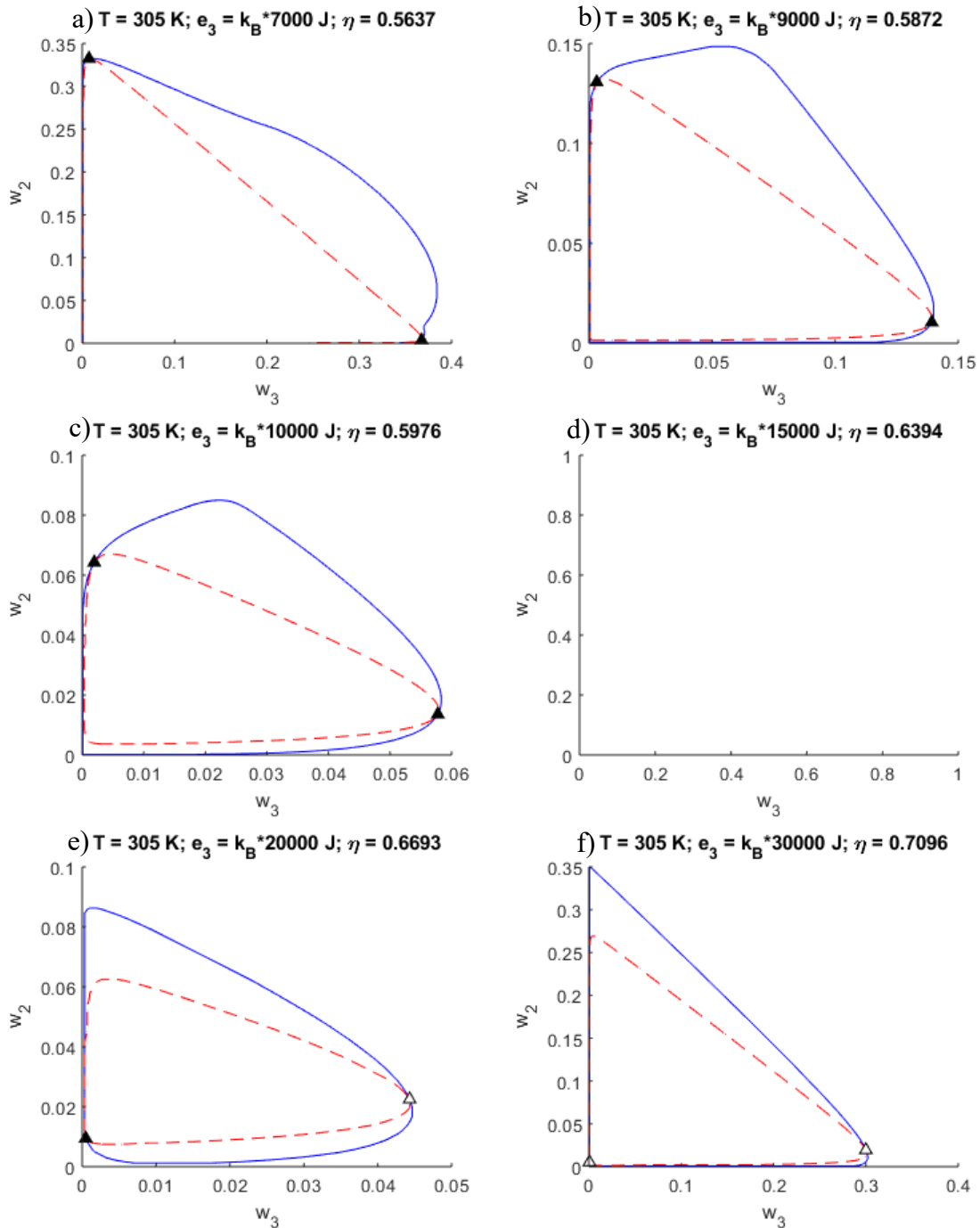
Figure 4.5 Ternary phase diagrams for cyclohexane + polystyrene + silica nanoparticles mixtures at 305K for different values of the nanoparticle dispersion energy. η designates the packing fraction of pure silica nanoparticles. The blue solid line is the binodal and the red dashed line is the spinodal. Solid triangles represent the critical points calculated with "critical_point_ternary". Open triangles represent critical points for which the graphic test failed. a) $\varepsilon_3 = k_B 7000$ J, b) $\varepsilon_3 = k_B 9000$ J, c) $\varepsilon_3 = k_B 10000$ J, d) $\varepsilon_3 = k_B 15000$ J, e) $\varepsilon_3 = k_B 20000$ J, f) $\varepsilon_3 = k_B 30000$ J.

Table 4.2 Dispersion energies parameters for no association sites on the nanoparticles and $k_{ij}=0$

Component (i)	Cyclohexane (1)	Polystyrene (2)	Silica nanoparticles (3)
ε_i/k_B (K)	3 100	970	10 000

Model Variant 2: Self Association of Silica nanoparticles.

From the first set of experiments, it is clear that the position of C1 on the two-phase to one-phase boundary could be improved. In this second set of calculations the question whether self-association of nanoparticles qualitatively changes phase diagrams or not is addressed. It is assumed that 2000 semi-spheres with a diameter of 2.75 Ångström are added on the surface of each nanoparticle. Using the "kappa" function as above, the $\kappa_{A_iB_j}$ parameter is estimated to be 3.70 10⁻⁶. These values do not qualitatively change the following reasoning. Without changing the dispersion energy (and it is not possible to keep a packing fraction around 0.6 for nanoparticles if the dispersion energy is reduced so that to provide a qualitative change in the phase diagram), the Helmholtz association energy must be small in order to maintain a packing fraction for silica nanoparticles of ~ 0.6. The smallest possible value for X_{A_i} is 0.9989 (which corresponds to ~ 2 bonded association sites on one nanoparticle, an association energy parameter $\varepsilon_{A_iB_j} = k_B$ 2.904 J and packing fraction for silica nanoparticles of 0.6229, which is in agreement with the random close packing fraction value). However, calculating the ternary diagram with this additional term does not lead to visible change in the placement of phase boundaries and critical points. For values of $\varepsilon_{A_iB_j}$ slightly greater (the standard double precision accuracy in MATLAB i.e. eps ≈ 2.22 10⁻¹⁶), the value of X_{A_i} drops to 0.7210 leading to a packing fraction of 0.9500 which is then greater than τ (this change appears to be discontinuous with the available precision). Thus, one can conclude that self-association of silica nanoparticles does not explain a significant fraction of the phase behavior of silica nanoparticle + cyclohexane +polystyrene mixtures, at least regarding association as it is modeled in SAFT.

Model Variant 3: Association between silica nanoparticles and cyclohexane.

Depletion interaction is a phenomenon that appears for nanoparticles in solution. Thus, it is reasonable to think that association between the solvent and nanoparticles could impact the phase diagrams. Association is only attractive and thus there cannot be any association between polymers and nanoparticles as polymers must not adsorb onto the surface of nanoparticles. In order to model association between the solvent and nanoparticles, the chosen value for $\kappa_{A_i B_j}$ between the two association sites of the solvent and association sites of nanoparticles is set at 3.70 10^{-6}. This value is four orders of magnitude smaller than the one between cyclohexane and polystyrene association sites, so it is reasonable to think that the overlapping volume between cyclohexane association sites and silica nanoparticles association sites is the volume of an association site on the nanoparticle (from geometrical reasons). Again, even if this value is not accurate, this is not an issue as it can be compensated by the value of $\varepsilon_{A_i B_j}$. What can be seen is that association in this case does not show a qualitative difference. The two-phases region does disappear at a lower temperature but the phase diagrams are qualitatively similar to the ones that are shown in Figure 4.5. For instance, at 307 K, a value for $\varepsilon_{A_i B_j}$ between cyclohexane and silica nanoparticles of k_B 20 J makes the entire two-phase region vanish. Smaller values such as k_B 5 J have the same effect but at higher temperature. Calculations with association for different values of the dispersion energy cannot have a qualitative impact on results either (in this case, the combination of two effects, dispersion and association, that do not have a qualitative impact on results separately, do not lead to a qualitative change). Thus, association between the solvent and nanoparticles does not impact the orientation of the tie lines and critical points.

Model Variant 4: non-zero k_{ij} values.

One could vary k_{ij} values, especially k_{23} between polystyrene and silica nanoparticles. Polystyrene should not adsorb onto the surface of nanoparticles. One way to reduce the attraction between these two components (inherent in the SAFT HS model) is to increase k_{23}. However, one sees the same outcome as for association between the solvent and nanoparticles. No qualitative difference is observed when either k_{12}, k_{13} and k_{23} are changed. Thus, non-zero k_{ij} values are also not warranted. Association parameters are summarized in Table 4.3.

Table 4.3 Association parameters for the cyclohexane + polystyrene + silica nanoparticles mixture

Components (i)	Cyclohexane (1)	Polystyrene (2)	Silica nanoparticles (3)
n_{A_i}	2	$2m_2$	0
$e_{A_1B_i}/k_B$(K)	0	500	0
$e_{A_2B_i}/k_B$(K)	500	230	0
$\kappa_{A_1B_i}$	0	0.0873	0
$\kappa_{A_2B_i}$	0	0.0873	0
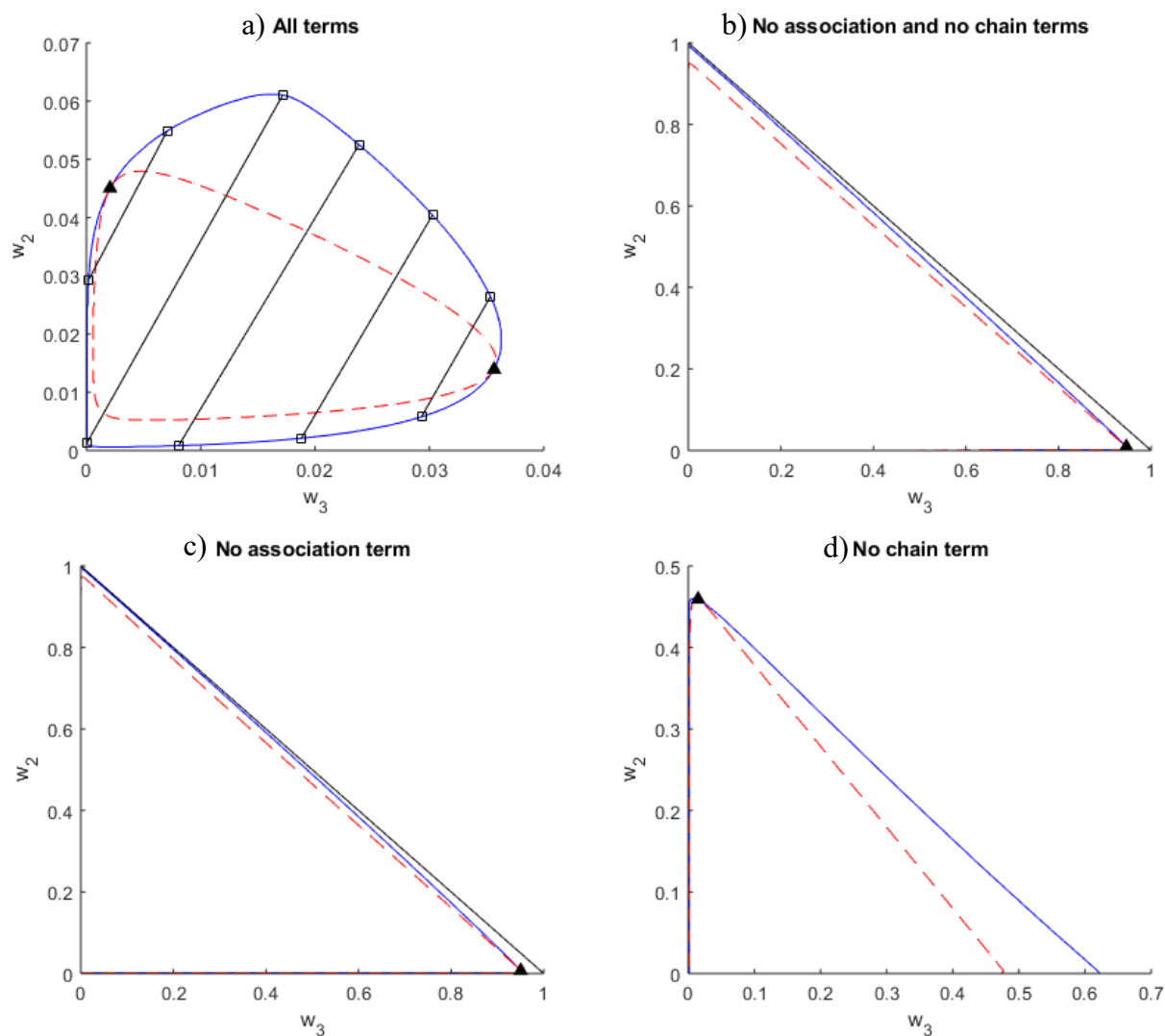
Figure 4.6 Ternary phase diagrams of cyclohexane + polystyrene + silica nanoparticles mixtures at 307K when different contributions in the equation of state (3.1) are accounted for. a) All the terms, b) All the terms except the association and chain terms, c) All the terms except the association term, d) All the terms except the chain term.

In Figure 4.6, phase diagrams obtained by neglecting the association term, the chain term and both of these terms are compared to the phase diagram obtained with all the terms present in equation (3.1) at 307 K. Dispersion energies were adjusted in each case to match the liquid densities of pure cyclohexane and polystyrene. One can see that association has a significant impact on the phase diagram. In cases where it is not present, the two-phase region expands significantly. The effect of

43

the chain term when association is not accounted for is very small. However, when only the chain term is omitted, the phase diagram is still qualitatively changed. Thus, association tends to form critical point C2 and thus horizontal tie lines. This is easily understandable because association between cyclohexane and polystyrene prevents a phase with a high polystyrene concentration separating from a phase with a high cyclohexane concentration. Regarding the chain formation term, it favors the formation of C1 and so near vertical tie lines. As one can expect, the chain formation term does not involve attraction between unlike components. Thus, the main repulsive effect is due to the size of nanoparticles. This explains the similarity between the no association and no chain term case with the no association only case. When both terms are accounted for, tie lines are more oblique. A better qualitative match with experiments would be obtained if tie lines were nearly horizontal. This suggests that modification of these terms or use of different SAFT models might be productive routes to explore in a subsequent study.

Figures 4.7 and 4.8 give phase diagrams obtained with the final parameters (Tables 4.1, 4.2, and 4.3) for temperatures below and above the UCEP. At low temperatures, the two-phase region is very close to the axes. Thus, for certain overall compositions, one of the phases has a very low polystyrene or silica nanoparticles mass fraction. This leads to numerical difficulties and the MATLAB function which finds tie lines does not converge or, if it does, very slowly. No appropriate scaling of the variables has been found in this work to calculate tie lines robustly. As an example for a failure of the code, two tie lines corresponding to two cases where the solver did not converge are included in Figure 4.7 (for 280 and 285K). At higher temperatures, the two-phase region moves away from the axis and it becomes easier to calculate tie lines. By contrast, critical points were calculated without difficulty.

At 280K and 285K, the two-phase region is similar to the low temperature case of Figure 2.2 except that critical point C1 is on the right of the two-phase region instead of being in the low silica nanoparticle mass fraction area. As temperature increases and gets closer to the UCEP temperature, the spinodal gets closer to the binodal at high polystyrene mass fraction and the two-phase region starts to move away from the polystyrene mass fraction axis. Thus, critical point C2 appears, between 285K and 290K. At 290K and 295K, as the two-phase region still touches the polystyrene mass fraction axis, a three-phase region must arise. In this case, Gibbs' phase rule implies that this three-phase region must be a triangle whose three vertices are located on the

binodal. One side of this triangle must be the part of the multiphase region that touches the polystyrene mass fraction axis. Thus, two vertices of this triangle are already known.
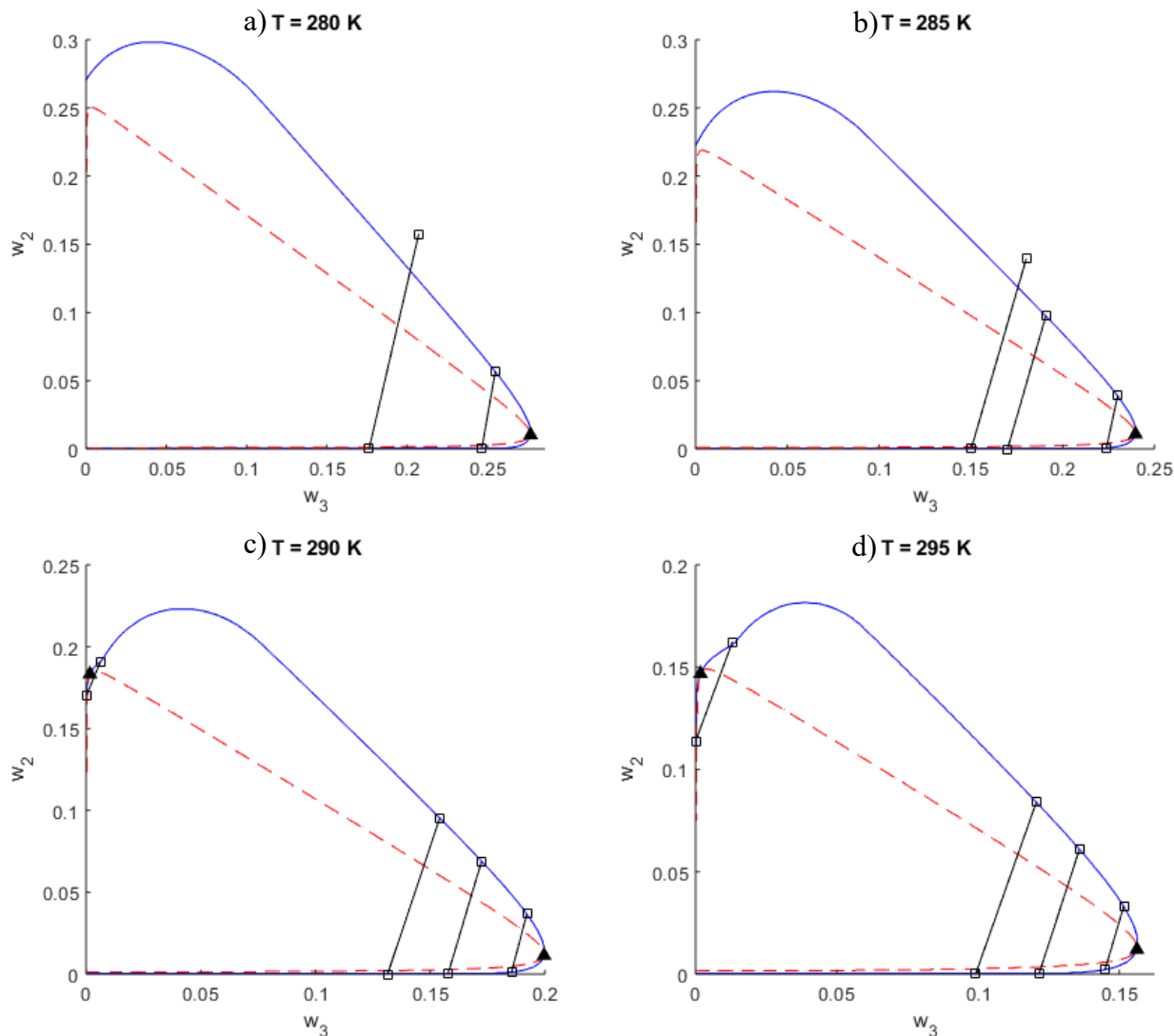
Figure 4.7 Ternary phase diagrams of cyclohexane + polystyrene + silica nanoparticles mixtures at different temperatures. The blue solid line is the binodal and the red dashed line is the spinodal. Solid triangles represent the critical points calculated with "critical_point_ternary". Open squares and lines joining them represent tie lines. a) T=280K, b) T=285K, c) T=290K, d) T=295K.
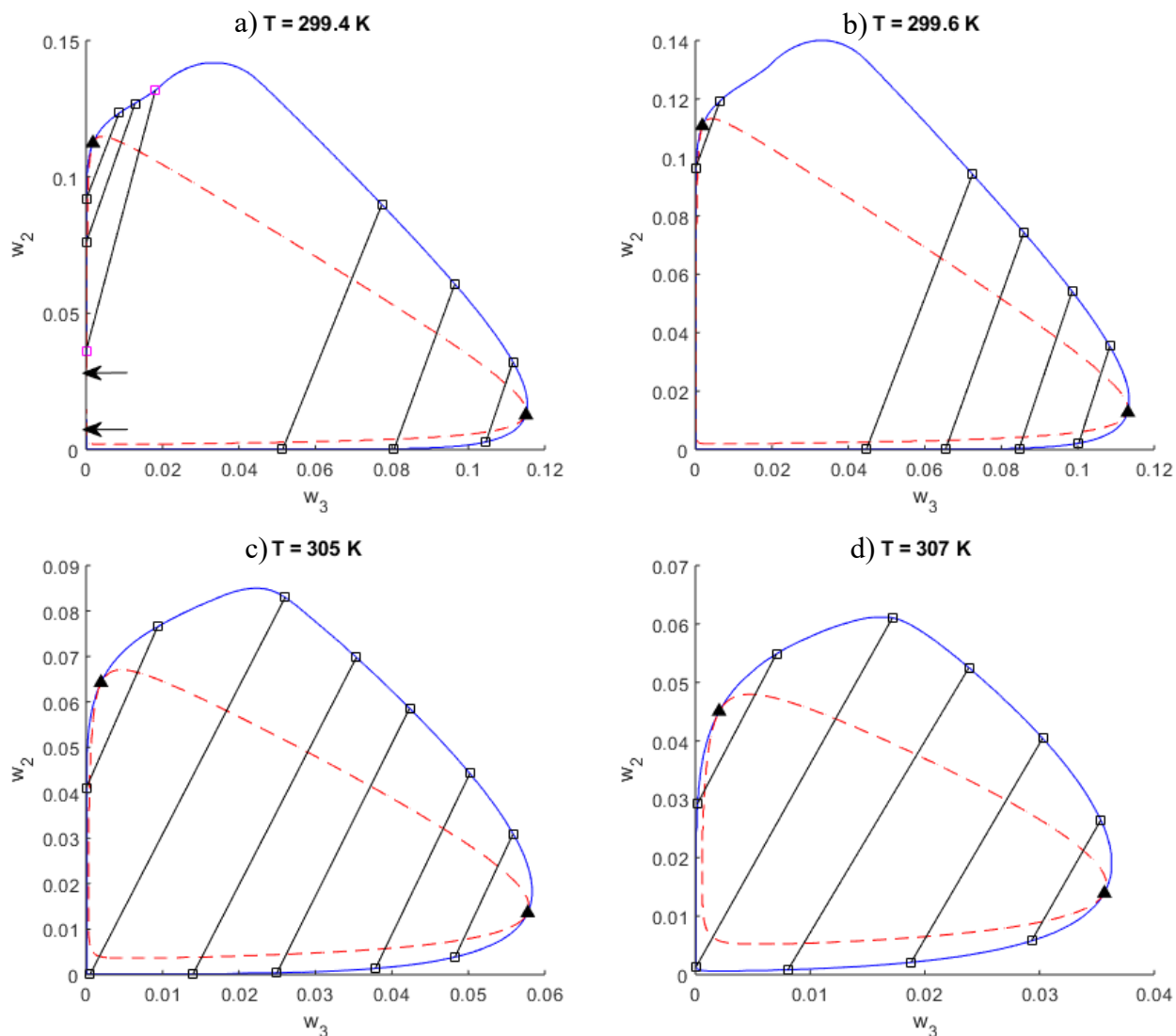
Figure 4.8 Ternary phase diagrams of cyclohexane + polystyrene + silica nanoparticles mixtures at different temperatures. The blue solid line is the binodal and the red dashed line is the spinodal. Solid triangles represent the critical points calculated with "critical_point_ternary". Open squares and lines joining them represent tie lines. Magenta squares are stationary points. a) T=299.4K, b) T=299.6K, c) T=305K, d) T=307K.

The computed multiphase behavior is composed of a triangular three-phase region, two two-phase ternary regions, as well as the solvent + polymer binary two-phase behaviour. In the two two-phase ternary regions and close to the three-phase region, tie lines must have different orientations. This results in a discontinuity of the slope of the binodal (although it is slight) around the third point

defining the three-phase region. This becomes more visible at higher temperatures as the appearance of C2 starts to open up the three-phase region. At 290K and 295K, tie lines close to the left of the three-phase region were calculated. Thus, they are almost where the three-phase region is situated (almost defining two of its vertices and the last one being around (0,0); see Figure 4.3 for a more accurate value of the two vertices situated on the polystyrene mass fraction axis).

Right below the UCEP temperature, at 299.4K, the two-phase region almost does not touch the polystyrene mass fraction axis anymore. Two arrows show contact points. The tie line with magenta squares has not been calculated by solving equilibrium equations but they are the minima of the tangent plane distance for some overall composition. Using the MATLAB code with these points does not work but it must be noted that stationary points (i.e. minima of the tangent plane distance) are usually close to the actual phase compositions. As temperature is increased further, the three-phase region tends toward a line because two of its points are merging. Exactly at the UCEP temperature, the three-phase region must be a tie line and thus the three-phase region ceases to exist. In addition, at this temperature and this temperature only, there should be three critical points. Above the UCEP temperature, there remains one two-phase region only with two critical points. At temperatures above the UCEP, the two critical points get closer until the two-phase region vanishes. In order to show how close the two phase region can be to axes, one provides the following compositions of one of the two phases at 299.4K ($w_2 = 1.52 \cdot 10^{-6}$, $w_3 = 0.0514$) and at 307K ($w_2 = 0.00132$, $w_3 = 5.75 \cdot 10^{-5}$).

The evolution of the multiphase region with temperature (from below to above the UCEP) is summarized in Figure 4.9 and comprises a major contribution of this work as it provides an alternate hypothesis for the origin and movement of critical point C2 in such phase diagrams. In the prior experimental work, C2 was hypothesized to emerge from the UCEP of the solvent + polymer binary. In this computational work, C2 and the UCEP are shown to coexist and to be separate phenomena. For example, critical point C2 is shown to move down and to the right (in phase diagrams with polymer composition (y-axis) and nanoprarticle composition (x-axis)) as temperature increases. At 290K, it is located at ($w_2 = 0.1833$, $w_3 = 0.0016$) and at 307K it is located at ($w_2 = 0.0451$, $w_3 = 0.0021$). This movement agrees with experiments, if the apparent upward motion, in the experiments, is due to the presence of a three-phase region just below the UCEP. Critical point C1 is not temperature independent according to calculations: at 280K, it is

located at ($w_2 = 0.0103$, $w_3 = 0.2769$) and at 307K it is located at ($w_2 = 0.0139$, $w_3 = 0.0357$). Below the UCEP temperature when there still is not critical point C2, the computed tie lines are nearly vertical remote from critical point C1 (i.e. close to the polymer mass fraction axis) and oblique near it. Experimental results show that tie lines trend to vertical near the polymer mass fraction axis, but they are horizontal near critical point C1. Above the UCEP temperature, the computed tie lines are oblique while they are horizontal in experimental results. If C2 is present and below the UCEP temperature, the three-phase region is thin and all the tie lines are oblique even though they have a slightly different orientation in the two different two-phase regions. The fact that the three-phase region is thin is of great importance. As one can see in Figure 4.9 b), it is possible to have tie lines nearly vertical close to the polymer mass fraction axis and still have a three-phase region with a critical point C2. As it is still possible for critical point C2 to move along the critical point locus of Figure 2.4 and have the apparent rapid motion of Figure 2.2 between the UCEP temperature (299K) and 303 K, it could also be possible that a three-phase region exists between 296K and the UCEP temperature. A three-phase region could also explain the drastic change of orientation of the tie lines of Figure 2.2 from nearly vertical below the UCEP temperature to nearly horizontal above the UCEP temperature.
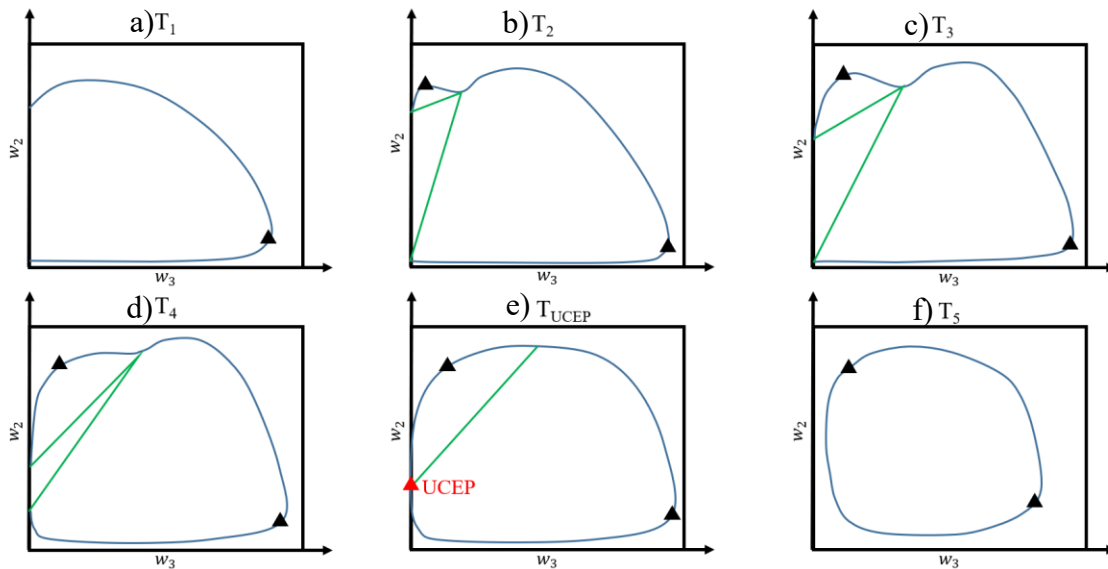
Figure 4.9 Sketches of the evolution of the phase diagrams with temperature. a) $T_1 <$ b) $T_2 <$ c) $T_3 <$ d) $T_4 <$ e) $T_{UCEP} <$ f) T_5. Blue lines represent the binodal, black triangles represent critical points and green triangles represent three-phase region.

Chapter 5: Conclusion and Future Work

5.1 Conclusions

The SAFT HS equation of state reproduces qualitatively some aspects of the phase behavior observed experimentally when physically meaningful parameters are employed. The temperature-composition phase diagram of cyclohexane + polystyrene presents the expected characteristics when the model includes association sites on the polymer with a predicted chain length and usual size parameters for cyclohexane and polystyrene, which is not achievable by adjusting k_{ij} values only. Association between cyclohexane and polystyrene permits the two-phase region of the ternary phase diagram to intersect the polymer mass fraction axis below the UCEP temperature. The entropic effect due to the size of silica nanoparticles and polystyrene chains, balanced by the cyclohexane/polystyrene interaction, qualitatively explains the shape of the binodal. However, it is not the only effect that is required to model the depletion interaction.

For temperatures low enough compared to the UCEP temperature, there is only one critical point C1. This critical point is not the expected depletion interaction critical point but the spinodal has a tendency to remain close to the binodal where the latter critical point is expected to be. For temperatures closer to the UCEP temperature, a second critical point C2 appears and thus a three-phase region. Above the UCEP temperature, the three-phase region vanishes which shows that in this case, critical point C2 does not move along a critical locus as indicated in Figure 2.4 but there would actually be two independent critical points (the UCEP and C2).

The following hypotheses may resolve the outstanding differences between the experiments and the SAFT HS model:

- This model does not include medium-range interactions, which is one of the main characteristics of nanoparticles as it can be seen from DLVO theory. Including this type of attraction in the model might be sufficient to explain the observed characteristics of this kind of phase diagram even if it would not be the only necessary effect. The "big atom" point of view would not be enough to understand the nanoparticles behavior because colloids show a specific kind of potential and surfaces energies that may explain how nanoparticles interact with the other species present. An association interaction between

49

the solvent and the nanoparticles does not change the computed results qualitatively. Overall, it seems that the potential energy of the nanoparticles is not well modeled. Ionic interactions could also be included as nanoparticles have a surface charge. However, it is theoretically difficult to include more interactions in the theory while still keeping a rigorous physical meaning. A perturbation theory is required for each new interaction.

- The behavior of cyclohexane + polystyrene is qualitatively reproduced but not quantitatively reproduced. It is possible that a quantitative reproduction of the phase behavior of this binary is sufficient to have critical point C1 located at a low silica nanoparticles mass fraction. For example, Wertheim's first order TPT does not include the formation of ring-like structures (e.g.: intramolecular interactions for the polymer), and the SAFT HS equation of state might not model the behavior of polymer molecules.

- Overall, it is very difficult to tell which interactions explain the phase behavior obtained experimentally. Using a more elaborated model such as PC SAFT[12] (with nanoparticles also modeled as chains) permits quantitative agreement (at low polystyrene and nanoparticle mass fraction) but fails to reproduce, even qualitatively, the remaining part of the phase diagram. However, it is still not clear what physics is happening at the molecular/nanoparticle scale. Adding more terms in the equation of state in order to include more interactions may be enough to model these types of system but one would want to make sure that the influence of all these interactions is properly taken into account (by the means of perturbation theories) and appropriate physics is modeled or simulated. So there is a real risk that models that are more sophisticated than SAFT HS but that require parameters fitted, for example, in the dispersion term, as is the case for SAFT HR and PC SAFT, that the quality of computed outcomes may be a consequence of fitting and not a consequence of the phenomena being modelled.

5.2 Future work

There are a number of short term and longer term works that follow naturally from this exploratory contribution.

1. One might enhance the efficiency and accuracy of the code for generating phase diagrams by translating it into another language. For example, MATLAB[14] minimization routines are not appropriate for these kinds of equations and do not provide robust results.

2. The polymer plays a major role in these phase diagrams. Thus, it is also recommended to modify the chain term according to equation (A.215) in Appendix A1, before changing the dispersion term. Equation (A.215) is very similar to equation (7) and so would not significantly impact computation time. The chain length values might differ and so they have to be fitted to experimental data directly.

3. Another SAFT equation of state with an improved dispersion term could be used. PC SAFT is appropriate as it has been widely used and tested. It also has a rigorous theoretical background. One may want to change the potential energy parameters (such as the square-well width) as the ones used for atoms might not be appropriate for nanoparticles, especially if the "big atom" point of view is not appropriate. An ionic interaction term could also be added to one of the SAFT equations of state, but as previously explained, this should be done with care.

4. Additional experiments are warranted to determine whether a three-phase region can be detected near the UCEP. These experiments would require tight temperature control to be meaningful and compositions close to the UCEP and C2 compositions would need to be explored in detail.

5. Wertheim's first order TPT does not allow the formation of ring-like structures, which are actually present within long polymer chains. It might be relevant to include more terms in the TPT so that attraction between association sites in the same molecule can be accounted for. This would significantly increase the complexity of the physics modeled and would increase the computation time dramatically.

Bibliography

1. Kumar, A. The Interaction between Depletion Flocculation and Molecular Liquid-Liquid Phase Separation Mechanisms, University of Alberta, 2018.

2. Kim, S.; Hyun, K.; Moon, J. Y.; Clasen, C.; Ahn, K. H. Depletion stabilization in nanoparticle-polymer suspensions: multi-length-scale analysis of microstructure. *Langmuir : the ACS journal of surfaces and colloids* **2015***, 31*, 1892.

3. Chowdhury, S. Phase Diagrams for Asphaltene and Asphaltene-Rich Hydrocarbons + Polystyrene + Toluene mixtures, University of Alberta, 2018.

4. Gast, A. P.; Hall, C. K.; Russel, W. B. Polymer-induced phase separations in nonaqueous colloidal suspensions. *Journal of Colloid And Interface Science* **1983***, 96*, 251-267.

5. Vincent, B.; Edwards, J.; Emmett, S.; Croot, R. Phase separation in dispersions of weakly-interacting particles in solutions of non-adsorbing polymer. *Colloids and Surfaces* **1988***, 31*, 267-298.

6. Lekkerkerker, H. N. W.; Poon, W. C. K.; Pusey, P. N.; Warren, P. B.; Stroobants, A. Phase Behaviour of Colloid + Polymer Mixtures. *Europhysics Letters* **1992***, 20*, 559.

7. Fleer, G. J.; Tuinier, R. Analytical phase diagrams for colloids and non-adsorbing polymer. *Advances in Colloid and Interface Science* **2008***, 143*, 1-47.

8. Chapman, W. G.; Gubbins, K. E.; Jackson, G.; Radosz, M. New reference equation of state for associating liquids. *Industrial & Engineering Chemistry Research* **1990***, 29*, 1709-1721.

9. ter Horst, M. H.; Behme, S.; Sadowski, G.; de Loos, T. W. The influence of supercritical gases on the phase behavior of polystyrene–cyclohexane and polyethylene–cyclohexane systems: experimental results and modeling with the SAFT-equation of state. *The Journal of Supercritical Fluids* **2002***, 23*, 181-194.

10. Garcia-Lisbona, M. N.; Galindo, A.; Jackson, G.; Burgess, A. N. An Examination of the Cloud Curves of Liquid-Liquid Immiscibility in Aqueous Solutions of Alkyl Polyoxyethylene Surfactants Using the SAFT-HS Approach with Transferable Parameters. *Journal of the American Chemical Society* **1998***, 120*, 4191.

11. Garcia-Lisbona, M. N.; Galindo, A.; Jackson, G. Predicting the high-pressure phase equilibria of binary aqueous solutions of 1-butanol, n- butoxyethanol and n-decylpentaoxyethylene ether (C10E5) using the SAFT-HS approach. *Molecular Physics* **1998***, 93*, 57.

12. AlHammadi, A. A.; Chapman, W. G. Modeling the Polystyrene−Asphaltenes−Toluene Mixture Using the Perturbed-Chain Form of Statistical Associating Fluid Theory Equation of State. *Energy & Fuels* **2017***, 31*, 6019.

13. Bymaster, A.; Jain, S.; Chapman, W. G. Microstructure and depletion forces in polymer-colloid mixtures from an interfacial statistical associating fluid theory. *The Journal of chemical physics* **2008***, 128*, 164910.

14. The MathWorks Inc. MATLAB. **2017***, Release 2017b*.

15. Asakura, S.; Oosawa, F. Surface Tension of High-Polymer Solutions. *The Journal of Chemical Physics* **1954***, 22*, 1255.

16. H. De Hek; A. Vrij Interactions in Mixtures of Colloidal Silica Spheres and Polystyrene Molecules in Cyclohexane. *Journal of Colloid and Interface Science* **1981***, 84*, 409-422.

17. Kumar, A.; Shaw, J. M. Combining Depletion Re-stabilization and Depletion Flocculation Effects in Phase Diagrams for NanoColloid + Polymer Mixtures. *(In preparation)* **2018**.

18. Sun, S.; Nishio, I.; Swislow, G.; Tanaka, T. The coil–globule transition: Radius of gyration of polystyrene in cyclohexane. *The Journal of Chemical Physics* **1980***, 73*, 5971.

19. Derjaguin, B.; Landau, L. Theory of the stability of strongly charged lyophobic sols and of the adhesion of strongly charged particles in solutions of electrolytes. *Acta Physiochim USSR* **1941***, 14*, 633-662.

20. Verwey, E. J.; Overbeek, J. T. G. Theory of the stability of lyophobic colloids. *The Journal of Physical Chemistry* **1947***, 51*, 631-636.

21. Poon, W. Colloids as Big Atoms. *Science* **2004***, 304*, 830-831.

22. Poon, W. Colloids as big atoms: the genesis of a paradigm. *Journal of Physics A: Mathematical and Theoretical* **2016***, 49*, 401001.

23. Zwanzig, R. W. High-Temperature Equation of State by a Perturbation Method. I. Nonpolar Gases. *The Journal of Chemical Physics* **1954***, 22*, 1420.

24. Zwanzig, R. W. Erratum : High-Temperature Equation of State by a Perturbation Method. I. Nonpolar Gases. *The Journal of Chemical Physics* **1954***, 22*, 2099.

25. Barker, J. A. Perturbation Theory and Equation of State for Fluids: The Square-Well Potential. *The Journal of Chemical Physics* **1967***, 47*, 2856.

26. Barker, J. A. Perturbation Theory and Equation of State for Fluids. II. A Successful Theory of Liquids. *The Journal of Chemical Physics* **1967***, 47*, 4714.

27. Wertheim, M. S. Fluids with Highly Directional Attractive Forces. I. Statistical Thermodynamics. *Journal of Statistical Physics* **1984***, 35*.

28. Wertheim, M. S. Fluids with highly directional attractive forces. II. Thermodynamic perturbation theory and integral equations. *Journal of Statistical Physics* **1984***, 35*, 35-47.

29. Wertheim, M. S. Fluids with Highly Directional Attractive Forces. III. Multiple Attraction Sites. *Journal of Statistical Physics* **1986***, 42*.

30. Wertheim, M. S. Fluids with highly directional attractive forces. IV. Equilibrium polymerization. *Journal of Statistical Physics* **1986***, 42*, 477-492.

31. Boublík, T. Hard Sphere Equation of State. *The Journal of Chemical Physics* **1970***, 53*, 471.

32. Mansoori, G. A.; Carnahan, N. F.; Starling, K. E.; Leland, T. W. Equilibrium Thermodynamic Properties of the Mixture of Hard Spheres. *The Journal of Chemical Physics* **1971***, 54*, 1523-1525.

33. Chapman, W. G.; Jackson, G.; Gubbins, K. E. Phase equilibria of associating fluids Spherical molecules with multiple bonding sites. *Molecular Physics* **1988***, 65*, 1-31.

34. Chapman, W. G.; Jackson, G.; Gubbins, K. E. Phase equilibria of associating fluids Chain molecules with multiple bonding sites. *Molecular Physics* **1988***, 65*, 1057-1079.

35. Galindo, A.; Davies, L. A.; Gil-Villegas, A.; Jackson, G. The thermodynamics of mixtures and the corresponding mixing rules in the SAFT-VR approach for potentials of variable range. *Molecular Physics* **1998***, 93*, 241.

36. Gross, J.; Sadowski, G. Application of perturbation theory to a hard-chain reference fluid: an equation of state for square-well chains. *Fluid Phase Equilibria* **2000***, 168*, 183-199.

37. Gross, J.; Sadowski, G. Perturbed-Chain SAFT: An Equation of State Based on a Perturbation Theory for Chain Molecules. *Industrial & Engineering Chemistry Research* **2001***, 40*, 1244-1260.

38. Huang, S. H.; Radosz, M. Equation of state for small, large, polydisperse, and associating molecules. *Industrial & Engineering Chemistry Research* **1990***, 29*, 2284-2294.

39. Huang, S. H.; Radosz, M. Equation of state for small, large, polydisperse, and associating molecules: extension to fluid mixtures. *Industrial & Engineering Chemistry Research* **1991***, 30*, 1994-2005.

40. Huang, S. H.; Radosz, M. Equation of state for small, large, polydisperse, and associating molecules. *Industrial & Engineering Chemistry Research* **1993***, 32*, 762.

41. Ioannis G. Economou Statistical Associating Fluid Theory: A Successful Model for the Calculation of Thermodynamic and Phase Equilibrium Properties of Complex Fluid Mixtures. **2002**.

42. Peters, C. J.; Goodwin, A. R. H.; Sengers, J. V. SAFT Associating Fluids and Fluid Mixtures. In *Applied Thermodynamics of Fluids*Royal Society of Chemistry: 2010; pp 1.

43. Green, D. G.; Jackson, G. Theory of Phase Equilibria for Model Aqueous Solutions of Chain Molecules: Water + Alkane Mixtures. *Journal of the Chemical Society, Faraday Transactions* **1992***, 88*, 1395.

44. Xu, G.; Brennecke, J. F.; Stadtherr, M. A. Reliable Computation of Phase Stability and Equilibrium from the SAFT Equation of State. *Industrial and Engineering Chemistry Research* **2001***, 41*, 938.

45. Octavio, L. M. Numerical Aspects of the SAFT Equation of State. **2006**.

46. Michelsen, M. L. The isothermal flash problem. Part I. Stability. *Fluid Phase Equilibria* **1982***, 9*, 1-19.

47. Quiñones-Cisneros, S. E. Critical Behavior in Fluid Systems, University of Minnesota, 1992.

48. Quiñones-Cisneros, S. E. Barotropic phenomena in complex phase behaviour. *Phys. Chem. Chem. Phys* **2004***, 6*, 2307-2313.

49. NIST Chemistry WebBook*;* NIST Standard Reference Database Number 69; Eds. P.J. Linstrom and W.G. Mallard: .

50. Gross, J.; Sadowski, G. Modeling Polymer Systems Using the Perturbed-Chain Statistical Associating Fluid Theory Equation of State. *Industrial & Engineering Chemistry Research* **2002***, 41*, 1084-1093.

51. Nakata, M.; Kuwahara, N.; Kaneko, M. Coexistence curve for polystyrene–cyclohexane near the critical point. *The Journal of Chemical Physics* **1974***, 62*, 4278.

52. Pubchem, 2004: Styrene *https://pubchem.ncbi.nlm.nih.gov/compound/styrene#section=Top* (Accessed July 25, 2018)

53. Shultz, A. R.; Flory, P. J. Phase Equilibria in Polymer—Solvent Systems1,2. *Journal of the American Chemical Society* **1952***, 74*, 4760.

54. Scott, G. D.; Kilgour, D. M. The density of random close packing of spheres. *Journal of Physics D: Applied Physics* **1969***, 2*, 863-866.

Appendices

A1: SAFT HS Equation of State Derivation

Contents

In this section, I derive the Statistical Associating Fluid Theory [1] (SAFT). The different concepts involved in this derivation may be interesting to people who want to use any SAFT equation of state. However they are not always easily accessible and they can be difficult to understand without a solid knowledge of statistical physics. The purpose of this section is to show where the SAFT HS equation of state comes from by condensing the main physical concepts in one document and by detailing the underlying mathematics. I reiterate the required ideas of Statistical Physics here but I advise reading any introduction to Statistical Physics beforehand to understand the underlying concepts. I suggest, for instance, reading *Statistical Mechanics* by Davidson [2] up to chapter 13 (chapter 8 to 12 may be skipped). Then I introduce graph theory as it is the main theory on which SAFT is based. Following this, I expose the main equations needed to get the hard sphere equation of state but I do not solve them as it is not my main focus here. From graph theory I then derive the Thermodynamic Perturbation Theory developed by Wertheim [3–6] which will directly lead to SAFT. Finally I give the derivatives of the Helmholtz energy formula needed in the model.

1   Statistical Physics

The objective of this derivation is to obtain an equation of state for mixtures. An equation of state is an equation that relates some thermodynamic variables of interest together. For example these variables can be temperature T, volume V, the total number of particles N and mole fractions x_i of each type of particles i. All these variables are related to a system that has to be defined. It is sometimes better to use pressure P rather than volume. In the frame of this derivation, two types of system will be studied and most of the time the system will contain only one type of particles. I will show in each case how the properties for mixtures can be obtained from the ones for a pure component.

The two main systems (with only one component) that are usually used are linked to one statistical ensemble each. The first one is called the canonical ensemble. It is used for systems with a fixed volume and a fixed number of particles but energy can cross the boundaries of the system. At equilibrium, the system has the same temperature T_s as the surrounding one (it is assumed that the surrounding is so big that its temperature remains constant). The mathematical tool used to describe this type of system is called the canonical partition function $\mathcal{Z}$ and can be written, in the semiclassical case and for a pure component, as:

$$\mathcal{Z} = \frac{1}{N!}\frac{1}{h^{3N}} \int e^{-\beta E(r_1,p_1,r_2,p_2,...,r_N,p_N)} \mathrm{d}^3r_1\mathrm{d}^3p_1\mathrm{d}^3r_2\mathrm{d}^3p_2 \cdots \mathrm{d}^3r_N\mathrm{d}^3p_N \qquad \text{(A.1)}$$

Where $\beta = 1/k_B T$, k_B is Boltzmann constant, h is Planck constant, r_i is the position vector of

particle i, p_i is the momentum of particle i and E is the energy which depends on the position vector and the momentum of each particle. The integration has to be done over all the possible position vectors and momenta of each particle (in the most general case over the whole phase space which can include other type of degrees of freedom). The canonical partition function is related to the Helmholtz energy A of the system by:

$$A = -k_B T \ln(\mathcal{Z}) \tag{A.2}$$

The second system is called the grand canonical ensemble. It is used for systems with a fixed volume but with energy and particles that can cross the boundaries of the system. At equilibrium, the system has the same temperature T_s and chemical potential μ_s as the surrounding (it is assumed that the surrounding is so big that its temperature and chemical potential remain constant). The mathematical tool used to describe this type of system is called the grand canonical partition function Ξ and can be written, in the semiclassical case and for pure component, as:

$$\Xi = \sum_{s \geq 0} z^s \mathcal{Z}_s \tag{A.3}$$

With the configuration integral $\mathcal{Z}_s$ given by:

$$\mathcal{Z}_s = \frac{1}{s!} \int e^{-\beta V(r_1, r_2, \ldots, r_s)} \mathrm{d}^3 r_1 \mathrm{d}^3 r_2 \ldots \mathrm{d}^3 r_s \tag{A.4}$$

And the fugacity z given by:

$$z = \frac{e^{\beta \mu}}{\lambda^3} \tag{A.5}$$

In equation (A.4), V is the potential energy and in equation (A.5), λ is the thermal de Broglie wavelength. Recall that:

$$\lambda = \frac{h}{\sqrt{2\pi m k_B T}} \tag{A.6}$$

With m the mass of one particle. In equation (A.3), the sum is over all the possible number of particles s in the system (which can vary in the grand canonical ensemble). The grand canonical partition function is related to the grand potential Ω of the system by:

$$\Omega = -k_B T \ln(\Xi) \tag{A.7}$$

It can be useful to rewrite this equation in the following manner, knowing that $\Omega = -PV$:

$$Z = \frac{PV}{k_B T} = \ln(\Xi) \tag{A.8}$$

With Z the compressibility factor. Davidson[2] details these concepts.

A first application of these results is the ideal gas law which is needed in any equation of state. In this framework, an ideal gas is represented by a potential energy function $V = 0$ which means that it is a set of non interacting indiscernible point particles (the indistinguishability actually comes from the presence of a $1/N!$ factor inside the canonical partition function or a $1/s!$ factor inside the grand canonical partition function; these factors must be removed if the particles are distinguishable). In the case of an ideal gas inside a closed box and surrounded by a medium of temperature T, E is reduced to kinetic energy only and equation (A.1) becomes:

$$\mathcal{Z} = \frac{1}{N!} \frac{1}{h^{3N}} \int \exp\left(-\beta \sum_{i=1}^{N} \frac{p_i^2}{2m}\right) \mathrm{d}^3 r_1 \mathrm{d}^3 p_1 \mathrm{d}^3 r_2 \mathrm{d}^3 p_2 \cdots \mathrm{d}^3 r_N \mathrm{d}^3 p_N \tag{A.9}$$

With the fundamental property of the exponential function and Fubini's theorem, it becomes:

$$\mathcal{Z} = \frac{1}{N!} \frac{1}{h^{3N}} \prod_{i=1}^{N} \left(\int_{-\infty}^{\infty} e^{\frac{-\beta p^2}{2m}} \mathrm{d}p\right)^3 \int_V \mathrm{d}^3 r_i \tag{A.10}$$

Where $p = p_x = p_y = p_z$ as no direction is favored in the absence of potential energy i.e. the phase space is isotropic. Using the well known result about Gaussian integrals $\int_{-\infty}^{\infty} \exp(-ax^2)\mathrm{d}x = \sqrt{\frac{\pi}{a}}$, equation (A.10) becomes:

$$\mathcal{Z} = \frac{V^N}{N!\lambda^{3N}} \tag{A.11}$$

Using Stirling's approximation and equation (A.2), the ideal gas Helmholtz energy A_{ig} can be found:

$$\frac{A_{\mathrm{ig}}}{Nk_B T} = \frac{a_{\mathrm{ig}}}{RT} = \ln(N_a \rho \lambda^3) - 1 \tag{A.12}$$

With ρ the molar density, R the ideal gas constant and N_a the Avogadro number. It is possible to get this result in the case of a mixture. In a general case, one can simply rewrite one of the partition functions in the case of mixtures. As noticed by Morita and Hiroike[7], the case of a mixture and of a pure component are mathematically similar. The two main differences are that there usually are interactions between different components (this is written inside the potential energy V) and the entropy of the system changes if different components are discernible (and this implies changes in the partition function). In the case of the grand canonical partition function, it can be written as[7]:

$$\Xi = \sum_{s_1, s_2, \ldots, s_\sigma} \frac{z_1^{s_1} z_2^{s_2} \cdots z_\sigma^{s_\sigma}}{s_1! s_2! \ldots s_\sigma!} \int e^{-\beta V_{s_1, s_2, \ldots, s_\sigma}(r_1, r_2, \ldots, r_s)} \mathrm{d}^3 r_1 \mathrm{d}^3 r_2 \ldots \mathrm{d}^3 r_s \tag{A.13}$$

Here the subscripts 1 to σ designate the σ different type of components. So z_i is the fugacity of component i, s_i is the number of particles i in the system and $V_{s_1, s_2, \ldots, s_\sigma}$ is the potential energy for a given set of particles. The fugacity z_i depends on the mass m_i and the chemical potential μ_i of

component i. The total number of particles s in the system is the sum of all the s_i. The different interactions between all kinds of particles must be taken into account inside $V_{s_1,s_2,...,s_\sigma}$ and the factor $\dfrac{1}{s_1!s_2!\ldots s_\sigma!}$ in front of the integral is there to take the entropy effect into account (related to the different possibilities of counting the indistinguishable particles). It is possible to rewrite equation (A.13) as:

$$\Xi = \sum_{s\geq 0} \mathcal{Z}'_s \tag{A.14}$$

Where $\mathcal{Z}'_s$ is a function of the different $V_{s_1,s_2,...,s_\sigma}$. The interesting result that Morita and Hiroike[7] show is that one can treat $\mathcal{Z}'_s$ in the same way that one would treat $z^s \mathcal{Z}_s$ in equation (A.3). Thus in sections 2 and 4, only the pure component system will be studied as was done in the literature[3–6,8]. Then in section 5, the potential energy for a mixture will be introduced and the results for mixtures will be directly obtained, as Chapman did[9]. It may be instructive to detail this calculation in the case of an ideal gas. In this case, it is easier to work with the canonical partition function. Some particles become discernible from each others if they are not related to the same component. Thus, if there are σ different components and if the total number of particles N is related to the number of particles $N_i, i \in [1\ldots\sigma]$ by $N = \sum_i N_i$, the number of permutations of particles becomes $N_1!N_2!\ldots N_\sigma!$ instead of $N!$. So equation (A.10) becomes:

$$\mathcal{Z} = \prod_{i=1}^{\sigma} \frac{1}{N_i!}\frac{1}{h^{3N_i}} \prod_{k=1}^{N_i} \left(\int_{-\infty}^{\infty} e^{\frac{-\beta p^2}{2m_i}}\, \mathrm{d}p \right)^3 \int_V \mathrm{d}^3 r_i = \prod_{i=1}^{\sigma} \frac{V^{N_i}}{N_i!\lambda_i^{3N_i}} \tag{A.15}$$

With equation (A.2) and a calculation similar to the one that leads to equation (A.12), the Helmholtz energy for an ideal gas mixture is:

$$\frac{A_{\mathrm{ig}}}{Nk_BT} = \frac{a_{\mathrm{ig}}}{RT} = \sum_{i=1}^{\sigma} x_i \left(\ln(N_a\rho x_i\lambda_i^3) - 1 \right) \tag{A.16}$$

With $x_i = \frac{N_i}{N}$ the mole fraction of component i.

2 Graph Theory

This section is mainly a detailed version of a work made by Stell[8] using ideas from Morita and Hiroike[7] and Zmpitas[10]. Morita and Hiroike[7] provide a very helpful and rigorous presentation of all the concepts introduced here. Zmpitas[10] gave a version of this theory (and of Wertheim's Thermodynamic Perturbation Theory) that is simpler to understand but which does not explain certain points. The purpose of this section is to rewrite equation (A.8) in a way that is easier to

manipulate and in particular as a function of density instead of fugacity (in the case of a system with only one component as explained before). The general idea is developed here and then used in section 4. The concepts introduced in this section are the ones that are used to derive the hard sphere equation of state. This section will show the main equation to solve for the latter purpose and the next presents the final solution (but skips the major part of the calculations as it is not the purpose of this derivation).

2.1 Mathematical needs

Before doing any calculation, one can introduce the following notation: all the coordinates related to a given particle i will be noted i. For instance, if a particle 1 has six degrees of freedom (three translational and three rotational) represented by three coordinates $r_1 = (x_1, y_1, z_1)$ and three angles $\omega_1 = (\theta_1, \phi_1, \psi_1)$ (in Euler's representation), a given differential form $d^3 r_1 d^3 \omega_1 = dx dy dz |r_1| \sin(\theta) d\theta d\phi d\psi$ will simply be written $d(1)$. In the same way, the potential energy depending on N particles will be written $V(1, 2, \ldots, N)$. With this notation, equation (A.3) becomes:

$$\Xi = \sum_{s \geq 0} \frac{z^s}{s!} \int e^{-\beta V(1,2,\ldots,s)} d(1) d(2) \ldots d(s) \tag{A.17}$$

The origin of any deviation to equation (A.16) is the existence of a potential energy that is not zero. In the most general case, each particle interacts with all the other particles and with any external force (even a force caused by the particle itself). Knowing that, it is assumed that the potential energy for a system with N particles can be written in the following way:

$$V(1, 2, \ldots, N) = \sum_{1 \leq i \leq N} \varphi_1(i) + \sum_{1 \leq i < j \leq N} \varphi_2(i, j) + \sum_{1 \leq i < j < k \leq N} \varphi_3(i, j, k) + \ldots \tag{A.18}$$

Where φ_1 describes potentials that depend on only one particle (i.e. due to external forces or a field created by the particle itself) and φ_n describes potentials that depend on n particles. In equation (A.18), potentials that depend on up to N particles are included. However what is usually assumed is that only φ_1 and the pair potential φ_2 contribute to V i.e. that the potential energy is pairwise additive. Sometimes φ_3 is included as well (see for example Rushbrook et al.[11]). In SAFT and in this graph theory, it is assumed that the potential energy is pairwise additive. Introducing $z_1(i) = z \exp(-\beta \varphi_1(i))$ and $e(i, j) = \exp(-\beta \varphi_2(i, j))$ for any given particle i and j, equation (A.17) becomes:

$$\Xi = \sum_{s \geq 0} \frac{1}{s!} \int \prod_{1 \leq i \leq s} z_1(i) \prod_{1 \leq i < j \leq s} e(i, j) \prod_{1 \leq i \leq s} d(i) \tag{A.19}$$

An important concept in graph theory is functional derivative. Let F be a function that takes other functions as argument i.e. a functional. For all functions of real variables f and h, the functional δF is defined such that:

$$\lim_{\|h\|\to 0} F[f+h] - F[f] - \delta F[h] = 0 \tag{A.20}$$

It is assumed here that all these functions are in the appropriate mathematical spaces, especially so that it is possible to define a norm $\| \cdot \|$. Riesz representation theorem says that there exists a function noted $\dfrac{\delta F}{\delta f}$ which is called the functional derivative of F and which verifies:

$$\delta F[h] = \int \frac{\delta F}{\delta f}(y) h(y) \mathrm{d}y \tag{A.21}$$

This derivation does not include all the mathematical details related to functional derivatives. It will be assumed that it mostly behaves like regular derivatives and equation (A.21) will be used in calculations.

The singlet density ρ_1 (also known as grand canonical 1-particle distribution function) is given by Zmpitas[10]:

$$\rho_1(1) = \left\langle \sum_i \delta(1,i) \right\rangle_\Xi \tag{A.22}$$

Where δ is the Dirac delta function defined here so that it verifies $\int \delta(i,j) f(j) d(j) = f(i)$ for all i and all function f. The bracket here means an average defined by the probability on the grand canonical ensemble. The singlet density is the probability of finding a particle at a given point of the phase space so the definition given by (A.22) makes it clearer than the definition given by Stell[8]. Equation (A.22) can be written by calculating the average:

$$\rho_1(1) = \frac{1}{\Xi} \sum_{s\geq 0} \frac{1}{s!} \int \left(\prod_{1\leq i\leq s} z_1(i) \prod_{1\leq i<j\leq s} e(i,j) \left(\sum_{i=1}^{s} \delta(1,i) \right) \prod_{1\leq i\leq s} \mathrm{d}(i) \right) \tag{A.23}$$

Note that the 1 in $\rho_1(1)$ is not the same as the one inside the integral (when the dummy variable $i = 1$) but we note them the same way for simplicity. Using the property of δ and remembering that particles are indiscernible (which means one can choose i to be 1 s times in $\sum_{i=1}^{s} \delta(1,i)$ with an appropriate change of dummy variables) it becomes:

$$\rho_1(1) = \frac{1}{\Xi} \sum_{s\geq 1} \frac{1}{(s-1)!} z_1(1) \int \left(\prod_{2\leq i\leq s} z_1(i) \prod_{1\leq i<j\leq s} e(i,j) \prod_{2\leq i\leq s} \mathrm{d}(i) \right) \tag{A.24}$$

The first term of the main sum vanishes as there is no integral. In order to simplify the previous equation, it is possible to calculate the functional derivative of Ξ with respect to z_1. Ξ is a sum of

many terms with the following form: $F = \int \prod_{1 \leq i \leq s} z_1(i) A \prod_{1 \leq i \leq s} \mathrm{d}(i)$ where A doesn't contain any z_1 function. With this functional, $\delta F[h] = \sum_{1 \leq j \leq s} \int h(j) \prod_{i \neq j} z_1(i) A \prod_{1 \leq i \leq s} \mathrm{d}(i)$ (only keep integrals with an integrand linear in h) so that $\frac{\delta F}{\delta z_1} = \sum_{1 \leq j \leq s} \int \prod_{i \neq j} z_1(i) A \prod_{i \neq j} \mathrm{d}(i)$. Knowing that particles are indistinguishable:

$$\frac{\delta \Xi}{\delta z_1}(1) = \sum_{s \geq 1} \frac{1}{(s-1)!} \int \left(\prod_{2 \leq i \leq s} z_1(i) \prod_{1 \leq i < j \leq s} e(i,j) \prod_{2 \leq i \leq s} \mathrm{d}(i) \right) \tag{A.25}$$

And so

$$\rho_1(1) = \frac{z_1(1)}{\Xi} \frac{\delta \Xi}{\delta z_1}(1) \tag{A.26}$$

The singlet density is related to the number density $\overline{\rho}$ if the system is uniform by:

$$\overline{\rho} = \rho_1 \Omega \tag{A.27}$$

Where Ω is the integration over all coordinates that are not position (for instance three angles of orientation). Indeed, in a uniform system $N = \int \rho_1(1) \mathrm{d}(1) = \rho_1 \int \mathrm{d}(1)$ (N being the average number of particles i.e. the number of particles that can be found in the whole phase space) and one can extract the volume from the last integral.

Likewise it is possible to define the grand canonical s-particle distribution function:

$$\rho_s(1, 2, \ldots, s) = \left\langle \sum_i \sum_{j \neq i} \sum_{k \neq i,j} \cdots \sum_{l \neq i,j,k,\ldots} \delta(1,i)\delta(2,j)\delta(3,k) \ldots \delta(s,l) \right\rangle_{\Xi} \tag{A.28}$$

As was done for the singlet density, the relation between ρ_s and Ξ is:

$$\rho_s(1, 2, \ldots, s) = \frac{1}{\Xi} \prod_{1 \leq i \leq s} z_1(i) \frac{\delta^s \Xi}{\delta z_1^s}(1, 2, \ldots, s) \tag{A.29}$$

In this derivation, only the case with $s = 2$ will be used. The results for $s > 2$ will always be given but not always derived as they are not useful here. Another kind of functions that are useful in graph theory are Ursell functions. Stell[8] gives them with the following definition: they are the functions $u_s(1, 2, \ldots, s)$ that verify:

$$\rho_s(1, 2, \ldots, s) = \sum_{P(1,2,\ldots,n)=\{\gamma\}} \prod_{\gamma=\{e_\alpha\}} u_\alpha(i_1, i_2, \ldots, i_\alpha) \tag{A.30}$$

Where the sum is carried out over all possible partitions γ of the set $\{1, 2, \ldots, n\}$. The product is then carried out over each element of γ noted e_α where α is the length of e_α (elements of e_α are noted i_β with β being a number between 1 and α). For instance $P(1,2) = \{(\{1\}, \{2\}), (\{1, 2\})\}$

and $P(1,2,3) = \{(\{1\},\{2\},\{3\}), (\{1,2\},\{3\}), (\{1,3\},\{2\}), (\{2,3\},\{1\}), (\{1,2,3\})\}$ and so:

$$
\begin{aligned}
\rho_1(1) &= u_1(1) \\
\rho_2(1,2) &= u_1(1)u_1(2) + u_2(1,2) \\
\rho_3(1,2,3) &= u_1(1)u_1(2)u_1(3) + u_2(1,2)u_1(3) \\
&\quad + u_2(1,3)u_1(2) + u_2(2,3)u_1(1) + u_3(1,2,3)
\end{aligned}
\tag{A.31}
$$

Ursell functions are given as functions of the grand canonical partition function with:

$$
u_s(1,2,\ldots,s) = \prod_{1 \le i \le s} z_1(i) \frac{\delta^s \ln(\Xi)}{\delta z_1^s}(1,2,\ldots,s)
\tag{A.32}
$$

With $\ln$ the natural logarithm defined for functionals by the Mercator series. It can be showed that it has the same properties as the real-valued function with respect to functional derivatives. Thus equation (A.32) is obviously true for $s = 1$ and it can be easily shown that it is true as well for $s = 2$ by direct calculation. The general case can be proved by induction. The functions g_s and h_s with $s \ge 2$ are defined by the following equations:

$$
g_s(1,2,\ldots,s) = \frac{\rho_s(1,2,\ldots,s)}{\rho_1(1)\rho_1(2)\ldots\rho_1(s)}
\tag{A.33}
$$

$$
h_s(1,2,\ldots,s) = \frac{u_s(1,2,\ldots,s)}{\rho_1(1)\rho_1(2)\ldots\rho_1(s)}
\tag{A.34}
$$

For $s = 1$, h_1 can be defined:

$$
h_1(1) = \ln\left(\frac{u_1(1)}{z_1(1)}\right) = \ln\left(\frac{\rho_1(1)}{z_1(1)}\right)
\tag{A.35}
$$

For the special case where $s = 2$:

$$
g_2(1,2) = \frac{u_1(1)u_1(2) + u_2(1,2)}{\rho_1(1)\rho_1(2)} = h_2(1,2) + 1
\tag{A.36}
$$

In a system of coordinates where the origin is particle 1 and if $(1,2)$ only represents translation degrees of freedom, $(1,2) = |r_1 - r_2|$ and g_2 (or simply written g) is called the radial distribution function which is related to the probability of finding a second particle at a distance $|r_1 - r_2|$ from particle 1. h_2 is called the two particle correlation function.

One need to introduce the Ornstein-Zernike direct correlation function for the next section (Hard Sphere Equation of State). It is the function $c(1,2)$ that verifies the Ornstein-Zernike equation:

$$
h_2(1,2) = c(1,2) + \int c(1,3)h_2(3,2)\rho_1(3)\mathrm{d}(3)
\tag{A.37}
$$

It can be shown that this is equivalent to:

$$
c(1,2) = \frac{\delta}{\delta\rho_1(2)}\left[\ln\left(\frac{\delta\ln(\Xi)}{\delta z_1(1)}\right)\right]
\tag{A.38}
$$

2.2   Graphs

The definition and vocabulary given by Stell[8] will be used:

Definition 1. A **linear graph** is a collection of circles between some pairs of which there are bonds.

An example of such a graph is given on Figure A1.1.
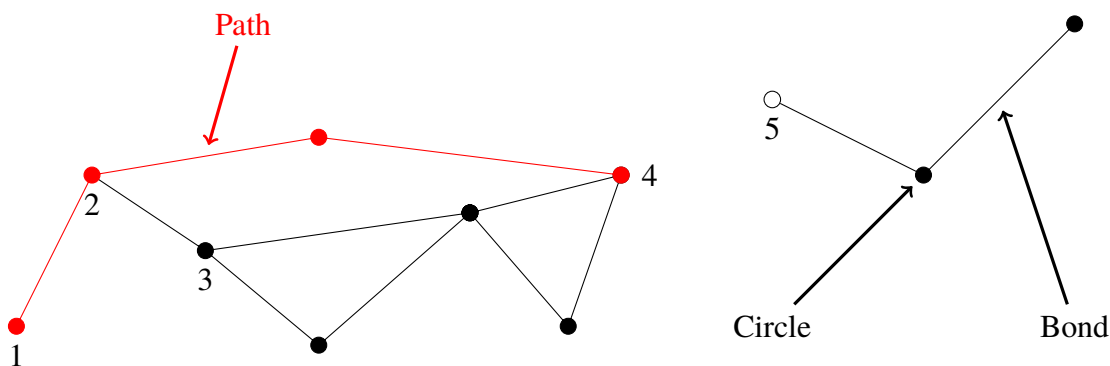
Figure A1.1: Example of one graph.

Definition 2. Two circles are said to be **adjacent** if there is one bond joining them directly.

For instance circles 1 and 2 on Figure A1.1 are adjacent but not circles 1 and 3.

Definition 3. A **path** is a sequence of adjacent circles joined by bonds.

The red part of the graph in Figure A1.1 is a path.

Definition 4. Two paths between two circles are **independent** if they have no intermediate circles in common.

For instance there are two independent paths between circles 2 and 4 but there is just one between circles 3 and 4. Two kind of circles will be considered: black and white (such as circle 5 on Figure A1.1). A meaning will be given to each kind of circle later. It is also possible to define different types of bond.

Definition 5. A graph is **connected** if there exists a path between any pair of circles in the graph.

Thus the graph in Figure A1.1 is not connected.

Definition 6. A graph is said to be **at-least-n-tuply-connected** if there are at least n independent paths between any pair of circles in the graph.

Definition 7. A graph is said to be **root-connected** if there is a path from each black circle to a white circle.

Definition 8. A **subgraph** is a part of a graph i.e. any collection of circles and bonds of a graph.

Definition 9. A **maximal** subgraph possessing a given property is a subgraph which is not contained in another subgraph with the same property. Likewise, a **minimal** subgraph possessing a given property is a subgraph that contains no other subgraph with the same property.

Definition 10. A **component** is a maximal connected subgraph.

For instance the graph in Figure A1.1 has two components.

Definition 11. A **simple** graph is a graph such that between any pair of adjacent circles there is only one path which is a single bond.

For instance the graph in Figure A1.1 is simple but not the graph in Figure A1.2. A graph that is not simple is called **composite**.
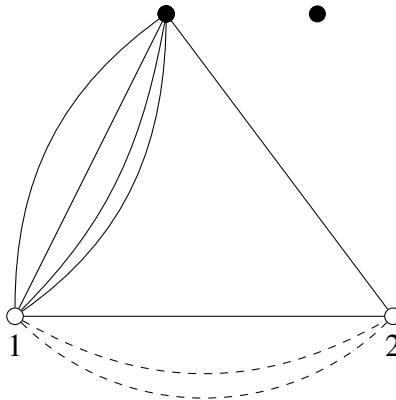
Figure A1.2: Example of a composite graph.

The purpose of these graphs is to simplify integrals that can appear in equation (A.19) and also to represent with one single graph different integrals that could be equal. Indeed, the idea is to attach a function to each part of a graph. A circle will always represent a particle and a bond will always represent an interaction between two particles. These interactions will come from the potential energy. Thus, if a triplet potential was kept in equation (A.18), a graph with surfaces joining three circles should be added to the graphs. In the case of this derivation, typical integrals that will appear will have the following form:

$$\int \left[\prod_S \prod_{a \in A} B_a(i,j) \right] \left[\prod_{1 \leq i \leq n} \gamma_1(i) \right] \left[\prod_{n+1 \leq i \leq N} \gamma_2(i) \mathrm{d}(i) \right]$$

Where S is a subset of all the pairs $\{i, j\}, 1 \leq i < j \leq N$, A is the set of different type of bond (that will be introduced later), B_a is a function that verifies $B_a(i, j) = B_a(j, i)$, γ_1 and γ_2 are two functions. Functions B_a will be represented by a bond, γ_1 will be represented by a white circle with a label i (note that there is no integration for all i between 1 and n) and γ_2 will be represented by a black circle (with no label as this function is integrated and so it does not depend on any coordinate). Note that the graph in Figure A1.2 is not the representation of any integral with the previous form as it is not a simple graph. Otherwise terms with a factor $B_a(i, j)^{m_a(i,j)}$ should be included with $m_a(i, j)$ the number of bonds B_a between i and j.

Thus in equation (A.19), the term $\int z_1(1)z_1(2)z_1(3)e(1, 2)e(1, 3)e(2, 3)\mathrm{d}(1)\mathrm{d}(2)\mathrm{d}(3)$ is represented by the graph . In some cases (but not in equation (A.19)), several identical integrals can appear in an equation as integrals can be invariant by permutations of the variable names. For instance the previous integral does not change after the following permutations:

$$1 \rightarrow 2; 2 \rightarrow 3; 3 \rightarrow 1$$

$$1 \rightarrow 3; 2 \rightarrow 1; 3 \rightarrow 2$$

$$1 \rightarrow 1; 2 \rightarrow 2; 3 \rightarrow 3$$

$$1 \rightarrow 3; 2 \rightarrow 2; 3 \rightarrow 1$$

$$1 \rightarrow 1; 2 \rightarrow 3; 3 \rightarrow 2$$

$$1 \rightarrow 2; 2 \rightarrow 1; 3 \rightarrow 3$$

Which are the $3!$ permutations between three objects. So graphs defined as above have the same invariance to permutations as integrals. In order to simplify the manipulations of these graphs, the symmetry number of a graph can be introduced.

Definition 12. If temporary labels are given to black circles, the **symmetry number** of a graph is the number of permutations that can be done to the latter labels so that it does not change the original integral.

A given integral I is related to its graph Γ and symmetry number σ by the following formula:

$$I = \sigma\Gamma \tag{A.39}$$

One can also speak of the symmetry number of an integral (as the symmetry number of the graph representing the integral) but integrals and graphs are always related by the previous equation. Thus

one integral will represent all the different possible graphs that are equal by permutations of labels on black circles. For example:

$$\int z_1(1)z_1(2)z_1(3)e(1,2)e(1,3)e(2,3)\mathrm{d}(1)\mathrm{d}(2)\mathrm{d}(3) = 6 \times \triangle \tag{A.40}$$

$$\int z_1(1)z_1(2)z_1(3)z_1(4)e(1,2)e(2,3)e(3,4)e(4,1)\mathrm{d}(1)\mathrm{d}(2)\mathrm{d}(3)\mathrm{d}(4) = 8 \times \square \tag{A.41}$$

$$\int z_1(1)z_1(2)z_1(3)z_1(4)e(1,3)e(3,2)e(2,4)e(4,1)f(3,4)\mathrm{d}(3)\mathrm{d}(4) = 2 \times \quad 1 \diamondsuit 2 \tag{A.42}$$

Equation (A.40) corresponds to the term that was previously mentioned. The integrated functions z_1 are represented by black circles and the functions e by straight lines. The symmetry number is 3! as each circle is connected to all the other ones. The general result is that the symmetry number of a graph with N identical circles that are all connected between each other is $N!$. In equation (A.41), there is no connection between 2 and 4 and between 1 and 3. Thus when repositioning temporary labels, 1 is always between 4 and 2, 2 is always between 1 and 3,etc. 8 permutations similar to the ones for equation (A.40) can be found (4 "clockwise" and 4 "counterclockwise" circular permutations). In equation (A.42), non integrated z_1 functions are represented by white circles and the function f is represented by a zigzag line. There are only two ways to add labels to black circles, so the symmetry number is 2. If two graphs do not represent the same graph, they are called distinct. As integrals, graphs are functionals (of the functions defining bonds and circles).

With this definition, it will be possible to write equations with graphs only and no prefactors. It is also possible to have a definition different than (39) and keep prefactors as is done by Zmpitas[10] and Wertheim[3].

Finally it is possible to define the product of graphs that have some or no 1-white circles (white circles that represent non integrated functions $x \longmapsto 1$). Let Γ_1 and Γ_2 be two graphs with respectively n_1 and n_2 white 1-circles such that:

$$\Gamma_1 = \frac{I_1}{\sigma_1} = \frac{1}{\sigma_1}\int \left[\prod_{S_1}\prod_{a \in A_1} B_a(i,j)\right]\left[\prod_{1 \le i \le n_1}\gamma_1(i)\right]\left[\prod_{n_1+1 \le i \le N_1}\gamma_2(i)\mathrm{d}(i)\right]$$

$$\Gamma_2 = \frac{I_2}{\sigma_2} = \frac{1}{\sigma_2}\int \left[\prod_{S_2}\prod_{a \in A_2} B_a(i,j)\right]\left[\prod_{1 \le i \le n_2}\gamma_1(i)\right]\left[\prod_{n_2+1 \le i \le N_2}\gamma_2(i)\mathrm{d}(i)\right]$$

The product of graph $\Gamma_1 \times \Gamma_2$ is the collection of all black circles and bonds in Γ_1 and Γ_2 such that the white 1-circles with same labels are in common. It thus represents the integral $I_1 \times I_2$ (with the usual product). Its symmetry number σ_3 defined as before will usually be different from $\sigma_1 \times \sigma_2$. For example the product of the graphs in equation (A.40) and (A.41) is given in Figure
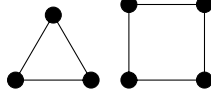
Figure A1.3: Product of graphs from equations (A.40) and (A.41).
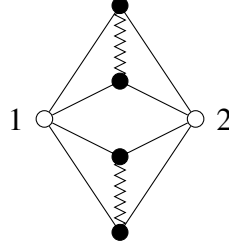
Figure A1.4: Product of two graphs.

A1.3 and the product of the graph in equation (A.42) by itself is in Figure A1.4. The symmetry number of the graph in Figure A1.3 is, in this case, the product of the symmetry numbers of each graph so $6 \times 8 = 48$. For the graph in Figure A1.4, both original graphs are identical so it is possible to exchange the labels between each subgraph without changing the integral it represents. The symmetry number of each subgraph is 2 so the symmetry number of the graph in Figure A1.4 is (number of permutations between identical graphs) $\times$ (product of the symmetry numbers of the original graphs) $= 2 \times 2^2 = 8$.

It is now possible to derive two lemmas that will be used further in order to express equations (A.8), (A.29), (A.32) and (A.34) (and so (A.36)) in terms of graphs.

Lemma 1: Let G be a set of an infinite number of distinct connected graphs Γ_i, each consisting of some or no black circles, some or no white 1-circles and some or no bonds such that no Γ_i is the product of other graphs in G. Let F be the set of all graphs in G and all products of graphs in G. Then, the sum of all graphs in F $=$ exp(the sum of all graphs in G)-1.

Proof. Any graph in F noted Γ_F can be written $\prod_{i=1}^{n} \Gamma_i^{p_i}$ by definition of F, with n different graphs Γ_i from G. p_i is the number of identical Γ_i in Γ_F. As in all the later other proofs regarding graph properties, the most difficult part is to find the symmetry number of new created graphs i.e. here Γ_F, knowing that the symmetry number of Γ_i is σ_i. Each factor $\Gamma_i^{p_i}$ as an independent set of labels as $\Gamma_i \neq \Gamma_j$ if $i \neq j$. Indeed if two graphs are different, they do not have the same set of bonds and/or the same number of circles (see for instance the case of the graph in Figure A1.3) so labels of a graph cannot be exchanged with a different graph. Another way to see that is to understand that two circles can exchange their labels if they are indistinguishable and two circles from two different graphs are distinguishable exactly because they are in two different graphs. So the number of permutations of labels in Γ_F are the combinations of all the permutations allowed in each factor $\Gamma_i^{p_i}$ and the

69

symmetry number of Γ_F is the product of the symmetry numbers of all the $\Gamma_i^{p_i}$. Conversely, in a factor $\Gamma_i^{p_i}$ it is possible to exchange labels between the p_i graphs Γ_i as they are all the same. However when exchanging labels, all the labels from one Γ_i have to be exchanged with all the labels from another Γ_i. For instance with the graph in Figure A1.4, if black circles are labeled 1,2,3 and 4 with a zigzag bond between 1 and 2 and between 3 and 4, it is not possible to exchange labels 2 and 3 as it would change the zigzag bonds (which would be between 1 and 3 and between 2 and 4). So the permutation of labels allowed between all the Γ_i are the permutations of the entire set of labels of each Γ_i. There are $p_i!$ such permutations as all Γ_i are indistinguishable. Once one of the $p_i!$ permutations is chosen, it is then possible to exchange labels inside each Γ_i. By definition, the number of such permutations is σ_i and the combinations of all permutations in $\Gamma_i^{p_i}$ is $\sigma_i^{p_i}$ once one of the $p_i!$ previous permutations is chosen. So overall the symmetry number of $\Gamma_i^{p_i}$ is $p_i!\sigma_i^{p_i}$ and the permutation number σ_F of Γ_F is:

$$\sigma_F = \prod_{i=1}^{n} p_i!\sigma_i^{p_i}$$

The integral represented by Γ_F is $\prod_{i=1}^{n} I_i^{p_i}$ if I_i is the integral represented by Γ_i. So:

$$\Gamma_F = \frac{\prod_{i=1}^{n} I_i^{p_i}}{\sigma_F} = \frac{\prod_{i=1}^{n} \left(\frac{I_i}{\sigma_i}\right)^{p_i}}{\prod_{i=1}^{n} p_i!}$$

Using $\exp$ as its Taylor series, the right hand side of the equation to be proved can be written:

$$\exp\left(\sum_i \Gamma_i\right) - 1 = \sum_{k=1}^{\infty}\left(\frac{\left(\sum_i \Gamma_i\right)^k}{k!}\right)$$

Where the sum over index i represents the sum carried out over all the infinite (but countable) number of graphs in G. Using the multinomial theorem, it becomes:

$$\exp\left(\sum_i \Gamma_i\right) - 1 = \sum_{k=1}^{\infty}\left(\frac{1}{k!}\sum_{p_1+p_2+...+p_i+...=k}\left(\frac{k!}{\prod_i p_i!}\prod_i \Gamma_i^{p_i}\right)\right)$$

The second sum in the right hand side means that the sum must be carried out over all the infinite numbers of p_i (some can be zero) as there are an infinite number of graphs Γ_i in $\sum_i \Gamma_i$. Similarly $\prod_i p_i!$ and $\prod_i \Gamma_i^{p_i}$ are products over all the p_i defined by the previous sum. Finally:

$$\exp\left(\sum_i \Gamma_i\right) - 1 = \sum_{k=1}^{\infty}\sum_{p_1+p_2+...+p_i+...=k}\frac{\prod_i \left(\frac{I_i}{\sigma_i}\right)^{p_i}}{\prod_i p_i!} \qquad (\star)$$

It is now easy to see that the right hand side of $(\star)$ is the sum of all the graphs in F. In order to prove that, it is required to prove that each term in the right hand side of $(\star)$ is a graph from F (which is obvious with the previously given form of a graph in F) and that each graph in F is in the right

hand side ($\star$). A graph Γ_F in F is characterized by some p_i and some Γ_i. All combinations of p_i are allowed by the right hand side of ($\star$) (some have to be zero if a given Γ_i is not in Γ_F). So each graph in F is in the right hand side of ($\star$) which proves lemma 1. $\qquad\square$

Lemma 2: Let Γ be a graph with some bonds, some black γ_2-circles and some white circles and let n be any natural number other than 0. Then

$$\frac{\delta^n \Gamma}{\delta \gamma_2^n}(1, 2, \ldots, n) \quad = \text{the sum of all the distinct graphs that are obtained from } \Gamma \text{ by changing}$$

$$n \text{ black } \gamma_2\text{-circles into } n \text{ white 1-circles labeled by } 1, 2, \ldots, n \text{ respectively}$$

Proof. The case for $n = 1$ must be proved first. Then the case for any n is evident by induction. A graph Γ can be written $\frac{I}{\sigma}$ by definition. The functional derivative is calculated for the functional I as was done before. Then the challenge is to verify that the symmetry numbers are correct.

First if there is no black γ_2-circle in Γ, then the functional derivative of I is 0 and so is the functional derivative of Γ and lemma 2 is verified in the sense that there is no graph that can be obtained from Γ by changing a black γ_2-circle into a white 1-circle. If there is at least one black γ_2-circle:

$$\frac{\delta \Gamma}{\delta \gamma_2}(1) = \frac{1}{\sigma} \frac{\delta}{\delta \gamma_2} \left(\int A \times \prod_{1 \leq i \leq s} \gamma_2(i) \mathrm{d}(i) \right)$$

Where s is the number of black γ_2-circles and A a product of bonds and white circles (such that none of them has a label 1). There are s γ_2 functions so:

$$\frac{\delta \Gamma}{\delta \gamma_2}(1) = \frac{1}{\sigma} \sum_{k=1}^{s} \left(\int A \times \prod_{\substack{1 \leq i \leq s \\ i \neq k}} \gamma_2(i) \mathrm{d}(i) \right)$$

The problem is that σ might not be the symmetry number of the graphs representing the integrals inside the sum.

If there was no white circle in Γ and a bond between each pair of black circles, σ would be $s!$ as all black circles would be indistinguishable and so all the terms inside the sum would be equal. So the sum would become a prefactor s and the overall prefactor would be $\frac{s}{s!} = \frac{1}{(s-1)!}$ and the lemma would be verified as there would be only one distinct graph with a symmetry number of $(s-1)!$ (which is the symmetry number of a graph with one white circle and bonds between each of the s circles as one label is already fixed).

In general there is not a bond between each pair of black circles and so the sum will not be entirely simplified as above (some graphs will not be identical anymore). In the general case it can

71

be written:

$$\frac{\delta\Gamma}{\delta\gamma_2}(1) = \sum_{k=1}^{r} \left(\frac{t_k}{\sigma} \int A \times \prod_{\substack{1 \leq i \leq s \\ i \neq k}} \gamma_2(i)\mathrm{d}(i) \right)$$

Where r is the number of distinct graphs Γ_k and t_k is the number of identical integrals of type k (that appeared in the former equation). In order to finish the proof, it is required to show that the symmetry number of each graph Γ_k representing integrals in the sum is $\frac{\sigma}{t_k}$. Let σ_k be the symmetry number of each graph Γ_k. Then the lemma is proved if $t_k\sigma_k = \sigma$. In order to better understand the following explanation, the graph in Figure A1.5 will be used. The symmetry number of the
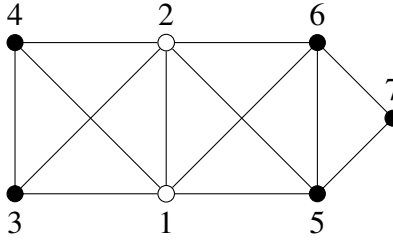
Figure A1.5: Graph with two white circles and five black γ_2-circle. Its symmetry number is 4.

graph in Figure A1.5 is 4 as the labels 3 and 4 can be exchanged and so can labels 5 and 6 (all combinations gives 4 different configurations). It is not possible to exchange labels 3 and 4 with labels 5 and 6 as the latter have to be connected to the circle with the label 7. When taking the functional derivative of this graph, any black circle can be transformed into a white 1-circle. This gives three distinct types of graphs whether the white 1-circle is placed on labels 3 and 4 or 5 and 6 or 7. If the graph with a white 1-circle on either label 3 or 4 is chosen, t_k is 2 as it is possible to have a white 1-circle on these two different places without changing the integral that the graph represents. Then the symmetry number σ_k of the graph is 2 as it is possible to exchange labels 5 and 6. So in this case $t_k\sigma_k = 4 = \sigma$. With any other graph, its symmetry number can always be calculated in the following way:

First place one fixed label, where there will be one more white circle, on any black circle and calculate the different ways to place this label so that it gives the same graph. The number of different ways is exactly t_k. Then it is possible to calculate the number of ways to place temporary labels on the remaining black circles. This is the symmetry number of the graph with a fixed label i.e. σ_k. So $\sigma = \sigma_k t_k$.

The idea behind this result is that a first classification is done to all the allowed permutations (when the first fixed label is placed) and then temporary labels are placed so that all permutations are found. The underlying mathematical result is that the group of permutations among the temporary

labels on black circles, once some fixed labels have been placed, is a subgroup of the group of permutations of the graph among all the labels (fixed and temporary) on black circles. This is illustrated in the following array for the graph on Figure A1.5 with 3 or 4 that can be a fixed label:

3	6	7	3	5	7
4	5		4	6	
4	6	7	4	5	7
3	5		3	6	

Each row represents a choice of a first fixed (red) label and each column represent a permutation of the remaining labels. The symmetry number is thus the number of column (σ_k) times the number of rows (t_k) which is the result proved before. There will be a similar idea for lemma 3, which was noticed by Stell[8]. □

2.3 Fugacity expansions

It is now possible to rewrite equation (A.19) in terms of graphs. z_1 functions will be represented as black circles if integrated or as white circles otherwise and e functions will be represented as solid lines for now. Note that in equation (A.19), there is one e-bond between each pair of particles so all particles are indistinguishable and so are circles of graphs representing these integrals. Thus the symmetry number of these graphs are $s!$ and so Ξ already has the form of a sum of graphs. When $s = 0$ the term is one by convention with the notation $\prod$. So:

$$\Xi = 1 + \bullet + \bullet\!\!-\!\!\bullet + \triangle + \boxtimes + \pentagram + \dots$$

This type of results will always be given with words as well instead of graphs. Indeed the most interesting aspect of graphs is that it is possible to describe them with topological properties only (connected, simple, distinct, etc.). Thus:

Ξ = the sum of all the distinct simple graphs consisting of black z_1-circles and some or no e-bonds such that there is one e-bond between each pair of z_1-circles $\qquad$ (A.43)

This equation is called a fugacity expansion of Ξ as it gives Ξ as a sum of terms that depend on fugacity. However it is more appropriate to rewrite it by introducing the Mayer f-function defined by $f(i,j) = e(i,j) - 1$. All the e-bonds in the previous equation will be replaced by f-bonds and 1-bonds. Now and until the end of this section solid lines will represent f-bonds. 1-bonds represent the fact that there is no bond between two particles. Putting $e = 1 + f$ in equation (A.43), it is easy

to realize that each e-bond can become an f-bond or no bond (a 1-bond) and this in all the possible configurations. Indeed, choosing any graph from equation (A.43) and an e-bond in it, transforming it into an f-bond and a 1-bond results in duplicating the graph and replacing the e-bond by an f-bond or no bond. Doing this and remembering that graphs that represent identical integrals must be counted as one graph:

$$\Xi \quad = 1 + \bullet + \bullet \;\; \bullet + \bullet\!\!-\!\!\bullet + \ldots + \ldots + \ldots + \ldots + \ldots + \ldots$$

(A.44)

= 1 + the sum of all distinct simple graphs consisting of black z_1-circles and some or no f-bonds

It can be verified by the same reasoning as the one used to prove lemma 2 (but by labeling bonds instead of circles for the classification) that, by summing identical graphs, prefactors in front of each integral is the inverse of the symmetry number of each graph. This is actually the whole purpose of symmetry numbers, most of the time the prefactor of each integral is the inverse of the symmetry number of the corresponding graph. Indeed, transforming a graph changes its symmetry but there usually are symmetrical ways to do the same transformation.

In equation (A.44), all the graphs that are not connected are products of graphs and so by direct application of lemma 1 ($\Xi - 1 = \exp(\ln(\Xi)) - 1$):

$$\ln(\Xi) \quad = \bullet + \bullet\!\!-\!\!\bullet + \ldots + \ldots + \ldots + \ldots + \ldots$$

(A.45)

= the sum of all distinct connected simple graphs consisting of black z_1-circles and some or no f-bonds

With equation (A.8), this gives the fugacity expansion of the equation of state for the given potential (A.18). It is now useful to find the fugacity expansion of the singlet density and s-particle distribution function using equation (A.30). With lemma 2 and equations (A.32) and (A.45), it results in:

$$u_n(1, 2, \ldots, n) \quad = \text{the sum of all distinct connected simple graphs consisting of n}$$

white z_1-circles labeled by 1,2,…,n respectively, some or no black z_1-circles and some or no f-bonds

(A.46)

White circles are z_1-circles and not 1-circles because in equation (A.32) the functional derivative is multiplied by n z_1 functions. In the case where $s = 2$ this gives:

$$u_2(1, 2) = \underset{1 \;\; 2}{\circ\!\!-\!\!\circ} + \underset{1 \;\; 2}{\ldots} + \underset{1 \;\; 2}{\ldots} + \underset{1 \;\; 2}{\ldots} + \underset{1 \;\; 2}{\ldots} + \underset{1 \;\; 2}{\ldots} + \ldots$$

74

Then the s-particle distribution function can easily be obtained from equation (A.30). Indeed, in this case, equation (A.30) means that the s-particle distribution function will be a sum of product of graphs of Ursell functions so that there are s white z_1-circles. The important point is that, except for $s = 1$, these graphs will not be connected anymore as the Ursell functions considered have white circles with different labels (the product of two graphs with different white circles is not a connected graph). However each component will be connected and so each black circle will be connected to a white circle. Then the sum over all the different partitions means that all the configurations of Ursell functions that give s white circles have to be considered. The result is:

$$\rho_n(1, 2, \ldots, n) = \text{the sum of all distinct simple graphs consisting of n white}$$

z_1-circles labeled by 1,2,...,n respectively, some or no black
z_1-circles and some or no f-bonds such that the graphs are
root-connected

(A.47)

When $s = 1$ this result is obvious (from equation (A.46)) and gives the singlet density:

$$\rho_1(1) = u_1(1) = \underset{1}{\circ} + \underset{1}{\circ\!\!-\!\!\bullet} + \underset{1}{\text{graph}} + \underset{1}{\text{graph}} + \underset{1}{\text{graph}} + \underset{1}{\text{graph}} + \ldots$$

If equation (A.47) does not seem obvious, it can be easily understood with the case $s = 2$ because $\rho_2(1, 2) = u_2(1, 2) + u_1(1)u_1(2)$ and so the 2-particle distribution function is the sum of the graphs in u_2 plus product of graphs in u_1 with labels 1 and 2:

$$\rho_2(1, 2) = \underset{1 \quad 2}{\circ \quad \circ} + \underset{1 \quad 2}{\text{graph}} + \underset{1 \quad 2}{\text{graph}} + \underset{1 \quad 2}{\text{graph}} + \underset{1 \quad 2}{\text{graph}} + \underset{1 \quad 2}{\text{graph}} + \underset{1 \quad 2}{\text{graph}} + \ldots$$

The first three terms come from $u_1(1)u_1(2)$ and the other ones from u_2. A useful version of equation (A.47) is the following:

$$\rho_n(1, 2, \ldots, n) = \text{the sum of all distinct connected simple graphs consisting of n}$$

white z_1-circles labeled by 1,2,...,n respectively, some or no black
z_1-circles and some or no f-bonds and an e-bond between every
pair of white circles

(A.48)

The transformation between equations (A.47) and (A.48) is obvious by changing each e-bond in equation (A.48) by $f + 1$. Indeed, this transformation doesn't change the connections involving black circles so there is always one path from each black circle to a white circle and all e-bonds become a f-bond or nothing (and so the graphs are not all connected anymore).

2.4 Topological reduction

The previous equations express certain quantities as functionals of fugacity. However it is usually preferred to have these quantities as functionals depending on singlet density (and so density via equation (A.27)) as it is more easily measured. Moreover such transformation simplifies equations as will be explained below.

It is convenient to introduce the concept of articulation circles for the purpose of this section.

Definition 13. An **articulation circle** is a circle which, when removed, separates a component of a graph into two or more parts with at least one without a white circle.

Definition 14. A graph without articulation circles is called **1-irreducible** or **irreducible**. In a graph with no more than one white circle, irreducible and at-least-doubly-connected are equivalent terms.

For instance on Figure A1.6, the white circle labeled 2 is an articulation circle (and the only one on this graph). The transformation that will be shown in this section makes possible to rewrite
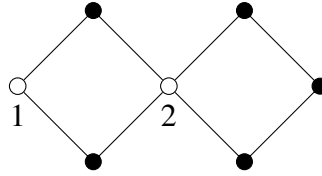
Figure A1.6: Example of graph with an articulation circle.

quantities as functionals of singlet density and to have graphs without articulation circles. Thus all "sum of distinct connected graph" will concern graphs with ρ_1-circles and without articulation circles which permits fewer possibilities for the topology of the graphs i.e. their general form. That is why this step is often called topological reduction. Still following Stell[8] it is convenient to first reduce graphs in h_n given by equation (A.34) and equation (A.35) for $n = 1$. Indeed, it is easy to first get rid of white articulation circles by noticing that:

$$
\begin{aligned}
h_n(1, 2, \ldots, n) \quad &= \text{the sum of all distinct connected simple graphs consisting of n} \\
&\quad \text{white 1-circles labeled by 1,2,\ldots,n respectively, some or no black} \\
&\quad z_1\text{-circles and at least one } f\text{-bond such that the graphs are free of} \\
&\quad \text{white articulation circles}
\end{aligned}
\tag{A.49}
$$

The case $n = 1$ is proved using lemma 1 and equation (A.35). Indeed, $u_1(1)/z_1(1)$ is the sum of all the graphs in equation (A.46) but with one 1-white circle instead of one z_1-circle (the graph

consisting of one z_1-circle divided by z_1 being equal to 1). The white circle in this type of graph may be an articulation circle like in ⊶ in the given fugacity expansion of u_1 which is the product of two graphs ⊶ . If the white circle is not an articulation circle, the graph can still be seen as a product as it can be a product with the 1-white circle. So using lemma 1, $u_1(1)/z_1(1) = \exp(h_1(1))$ (1 is included in the sum of graphs $u_1(1)/z_1(1)$) makes the link between equations (A.35) and (A.49). Note that the simplest graph in h_1 is ⊶ as there must be at least one f-bond.

When $n \geq 2$, it is proved using equation (A.34) written as $h_n(1, 2, \ldots, n)\rho_1(1)\rho_1(2) \ldots \rho_1(n)$ $= u_n(1, 2, \ldots, n)$. Indeed in this case, graphs in u_n that have white articulation circles can be written as a product of one graph without white articulation circles times the parts in the graphs that were the cause of the presence of articulation circles (as before if there is no articulation circle, it can be written as the product with a single white circle). As the latter parts are connected and have one white z_1-circle, they are inside ρ_1. For instance:
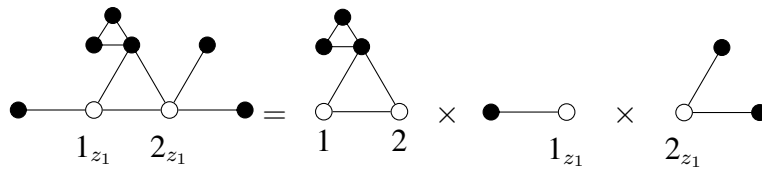
The graph on the left hand side belongs to u_2. z_1 subscripts have been added to show the difference between 1-circles and z_1-circles. The first graph of the right hand side is a graph of equation (A.49) and the two others are in the singlet density. Here it is not necessary to pay attention to symmetry numbers as no prefactor is changing (all terms in $h_n(1, 2, \ldots, n)\rho_1(1)\rho_1(2) \ldots \rho_1(n)$ are obviously distinct because graphs in h_n are distinct).
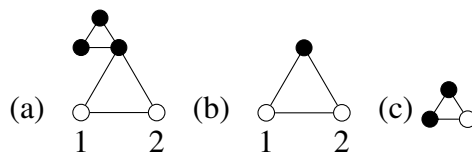
Figure A1.7: (a):Example of a graph; (b): The maximal 1-irreducible rooted subgraph of graph (a). The original graph on figure (a) is obtained by replacing the black circle on graph (b) by the graph (c) and making the white circle black.

Some graphs in h_n still have black articulation circles. Thus it is possible to define the maximal 1-irreducible rooted subgraph of a graph Γ. It is the largest subgraph Γ_m of Γ that contains all the white circles (white circles are sometimes called rooted circles) but no articulation circle. The differences between a graph and its maximal 1-irreducible rooted subgraph are only some more

parts attached to the original graph. These parts are attached at the articulation circle and are connected graphs. They actually are graphs from the singlet density with a black circle instead of a white circle. An example is shown on Figure A1.7. This fact is summarized in the following lemma:

Lemma 3: The sum of all graphs appearing in the expansion of h_n given by equation (A.49) that have the same maximal 1-irreducible rooted subgraph Γ_m is equal in value to the graph $\overline{\Gamma_m}$ obtained by replacing all the black z_1 circles of Γ_m by ρ_1-circles.

Proof. The singlet density can be written as an infinite sum of graphs that are functionals of z_1 (and f):

$$\rho_1(i) = \sum_\alpha \Gamma_\alpha(i) = \sum_\alpha \frac{I_\alpha(i)}{\sigma_\alpha}$$

Where all the Γ_α are for instance given by equation (A.47) and I_α and σ_α are respectively the integrals they represent and their symmetry number. Let Γ_m be one of the maximal 1-irreducible rooted subgraph found in a graph of h_n with m black circles and $\overline{\Gamma_m}$ the corresponding graph with ρ_1-circles instead of z_1-circles. $\overline{\Gamma_m}$ can be written as $\overline{I_m}/\sigma_m$ where $\overline{I_m}$ is the integral represented by $\overline{\Gamma_m}$ and σ_m is its symmetry number (and the symmetry number of Γ_m). Rewriting each $\rho_1(i)$ appearing in $\overline{\Gamma_m}$ as a sum of graphs and expanding the products, a new infinite sum of terms (they are not graphs yet) appears but this time as functionals of z_1. Let t be one of these new terms. It obviously has the following form:

$$t = \frac{1}{\sigma_m \sigma_{\alpha_1} \sigma_{\alpha_2} \ldots \sigma_{\alpha_m}} I$$

Where each σ_{α_i} is the symmetry number of a graph Γ_{α_i} that has been used in the product that creates t. I divided by its symmetry number is a graph of h_n and it has Γ_m for maximal 1-irreducible rooted subgraph. As for previous proofs with graphs, the only thing that has to be proved is that prefactors in front of integrals have the correct symmetry number. But in general, $\sigma_m \sigma_{\alpha_1} \sigma_{\alpha_2} \ldots \sigma_{\alpha_m}$ is not the symmetry number of t. In this case it means that there are other terms in the expanded form of $\overline{\Gamma_m}$ that have the same integral I (in value but with different dummy variables). Let T be the sum of all the terms that have the same integral I and s the number of such terms. All the terms naturally have the same prefactor $\frac{1}{\sigma_m \sigma_{\alpha_1} \sigma_{\alpha_2} \ldots \sigma_{\alpha_m}}$ as they have the same integral. So:

$$T = \frac{s}{\sigma_m \sigma_{\alpha_1} \sigma_{\alpha_2} \ldots \sigma_{\alpha_m}} I$$

$\overline{\Gamma_m}$ is the sum of all these terms T and each T (with the good prefactor) is one graph in the expansion of h_n that has Γ_m as its maximal 1-irreducible rooted subgraph. In order to reach a conclusion, it is required to prove that $\frac{\sigma_m \sigma_{\alpha_1} \sigma_{\alpha_2} \ldots \sigma_{\alpha_m}}{s}$ is the symmetry number σ_T of each T (and so T will be a

graph). This proof is essentially the same kind of proof that has been done for lemma 2 but with two different classifications. Figure A1.8 will be used as an example to explain the reasoning.
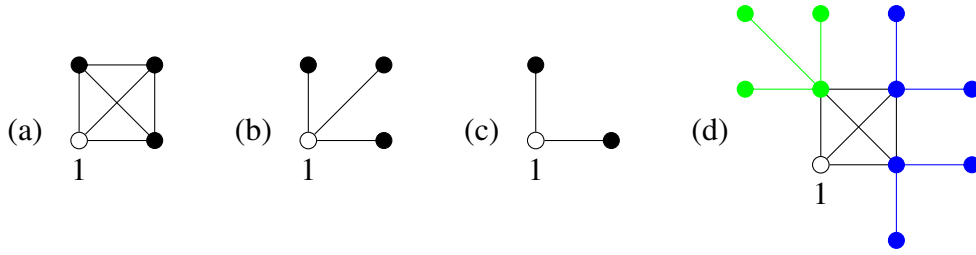
Figure A1.8: (a): Graph Γ_m; (b): Graph Γ_{α_1}; (c): Graph Γ_{α_2}; (d): Graph representing T

T (Figure A1.8(d) gives an example of such a graph) has some articulation circles because of the subgraphs Γ_{α_i} coming from the singlet density (figures A.8(b) and A.8(c)). Any label given to one circle of these subgraphs must remain inside the same subgraph when a permutation is applied to any label, unless all labels in identical subgraphs are switched (for instance all the labels of one blue subgraph can be switched with all the labels of the other blue subgraph). Each black circle of T that belongs to Γ_m (Figure A1.8(a)) receives a label α_i corresponding to a graph Γ_{α_i}. In Figure A1.8(d), the green color represents a label α_1 and the blue color a label α_2. In order to count the different possible permutations of some temporary labels given to the black circles of T, one can first count the number of permutations of identical graphs Γ_{α_i} and then multiply it by the symmetry number of the latter graphs. This gives a classification of allowed permutations for T. So $\sigma_T = \bar{\sigma}\sigma_{\alpha_1}\sigma_{\alpha_2}\ldots\sigma_{\alpha_m}$ where $\bar{\sigma}$ is the number of permutations of labels α_i that do not change the labeling. In Figure A1.8(d), $\bar{\sigma} = 2$ (the two blue subgraphs can be switched i.e. the two labels α_2), $\sigma_{\alpha_1} = 6$, $\sigma_{\alpha_2} = 2$ and $\sigma_T = 48$.

Now it must be proved that $s\bar{\sigma} = \sigma_m$ to conclude. In order to prove this, one must find a classification of the permutations of Γ_m. The equation to be proved involves $\bar{\sigma}$ so the α_i labels need to be considered. As before, in order to count the number of permutations of temporary labels on black circles, one can first count the permutations of the α_i labels which is $\bar{\sigma}$ by definition. But doing so, some permutations have been missed, unless all the α_i are identical. So one has to multiply $\bar{\sigma}$ by the number of distinct ways to place the α_i labels so that T is unchanged. This means that the configurations where the graphs Γ_{α_i} have been placed in a different way, but so that the integral represented by T is still the same, have to be counted. This number is s by definition and it may be seen by expanding the product that first appears when the singlet density is changed into a sum of graphs in $\overline{\Gamma_m}$. In the case of Figure A1.8(d), the green subgraph can be switched with any of the two blue subgraphs so that $s = 3$. $\bar{\sigma} = 2$ and $\sigma_m = 6$ so $s\bar{\sigma} = \sigma_m$ is verified for this example. The different configurations of α_i labels is summarized in the following array:

α_1	α_2	α_2	α_1	α_2	α_2
	α_2		α_2		α_1

For each of these configurations, labels α_2 can be switched and it gives the six ways to label Γ_m.   □

This lemma can now be used to express h_n as a sum of irreducible graphs. Equation (A.49) becomes:

$h_n(1, 2, \ldots, n)$ = the sum of all distinct connected simple graphs consisting of n white 1-circles labeled by 1,2,…,n respectively, some or no black (A.50) ρ_1-circles and at least one f-bond such that the graphs are irreducible

Combining equations (A.30), (A.33) and (A.34), one can see that g_n will be a sum of all possible products of functions h_m ($2 \leq m \leq n$). So graphs in g_n will not be connected anymore but will still be root-connected:

$g_n(1, 2, \ldots, n)$ = the sum of all distinct simple graphs consisting of n white 1-circles labeled by 1,2,…,n respectively, some or no black ρ_1-circles and some or no f-bonds such that the graphs are irreducible and (A.51) root-connected

The different terms $u_1(i)/\rho_1(i)$ correspond to unconnected white 1-circles. Thus the only parts of the graphs of g_n which are not connected are white 1-circles. With the same reasoning that allows to go from equation (A.47) to equation (A.48), g_n can be given as a sum of connected graphs by changing f-bonds between white 1-circles into e-bonds:

$g_n(1, 2, \ldots, n)$ = the sum of all distinct and at-least-doubly-connected simple graphs consisting of n white 1-circles labeled by 1,2,…,n respectively, some or no black ρ_1-circles, some or no f-bonds and an e-bond between (A.52) each pair of white circle

It is not required to go any further here as topological reduction of other quantities will be done in section 4.

3   Hard Sphere Equation of State

The hard sphere (hs) equation of state written here is given by Mansoori[12]. The main idea is to find first the radial distribution function g_2^{hs} (or simply noted g^{hs}) using equations (A.36) and (A.37)

for hard spheres. Equation (A.38) shows the dependency in the potential energy. In the case of N identical hard spheres, this potential energy V_{hs} is related to the pair potential φ_{hs}:

$$V_{hs}(1, 2, \ldots, N) = \sum_{1 \leq i < j \leq N} \varphi_{hs}(|r_i - r_j|) \tag{A.53}$$

$$\varphi_{hs}(r) = \begin{cases} \infty & , \quad \text{if } r \leq \sigma \\ 0 & , \quad \text{otherwise} \end{cases} \tag{A.54}$$

Where σ here is the diameter of a sphere and there are only translation degrees of freedom here, so the previously introduced notation i reduces to the position vector r_i. In the case of a mixture of hard spheres different values of σ and the radial distribution function g_{ij}^{hs} between each pair of components $\{i, j\}$ have to be considered. Equation (A.37) is solved using the Percus-Yevick approximation (approximation explained for instance by Stell[8]). It is then possible to find the compressibility factor Z_{hs}. In SAFT, the solutions for the radial distribution function and the compressibility factor for mixtures are given by Boublik[13] and Mansoori[12]. The following forms of the two given equations are usually used:

$$g_{ij}^{hs} = \frac{1}{1 - \xi_3} + \frac{\sigma_i \sigma_j}{\sigma_i + \sigma_j} \frac{3\xi_2}{(1 - \xi_3)^2} + \left(\frac{\sigma_i \sigma_j}{\sigma_i + \sigma_j}\right)^2 \frac{2\xi_2^2}{(1 - \xi_3)^3} \tag{A.55}$$

$$Z_{hs} = \frac{1}{1 - \xi_3} + \frac{3\xi_1 \xi_2}{\xi_0 (1 - \xi_3)^2} + \frac{3\xi_2^3 - \xi_2^3 \xi_3}{\xi_0 (1 - \xi_3)^3} \tag{A.56}$$

$$\xi_k = \frac{\pi}{6} N_a \rho_s \sum_i x_i \sigma_i^k \tag{A.57}$$

Where the sum in equation (A.57) is carried out over every component i, σ_i is the diameter of the spheres of component i and ρ_s is the overall molar density of spheres. In order to get the Helmholtz energy change A_{hs} due to the presence of V_{hs}, the following departure function is used:

$$\frac{A_{hs}}{N_s k_B T}(\rho_s, N_{s_i}) = \frac{A - A_{ig}}{N_s k_B T}(\rho_s, N_{s_i}) = \int_0^{\rho_s} (Z_{hs}(\rho) - 1) \frac{d\rho}{\rho} \tag{A.58}$$

Where N_s is the overall number of spheres in the system and N_{s_i} is the number of spheres of component i (the dependence is for all i). The density dependence of Z_{hs} has been noted with the dummy variable ρ. Skipping the tedious but not difficult calculations, the result is:

$$\frac{A_{hs}}{N_s k_B T}(\rho_s, N_{s_i}) = \frac{1}{\xi_0} \left(\frac{3\xi_1 \xi_2}{1 - \xi_3} + \frac{\xi_2^3}{\xi_3 (1 - \xi_3)^2} + \ln(1 - \xi_3) \left(\frac{\xi_2^3}{\xi_3^2} - \xi_0 \right) \right) \tag{A.59}$$

SAFT allows the presence of chains of molecules as will be explained further on. Thus in the general case molecules will not be modeled as spheres but as chains of spheres. If component i is a chain of m_i spheres the number N_i of molecules i is given by:

$$N_i = \frac{N_{s_i}}{m_i} \tag{A.60}$$

So the functions ξ_k become functions of the molar density of molecules:

$$\xi_k = \frac{\pi}{6} N_a \rho \sum_i x_i m_i \sigma_i^k \tag{A.61}$$

As it is more convenient to work with molar Helmholtz energy (per mole of molecules):

$$\frac{a_{\text{hs}}}{RT}(\rho, N_i) = \frac{A_{\text{hs}}}{N_s k_B T}(\rho_s, N_{s_i})\frac{N_s}{N} = \frac{A_{\text{hs}}}{N_s k_B T}(\rho_s, N_{s_i})\frac{\sum_i m_i N_i}{N} = \frac{A_{\text{hs}}}{N_s k_B T}(\rho_s, N_{s_i})m_x \tag{A.62}$$

With $m_x = \sum_i x_i m_i$ the average number of spheres in a component. So overall, without showing dependencies:

$$\frac{a_{\text{hs}}}{RT} = \frac{6}{\pi N_a \rho}\left(\frac{3\xi_1\xi_2}{1-\xi_3} + \frac{\xi_2^3}{\xi_3(1-\xi_3)^2} + \ln(1-\xi_3)\left(\frac{\xi_2^3}{\xi_3^2} - \xi_0\right)\right) \tag{A.63}$$

The overall molar Helmholtz energy a is given by the sum of equations (A.16) and (A.63) times RT. This is the hard sphere equation of state.

4 Wertheim's Thermodynamic Perturbation Theory

The previous section showed an equation of state for a potential energy that only allows repulsion. In this section it will be shown how an attractive interaction with specific directions can be rigorously added on the top of V_{hs} or any other repulsive potential, in the case of a pure component. As explained in the first section, it will be then possible (in section 5) to extend these results to mixtures. Here the derivation made by Wertheim[3–6] is followed. It will be assumed that the system is uniform i.e. $\varphi_1 = 0$ and the pair potential φ_2 that will be considered here is the following:

$$\varphi_2(1,2) = \varphi_R(1,2) + \sum_A \sum_B \varphi_{AB}\left(|r_2 + d_B(\Omega_2) - r_1 - d_A(\Omega_1)|\right) \tag{A.64}$$

Where φ_R is the reference pair potential that is only repulsive and represents the hardcore of the particle (it will be φ_{hs} in the version of SAFT of interest) and φ_{AB} is the attractive interaction potential between what are called association sites A and B. The sums are carried out over all association sites. The $(1,2)$ dependence of φ_{AB} has been written: $|r_2 + d_B(\Omega_2) - r_1 - d_A(\Omega_1)| = x$. As before r_1 and r_2 are the position vectors of particles 1 and 2. Ω_1 and Ω_2 designate the orientation of particles 1 and 2. These can be for instance a vector with three elements that are Euler angles. In the case where there would be no association site, molecules would be perfectly symmetrical and Ω in equation (A.27) would be $\int_{\theta=0}^{\pi} \int_{\phi=0}^{2\pi} \int_{\psi=0}^{2\pi} \sin(\theta)\mathrm{d}\theta\mathrm{d}\phi\mathrm{d}\psi = 8\pi^2$. When there are association sites, their relative position from the center of the particle is given by the vectors

d_A, for an association site A, which naturally must depend on the orientation of the particle. For educational purposes, the case with one association site is studied first following Wertheim[3,4]. In this case $\varphi(1,2) = \varphi_R(1,2) + \varphi_A(1,2)$ with $\varphi_A = \varphi_{AA}$. The simplest case for φ_A is considered:

$$\varphi_A(1,2) = \varphi_A(x) \begin{cases} < 0 & , \quad \text{if } x \leq a \\ 0 & , \quad \text{otherwise} \end{cases} \tag{A.65}$$

Where x was defined above. Thus here an association site is a sphere with a square-well potential situated at a distance $|d_A| = d$ from the center of the hardcore of the particle. If, as in the previous section, σ is the diameter of the hardcore, then the whole situation is explained in Figure A1.9. In
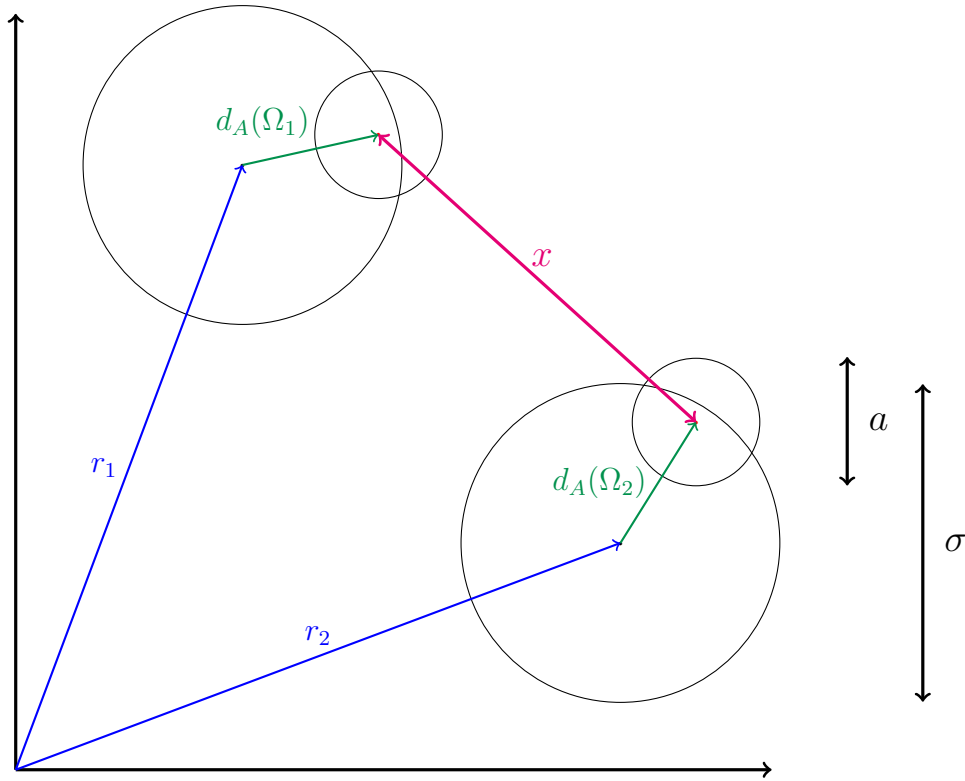
Figure A1.9: 2-D section of two particles 1 and 2 with both one association site.

order to have an impact, association sites must be at least partially outside of hardcores and it is assumed that the center of these association sites must be inside the hardcore so that:

$$\frac{(\sigma - a)}{2} < d < \frac{\sigma}{2} \tag{A.66}$$

4.1 Pair potential with one association site

Adaptation of Graph Theory

In order to use Graph Theory, one must define what will be circles and bonds. Circles will become z-circles as it is assumed the system is uniform $(\exp(-\beta\varphi_1) = 1)$ and bonds will be written in a more natural way which takes advantage of the form of equation (A.64). For the case first considered of only one association site, equation (A.64) becomes:

$$\varphi_2(1, 2) = \varphi_R(1, 2) + \varphi_A(1, 2) \tag{A.67}$$

The e function then become:

$$
\begin{aligned}
e(1, 2) &= \exp(-\beta\varphi_2(1, 2)) = e_R(1, 2)e_A(1, 2) \\
&= e_R(1, 2)(1 + f_A(1, 2)) = e_R(1, 2) + e_R(1, 2)f_A(1, 2)
\end{aligned} \tag{A.68}
$$

Where the fundamental property of $\exp$ has been used and any function e_X is naturally defined by $\exp(-\beta\varphi_X)$ and any function f_X is naturally defined by $e_X - 1$. In equation (A.68), e_R has not been transformed into an f_R function as it is already done when f-bonds are considered:

$$f(1, 2) = e(1, 2) - 1 = f_R(1, 2) + e_R(1, 2)f_A(1, 2) = f_R(1, 2) + F(1, 2) \tag{A.69}$$

This decomposition is inspired by an idea of Lockett[14]. It is now possible to put equation (A.69) into equation (A.45). Each f-bond in equation (A.45) will become an f_R-bond plus an F-bond. Doing this f-bond by f-bond, each graph will be transformed into a new graph which symmetry might have changed. As it was done several times in section 2, all graphs representing the same integral are summed so that the prefactor in front of each integral is its symmetry number. One can notice now that a transformation $a = b + c$ of a bond can change the symmetry of a graph if and only if this transformation can be done in a symmetric manner to other bonds. That is the reason why there is no need to add any prefactor with such transformations. Thus:

$$\ln(\Xi) \quad = \bullet + \bullet\!\!-\!\!\bullet + \bullet\!\!\sim\!\!\bullet + \begin{array}{c}\bullet\\ \end{array} + \begin{array}{c}\bullet\\ \end{array} + \begin{array}{c}\bullet\\ \end{array} + \begin{array}{c}\bullet\\ \end{array} + \begin{array}{c}\bullet\\ \end{array} + \begin{array}{c}\bullet\\ \end{array} + \begin{array}{c}\bullet\\ \end{array} + \ldots$$

= the sum of all distinct connected simple graphs consisting of black z-circles, some or no f_R-bonds and some or no F-bonds

$$\tag{A.70}$$

F-bonds are represented with zigzag lines and f_R-bonds with solid lines. e_R-bonds will be represented with dashed lines. One more step can be done. Although graphs in the previous equation are connected, there still are some pairs of black z-circles which are not connected. In particular there might still be no bond between a pair of black z-circles inside a maximal subgraph which is only made of F-bonds. Such a subgraph is for instance in Figure A1.10 (a). In Figure A1.10 prefactors have been shown in order to better understand what happens. In order to simplify graphs
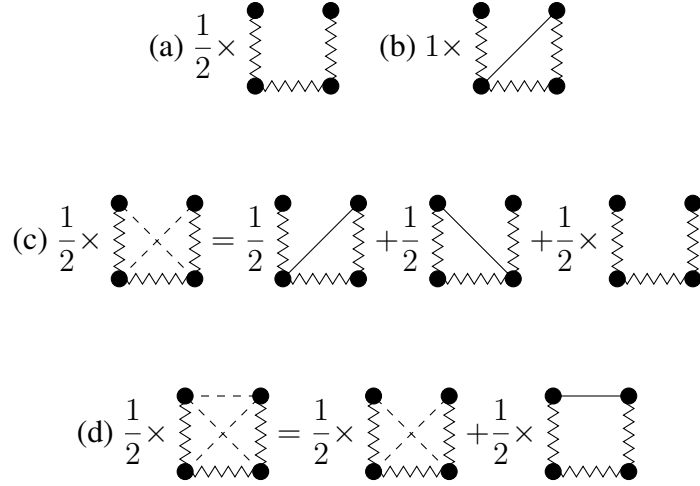
Figure A1.10: Filling s-mers with e_R-bonds.

it is assumed that the graph in Figure A1.10 (a) is the entire graph found in equation (A.70) (otherwise other f-bonds and black z-circles should be included but they would not be affected by these transformations). Equation (A.70) shows as well graphs corresponding to the missing bonds. Such a graph is in Figure A1.10 (b). The symmetry number (and so the prefactor) is different from the graph in Figure A1.10 (a) but this is not a problem as it can be written as the sum of the first two terms of the right hand side of Figure A1.10 (c). Then using the definition of f_R, it can be seen in Figure A1.10 (c) that adding graph (b) to graph (a) makes two e_r-bonds appear and the prefactor still corresponds to the symmetry number. In Figure A1.10 (d) is showed how the last missing bond can be added. Subgraphs created in that way are called s-mers.

Definition 15. An **s-mer** is a connected simple graph consisting of s z-circles, some or no F-bonds (such that the graph would be connected with only F-bonds) and a e_R-bond between each pair of circle that are not directly connected by an F-bond. A z-circle without bonds is a 1-mer or monomer.

So it is possible to sum together graphs with identical incomplete s-mers (i.e. with missing e_R-bonds and the same set of F-bonds) with the same procedure explained in Figure A1.10 in order to form complete s-mers. When doing such a sum, if prefactors are not identical between all the graphs, it means that some graphs can be decomposed into a sum of graphs with f_R-bonds placed in a different way but still representing the same integral (this is the case for graph (b) in Figure A1.10). Then in equation (A.70) all maximal subgraphs which are only made of F-bonds belong

to a s-mer. Thus it becomes clear that:

$$\ln(\Xi) = \text{the sum of all distinct connected simple graphs consisting of s-mers } (s = 1 \dots \infty)$$
$$\text{and } f_R\text{-bonds between pairs of black } z\text{-circles in distinct s-mers}$$

(A.71)

Note that a single z-circle is a monomer. That is why in equation (A.71) f_R-bonds are only joining s-mers. All the s-mers for s= $1 \dots 4$ are showed in Figure A1.11. Any s-mer with s≤ 4 satisfying definition 15 must be equivalent to one of these graphs even if it may look different at first.
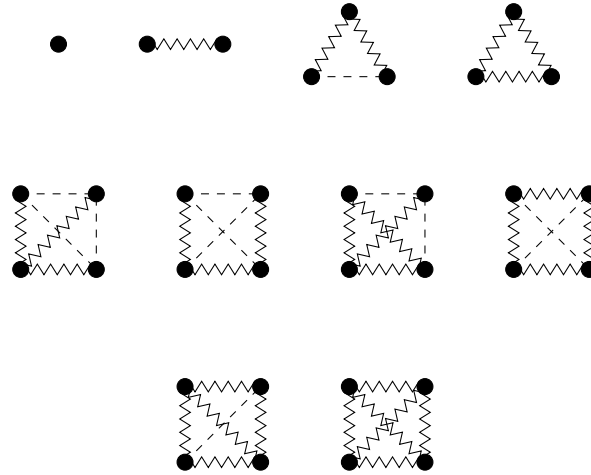
Figure A1.11: All s-mers for s= $1 \dots 4$.

Using equations (A.31) and (A.32) and lemma 2, it is possible to get the singlet density ρ_1, as in section 2, by summing all the distinct graphs obtained from $\ln(\Xi)$ by changing a black z-circle into a white z-circle. As only ρ_s with $s = 1$ will be used from now on, the singlet density should be only noted ρ in order to simplify forthcoming notations.

Topological reduction

Still from an idea of Lockett[14], Wertheim[3] introduces a multi-density formalism. The idea is to distinguish particles that are bonded at certain association sites. In a graph of the singlet density ρ, the white z-circle represents a particle 1 and the graph represents a possibility of how particle 1 can interact with other particles (and all these graphs are summed to take all configurations into account). Each particle in the real system should correspond (on average at equilibrium) to such a graph. Assuming there is just one association site, if the graph corresponding to a particle has no F-bond connected to its white z-circle, it means that the particle itself is not attracted to any other

particle and so is a monomer. This is how ρ_0 is defined:

$\rho_0(1)$ = sum of graphs in the singlet density $\rho(1)$ such that the white z-circle labeled 1 has no incident F-bond

$$(A.72)$$

Furthermore ρ_1 can be defined:

$\rho_1(1)$ = $\rho(1) - \rho_0(1)$

$$(A.73)$$

The previous graphs are still made of s-mers but containing a white z-circle. There should still be referred to as s-mers. Now that this has been done, it is possible to reproduce what has been done in section 2 in order to have quantities made of irreducible graphs. First it is possible to create a quantity from ρ_0 which has no white articulation circle. This quantity is equivalent to h_1 concerning the singlet density. In this case, it will be noted c_0 following Wertheim[3]:

$$c_0(1) = \ln\left(\frac{\rho_0(1)}{z}\right)$$
= subset of graphs in $\frac{\rho_0(1)}{z}$ that are free of white articulation circles

= subset of graphs in $\frac{\rho_0(1)}{z}$ that remain connected when all connections

at the white 1-circle are broken

$$(A.74)$$

As for h_1 this is proved using lemma 1 but with ρ_0 instead of u_1. The proof is exactly the same. Indeed, even if there are more types of bonds in this case, they are not connected to the white circle by definition.

Now considering ρ_1, it is possible to notice that ρ_0 is a factor of this quantity. Indeed, there are two types of graphs in ρ_1 whether their white z-circle is an articulation circle or not. If the white z-circle is not an articulation circle then it is part of one and only one s-mer with s ≥ 2 by definition of a s-mer (each black circle connected to the white circle by a F-bond must also be connected to the white circle by at least one e_R-bond) and is the product of itself by the white circle. If the white z-circle is an articulation circle then it means that the graph can be written as the product of two graphs: by definition of ρ_1, the white z-circle is part of one and only one s-mer with s ≥ 2; the subgraph containing this s-mer is the first graph of the product and the remaining part of the

87

graph is the second (they are independent because the white circle is an articulation circle). In the second graph, the white circle cannot be part of an s-mer with s $\geq$ 2 otherwise it could not be an articulation circle. So the second graph is in the sum defining ρ_0. For instance

$$\underset{1}{\vcenter{\hbox{\includegraphics{}}}} = \underset{1}{\vcenter{\hbox{\includegraphics{}}}} \times \underset{1}{\vcenter{\hbox{\includegraphics{}}}}$$
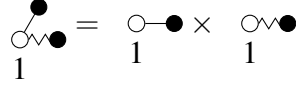
So the quantity c_1 is defined as follows:

$$
\begin{aligned}
c_1(1) \quad &= \frac{\rho_1(1)}{\rho_0(1)} \\
&= \text{subset of graphs in } \rho_1(1) \text{ that are free of white articulation circles} \\
&= \text{subset of graphs in } \rho_1(1) \text{ that remain connected when all connections} \\
&\quad \text{at the white 1-circle are broken, 1 being part of an s-mer with s} \geq 2
\end{aligned}
\tag{A.75}
$$

The second equality immediately follows from what has been discussed above. Note that c_1 is built in a similar manner to h_2 was. As c_0 and c_1 are similar to h_n functions, lemma 3 can be used in order to get rid of black articulation circles. However this lemma must be slightly changed. Indeed, considering a black articulation circle that is part of an s-mer with s $\geq$ 2, the part of the graph attached to this circle cannot be any graph in the singlet density. If it was a graph from ρ_1, it would mean that there would be missing e_R-bonds in the s-mer by definition. So if a black circle is part of an s-mer with s $\geq$ 2, it must be replaced by a ρ_0-circle instead of a ρ-circle. Thus:

$$
\begin{aligned}
c_0(1) \quad &= \text{sum of all distinct irreducible connected simple graphs consisting of some} \\
&\quad \text{or no s-mers (s} \geq 2) \text{ made of } \rho_0\text{-cirles, some or no monomers made of a single} \\
&\quad \rho\text{-circle, } f_R\text{-bonds between pairs of circles (not necessarily black) in distinct} \\
&\quad \text{s-mers, one white 1-circle with no incident } F\text{-bond and there must be at least} \\
&\quad \text{one bond}
\end{aligned}
\tag{A.76}
$$

$$
\begin{aligned}
c_1(1) \quad &= \text{sum of all distinct irreducible connected simple graphs consisting of s-mers} \\
&\quad \text{(s} \geq 2) \text{ made of } \rho_0\text{-cirles, monomers made of a single } \rho\text{-circle, } f_R\text{-bonds} \\
&\quad \text{between pairs of circles (not necessarily black) in distinct s-mers and one} \\
&\quad \text{white 1-circle with at least one incident } F\text{-bond}
\end{aligned}
\tag{A.77}
$$

Defining the following quantity:

$$
\begin{aligned}
c^{(0)} \quad &= \text{sum of all distinct irreducible connected simple graphs consisting of s-mers} \\
&\quad \text{(s} \geq 2) \text{ made of } \rho_0\text{-cirles, monomers made of a single } \rho\text{-circle, } f_R\text{-bonds} \\
&\quad \text{between pairs of circles in distinct s-mers and there must be at least one bond}
\end{aligned}
\tag{A.78}
$$

It follows that:

$$c_0(1) = \frac{\delta c^{(0)}}{\delta \rho}(1) \tag{A.79}$$

$$c_1(1) = \frac{\delta c^{(0)}}{\delta \rho_0}(1) \tag{A.80}$$

The first terms of $c^{(0)}$ are shown in Figure A1.12.
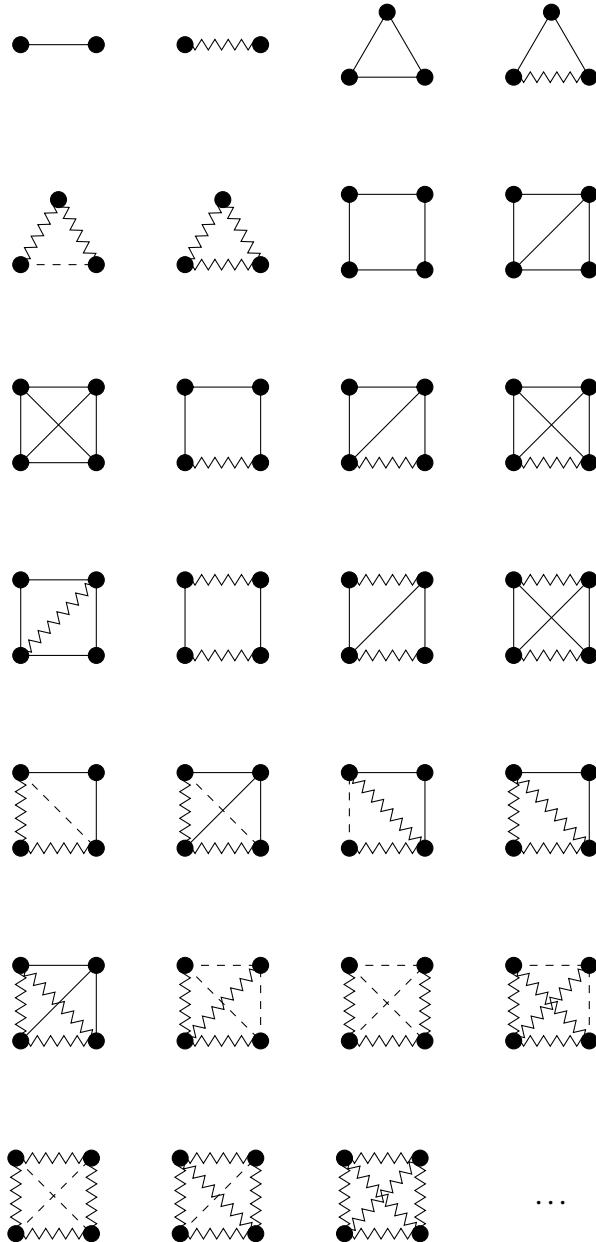
Figure A1.12: First terms of $c^{(0)}$; black circles inside s-mers (s $\geq$ 2) are ρ_0-circles and others are ρ-circles.

89

Thermodynamics

As mentioned at the very beginning of the first section, the objective is to relate thermodynamic quantities between each other starting from a certain potential energy. The link between thermodynamic properties and potential energy is then provided by equations (A.8) and (A.32) (with $s = 1$ and remember that $\rho = u_1$):

$$\rho(1) = z \frac{\delta \ln(\Xi)}{\delta z} = z \frac{\delta(\beta PV)}{\delta z} \tag{A.81}$$

However this equation still has z in it and it would be better to have densities which can be measured instead. Previously introduced quantities can be used for that. Moreover in equation (A.81), it is the functional derivative of βPV that appears and not βPV itself. So this equation needs to be integrated and it is not necessary to keep the constant that should appear as energies are given with a certain reference energy. It is easier, for the purpose of this derivation, to start from the result and then prove that it is equivalent to equation (A.81). The result is:

$$\beta PV = \int \rho_0(1)\mathrm{d}(1) - \int \rho(1)c_0(1)\mathrm{d}(1) + c^{(0)} \tag{A.82}$$

In order to show that this is equivalent to equation (A.81), one must calculate the variation of (A.82):

$$\delta(\beta PV) = \int \delta\rho_0(1)\mathrm{d}(1) - \int \delta\rho(1)c_0(1)\mathrm{d}(1) - \int \rho(1)\delta c_0(1)\mathrm{d}(1) + \delta c^{(0)} \tag{A.83}$$

Noting that $c^{(0)}$ is a functional of two functions ρ and ρ_0, using equation (A.21) and equations (A.79) and (A.80), the result is:

$$\delta c^{(0)} = \int c_1(1)\delta\rho_0(1)\mathrm{d}(1) + \int c_0(1)\delta\rho(1)\mathrm{d}(1) \tag{A.84}$$

Regarding $c_0(1)$, one easily finds:

$$\delta c_0(1) = \frac{\delta\rho_0(1)}{\rho_0(1)} - \frac{\delta z}{z} \tag{A.85}$$

Substituting equations (A.84) and (A.85) in equation (A.83) and canceling identical terms gives:

$$\delta(\beta PV) = \int \frac{\delta z}{z}\rho(1)\mathrm{d}(1) \iff \frac{\delta(\beta PV)}{\delta z} = \frac{\rho(1)}{z} \tag{A.86}$$

Which is equation (A.81) and so equation (A.82) is proved. In general for perturbation theories, Helmholtz energy is used. Using Euler's theorem for homogeneous functions, the Helmholtz energy is given by $A = N\mu - PV$. With equations (A.74) and (A.5):

$$\beta\mu = \ln\left(\frac{\rho_0(1)}{\Lambda}\right) - c_0(1) \tag{A.87}$$

Where $\Lambda = 1/\lambda^3$. Multiplying the previous equation by $\rho(1)$ and integrating:

$$\beta \mu N = \int \beta \mu \rho(1) \mathrm{d}(1) = \int \rho(1) \left[\ln \left(\frac{\rho_0(1)}{\Lambda} \right) - c_0(1) \right] \mathrm{d}(1) \tag{A.88}$$

Where the first equality comes from the fact that chemical potential and temperature are the same everywhere in the system at equilibrium. So overall:

$$\beta A = \int \left[\rho(1) \ln \left(\frac{\rho_0(1)}{\Lambda} \right) - \rho_0(1) \right] \mathrm{d}(1) - c^{(0)} \tag{A.89}$$

Perturbation Theory

Equation (A.89) is the general equation that gives the Helmholtz energy for a pair potential given by equation (A.67). Even though the first term of equation (A.89) itself is not complicated, $c^{(0)}$ as can be seen in Figure A1.12, it contains many complicated terms. Terms with many F-bonds become more complicated to calculate as the number of F-bonds increases even if this is not theoritically impossible as showed by Zmpitas[10]. That is why perturbation theories are usually used. It consists in only keeping terms (here in $c^{(0)}$) up to a certain order of effects added to a reference potential (here φ_R). These effects called perturbations have to be small enough to justify that not all terms are kept. It is especially important that they be small enough so that high orders terms are smaller that low order terms. For instance here the perturbation potential is of course φ_A and it appears in $c^{(0)}$ as F-bonds. A term of the first order only contains one of such bonds, a term of the second order contains two, etc. Thus a term of the first order has an order of magnitude proportional to the order of magnitude of F, F^2 for a term of the second order, etc. Higher order terms need to have a smaller order of magnitude in order to be neglected so the function F has to give values smaller than 1 and in general very small compared to 1 so that the perturbation theory works even better. Looking at the definition of F in equation (A.69), it can in general provide conditions on φ_A. However in the specific case of potential (A.67) when parameter a in equation (A.65) is small enough compared to σ, steric effects appear. In the case of one association site, this is showed in Figure A1.13.

Considering first two particles 1 and 2 both with one association site, the only way the particles can attract each other is that they are close enough and with an orientation such that the parts of the association site which are outside of the hardcore overlap. Assuming that these two particles do not have too much inertia and that temperature is not too high, once they attract each other, they stay in this attraction state for a while. Assuming now that a third particle arrives with a configuration such as particle 3 in Figure A1.13, it is easy to see that if the size of the association site a is small enough compared to the size σ of the hardcore, it is not possible for three particles to be bonded at the same time. If this is actually the case in a real system, it means that even without doing
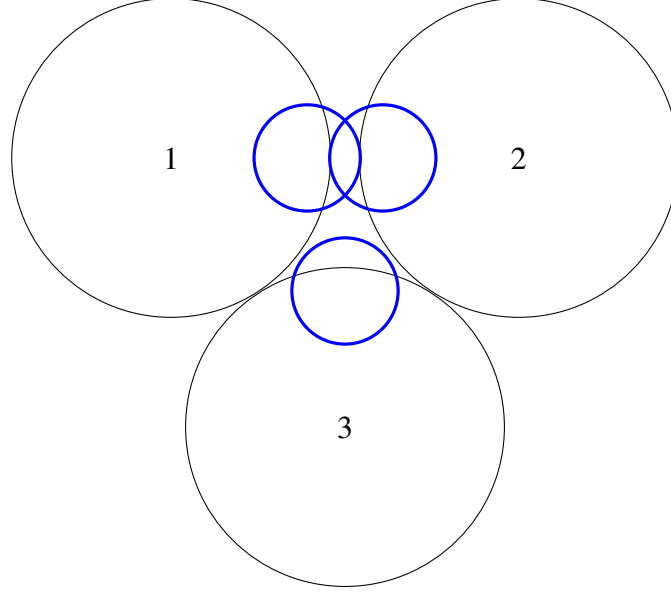
Figure A1.13: Steric effect between three molecules having each one identical association site. Sketch inspired by Chapman[1].

any approximation, all the graphs in $c^{(0)}$ that have at least two consecutive F-bonds vanish. All that remain are graphs without F-bonds or graphs with separated F-bonds. For example, with an obvious numbering, graphs 5,6,17,18,19,20,21,22,23,24,25,26 and 27 in Figure A1.12 are equal to 0. Thus, in such a case, a first order theory only assumes that graphs with multiple separate F-bonds vanish. For the example of Figure A1.12, the first order theory would get rid of graphs 14,15 and 16 on the top of the ones previously mentioned.

From now on, and even when multiple association sites will be dealt with, the first order perturbation theory will be considered (See Zmpitas[10] for any order). In this case, as explained before, only graphs with one F-bond or none are kept in $c^{(0)}$. Graphs that have no F-bond obviously correspond to the case when there is no association. The system without association is the reference system (related to the reference potential) and $c^{(0)}$ will be noted $c_R^{(0)}$ in this case. Equation (A.89) in the case of the reference potential is assumed to be known and will be given by results of section 3 in the case of this derivation. As there is no association in this case, $\rho_0 = \rho$ and equation (A.89) becomes:

$$\beta A_R = \int \left[\rho(1) \ln \left(\frac{\rho(1)}{\Lambda} \right) - \rho(1) \right] \mathrm{d}(1) - c_R^{(0)} \tag{A.90}$$

Thus the only thing that is needed is the difference:

$$\beta A_{\mathrm{assoc}} = \beta(A - A_R) = \int \left[\rho(1) \ln \left(\frac{\rho_0(1)}{\rho(1)} \right) - \rho_0(1) + \rho(1) \right] \mathrm{d}(1) - (c^{(0)} - c_R^{(0)}) \tag{A.91}$$

Where A_{assoc} is the contribution to the Helmholtz energy due to association sites. $c^{(0)} - c_R^{(0)}$ is the

sum of all the graphs in $c^{(0)}$ that have exactly one F-bond. So it can be formulated as follows:

$c^{(0)} - c_R^{(0)}$ = sum of all distinct irreducible connected simple graphs consisting of
one F-bond connecting two ρ_0-circles, some or no ρ-circle and some or   (A.92)
no f_R-bonds

Now, rewriting equation (A.52) in the case $n = 2$ for pair potential φ_R (which defines $g_R = g_2$):

$g_R(1,2)$ = sum of all distinct and at-least-doubly-connected simple graphs
consisting of one e_R-bond connecting two white 1-circle labeled 1 and 2,   (A.93)
some or no ρ-circles and some or no f_R-bonds

Then the following relation holds:

$$c^{(0)} - c_R^{(0)} = \frac{1}{2} \int \rho_0(1) g_R(1,2) f_A(1,2) \rho_0(2) \mathrm{d}(1)\mathrm{d}(2) \tag{A.94}$$

Indeed, considering a graph in the sum (A.93), it can be transformed into a graph in the sum (A.92) using the "transformation rule" defined by equation (A.94): first multiplying a graph from (A.93) by $\rho_0(1) f_A(1,2) \rho_0(2)$ transforms the e_R-bond into a F-bond and white 1-circles into white ρ_0-circles; integrating transforms the two white circles into black circles; finally a factor $1/2$ is needed so that graphs have good symmetry numbers (having black circles instead of white circles allows two kinds of labeling whether former white circles labeled 1 and 2 are respectively given temporary labels 1 and 2 or 2 and 1). Obviously the reversed transformation can be done for each graph of the sum (A.92) to get one or two (depending on the symmetry) graphs from the sum (A.93).

One can get a simple expression for c_1 as well using lemma 2:

$$c_1(1) = \frac{\delta c^{(0)}}{\delta \rho_0}(1) = \int g_R(1,2) f_A(1,2) \rho_0(2) \mathrm{d}(2) \tag{A.95}$$

And the factor $1/2$ vanishes as there are two ways of turning a ρ_0-circle into a white 1-circle. Moreover, by definition of c_1, $\rho/\rho_0 = 1 + \rho_1/\rho_0 = 1 + c_1$ so:

$$\rho(1) = \rho_0(1) + \rho_0(1) \int g_R(1,2) f_A(1,2) \rho_0(2) \mathrm{d}(2) \tag{A.96}$$

Putting equation (A.94) in equation (A.91), one gets:

$$\beta A_{\mathrm{assoc}} = \int \left[\rho(1) \ln \left(\frac{\rho_0(1)}{\rho(1)} \right) - \rho_0(1) + \rho(1) \right] \mathrm{d}(1) - \frac{1}{2} \int \rho_0(1) g_R(1,2) f_A(1,2) \rho_0(2) \mathrm{d}(1)\mathrm{d}(2) \tag{A.97}$$

Using now equation (A.96):

$$\beta A_{\mathrm{assoc}} = \int \left[\rho(1) \ln \left(\frac{\rho_0(1)}{\rho(1)} \right) - \rho_0(1) + \rho(1) \right] \mathrm{d}(1) - \frac{1}{2} \int [\rho(1) - \rho_0(1)] \mathrm{d}(1) \tag{A.98}$$

Defining the fraction of association sites that are not bonded x (which does not depend on coordinates "1" for the uniform system case as densities are constant) verifying:

$$x = \frac{\rho_0(1)}{\rho(1)} = \frac{1}{1 + \int g_R(1,2) f_A(1,2) \rho_0(2) \mathrm{d}(2)} \tag{A.99}$$

It is possible to rewrite equation (A.98) as:

$$\beta A_{\text{assoc}} = \int \rho(1) \left[\ln(x) - \frac{x}{2} - \frac{1}{2} \right] \mathrm{d}(1) = N \left(\ln(x) - \frac{x}{2} - \frac{1}{2} \right) \tag{A.100}$$

Where the second equality arises from the fact that the system is uniform. Equation (A.100) gives the association contribution of an equation of state for a system consisting of a pure component with one associating site.

4.2   General case of multiple association sites

It will now be shown how results of the previous part can be generalized to systems consisting of a pure component with any number of association sites. The physical concepts are the same but the mathematical aspect is more difficult.

The entire pair potential given by equation (A.64) will now be considered. Let Γ be the set of all the association sites $\{A, B, C, \ldots\}$ so that:

$$\varphi_2(1,2) = \varphi_R(1,2) + \sum_{A \in \Gamma} \sum_{B \in \Gamma} \varphi_{AB}(1,2) \tag{A.101}$$

With:

$$\varphi_{AB}(1,2) = \varphi_{AB}(x) \begin{cases} < 0 & , \quad \text{if } x \leq a_{AB} \\ 0 & , \quad \text{otherwise} \end{cases} \tag{A.102}$$

a_{AB} being relative to a couple $\{A, B\}$. Then e-functions and f-functions are defined as before and:

$$e(1,2) = e_R(1,2) \prod_{A \in \Gamma} \prod_{B \in \Gamma} e_{AB}(1,2) \tag{A.103}$$

$$f(1,2) = e_R(1,2) \left(\prod_{A \in \Gamma} \prod_{B \in \Gamma} 1 + f_{AB}(1,2) \right) - 1$$

Noticing that $-1 = f_R - e_R$:

$$f(1,2) = f_R(1,2) + e_R(1,2) \left[\left(\prod_{A \in \Gamma} \prod_{B \in \Gamma} 1 + f_{AB}(1,2) \right) - 1 \right] \tag{A.104}$$

94

Equation (A.104) is very similar to equation (A.69) except that f_A is replaced by $(\prod_{A \in \Gamma} \prod_{B \in \Gamma} 1 + f_{AB}(1,2)) - 1$. It is possible to better understand the meaning of the latter term with the following lemma that will be useful for later calculations:

Lemma 4: Let Γ be any type of finite set and let $\{z_A\}_{A \in \Gamma}$ be a set of any type of objects numbered with elements A belonging to Γ (such that commutative and associative product and sum are defined). Then:

$$\prod_{A \in \Gamma} (1 + z_A) = \sum_{\gamma \subseteq \Gamma} \prod_{A \in \gamma} z_A$$

Where the sum is carried out over all subsets γ of Γ ($\varnothing$ included).

This lemma is easily proved by induction on the number of elements of Γ. So the term between square brackets in equation (A.104) is a sum of all the different possible combinations of f_{AB}-functions (no more than one of each) with different pairs of association sites $\{A, B\}$ (with at least one of such pair). The remaining part of equation (A.104) means that there is an e_R-bond between two particles when some association sites among them are connected, otherwise there is a f_R-bond joining them.

Adaptation of Graph theory

It is now convenient to change the graphs that will be used. Black circles will now always be represented as an empty circle with some points inside it representing association sites. A label will be added to a circle if it is a white circle. Bonds will be represented as before except that f_{AB}-bonds (or previously f_A-bonds) will join association sites and not directly circles. Thus in the case of two association sites A and B, some graphs with two circles are presented in Figure A1.14.
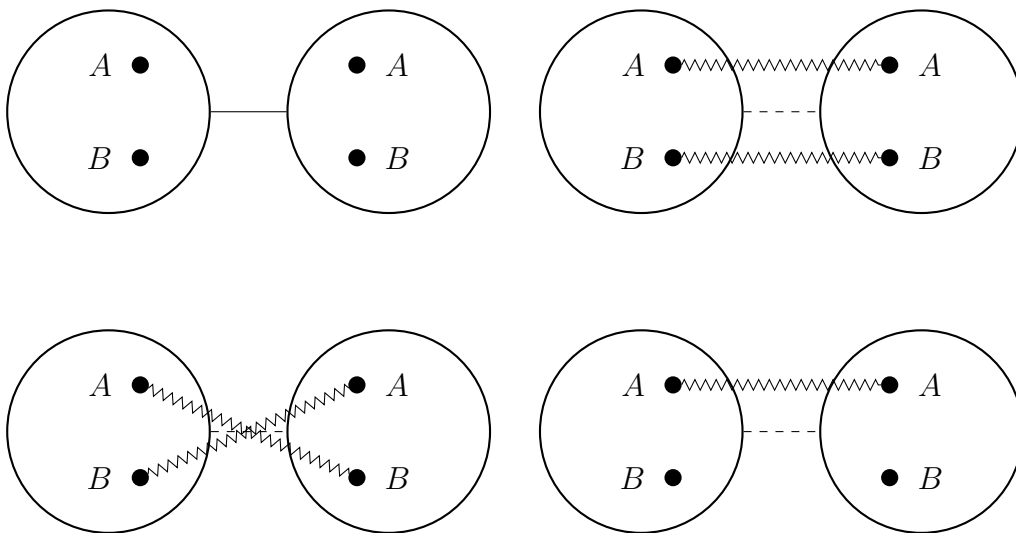
Figure A1.14: Graphs for a system with two association sites.

95

$\ln(\Xi)$ can still be obtained with equation (A.70) except that F-bonds are replaced by an e_R-bond (always) with some f_{AB}-bonds. The singlet density can still be obtained from $\ln(\Xi)$ as it was done before.

Now the problem is to find an efficient way to organize e_R-bonds and f_R-bonds as the former can be written as the sum of no bond and an f_R bond. In the case of one association site, the way it has been done was actually motivated by the steric effect presented on Figure A1.13. Indeed, filling graphs with e_R-bonds implies that the s-mers are irreducible. So when topological reduction is done, all the graphs with the same configuration of attractive bonds (i.e. the same maximal subgraph which is only made of F-bonds) are reduced to the same graph in $c^{(0)}$. That way, steric effect configurations represented by the same s-mers are gathered in only one graph. In the case of multiple association sites, new steric effects can appear and so it will not be the best choice anymore to fill s-mers with e_R-bonds. Before tackling this point, the different steric effects that will be considered should be presented.

The first steric effect, that will be noted I, is the same that was presented in the case of a single association site and in Figure A1.13. The second steric effect (II) is similar to the previous one but it involves one association site on one particle and two on another one. This effect implies that it is not possible for one association site to bond with two association sites of another molecule. This is especially true when association sites are not too close to each other. The third steric effect (III) involves two association sites on one particle and two as well on another one. This effect implies that two bonds between two molecules cannot appear simultaneously. Again, this is especially true when association sites are not too close to each other. All these effects are summarized in Figure A1.15. There is another steric effect that could be considered but it will not be the case here. The reader can refer to Wertheim[5] for more information about this subject. It will be seen in the Perturbation Theory part how these steric effects are taken into account.
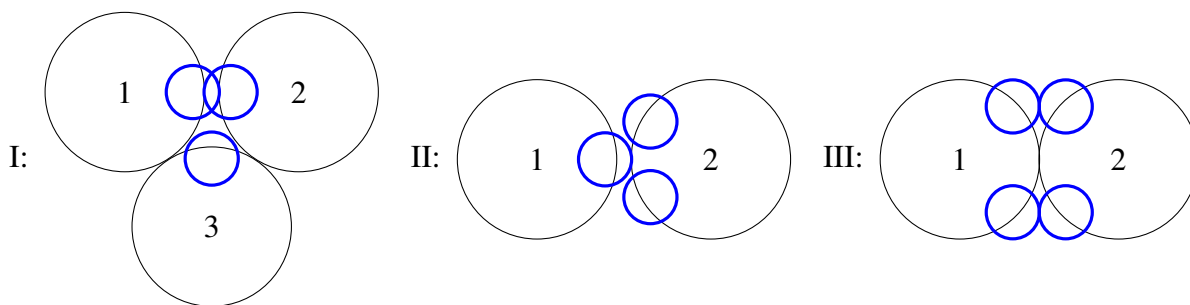
Figure A1.15: Steric effects considered in SAFT. Graphs that represent this type of configuration vanish. Sketch inspired by Chapman[1].

It is better to introduce the following definitions[5] before further development:

Definition 16. Two sites A and B are **bond-connected** if and only if there is a path consisting of attraction bonds (any kind of f_{CD}-bond) and association sites connecting A and B.

Definition 17. Two sites are **constraint-connected** if and only if they are inside the same circle.

Definition 18. A circle is called a **constraint-articulation circle** if upon deletion of the constraint connection (i.e. the circle around the association sites) the graph is separated into several connected, but not mutually connected, fragments. Unbonded sites are not counted as fragments. A graph is now **irreducible** if it is free of constraint-articluation circle.

These three definitions are illustrated in Figure A1.16.
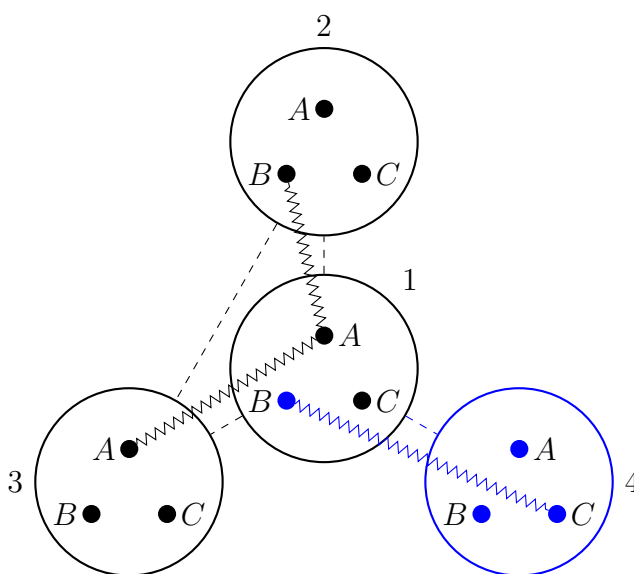
Figure A1.16: Illustration of definitions 16 to 18 on a s-mer. Labels have been added for clarity. Site B in circle 2 and site A in circle 3 are bond-connected. Site A and B in circle 1 are constraint-connected. Circle 1 is a constraint-articulation circle; one of the two associated fragment is blue; site C in circle 1 is not a fragment.

The new way to organize e_R-bonds and f_R will be given as a generalized definition of s-mers:

Definition 19. An **s-mer** is a connected simple graph consisting of s z-circles, some attraction bond (any f_{AB}-bond) such that all the z-circles are connected together by a network of attraction bonds and an e_R-bond between each pair of circles if a site inside one of the circles is bond-connected to a site inside the other circle.

This definition is motivated by steric effects and a justification is provided by Wertheim[5]. This obviously generalizes definition 15 as $F = e_R \times f_A$ and because, in the case of one association site,

97

connected is equivalent to bond-connected. Thus, in Figure A1.16, there is an e_R-bond between circles 2 and 3 because site B in 2 is connected to site A in 3. There is no such connection between circles 3 and 4 so there is no e_R-bond between these two circles. The connection between 3 and 4 is done via a constraint connection provided by circle 1 which is therefore a constraint-articulation circle.

With the exact same argument that was used in the case of one association site and the new definition of s-mers, equation (A.71) still holds and the singlet density is still obtained in the same way.

Topological reduction

As for the case with one association site, new densities will be introduced so that $\ln(\Xi)$ will not depend on z anymore. All graphs are kept and steric effects will be taken into account only in the approximations of the Perturbation Theory in the next part.

Let G be a graph in the singlet density $\rho(1)$. G has one white z-circle labeled 1 with a certain number of association sites depending on the model chosen. Let α be the set of all bonded sites in 1. Then $\rho_\alpha(1)$ is defined as the sum of all the graphs in $\rho(1)$ such that their set of all bonded sites in the white z-circle is exactly α. So:

$$\rho(1) = \sum_{\alpha \subseteq \Gamma} \rho_\alpha(1) \tag{A.105}$$

$\varnothing$ is included in the subsets of Γ (and will always be) so that the monomer density $\rho_0(1)$ is in the sum. The graph in Figure A1.16, with circle 1 as a white circle and the others as black circles, is a term of $\rho_{A,B}(1)$.

Again, the subset $c_0(1)$ of graphs in $\rho_0(1)/z$ for which circle 1 is not a constraint-articulation circle is given by:

$$c_0(1) = \ln\left(\frac{\rho_0(1)}{z}\right) \tag{A.106}$$

The proof is the same as the proof of equation (A.74) (using lemma 1). Still as in the case of one association site, $\rho_0(1)$ is a factor of $\rho_\alpha(1)$ for a given set α. Each $\dfrac{\rho_\alpha(1)}{\rho_0(1)}$ contains some graphs for which 1 is not a constraint-articulation circle. The sum of these graphs defines $c_\alpha(1)$. Regarding the others, 1 is a constraint-articulation circle so they are made of different fragments (or subgraphs) for which 1 is not a constraint-articulation circle anymore and they belong to different sum of graphs c_γ with $\gamma \subset \alpha$ and $\{\gamma\} = P(\alpha)$ (meaning the set of all the sets γ is a partition of α). So overall, it gives the following result:

$$\rho_\alpha(1) = \rho_0(1) \sum_{P(\alpha)=\{\gamma\}} \prod_\gamma c_\gamma(1) \tag{A.107}$$

$$\forall \gamma \neq \varnothing, c_\gamma(1) = \text{the subset of graphs in } \rho_\gamma \text{ for which 1 is not a constraint-articulation circle} \tag{A.108}$$

Where γ is any set of bonded association sites and the sum in equation (A.107) is carried out over all the partitions $\{\gamma\}$ of α (these partitions do not contain $\varnothing$). It is easier to understand this result with the graph in Figure A1.17.
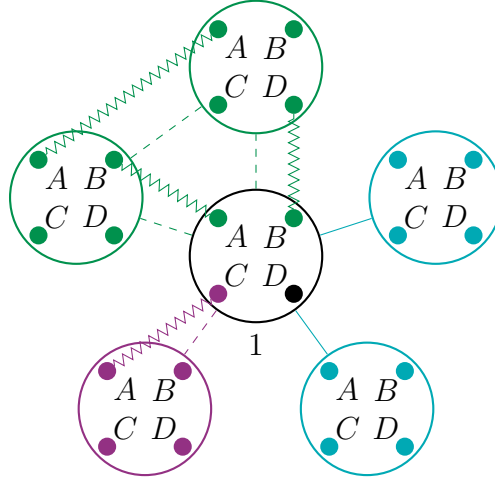
Figure A1.17: Illustration of equation (A.107). The graph in this figure belongs to the sum of graph $\rho_{\{A,B,C\}}(1)$. Only the central circle labeled 1 is a white z-circle.

The graph in Figure A1.17 belongs to the sum of graph $\rho_{\{A,B,C\}}$ because only association sites A, B and C in the white circle 1 are connected with attractive bonds. The green fragment belongs to $c_{\{A,B\}}$, the purple fragment belongs to $c_{\{C\}}$ and the blue part (two fragments) belongs to $\rho_0(1)$. The black central part belongs to each part (and each part with the central part forms a graph) and the overall graph is the product of three graphs thus belonging to $\rho_0(1)c_{\{A,B\}}c_{\{C\}}$. Of course there are other partitions of $\{A, B, C\}$ which explains the sum in (A.107). Seeing how c_γ were defined in equation (A.108) (or equation (A.106) when $\gamma = \varnothing \Rightarrow c_\gamma = c_0$) it is clear that they do not contain any white articulation circles. Moreover, because of the way they were filled by e_R-bonds, bond-connected subgraphs inside s-mers are free of constraint-articulation circles. Thus only constraint-articulation circles between not bond-connected subgraphs need to be removed inside s-mers. Any black constraint-articulation circle might still exist outside s-mers ($s \geq 2$).

As for the case of one association site, lemma 3 will be adapted and used, noticing that c_γ functions behave like h_n functions. Again, considering a black constraint-articulation circle i inside

a s-mer of G with s$\geq$ 2, a part G_p (which makes i a constraint articulation circle) of G attached to the s-mer cannot be any graph in the singlet density. This comes again from the manner s-mers have been filled with e_R-bonds. Indeed, let $\alpha(i)$ be the set of association sites of i which are connected. Then G_p cannot be bond-connected to (meaning one association site of G_p is bond-connected to) an association site in $\alpha(i)$. Otherwise according to definition 19, there would be e_R-bonds between G_p and each circle of the s-mer i is part of, and i would not be a constraint-articulation circle. This reasoning needs to be repeated for each part of the graph which makes i a constraint-articulation circle. Thus in lemma 3, each black z-circle i is not replaced by a ρ-circle but by the sum $\sigma_{\Gamma-\alpha(i)}$ of all the graphs in ρ which are not connected to $\alpha(i)$. So the sums of graph σ_α verify:

$$\forall \alpha \subseteq \Gamma, \sigma_\alpha(1) = \sum_{\gamma \subseteq \alpha} \rho_\gamma(1) \tag{A.109}$$

The only difficulty in this adapted version of lemma 3 is again to prove that symmetry numbers are correct and that there is no need to add any prefactor. This is done by successively applying lemma 3 for each σ_α separately.

In the case of a monomer black circle, the set of connected association sites is $\alpha = \varnothing$ and $\sigma_{\Gamma-\alpha} = \sigma_\Gamma = \rho$. Indeed any graph in ρ can be connected to a monomer as all its association sites are free. If $\alpha = \Gamma$, $\sigma_{\Gamma-\alpha} = \sigma_\varnothing = \sigma_0 = \rho_0$ as only f_R-bonds can be used to connect them to another graph once all the association sites are connected.

So now $c^{(0)}$ is given by:

$c^{(0)}$ = the sum of all distinct irreducible connected simple graphs consisting of s-mers and f_R-bonds; each circle i is a black $\sigma_{\Gamma-\alpha(i)}$-circle where $\alpha(i)$ is the set of connected association sites in i

$$\tag{A.110}$$

And using lemma 2, it is easy to verify that:

$$c_\alpha(1) = \frac{\delta c^{(0)}}{\delta \sigma_{\Gamma-\alpha}}(1) \tag{A.111}$$

In the case of one association site, one can retrieve equations (A.78) to (A.80).

Site Operators

In order to simplify calculations, Wertheim[5] introduced site operators. For each site A in Γ of a circle i, the site operator $\varepsilon_A(i)$ is an operator which commutes and verifies:

$$\varepsilon_A^2(i) = 0 \tag{A.112}$$

It is called an operator because it is not a number but nor is it a function as the value of $\varepsilon_A(i)$ is not useful. It should be seen as something similar to the complex number i verifying $i^2 = -1$. Wertheim details a bit more what these operators are but it is not needed here. For a set α of connected association sites, ε_α is defined as follows:

$$\varepsilon_\alpha(i) = \prod_{A \in \alpha} \varepsilon_A(i) \tag{A.113}$$

With these operators, it is possible to create an object $\mathring{x}$ which gathers all the required values of a physical quantity x depending on the state of each site:

$$\mathring{x} = x_0 + \sum_{\substack{\alpha \subseteq \Gamma \\ \alpha \neq \varnothing}} x_\alpha \varepsilon_\alpha \tag{A.114}$$

Regular summation and multiplication can be applied to these objects. Equation (A.112) assures that when multiplying two objects of the form (A.114), it remains an object with the same form:

$$\mathring{x}\mathring{y} = x_0 y_0 + \sum_{\substack{\alpha \subseteq \Gamma \\ \alpha \neq \varnothing}} \left(\sum_{\beta \subseteq \Gamma} x_\beta y_{\alpha-\beta} \right) \varepsilon_\alpha \tag{A.115}$$

Because all terms containing the same site operator several times vanish. It is possible to define other functions for these objects using the general Taylor series of the functions of interest. For instance the following equations will be needed:

$$\ln(1 \pm \varepsilon) = \pm\varepsilon \tag{A.116}$$

$$\frac{1}{1+\varepsilon} = 1 - \varepsilon \tag{A.117}$$

For any object of the type given by equation (A.114), $\langle \mathring{x} \rangle$ is defined by:

$$\langle \mathring{x} \rangle = x_\Gamma \tag{A.118}$$

For instance, from equation (A.115), it follows that:

$$\langle \mathring{x}\mathring{y} \rangle = \sum_{\beta \subseteq \Gamma} x_\beta y_{\Gamma-\beta} \tag{A.119}$$

Now using this formalism for different quantities introduced before:

$$\mathring{\rho}(1) = \rho_0(1) + \sum_{\substack{\alpha \subseteq \Gamma \\ \alpha \neq \varnothing}} \rho_\alpha(1)\varepsilon_\alpha(1) \tag{A.120}$$

$$\mathring{\sigma}(1) = \sigma_0(1) + \sum_{\substack{\alpha \subseteq \Gamma \\ \alpha \neq \varnothing}} \sigma_\alpha(1)\varepsilon_\alpha(1) \tag{A.121}$$

$$\mathring{c}(1) = c_0(1) + \sum_{\substack{\alpha \subseteq \Gamma \\ \alpha \neq \varnothing}} c_\alpha(1) \varepsilon_\alpha(1) \tag{A.122}$$

The following relation will now be derived:

$$\mathring{\sigma}(1) = \mathring{\rho}(1) \prod_{A \in \Gamma} (1 + \varepsilon_A(1)) \tag{A.123}$$

This is the equivalent of equation (A.109) with site operators. Using equation (A.109) and remembering that $\sigma_0 = \rho_0$, the left hand side becomes:

$$\mathring{\sigma}(1) = \rho_0(1) + \sum_{\substack{\alpha \subseteq \Gamma \\ \alpha \neq \varnothing}} \sum_{\gamma \subseteq \alpha} \rho_\gamma(1) \varepsilon_\alpha(1) \tag{A.124}$$

In the sum, separating cases $\gamma = \alpha$ and $\gamma \neq \alpha$ and using equation (A.120), it becomes:

$$\mathring{\sigma}(1) = \mathring{\rho}(1) + \sum_{\substack{\alpha \subseteq \Gamma \\ \alpha \neq \varnothing}} \sum_{\gamma \subset \alpha} \rho_\gamma(1) \varepsilon_\alpha(1) \tag{A.125}$$

Using lemma 4 in the right hand side of equation (A.123) plus equation (A.120) again:

$$\mathring{\rho}(1) \prod_{A \in \Gamma} (1 + \varepsilon_A(1)) = \mathring{\rho}(1) + \mathring{\rho}(1) \sum_{\substack{\alpha \subseteq \Gamma \\ \alpha \neq \varnothing}} \varepsilon_\alpha(1) \tag{A.126}$$

$$= \mathring{\rho}(1) + \left(\rho_0(1) + \sum_{\substack{\gamma \subseteq \Gamma \\ \gamma \neq \varnothing}} \rho_\gamma(1) \varepsilon_\gamma(1) \right) \sum_{\substack{\alpha \subseteq \Gamma \\ \alpha \neq \varnothing}} \varepsilon_\alpha(1) \tag{A.127}$$

$$= \mathring{\rho}(1) + \rho_0(1) \sum_{\substack{\alpha \subseteq \Gamma \\ \alpha \neq \varnothing}} \varepsilon_\alpha(1) + \sum_{\substack{\gamma \subseteq \Gamma \\ \gamma \neq \varnothing}} \rho_\gamma(1) \varepsilon_\gamma(1) \sum_{\substack{\alpha \subseteq \Gamma \\ \alpha \neq \varnothing}} \varepsilon_\alpha(1) \tag{A.128}$$

Using equation (A.112), it becomes:

$$\mathring{\rho}(1) \prod_{A \in \Gamma} (1 + \varepsilon_A(1)) = \mathring{\rho}(1) + \rho_0(1) \sum_{\substack{\alpha \subseteq \Gamma \\ \alpha \neq \varnothing}} \varepsilon_\alpha(1) + \sum_{\substack{\alpha \subseteq \Gamma \\ \alpha \neq \varnothing}} \sum_{\substack{\gamma \subseteq \Gamma \\ \gamma \neq \varnothing \\ \gamma \cap \alpha = \varnothing}} \rho_\gamma(1) \varepsilon_{\gamma \cup \alpha}(1) \tag{A.129}$$

In the last term, the sum is done for all the (non-empty) possible sets $\gamma \cup \alpha$ so that $\varepsilon_{\gamma \cup \alpha}(1) \neq 0$ (implied by the condition $\gamma \cap \alpha = \varnothing$). For all these sets, there is a second summation over all the non-empty sets $\gamma \subseteq \Gamma$ and obviously the constraint $\gamma \subseteq \gamma \cup \alpha$ is more restrictive. So the first sum can be carried over all the non-empty sets $\gamma \cup \alpha \subseteq \Gamma$ and the second one over all the non-empty sets $\gamma \subset \gamma \cup \alpha$ (the inclusion symbol here is $\subset$ and not $\subseteq$ because α can not be empty). Simply renaming α all the sets $\alpha \cup \gamma$ (the outer sum does not depend on the inner one):

$$\mathring{\rho}(1) \prod_{A \in \Gamma} (1 + \varepsilon_A(1)) = \mathring{\rho}(1) + \rho_0(1) \sum_{\substack{\alpha \subseteq \Gamma \\ \alpha \neq \varnothing}} \varepsilon_\alpha(1) + \sum_{\substack{\alpha \subseteq \Gamma \\ \alpha \neq \varnothing}} \sum_{\substack{\gamma \subset \alpha \\ \gamma \neq \varnothing}} \rho_\gamma(1) \varepsilon_\alpha(1) \tag{A.130}$$

Including the second term corresponding to $\gamma = \varnothing$ in the third term:

$$\mathring{\rho}(1) \prod_{A \in \Gamma} (1 + \varepsilon_A(1)) = \mathring{\rho}(1) + \sum_{\substack{\alpha \subseteq \Gamma \\ \alpha \neq \varnothing}} \sum_{\gamma \subset \alpha} \rho_\gamma(1)\varepsilon_\alpha(1) \tag{A.131}$$

Equation (A.125) and (A.131) prove equation (A.123). By applying equation (A.117) for each factor in the product of equation (A.123), $\mathring{\rho}(1)$ is:

$$\mathring{\rho}(1) = \mathring{\sigma}(1) \prod_{A \in \Gamma} (1 - \varepsilon_A(1)) \tag{A.132}$$

The following relation will also be derived:

$$\frac{\mathring{\rho}(1)}{\rho_0(1)} = \exp(\mathring{c}(1) - c_0(1)) \tag{A.133}$$

This is the equivalent of equation (A.107) with site operators. Using equation (A.120) followed by equation (A.107), the left hand side becomes:

$$\frac{\mathring{\rho}(1)}{\rho_0(1)} = 1 + \sum_{\substack{\alpha \subseteq \Gamma \\ \alpha \neq \varnothing}} \left(\sum_{P(\alpha)=\{\gamma\}} \prod_\gamma c_\gamma(1) \right) \varepsilon_\alpha(1) \tag{A.134}$$

The right hand side of equation (A.133) can be written as:

$$\exp(\mathring{c}(1) - c_0(1)) = \prod_{\substack{\alpha \subseteq \Gamma \\ \alpha \neq \varnothing}} \exp(c_\alpha(1)\varepsilon_\alpha(1)) \tag{A.135}$$

With equation (A.112), is is easily seen that $\exp(\varepsilon) = 1 + \varepsilon$ so:

$$\exp(\mathring{c}(1) - c_0(1)) = \prod_{\substack{\alpha \subseteq \Gamma \\ \alpha \neq \varnothing}} (1 + c_\alpha(1)\varepsilon_\alpha(1)) \tag{A.136}$$

Now using lemma 4 (with $\alpha \subseteq \Gamma$ being equivalent to $\alpha \in$ the set $\{\Gamma\}$ of all the subsets in Γ) it becomes:

$$\exp(\mathring{c}(1) - c_0(1)) = \sum_{\gamma \subseteq \{\Gamma\}} \prod_{\alpha \in \gamma} c_\alpha(1)\varepsilon_\alpha(1) \tag{A.137}$$

According to equation (A.112), the product can be different from 0 only if all the α form a partition of the reunion of the sets forming γ. But the different α are elements of γ so that means that all the elements in γ must be disjointed. Thus it is equivalent to carrying out the sum over all the partitions of subsets of Γ (by first summing over all the subsets and then the partitions of each subset):

$$\exp(\mathring{c}(1) - c_0(1)) = \sum_{\gamma \subseteq \Gamma} \sum_{P(\gamma)=\{\alpha\}} \prod_\alpha c_\alpha(1)\varepsilon_\alpha(1) \tag{A.138}$$

103

Separating the term $\gamma = \varnothing$ and calculating the product of the association site operators:

$$\exp(\mathring{c}(1) - c_0(1)) = 1 + \sum_{\substack{\gamma \subseteq \Gamma \\ \gamma \neq \varnothing}} \left(\sum_{P(\gamma)=\{\alpha\}} \prod_\alpha c_\alpha(1) \right) \varepsilon_\gamma(1) \tag{A.139}$$

The right hand side of the previous equation is the same as the right hand side of equation (A.134) by exchanging the names of dummy variables α and γ so equation (A.133) is proved. Taking the logarithm of equation (A.133) and using equations (A.132) and (A.116):

$$\mathring{c}(1) - c_0(1) = \ln\left(\frac{\mathring{\sigma}(1)}{\sigma_0(1)} \right) - \sum_{A \in \Gamma} \varepsilon_A(1) \tag{A.140}$$

From now on, it is convenient to introduce the following notation for any quantity x:

$$\hat{x} = \frac{x}{x_0} \tag{A.141}$$

From equation (A.140), it is possible to calculate $c_\alpha(1)$ as a function of the more useful quantities σ_α. The second term of this equation means that if α is a set containing only one association site, there must be a -1 term added to $c_\alpha(1)$. Using the Taylor series of $\ln$, equation (A.140) becomes:

$$\sum_{\substack{\alpha \subseteq \Gamma \\ \alpha \neq \varnothing}} c_\alpha(1)\varepsilon_\alpha(1) = \sum_{n=0}^\infty \frac{(-1)^n}{n+1} \left(\sum_{\substack{\alpha \subseteq \Gamma \\ \alpha \neq \varnothing}} \hat{\sigma}_\alpha(1)\varepsilon_\alpha(1) \right)^{n+1} - \sum_{A \in \Gamma} \varepsilon_A(1) \tag{A.142}$$

Expanding the product in the first sum of the right hand side, each non-zero term appears $(n+1)!$ times. This can be seen from the multinomial theorem or from the fact that identical term appears with factors in a different order and that there are $(n+1)!$ different orders (for example a term containing a, b and c can appear as $3! = 6$ terms abc, acb, bac, bca, cab and cba). Therefore:

$$\sum_{\substack{\alpha \subseteq \Gamma \\ \alpha \neq \varnothing}} c_\alpha(1)\varepsilon_\alpha(1) = \sum_{n=0}^\infty (-1)^n n! \left(\sum_{\{\alpha,n+1\}} \prod_\alpha \hat{\sigma}_\alpha(1)\varepsilon_\alpha(1) \right) - \sum_{A \in \Gamma} \varepsilon_A(1) \tag{A.143}$$

Where the second sum is carried out over all the sets $\{\alpha, n+1\}$ of $n+1$ disjointed sets α. In the latter sum, if $n+1$ is greater than the total number of association sites, the following product is zero. So the sum carried out over n must go up to $n = n(\Gamma) - 1$ where for any set α, $n(\alpha)$ is the number of association sites inside the set α. As before, $\{\alpha, n+1\}$ must be the partition of a set γ. So the sum carried out over $\{\alpha, n+1\}$ can be replaced by a (double) sum carried out over all the sets (with at least $n+1$ elements) included in Γ and over all the partitions $\{\alpha\}$ of γ with $n+1$ elements. Exchanging the dummy variables α and γ, it becomes:

$$\sum_{\substack{\alpha \subseteq \Gamma \\ \alpha \neq \varnothing}} c_\alpha(1)\varepsilon_\alpha(1) = \sum_{n=0}^{n(\Gamma)-1} (-1)^n n! \left(\sum_{\substack{\alpha \subseteq \Gamma \\ n(\alpha) \geq n+1}} \sum_{P(\alpha)=\{\gamma,n+1\}} \prod_\gamma \hat{\sigma}_\gamma(1)\varepsilon_\alpha(1) \right) - \sum_{A \in \Gamma} \varepsilon_A(1) \tag{A.144}$$

In the right hand side, by exchanging the order of the first two sums, it is possible to get rid of the constraint $n(\alpha) \geq n+1$ and then the sum carried out over n can be included in the sum carried out over $P(\alpha) = \{\gamma, n+1\}$:

$$\sum_{\substack{\alpha \subseteq \Gamma \\ \alpha \neq \varnothing}} c_\alpha(1) \varepsilon_\alpha(1) = \sum_{\alpha \subseteq \Gamma} \left(\sum_{P(\alpha) = \{\gamma, n+1\}} (-1)^n n! \prod_\gamma \hat{\sigma}_\gamma(1) \right) \varepsilon_\alpha(1) - \sum_{A \in \Gamma} \varepsilon_A(1) \tag{A.145}$$

So the sum carried out over $P(\alpha) = \{\gamma, n+1\}$ means now over all the partitions γ of α, $n+1$ being the number of element in $P(\alpha)$ needed to calculate the inner product. Finally, c_α is given by:

$$c_\alpha(1) = \sum_{P(\alpha) = \{\gamma, n\}} (-1)^{(n-1)} (n-1)! \prod_\gamma \hat{\sigma}_\gamma(1) - \delta_{n(\alpha),1} \tag{A.146}$$

Where δ is the Kronecker delta.

Combining equations (A.106) and (A.133), one gets:

$$\exp\left[\mathring{c}(1)\right] = \frac{\mathring{\rho}(1)}{z} \tag{A.147}$$

Or again, using equations (A.132) and (A.116):

$$\mathring{c}(1) = \ln\left(\frac{\mathring{\sigma}(1)}{z}\right) - \sum_{A \in \Gamma} \varepsilon_A(1) \tag{A.148}$$

This equation will be useful later.

Thermodynamics

Repeating what as been done for the single association site case, it will now be proven that:

$$\beta PV = \int \langle \mathring{\sigma}(1) \left[1 - \mathring{c}(1)\right] \rangle \, \mathrm{d}(1) + c^{(0)} \tag{A.149}$$

Is equivalent to equation (A.81). Again, the variation of the previous equation must be taken:

$$\delta(\beta PV) = \int \langle \delta \mathring{\sigma}(1) - \delta \mathring{\sigma}(1) \mathring{c}(1) - \mathring{\sigma}(1) \delta \mathring{c}(1) \rangle \, \mathrm{d}(1) + \delta c^{(0)} \tag{A.150}$$

The variation of equation (A.148) gives:

$$\delta \mathring{c}(1) = \frac{\delta \mathring{\sigma}(1)}{\mathring{\sigma}(1)} - \frac{\delta z}{z} \Rightarrow \delta \mathring{\sigma}(1) - \mathring{\sigma}(1) \delta \mathring{c}(1) = \mathring{\sigma}(1) \frac{\delta z}{z} \tag{A.151}$$

Equation (A.111) implies:

$$\delta c^{(0)} = \int \sum_{\alpha \subseteq \Gamma} c_\alpha(1) \delta \sigma_{\Gamma - \alpha} \mathrm{d}(1) = \int \langle \mathring{c}(1) \delta \mathring{\sigma}(1) \rangle \, \mathrm{d}(1) \tag{A.152}$$

105

Where equation (A.119) has been used. Putting the two previous equations in (A.150) gives exactly equation (A.81) because $\langle \mathring{\sigma}(1) \rangle = \sigma_\Gamma(1) = \rho(1)$. Using equation (A.119), it is easy to notice that equation (A.149) can be written as:

$$\beta PV = \int \left[\rho(1) - \sum_{\alpha \subseteq \Gamma} \sigma_{\Gamma-\alpha}(1)c_\alpha(1) \right] \mathrm{d}(1) + c^{(0)} \tag{A.153}$$

Then using equation (A.88):

$$\beta A = \int \left[\rho(1) \ln\left(\frac{\rho_0(1)}{\Lambda}\right) - \rho(1) + \sum_{\substack{\alpha \subseteq \Gamma \\ \alpha \neq \varnothing}} \sigma_{\Gamma-\alpha}(1)c_\alpha(1) \right] \mathrm{d}(1) - c^{(0)} \tag{A.154}$$

It is useful to have an expression with densities only. Thus equation (A.146) can be used:

$$\beta A = \int \left[\sigma_\Gamma(1) \ln\left(\frac{\sigma_0(1)}{\Lambda}\right) + Q(1) \right] \mathrm{d}(1) - c^{(0)} \tag{A.155}$$

Where:

$$Q(1) = \sum_{\substack{\alpha \subseteq \Gamma \\ \alpha \neq \varnothing}} \sigma_{\Gamma-\alpha}(1) \left(\sum_{P(\alpha)=\{\gamma,n\}} (-1)^{n-1}(n-1)! \prod_\gamma \hat{\sigma}_\gamma(1) - \delta_{n(\alpha),1} \right) - \sigma_\Gamma(1) \tag{A.156}$$

Taking out the Kronecker delta and separating the case $\alpha = \Gamma$ in the first sum, one gets:

$$Q(1) = -\sum_{A \in \Gamma} \sigma_{\Gamma-A}(1) + \sigma_0(1) \sum_{P(\Gamma)=\{\gamma,n\}} (-1)^{n-1}(n-1)! \prod_\gamma \hat{\sigma}_\gamma(1) - \sigma_\Gamma(1) \tag{A.157}$$
$$+ \sigma_0(1) \sum_{\substack{\alpha \subseteq \Gamma \\ \alpha \neq \varnothing}} \sum_{P(\alpha)=\{\gamma,n\}} (-1)^{n-1}(n-1)! \hat{\sigma}_{\Gamma-\alpha}(1) \prod_\gamma \hat{\sigma}_\gamma(1)$$

Where equation (A.141) for $\sigma_{\Gamma-\alpha}(1)$ has been used. In the first sum, the case $n = 1$ gives a term $\sigma_\Gamma(1)$ which will cancel itself with the $-\sigma_\Gamma(1)$ term. In the last sum carried out over $P(\alpha) = \{\gamma, n\}$, one wants to introduce the $\hat{\sigma}_{\Gamma-\alpha}(1)$ term inside the product. Doing so, γ will become a partition of Γ with $n' = n + 1$ elements. It must be remembered that there is a outer sum carried out over all the α included in Γ. Performing the change $n \to n' - 1$, $Q(1)$ can be rewritten as follows:

$$Q(1) = -\sum_{A \in \Gamma} \sigma_{\Gamma-A}(1) + \sigma_0(1) \sum_{P(\Gamma)=\{\gamma,n \geq 2\}} (-1)^{n-1}(n-1)! \prod_\gamma \hat{\sigma}_\gamma(1) \tag{A.158}$$
$$+ \sigma_0(1) \sum_{\substack{\alpha \subseteq \Gamma \\ \alpha \neq \varnothing}} \sum_{\substack{P(\Gamma)=\{\gamma,n' \geq 2\} \\ \alpha \in \gamma}} (-1)^{n'-2}(n'-2)! \prod_\gamma \hat{\sigma}_\gamma(1)$$

For a given n', all the sums carried out over $P(\Gamma) = \{\gamma, n' \geq 2\}$ will be equal no matter what α is. So the outer sum carried out over α simply multiplies each inner sum for a given n' by the different

possible choices of α in $\{\gamma, n' \geq 2\}$. This is the number of elements n' in γ. Thus, changing the dummy variable n' to n:

$$Q(1) = -\sum_{A \in \Gamma} \sigma_{\Gamma-A}(1) + \sigma_0(1) \sum_{P(\Gamma)=\{\gamma,n\geq 2\}} (-1)^{n-1}(n-1)! \prod_\gamma \hat{\sigma}_\gamma(1) \qquad \text{(A.159)}$$
$$- \sigma_0(1) \sum_{P(\Gamma)=\{\gamma,n\geq 2\}} (-1)^{n-1} n(n-2)! \prod_\gamma \hat{\sigma}_\gamma(1)$$

Noticing that $n(n-2)! - (n-1)! = (n-2)!$:

$$Q(1) = -\sum_{A \in \Gamma} \sigma_{\Gamma-A}(1) + \sigma_0(1) \sum_{P(\Gamma)=\{\gamma,n\geq 2\}} (-1)^n (n-2)! \prod_\gamma \hat{\sigma}_\gamma(1) \qquad \text{(A.160)}$$

Equation (A.155) gives the exact value of Helmholtz energy for any number of association sites. $Q(1)$ given by equation (A.160) only depends on different density quantities and cannot be simplified any more for now. $c^{(0)}$ is the only term which depends on the attractive part of the pair potential. As before, a perturbation will be used in order to simplify that term.

Perturbation Theory

As evoked above, steric effects have to be taken into account and, in the case of SAFT, all three effects summarized in Figure A1.15. These configurations correspond to some type of graphs in $c^{(0)}$, the only part in Helmholtz energy which contains attractive energies. The first two steric effects I and II imply what Wertheim calls the single bonding condition which means that one association site can be either not bonded or bonded to only one other association site. Configurations where a site is bonded to multiple other association sites must be terms of order 2 (for instance containing a product $f_{AB}f_{AC}$) inside $c^{(0)}$ so they would be neglected in the first order perturbation theory. Thus in the square bracket of equation (A.104), only terms which satisfy steric effects I and II can be kept. It is convenient to create an operator $\mathring{f}$:

$$\mathring{f}(1,2) = \sum_{A \in \Gamma} \sum_{B \in \Gamma} f_{AB}(1,2) \varepsilon_A(1) \varepsilon_B(2) \qquad \text{(A.161)}$$

So that all the terms inside the square bracket of equation (A.104), which satisfy steric effects I and II, are inside the operator $\exp\left[\mathring{f}(1,2)\right] - 1$ (this is easily seen by considering the Taylor series of $\exp$). However it would still contain terms like $f_{AB}(1,2)f_{CD}(1,2)\varepsilon_A(1)\varepsilon_B(2)\varepsilon_C(1)\varepsilon_D(2)$ which are not allowed because of steric effect III. These terms are of order 2 as well because they contain at least two attractive bonds and so they are neglected in the first order perturbation theory. Attractive terms satisfying all three steric effects are then exactly the ones in $\mathring{f}$.

Using equation (A.155) directly with all the possible combinations of f_{AB}-bonds would lead to exactly the same result as only using it with combinations inside $\mathring{f}$ if association sites were not too

big and angles between them great enough. Thus using $\mathring{f}$ simplifies calculations and leads to the same results.

However even in this case there still are graphs containing more than one attractive bond which are difficult to take into account (again, the reader can refer to Zmpitas[10] to see a generalization of the perturbation theory to any order). That is why only graphs with one attractive bond will now be kept.

As for the one association site case, it is assumed that the Helmholtz energy is known in the case of the absence of association sites (it is given by equation (A.90)) and the following difference (similar to equation (A.91)) is considered:

$$\beta A_{\text{assoc}} = \beta(A - A_R) = \int \left[\sigma_\Gamma(1) \ln \left(\frac{\sigma_0(1)}{\sigma_\Gamma(1)} \right) + \sigma_\Gamma(1) + Q(1) \right] d(1) - (c^{(0)} - c_R^{(0)}) \quad \text{(A.162)}$$

$c^{(0)} - c_R^{(0)}$ is evaluated the same way as before (equation (A.94)), the only difference is that all the allowed attractive bonds have to be considered. These bonds are all the $f_{AB}(1,2)$. Monomer densities in equation (A.94) must be changed accordingly so that it satisfies equation (A.110) i.e. $\sigma_{\Gamma-A}(1)$ instead of $\rho_0(1)$ and $\sigma_{\Gamma-B}(2)$ instead of $\rho_0(2)$. The sums of all the products $\sigma_{\Gamma-A}(1)f_{AB}(1,2)\sigma_{\Gamma-B}(2)$ to be considered is noted $\left\langle \mathring{\sigma}(1)\mathring{f}(1,2)\mathring{\sigma}(2) \right\rangle_{1,2}$. Finally:

$$c^{(0)} - c_R^{(0)} = \frac{1}{2} \int g_R(1,2) \left\langle \mathring{\sigma}(1)\mathring{f}(1,2)\mathring{\sigma}(2) \right\rangle_{1,2} d(1)d(2) \quad \text{(A.163)}$$

$$= \sum_{A\in\Gamma} \sum_{B\in\Gamma} \frac{1}{2} \int g_R(1,2)\sigma_{\Gamma-A}(1)f_{AB}(1,2)\sigma_{\Gamma-B}(2)d(1)d(2) \quad \text{(A.164)}$$

And directly from equation (A.111):

$$c_A(1) = \sum_{B\in\Gamma} \int g_R(1,2)\sigma_{\Gamma-B}(2)f_{AB}(1,2)d(2) \quad \text{(A.165)}$$

$$c_\alpha = 0, \text{if } n(\alpha) \geq 2 \quad \text{(A.166)}$$

Then for all $\alpha \neq \varnothing$, it directly comes from equation (A.107):

$$\rho_\alpha(1) = \rho_0(1) \prod_{A\in\alpha} c_A(1) \quad \text{(A.167)}$$

$$\frac{\rho_\alpha(1)}{\rho_0(1)} = \prod_{A\in\alpha} \frac{\rho_A(1)}{\rho_0(1)} \quad \text{(A.168)}$$

Equation (A.168) is proved by noticing that equation (A.167) implies that $\rho_A(1) = \rho_0(1)c_A(1)$. Equation (A.140) can then be used to give a similar expression for the σ_α densities. Putting equation (A.166) into it and applying $\exp$ to both sides of the resulting equation:

$$\frac{\mathring{\sigma}(1)}{\sigma_0(1)} = \exp \left(\sum_{A\in\Gamma} (c_A(1) + 1)\varepsilon_A(1) \right) = \prod_{A\in\Gamma} \exp \left((c_A(1) + 1)\varepsilon_A(1) \right) \quad \text{(A.169)}$$

108

Then successively applying equation (A.116) written as $\exp(\varepsilon) = 1 + \varepsilon$ and lemma 4, one gets:

$$\frac{\mathring{\sigma}(1)}{\sigma_0(1)} = \sum_{\alpha \subseteq \Gamma} \prod_{A \in \alpha} (c_A(1) + 1)\varepsilon_\alpha(1) \tag{A.170}$$

From this, it directly follows that:

$$\hat{\sigma}_A = c_A(1) + 1 \tag{A.171}$$

And so:

$$\hat{\sigma}_\alpha = \prod_{A \in \alpha} \hat{\sigma}_A(1) \tag{A.172}$$

This is all that is needed in SAFT from Wertheim's work[3–6]. Chapman did some simplifications in his Ph.D. thesis[9] following what Wertheim did for the pure component case. They are shown below.

The first step is to introduce $\Delta_{AB}(1, 2)$:

$$\Delta_{AB}(1, 2) = g_R(1, 2)f_{AB}(1, 2) \tag{A.173}$$

Then combining equations (A.171) and (A.165):

$$\hat{\sigma}_A - 1 = \sum_{B \in \Gamma} \int \sigma_{\Gamma - B}(2)\Delta_{AB}(1, 2)\mathrm{d}(2) \tag{A.174}$$

Combining equations (A.164) and (A.165), one gets:

$$c^{(0)} - c_R^{(0)} = \frac{1}{2} \sum_{A \in \Gamma} \int c_A(1)\sigma_{\Gamma - A}(1)\mathrm{d}(1) = \frac{1}{2} \sum_{A \in \Gamma} \int (\hat{\sigma}_A(1) - 1)\sigma_{\Gamma - A}(1)\mathrm{d}(1) \tag{A.175}$$

Then a particular case of equation (A.172) gives:

$$\rho(1) = \sigma_\Gamma(1) = \frac{\sigma_A(1)\sigma_{\Gamma - A}(1)}{\sigma_0(1)} \tag{A.176}$$

Putting the previous equation in equation (A.175), one gets:

$$c^{(0)} - c_R^{(0)} = \frac{1}{2} \sum_{A \in \Gamma} \int \left[\rho(1) - \sigma_{\Gamma - A}(1)\right]\mathrm{d}(1) \tag{A.177}$$

Which is the generalized version of the last term of equation (A.98) in the case of multiple association sites. Q given by equation (A.160) can also be simplified. Using equation (A.172) in the product of equation (A.160):

$$Q(1) = -\sum_{A \in \Gamma} \sigma_{\Gamma - A}(1) + \sum_{P(\Gamma) = \{\gamma, n \geq 2\}} (-1)^n (n - 2)!\sigma_\Gamma(1) \tag{A.178}$$

It will now be shown that:

$$A_m = \sum_{P(\Gamma_m)=\{\gamma,n\geq 2\}} (-1)^n(n-2)! = n(\Gamma_m) - 1 = m - 1 \qquad (A.179)$$

Where Γ_m is any set with m association sites. This is not trivial. It can be shown by induction. For $m = 1$, there is only one partition of Γ_m with one element so $A_1 = 0 = n(\Gamma_1) - 1$. For $m = 2$, there is only one partition with at least two elements so $A_2 = (-1)^2 \times 0! = 1 = n(\Gamma_2) - 1$. Assuming that equation (A.179) is proved for all m up to a positive integer M, it is required to show that it is also true for $m = M + 1$ in order to prove equation (A.179). $P(\Gamma_{M+1})$ (with at least two elements) can be divided into two sets whether the subset $\{M + 1\}$ is added to a partition of Γ_M with at least two elements (first set) or if $M + 1$ is added to one of the subsets of the partitions of Γ_M (second set). There also is the partition $\{1, 2, \ldots, M\}, \{M + 1\}$ in $P(\Gamma_{M+1})$ which has two elements (and is not in one of the previous two sets). The partitions in the first set are essentially partitions of Γ_M but with one more subset so its contribution to A_{M+1} is:

$$\sum_{P(\Gamma_M)=\{\gamma,n\geq 2\}} (-1)^n(n-2)! \times (-1)(n-1)$$

Where $\times(-1)(n-1)$ appears because of the subset $\{M + 1\}$ but the sum is still carried out over $P(\Gamma_M) = \{\gamma, n \geq 2\}$ because there are as many partitions in the first set as in $P(\Gamma_M) = \{\gamma, n \geq 2\}$. The partitions in the second set are all the different partitions that can be made from the partitions in $P(\Gamma_M) = \{\gamma, n \geq 2\}$ by adding $M + 1$ inside one of their subsets. For each n, there are n possibilities of adding $M + 1$ as there are n subsets in the partitions. So the contribution of the second set to A_{M+1} is:

$$\sum_{P(\Gamma_M)=\{\gamma,n\geq 2\}} (-1)^n(n-2)! \times n$$

The contribution of $\{1, 2, \ldots, M\}, \{M + 1\}$ to A_{M+1} is 1 so finally:

$$A_{M+1} = \left(\sum_{P(\Gamma_M)=\{\gamma,n\geq 2\}} (-1)^n(n-2)! \times (-1)(n-1) \right)$$
$$+ \left(\sum_{P(\Gamma_M)=\{\gamma,n\geq 2\}} (-1)^n(n-2)! \times n \right) + 1 \qquad (A.180)$$

Using again the fact that $n(n-2)! - (n-1)! = (n-2)!$:

$$A_{M+1} = \left(\sum_{P(\Gamma_M)=\{\gamma,n\geq 2\}} (-1)^n(n-2)! \right) + 1 = A_M + 1 = n(\Gamma_M) - 1 + 1 = n(\Gamma_{M+1}) - 1 \quad (A.181)$$

Which therefore proves equation (A.179). So:

$$Q(1) = -\sum_{A\in\Gamma} \sigma_{\Gamma-A}(1) + \rho(1)(n(\Gamma)-1) \tag{A.182}$$

Putting equations (A.177) and (A.182) into equation (A.162), one gets after simplifications:

$$\beta A_{\text{assoc}} = \int \rho(1)\left[\ln\left(\frac{\rho_0(1)}{\rho(1)}\right) - \frac{1}{2}\sum_{A\in\Gamma}\frac{\sigma_{\Gamma-A}(1)}{\rho(1)} + \frac{n(\Gamma)}{2}\right]\mathrm{d}(1) \tag{A.183}$$

Introducing the fraction of sites A which are not bonded $x_A(1) = \frac{\sigma_{\Gamma-A}(1)}{\sigma_\Gamma(1)}$ and using equations (A.172) with $\alpha = \Gamma$ and (A.176):

$$\frac{\rho_0(1)}{\rho(1)} = \prod_{A\in\Gamma}\frac{\sigma_{\Gamma-A}(1)}{\sigma_\Gamma(1)} = \prod_{A\in\Gamma} x_A(1) \tag{A.184}$$

And so equation (A.183) becomes:

$$\beta A_{\text{assoc}} = \sum_{A\in\Gamma}\int \rho(1)\left[\ln\left(x_A(1)\right) - \frac{x_A(1)}{2} + \frac{1}{2}\right]\mathrm{d}(1) \tag{A.185}$$

It remains to show how the $x_A(1)$ terms can be calculated. Multiplying equation (A.174) by $\sigma_{\Gamma-A}(1)$ and using equation (A.176), it gives:

$$\rho(1) - \sigma_{\Gamma-A}(1) = \sigma_{\Gamma-A}(1)\sum_{B\in\Gamma}\int \sigma_{\Gamma-B}(2)\Delta_{AB}(1,2)\mathrm{d}(2) \tag{A.186}$$

Dividing both side of this equation by $\sigma_{\Gamma-A}(1)$ and rearranging:

$$x_A(1) = \frac{1}{1 + \sum\limits_{B\in\Gamma}\int \rho(2)x_B(2)\Delta_{AB}(1,2)\mathrm{d}(2)} \tag{A.187}$$

In the case of a uniform system, all the quantities related to densities do not depend on any coordinate so that:

$$x_A = \frac{1}{1 + \sum\limits_{B\in\Gamma}\rho x_B\Delta_{AB}} \tag{A.188}$$

With:

$$\Delta_{AB} = \int g_R(1,2)f_{AB}(1,2)\mathrm{d}(1)\mathrm{d}(2) \tag{A.189}$$

And:

$$\beta A_{\text{assoc}} = N\sum_{A\in\Gamma}\left(\ln\left(x_A\right) - \frac{x_A}{2} + \frac{1}{2}\right) \tag{A.190}$$

The latter equation can written in the form:

$$\frac{a_{\text{assoc}}}{RT} = \sum_{A\in\Gamma}\left(\ln\left(x_A\right) - \frac{x_A}{2} + \frac{1}{2}\right) \tag{A.191}$$

Improvements to the first order theory are discussed by Zmpitas[10].

5 SAFT HS

In this section it will be shown how everything that has been discussed before can be combined to create an equation of state which can describe a system made of a mixture of different chains of spheres (connected by covalent bonds) with association sites. This is the Statistical Association Fluid Theory, first developed by Chapman[1]. Here, works done by Chapman in his Ph.D. thesis and in later papers are followed[1,9,15,16].

What is presented here is the case where spheres are modeled by a pair potential given by equation (A.53) but this can be extended to any type of potential[17].

Wertheim's Thermodynamic Perturbation Theory has to be applied to a reference potential. In SAFT HS this is the Hard Sphere potential. The corresponding reference molar Helmholtz energy is then:

$$A_R(T, \rho_i) = A_{\text{ig}}(T, \rho_i) + A_{\text{hs}}(T, \rho_i) \tag{A.192}$$

Where here the choice of independent variables are temperature T and molar densities ρ_i of molecules i (for all molecules). This choice is motivated by the way partial derivatives will be calculated later and is subjected to the constraint that $V \sum \rho_i$ is the total number of moles in the system. It can also be useful to choose the more natural set of independent variables T, V, n_i with n_i the mole number of molecule i (for all molecules). The latter set has one more variable but it is not subjected to any constraint. The ideal gas term is obtained from equation (A.16) and the hard sphere term from equation (A.63), for now for the pure component case.

The total Helmholtz energy is then given by equation (A.190):

$$A(T, \rho_i) = A_R(T, \rho_i) + A_{\text{assoc}}(T, \rho_i) \tag{A.193}$$

It is now possible to extend this to mixtures. It has already been done for the reference term so only the association term needs changes. Quantities for different components will be noted with a subscript ι or κ. Only the main changes will be given as calculations do not change. First the potential energy of the system can be written. In order to simplify notation, the potential energy will still be written V and the pair potential $\varphi_{\iota\kappa}$. For homogeneous (uniform) systems, equation (A.18) becomes:

$$V(1, 2, \ldots, N) = \sum_{\iota, \kappa} \sum_{1 \leq i < j \leq N} \varphi_{\iota\kappa}(i, j) \tag{A.194}$$

Where the first sum is carried out over all combinations of components. Equation (A.101) for pair potential is given by:

$$\varphi_{\iota\kappa}(1, 2) = \varphi_{R\iota\kappa}(1, 2) + \sum_{A \in \Gamma_\iota} \sum_{B \in \Gamma_\kappa} \varphi_{A_\iota B_\kappa}(1, 2) \tag{A.195}$$

$\varphi_{R\iota\kappa}$ designate the reference hard sphere pair potential between components ι and κ. It is the pair potential used in the Hard Sphere Equation of State section for the case of a mixture. Γ_ι is the set of association sites on component ι and $\varphi_{A_\iota B_\kappa}$ is the attraction energy between site A of component ι and site B of component κ. Equation (A.104) for the Mayer f-functions becomes:

$$f_{\iota\kappa}(1,2) = f_{R\iota\kappa}(1,2) + e_{R\iota\kappa}(1,2)\left[\left(\prod_{A\in\Gamma_\iota}\prod_{B\in\Gamma_\kappa}1 + f_{A_\iota B_\kappa}(1,2)\right) - 1\right] \tag{A.196}$$

Molar density ρ_ι of component ι is given by:

$$\rho_\iota = x_\iota\rho \tag{A.197}$$

Where ρ is now the total molar density (instead of the number density) and x_ι is the mole fraction of component ι (different from x_A with a capital letter which is the fraction of sites A which are not bonded). Each number density $N_a\rho_\iota$ of component ι is associated with a singlet density $\rho_\iota(1_\iota)$. For all these new singlet densities, the topological reduction previously introduced can be applied noting that the only things that matter in this part are the connections at the white circle (either fugacity or density circles) labeled 1_ι. Modifications in the thermodynamics part appear in the fact that variation of βPV is implied by independent variations in the different components of the mixture. Mathematically, this is shown by the fact that, before any topological reduction is performed, $\ln(\Xi)$ is a functional of all the fugacities z_ι. Then equation (A.21) for $\ln(\Xi)$ becomes:

$$\delta(\beta PV) = \sum_\iota\int\frac{\delta\ln(\Xi)}{\delta z_\iota}(1_\iota)\delta z_\iota d(1_\iota) \tag{A.198}$$

Singlet densities $\rho_\iota(1_\iota)$ defined by equation (A.22) replacing 1 by 1_ι are then directly given by:

$$\rho_\iota(1_\iota) = z_\iota\frac{\delta\ln(\Xi)}{\delta z_\iota}(1_\iota) \tag{A.199}$$

Then equation (A.153) becomes:

$$\beta PV = \sum_\iota\int\left[\rho_\iota(1_\iota) - \sum_{\alpha_\iota\subseteq\Gamma_\iota}\sigma_{\Gamma_\iota-\alpha_\iota}(1_\iota)c_{\alpha_\iota}(1_\iota)\right]d(1_\iota) + c^{(0)} \tag{A.200}$$

Where:

$$c_{\alpha_\iota}(1_\iota) = \frac{\delta c^{(0)}}{\delta\sigma_{\Gamma_\iota-\alpha_\iota}}(1_\iota) \tag{A.201}$$

Which also defines $c^{(0)}$. Then equation (A.155) becomes:

$$\beta A = \sum_\iota\int\left[\sigma_{\Gamma_\iota}(1_\iota)\ln\left(\frac{\sigma_{0_\iota}(1_\iota)}{\Lambda_\iota}\right) + Q_\iota(1_\iota)\right]d(1_\iota) - c^{(0)} \tag{A.202}$$

The main difference appears in the perturbation theory because interactions are considered inside $c^{(0)}$ and so interactions between two different particles can happen. However, the only graphs that are kept still have only one attraction bond so that equation (A.163) becomes:

$$c^{(0)} - c_R^{(0)} = \frac{1}{2} \sum_{\iota,\kappa} \int g_{R\iota\kappa}(1,2) \left\langle \mathring{\sigma}_\iota(1) \mathring{f}_{\iota\kappa}(1,2) \mathring{\sigma}_\kappa(2) \right\rangle_{1,2} \mathrm{d}(1)\mathrm{d}(2) \tag{A.203}$$

Where 1_ι and 2_κ have been equivalently written 1 and 2. Calculations are then identical to the ones that were performed in the previous part. Finally, changing subscripts ι and κ to i and j respectively:

$$\frac{a_{\text{assoc}}}{RT} = \sum_i x_i \sum_{A_i \in \Gamma_i} \left(\ln(x_{A_i}) - \frac{x_{A_i}}{2} + \frac{1}{2} \right) \tag{A.204}$$

$$x_{A_i} = \frac{1}{1 + \sum\limits_j \sum\limits_{B_j \in \Gamma_j} N_a \rho_j x_B \Delta_{A_i B_j}} \tag{A.205}$$

$$\Delta_{A_i B_j} = \int g_{ij}(1,2) f_{A_i B_j}(1,2) \mathrm{d}(1)\mathrm{d}(2) \tag{A.206}$$

Where $g_{Rij}(1,2)$ has simply been written $g_{ij}(1,2)$. In general $g_{ij}(1,2)$ is a function of the distance $|r_2 - r_1|$ between two points 1 and 2 (where there can potentially be particles; the integration is formally done over the whole available space where a particle could be but that does not mean that in general there are particles at points 1 and 2). But it should be anticipated that g_{ij} will be usually given by equation (A.55) because of the fact that interaction energies for association sites have a short range and so it can be assumed that the hardcore of two bonded particles are touching. Also, x_i is the mole fraction of molecule i and is different from x_{A_i} (with a capital letter designating an association site).

In order to better understand the following calculations, it can be helpful to anticipate the final form of the SAFT HS equation of state. This is summarized in Figure A1.18 for a pure component.

In the top left corner of Figure A1.18, a system described by the ideal gas law is presented. Particles are represented by points having a mass. Then adding the hard sphere potential to the description of the system adds a spherical volume to each sphere. Using association sites (and this will be shown a bit later) it is then possible to create chains of particles, each chain containing exactly the same number of spheres. There are two properties implied by Wertheim's first order Thermodynamic Perturbation Theory. First, the relative position of each association site is of no importance as can be seen from the equations derived in the previous section. Thus chains can have any shape as long as no spheres overlap. The second property (closely related to the first one) is that no ring can be formed with this level of theory. Actually only tree structures can be formed i.e. there is only one path (made of hard spheres) joining any two spheres in such a structure. This is seen from equation (A.175) by the fact that the only c_α in this equation involves sets α made of one
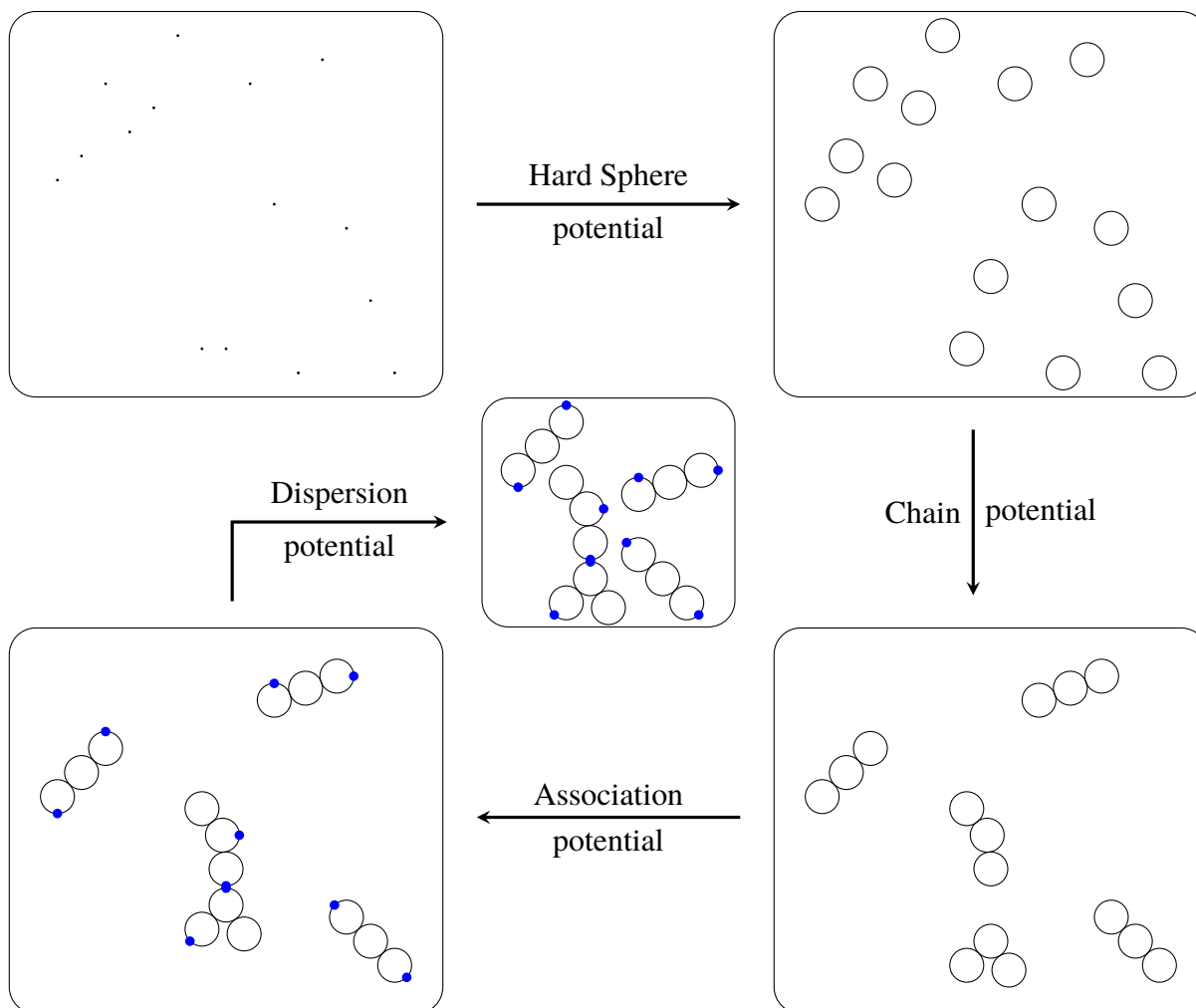
Figure A1.18: Physical meaning of the SAFT HS Equation of State.

site and so the corresponding graphs have only one attractive bond on their white circle. However that does not mean that only dimers can be formed like in the one association site case (even if the graphs that were kept in $c^{(0)}$ only have one attraction bond at most) because the contributions for each site are summed in equation (A.175). One of Chapman's[9] contributions here was to limit these tree structures to chains of equal length when association sites have a strong energy corresponding to covalent bonds.

In the general case, there can still be some association sites that were not used to form chains. They can then form bonds but these are not as strong as in chains because the corresponding association energy is usually weaker, satisfying the perturbation theory requirements.

All the previous contribution have been rigorously derived (as will be done further for the chain contribution) but a major issue arises if no other potential is added. Indeed, there would be no long range attraction energy that could force the system to be liquid under certain circumstances. That

is why a dispersion term must be added to the equation. This term can be more or less rigorously added to the equation in general. Usually it is considered as a perturbation potential as well and so two consecutive perturbation theories must be performed (the multidensity formalism used in the previous section is only suitable for short range potentials with a specific direction) which is very difficult considering the complexity of Wertheim's Thermodynamic Perturbation Theory. The manner to add a dispersion potential in SAFT HS will also be discussed.

As a consequence the next step will be to show how chains of definite length can be created in the system, only using association sites. The starting equation is (A.204). The way Chapman forces chains to form is the following:

Let component i form chains of m_i identical spheres of diameter σ_i. Each sphere has a number from 1 to m_i, 1 and m_i being the first and last spheres of the chain. If a sphere has neither 1 nor m_i as a number, then it receives two association sites; otherwise just one. If m_i is 1, then no association site is given. Let β_i be a number between 2 and $m_i - 1$. Then one association site on sphere β_i will be allowed to bond with only one association site of sphere $\beta_i - 1$ and the other will be allowed to bond with only one association site of sphere $\beta_i + 1$. If $\beta_i = 1$, its association site is allowed to bond with only one of the association site (always the same one) of sphere 2 and if $\beta_i = m_i$, its association site is allowed to bond with only one of the association site (always the same one) of sphere $m_i - 1$. This is summarized on Figure A1.19. On top of these association sites only allowed to create bonds in order to form the chain, there can be any other number of association sites and their position does not matter as it was noted above.
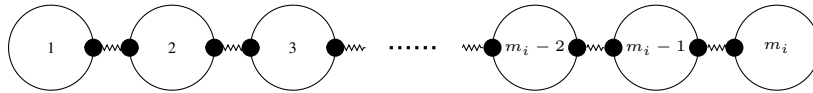
Figure A1.19: Chain formation. Sketch inspired by Chapman[9].

Each sphere in a component can be treated as a distinct component so that, separating terms involving association sites used to form chains, equation (A.204) becomes:

$$\frac{a_{\text{assoc}}}{RT} = \sum_i x_i \sum_{A_i \in \Gamma_i} \left(\ln\left(x_{A_i}\right) - \frac{x_{A_i}}{2} + \frac{1}{2} \right) + \sum_i \sum_{\beta_i = 1}^{m_i} x_{\beta_i} \sum_{A_{\beta_i} \in \Gamma'_{\beta_i}} \left(\ln\left(x_{A_{\beta_i}}\right) - \frac{x_{A_{\beta_i}}}{2} + \frac{1}{2} \right)$$

(A.207)

Where β_i designates as before the different spheres in a chain of component i, x_{β_i} is the mole fraction of sphere β_i and now Γ designates a set of association sites that are not used to form chains and on the opposite Γ' designates a set of association sites that are only used to form chains according to the manner previously explained. It is then possible to redefine a_{assoc}/RT as the first term of equation (A.207) (which thus does not change) and the second term will define the chain

contribution a_{chain}/RT. Noticing that the mole fraction of a sphere inside a chain is equal to the mole fraction of the chain itself (because there always is the same number m_i of spheres in a chain of component i), the chain term can be written as follows:

$$\frac{a_{\text{chain}}}{RT} = \sum_i x_i \sum_{\beta_i=1}^{m_i} \sum_{A_{\beta_i} \in \Gamma'_{\beta_i}} \left(\ln \left(x_{A_{\beta_i}} \right) - \frac{x_{A_{\beta_i}}}{2} + \frac{1}{2} \right) \tag{A.208}$$

Giving the same properties to each association site forming the chain, noticing that there are $2m_i - 2$ such sites in a chain (so that the two inner sum can be factorized) and factorizing by $(1 - m_i)$:

$$\frac{a_{\text{chain}}}{RT} = \sum_i x_i(1 - m_i) \left(x^{(i)} - 2\ln\left(x^{(i)}\right) - 1 \right) \tag{A.209}$$

Where $x^{(i)}$ is the fraction of not bonded association sites that form chains i. From equation (A.205), $x^{(i)}$ is given by:

$$x^{(i)} = \frac{1}{1 + N_a \rho_i \Delta_{ii} x^{(i)}} \tag{A.210}$$

$$\Leftrightarrow x^{(i)} = 1 - N_a \rho_i \Delta_{ii} x^{(i)2} \tag{A.211}$$

$$\Leftrightarrow x^{(i)2} = \frac{1 - x^{(i)}}{N_a \rho_i \Delta_{ii}} \tag{A.212}$$

With, from equation (A.206):

$$\Delta_{ii} = \int g_{ii}(1,2) f_{ii}(1,2) \mathrm{d}(1)\mathrm{d}(2) \tag{A.213}$$

And $f_{ii}(1,2) = \exp(-\beta\varphi_{ii}(1,2)) - 1$ with $\varphi_{ii}(1,2)$ the attraction potential between association sites forming a chain i. Using the fact that $-2\ln(x) = \ln(1/x^2)$ with equations (A.211) and (A.212), equation (A.209) becomes:

$$\frac{a_{\text{chain}}}{RT} = \sum_i x_i(1 - m_i) \left(\ln \left(\frac{N_a \rho_i \Delta_{ii}}{1 - x^{(i)}} \right) - N_a \rho_i \Delta_{ii} x^{(i)2} \right) \tag{A.214}$$

If covalent bonds are wanted between spheres inside a chain, then the limit $\varphi_{ii}(1,2) \to \infty$ must be considered. That is in agreement with the developed perturbation theory, even if the potential energy is not a perturbation anymore, because of the restrictions that have been given to the association sites forming chains. It implies that $\Delta_{ii} = \infty$ and so from equation (A.211) $x^{(i)} = 0$ ($x^{(i)}$ is always between 0 and 1 by definition). Putting this into the previous equation, it becomes:

$$\frac{a_{\text{chain}}}{RT} = \sum_i x_i(1 - m_i) \ln\left(N_a \rho_i \Delta_{ii}\right) \tag{A.215}$$

Further simplifications can be done based on the fact that association interaction energy has a short range (see Chapman[9,16]). As mentioned above the radial distribution function can be approximated by its value when two hard spheres i and j are actually touching i.e. for $|r_2 - r_1| = \sigma_{ij} =$

117

$(\sigma_i + \sigma_j)/2$ and so it is given by equation (A.55). For the same reason, it can be assumed that $\varphi_{A_i B_j}$ is a constant inside an association site (i.e. corresponding to a square well potential). Choosing one of the two particles as the origin of the system (particle 1) and using spherical coordinates, equation (A.206) becomes:

$$\Delta_{A_i B_j} = \int g_{ij}(r_{12}) f_{A_i B_j}(r_{12}, \omega_1, \omega_2) \mathrm{d}r_{12} r_{12}^2 \mathrm{d}\theta \sin(\theta) \mathrm{d}\phi \mathrm{d}\omega_1 \mathrm{d}\omega_2 \qquad (A.216)$$

Where $r_{12} = |r_2 - r_1|$ generally varies from 0 to ∞, θ varies from 0 to π, ϕ varies from 0 to 2π and ω_l is the different possible orientations of particle l depending on three angles in general. For the same reason evoked for the radial distribution function, r_{12} can be approximated by σ_{ij}. $f_{A_i B_j}$ only depends on the distance between association sites A_i and B_i. Thus:

$$\Delta_{A_i B_j} \simeq 4\pi \sigma_{ij}^2 g_{ij}(\sigma_{ij}) \int_{r_{12}} \left(\int_{\omega_1, \omega_2} f_{A_i B_j}(r_{12}, \omega_1, \omega_2) \mathrm{d}\omega_1 \mathrm{d}\omega_2 \right) \mathrm{d}r_{12} \qquad (A.217)$$

Remembering that $g_{ij}(\sigma_{ij})$ is given by equation (A.55), it shall simply be written g_{ij}. The integral over orientations (at constant r_{12}) will be dealt with first. Using Euler angles and the z's axes passing through the center of the particle and the center of the association site, each particle is invariant by a rotation around its z axis. However it is not invariant with respect to a rotation over the nutation angle θ and the precession angle ϕ. However, fixing the orientation of one particle, the system is symmetric with respect to a rotation on ϕ (the symmetry plane passing through the center of both particles and the center of the fixed association site) so it is actually convenient to calculate the average of $f_{A_i B_j}(r_{12}, \omega_1, \omega_2)$ over orientation (only depending on the two nutation angles from what has been said) instead of the actual integral. So:

$$\Delta_{A_i B_j} \simeq 4\pi \sigma_{ij}^2 g_{ij} \int_{r_{12}} \left\langle f_{A_i B_j}(r_{12}, \omega_1, \omega_2) \right\rangle_{\omega_1, \omega_2} \mathrm{d}r_{12} \qquad (A.218)$$

The average $\left\langle f_{A_i B_j}(r_{12}, \omega_1, \omega_2) \right\rangle_{\omega_1, \omega_2}$ will be calculated using Figure A1.20 for the case $A_i = B_j$. It was first done by Wertheim[18].

The first step is to calculate the average with respect to the orientation of particle 2. As explained above, considering the centers of the particles and their association sites in the same plane as in Figure A1.20, only the average with respect to the angle θ_2 (defined in Figure A1.20) needs to be done. This is equivalent to saying that $f_{A_i B_j}$ only depends on r_{12}, θ_1 and θ_2. With the definition of an average quantity and simply writing $f_{A_i B_j}$ as f for now, one gets:

$$\langle f(r_{12}, \omega_1, \omega_2) \rangle_{\omega_2} = \frac{\int f(x(\theta_2)) d \sin(\theta_2) \mathrm{d}\theta_2}{\int d \sin(\theta_2) \mathrm{d}\theta_2} \qquad (A.219)$$

Where the distance d is defined as the length of vectors d_1 and d_2 and θ_2 varies between 0 and π.
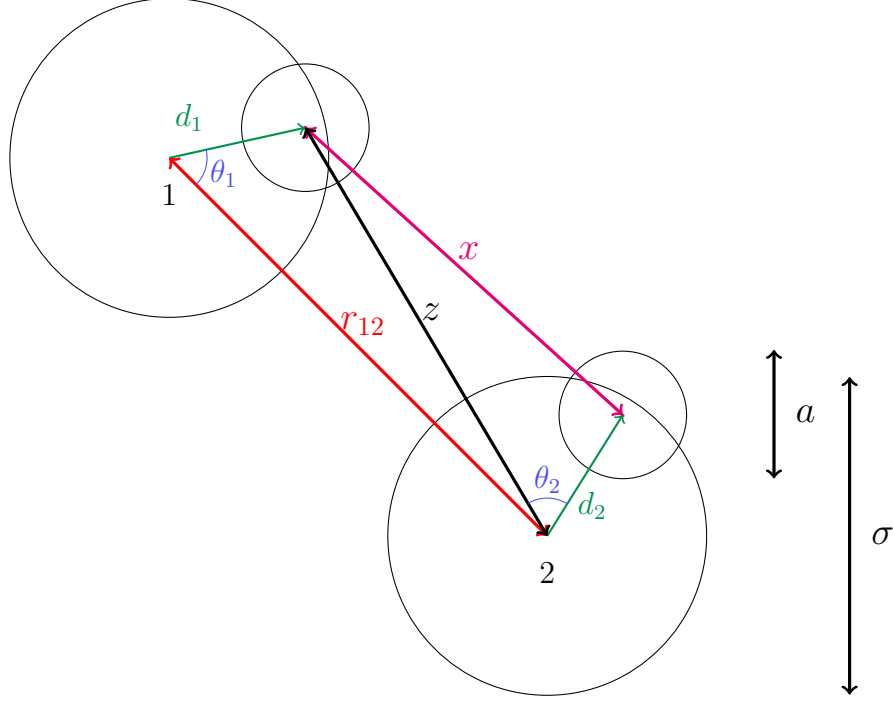
Figure A1.20: Calculation of the angle average in equation (A.218).

Using the law of cosines, one gets:

$$x^2 = z^2 + d^2 - 2zd\cos(\theta_2) \tag{A.220}$$

$$\Leftrightarrow \cos(\theta_2) = \frac{z^2 + d^2 - x^2}{2zd} \tag{A.221}$$

Differentiating the previous equation and remembering that z is fixed at constant θ_1:

$$d\theta_2 \sin(\theta_2) = \frac{x\,dx}{zd} \tag{A.222}$$

And changing variable θ_2 to x:

$$\langle f(r_{12}, \omega_1, \omega_2) \rangle_{\omega_2} = \frac{\int_{x=z-d}^{z+d} f(x) x\,dx}{\int_{x=z-d}^{z+d} x\,dx} \tag{A.223}$$

$f(x)$ is always zero if $x > a$ so:

$$g(z) = \langle f(r_{12}, \omega_1, \omega_2) \rangle_{\omega_2} = \frac{\int_{x=z-d}^{a} f(x) x\,dx}{2zd} \tag{A.224}$$

Similarly performing the average for θ_1 and applying again the law of cosines:

$$z^2 = d^2 + r_{12}^2 - 2dr_{12}\cos(\theta_1) \tag{A.225}$$

It becomes:

$$\langle f(r_{12}, \omega_1, \omega_2) \rangle_{\omega_1, \omega_2} = \frac{\int_{z=r_{12}-d}^{a+d} g(z) z\,dz}{2r_{12}d} \tag{A.226}$$

119

Combining equations (A.224) and (A.226), the required average is:

$$\langle f(r_{12}, \omega_1, \omega_2) \rangle_{\omega_1, \omega_2} = \frac{1}{4d^2 r_{12}} \int_{z=r_{12}-d}^{a+d} \int_{x=z-d}^{a} f(x) x \mathrm{d}x \tag{A.227}$$

The order of integration can be changed using Fubini's theorem. In order to do that, it must be noticed that when $z = r_{12} - d$ then $x = r_{12} - 2d$ and for a given x, $z = x + d$ so that:

$$\langle f(r_{12}, \omega_1, \omega_2) \rangle_{\omega_1, \omega_2} = \frac{1}{4d^2 r_{12}} \int_{x=r_{12}-2d}^{a} \int_{z=r_{12}-d}^{x+d} f(x) x \mathrm{d}x \mathrm{d}z \tag{A.228}$$

$$= \frac{1}{4d^2 r_{12}} \int_{x=r_{12}-2d}^{a} f(x) x (x + 2d - r_{12}) \mathrm{d}x \tag{A.229}$$

In the approximation mentioned above when f is constant inside an association site, the integration is easily calculated. Returning to full notations, it becomes:

$$\left\langle f_{A_i B_j}(r_{12}, \omega_1, \omega_2) \right\rangle_{\omega_1, \omega_2} = \frac{f_{A_i B_j}}{24 d^2 r_{12}} (a + 2d - r_{12})^2 (2a - 2d + r_{12}) \tag{A.230}$$

Where $f_{A_i B_j}$ is given by the constant value $\varphi_{A_i B_j}$ of the association energy inside an association site:

$$f_{A_i B_j} = \exp(-\beta \varphi_{A_i B_j}) - 1 \tag{A.231}$$

It must be noticed that if $\varphi_{A_i B_j}$ is given as its absolute value (as it is often done when using SAFT), then:

$$f_{A_i B_j} = \exp(\beta \varphi_{A_i B_j}) - 1 \tag{A.232}$$

The remaining integral in equation (A.218) can be directly calculated. The result is given by Chapman[16]. Defining for instance:

$$k_{A_i B_j} = \frac{4\pi}{\sigma_{ij} f_{A_i B_j}} \int_{r_{12}} \left\langle f_{A_i B_j}(r_{12}, \omega_1, \omega_2) \right\rangle_{\omega_1, \omega_2} \mathrm{d}r_{12} \tag{A.233}$$

$\Delta_{A_i B_j}$ gets its final form:

$$\Delta_{A_i B_j} = \sigma_{ij}^3 g_{ij} k_{A_i B_j} f_{A_i B_j} \tag{A.234}$$

With:

$$k_{A_i B_j} = \frac{4\pi}{72 d^2 \sigma} \left(\ln \left(\frac{a + 2d}{\sigma} \right) (6a^3 + 18a^2 d - 24d^3) \right.$$
$$\left. + (a + 2d - \sigma)(22d^2 - 5ad - 7d\sigma - 8a^2 + a\sigma + \sigma^2) \right) \tag{A.235}$$

When $A_i = B_j$. The previous equation is convenient to give a physical meaning to the equation but it can be preferred to leave $k_{A_i B_j}$ as a parameter. If $A_i \neq B_j$, it is usually better to use some kind of mixing rules or to simply leave $k_{A_i B_j}$ as a parameter.

In equation (A.215), it can be convenient to get rid of some factors inside the logarithm as they do not play any role, any energy being defined with a reference state. The form that is usually used is the following:

$$\frac{a_{\text{chain}}}{RT} = \sum_i x_i (1 - m_i) \ln(g_{ii}) \tag{A.236}$$

But the missing factor ρ_i might have a significant impact.

The dispersion term introduced by Chapman[15] can be explained as follows. In the pure component case, it can be considered that the internal energy due to the dispersion energy is proportional to the total number of spheres Nm (N is the number of molecules and m the number of spheres in a molecule) and an energy parameter ε corresponding to a mean field. It is also clear that in a liquid phase, this dispersion energy should be more important than in a gas phase so the dispersion energy can also be assumed to be proportional to the total packing fraction of the system v/V where v is the total volume taken by all the molecules and V is the volume of the system. The dispersion energy must be attractive so, choosing ε as a positive number, the dispersion contribution to the internal energy is U_{disp}:

$$U_{\text{disp}} = -Nm\frac{v}{V}\varepsilon \tag{A.237}$$

The previous equation does not depend on temperature so it is the same expression for the Helmholtz energy dispersion contribution. Molecules being made of m spheres of diameter σ, one gets:

$$A_{\text{disp}} = -N\frac{\pi N_a}{6}\rho m^2 \sigma^3 \varepsilon \tag{A.238}$$

With ρ again being the molar density. With molar Helmholtz energy it becomes:

$$a_{\text{disp}} = -N_a\frac{\pi N_a}{6}\rho m^2 \sigma^3 \varepsilon \tag{A.239}$$

This can be extended to mixtures using Van der Waals mixing rules:

$$a_{\text{disp}} = -N_a\frac{\pi N_a}{6}\rho \sum_{i,j} \sigma_{ij}^3 \varepsilon_{ij} m_i m_j x_i x_j \tag{A.240}$$

With as before:

$$\sigma_{ij} = \frac{\sigma_i + \sigma_j}{2} \tag{A.241}$$

And:

$$\varepsilon_{ij} = (1 - k_{ij})\sqrt{\varepsilon_i \varepsilon_j} \tag{A.242}$$

Where ε_i is the dispersion energy parameter for component i and k_{ij} is the binary interaction parameter between components i and j.

Finally, combining all previous equations, the SAFT HS equation of state is given by:

$$A(T, V, n_i) = A_{\text{ig}}(T, V, n_i) + A_{\text{hs}}(T, V, n_i) + A_{\text{chain}}(T, V, n_i) + A_{\text{assoc}}(T, V, n_i) + A_{\text{disp}}(T, V, n_i)$$
(A.243)

It can be written with different forms depending on whether the molar Helmholtz energy is used or if the set of independent variables is different. For instance one can use:

$$a(T, \rho_i) = a_{\text{ig}}(T, \rho_i) + a_{\text{hs}}(T, \rho_i) + a_{\text{chain}}(T, \rho_i) + a_{\text{assoc}}(T, \rho_i) + a_{\text{disp}}(T, \rho_i)$$
(A.244)

The ideal gas term is given by equation (A.16), the hard sphere term by equation (A.63), the chain term by equation (A.236), the association term by equation (A.204) and the dispersion term by equation (A.240).

6 Chemical Potentials

In order to calculate chemical potentials, it is convenient to use the set of independent variables (T, V, n_i). But before performing any derivative calculation, it is useful to rewrite all the required equations so all the products ρx_i becomes ρ_i. Looking at the equations, it is indeed possible and then derivatives of factors ρ or x_i with respect to n_i are avoided. Then using the definition of the chemical potential μ_i of component i:

$$\mu_i = \frac{\partial A}{\partial n_i}_{|T, V, n_{j \neq i}}$$
(A.245)

One gets after another change of (more convenient) variables:

$$\mu_i(T, \rho_i) = \mu_{i,\text{ig}}(T, \rho_i) + \mu_{i,\text{hs}}(T, \rho_i) + \mu_{i,\text{chain}}(T, \rho_i) + \mu_{i,\text{assoc}}(T, \rho_i) + \mu_{i,\text{disp}}(T, \rho_i)$$
(A.246)

The ideal gas term is easily calculated:

$$\frac{\mu_{i,\text{ig}}}{RT} = \ln(N_a \rho x_i \lambda_i^3)$$
(A.247)

The hard sphere term is given by Xu et al. [19]:

$$\frac{\mu_{i,\text{hs}}}{RT} = \frac{3B_i C\xi + 3BC_i\xi - 3C^2 C_i/D + 2C^3 D_i/D^2}{D(1-\xi)}$$
$$+ \frac{1}{D(1-\xi)^2}\left[\left(3BC\xi - \frac{C^3}{D}\right)\zeta_i + \frac{3C^2 C_i}{D} - \frac{2C^3 D_i}{D^2}\right] + \frac{2C^3\zeta_i}{D^2(1-\xi)^3}$$
$$+ \left[\frac{3C^2 C_i}{D^2} - \frac{2C^3 D_i}{D^3} - A_i\right]\ln(1-\xi) - \left[\frac{C^3}{D^2} - A\right]\frac{\zeta_i}{1-\xi}$$
(A.248)

Where:

$$\xi = \xi_3 = \frac{\pi}{6} N_a \rho \sum_i x_i m_i \sigma_i^3 \qquad\qquad \zeta_i = \frac{\pi}{6} N_a m_i \sigma_i^3 \qquad (A.249)$$

$$A = \frac{6\xi_0}{\pi N_a} = \sum_i \rho_i m_i \qquad\qquad A_i = m_i \qquad (A.250)$$

$$B = \frac{6\xi_1}{\pi N_a} = \sum_i \rho_i m_i \sigma_i \qquad\qquad B_i = m_i \sigma_i \qquad (A.251)$$

$$C = \frac{6\xi_2}{\pi N_a} = \sum_i \rho_i m_i \sigma_i^2 \qquad\qquad C_i = m_i \sigma_i^2 \qquad (A.252)$$

$$D = \frac{6\xi_3}{\pi N_a} = \sum_i \rho_i m_i \sigma_i^3 \qquad\qquad D_i = m_i \sigma_i^3 \qquad (A.253)$$

The chain term is given by Xu et al.[19] or Chapman[1]

$$\frac{\mu_{i,\text{chain}}}{RT} = (1 - m_i) \ln(g_{ii}) + \sum_j \rho_j (1 - m_j) \frac{1}{g_{jj}} \frac{\partial g_{jj}}{\partial \rho_i}_{|T,\rho_{j\neq i}} \qquad (A.254)$$

Where:

$$\frac{\partial g_{ij}}{\partial \rho_k}_{|T,\rho_{l\neq k}} = \frac{\pi N_a}{6} \frac{m_k \sigma_k^2}{(1-\xi)^2} \left\{ \sigma_k + \frac{3\sigma_i \sigma_j}{\sigma_i + \sigma_j} \left[1 + \frac{2\sigma_k \xi_2}{1-\xi} \right] + 2 \left(\frac{\sigma_i \sigma_j}{\sigma_i + \sigma_j} \left[\frac{2\xi_2}{1-\xi} + \frac{3\sigma_k \xi_2^2}{(1-\xi)^2} \right] \right) \right\} \qquad (A.255)$$

The dispersion term is easily calculated:

$$\frac{\mu_{i,\text{disp}}}{RT} = -2 m_i N_a \frac{\pi N_a}{6} \sum_j \sigma_{ij}^3 \varepsilon_{ij} m_j \rho_j \qquad (A.256)$$

The association term is given by Xu et al.[19] or Chapman[1]:

$$\frac{\mu_{i,\text{assoc}}}{RT} = \sum_{A_i} \left(\ln(x_{A_i}) - \frac{x_{A_i}}{2} + \frac{1}{2} \right) + \sum_j \rho_j \left[\sum_{A_j} \frac{\partial x_{A_j}}{\partial \rho_i}_{|T,\rho_{k\neq i}} \left(\frac{1}{x_{A_j}} - \frac{1}{2} \right) \right] \qquad (A.257)$$

Where $A_i \in \Gamma_i$ has simply been written A_i. As noticed by Xu et al.[19], all the $\frac{\partial x_{A_i}}{\partial \rho_k}_{|T,\rho_{j\neq k}}$ for each site form a vector y_k which is the solution of the following linear system (once the non linear system defined by equation (A.205) is solved):

$$Q y_k = c_k \qquad (A.258)$$

Where Q is a matrix whose coefficients are:

$$(Q)_{A_i,B_j} = \delta_{A_i,B_j} + N_a \rho_j x_{A_i}^2 \Delta_{A_i B_j} \qquad (A.259)$$

And c_k is given by:

$$(c_k)_{A_i} = -N_a x_{A_i}^2 \left(\sum_{B_k} x_{B_k} \Delta_{A_i B_k} + \sum_j \sum_{B_j} \rho_j x_{B_j} \frac{\partial \Delta_{A_i B_j}}{\partial \rho_k}_{|T,\rho_{l\neq k}} \right) \qquad (A.260)$$

123

There is a small mistake in the expression of c_k provided by Xu et al.[19]. The partial derivative in the previous equation is easily calculated with equations (A.234) and (A.255) as only the radial distribution function depends on molar densities. The characteristic size of this system is the total number of association sites considered.

7 Pressure

Regarding pressure, the same set of independent variable as before will be used but, as volume does not explicitly appear in the SAFT HS equation, it is convenient to calculate pressure as a partial derivative with respect to the total molar density. One has:

$$P = -\frac{\partial A}{\partial V}\Big|_{T,n_i} = -\frac{\partial (A/n)}{\partial (V/n)}\Big|_{T,n_i} = -\frac{\partial a}{\partial \rho}\Big|_{T,n_i}\frac{\partial \rho}{\partial (1/\rho)}\Big|_{T,n_i} \tag{A.261}$$

And so:

$$P = \rho^2 \frac{\partial a}{\partial \rho}\Big|_{T,n_i} \tag{A.262}$$

Explaining each contribution and changing variables, one get:

$$P(T, \rho_i) = P_{\text{ig}}(T, \rho_i) + P_{\text{hs}}(T, \rho_i) + P_{\text{chain}}(T, \rho_i) + P_{\text{assoc}}(T, \rho_i) + P_{\text{disp}}(T, \rho_i) \tag{A.263}$$

The ideal gas term is:

$$P_{\text{ig}}(T, \rho_i) = \rho RT \tag{A.264}$$

The hard sphere term is:

$$P_{\text{hs}}(T, \rho_i) = RT\rho Z_{\text{hs}} \tag{A.265}$$

With Z_{hs} given by equation (A.56). The chain term is given by Chapman[9]:

$$P_{\text{chain}}(T, \rho_i) = RT\rho \sum_i \rho_i(1 - m_i)\frac{\partial \ln(g_{ii})}{\partial \rho}\Big|_{T,n_j} \tag{A.266}$$

Where:

$$\frac{\partial \ln(g_{ii})}{\partial \rho}\Big|_{T,n_j} = \frac{1}{g_{ii}}\frac{1}{(1-\xi)^2}\left[\xi_3 + \frac{3}{2}\sigma_i\xi_2 + \frac{3\sigma_i\xi_2\xi_3}{1-\xi} + \frac{\sigma_i^2\xi_2^2}{1-\xi} + \frac{3\sigma_i^2\xi_2^2\xi_3}{2(1-\xi)^2}\right] \tag{A.267}$$

The dispersion term is easily calculated:

$$P_{\text{disp}}(T, \rho_i) = -N_a\frac{\pi N_a}{6}\rho^2 \sum_{i,j} \sigma_{ij}^3\varepsilon_{ij}x_im_ix_jm_j \tag{A.268}$$

The association term is given for instance by Zmpitas[10]

$$P_{\text{assoc}}(T, \rho_i) = \sum_i \rho_i \left[\sum_{A_i} \frac{\partial x_{A_i}}{\partial \rho} \bigg|_{T, n_j} \left(\frac{1}{x_{A_i}} - \frac{1}{2} \right) \right] \tag{A.269}$$

The partial derivative in the previous equation can be calculated in a similar manner as for chemical potentials. The system given by equation (A.258) still needs to be solved but with c_k given by:

$$(c_k)_{A_i} = -N_a x_{A_i}^2 \left(\sum_j \sum_{B_j} x_j x_{B_j} \left[\Delta_{A_i B_j} + \rho \frac{\partial \Delta_{A_i B_j}}{\partial \rho} \bigg|_{T, n_l} \right] \right) \tag{A.270}$$

In order to calculate the partial derivative in the previous equation, one must calculate the partial derivative of the radial distribution function with respect to the total molar density. A direct calculation gives:

$$\begin{aligned}
\frac{\partial g_{ij}}{\partial \rho} \bigg|_{T, n_l} = \frac{1}{\rho(1 - \xi_2)^2} &\left\{ \xi_3 + \frac{3\sigma_i \sigma_j}{\sigma_i + \sigma_j} \left(\xi_2 + \frac{2\xi_2 \xi_3}{(1 - \xi_3)} \right) \right. \\
&\left. + 2 \left(\frac{\sigma_i \sigma_j}{\sigma_i + \sigma_j} \right)^2 \left(\frac{2\xi_2^2}{(1 - \xi_3)} + \frac{3\xi_2^2 \xi_3}{(1 - \xi_3)^2} \right) \right\}
\end{aligned} \tag{A.271}$$

8   Hessian

It is also required for this work to calculate the Hessian of the Helmholtz energy density A/V. For this purpose, the chosen set of independent variables is (T, ρ_i). The wanted Hessian $(H)_{i,j}$ is then defined by:

$$(H)_{i,j} = \frac{\partial^2 (A/V)}{\partial \rho_i \partial \rho_j} \bigg|_{T, \rho_{k \neq i,j}} \tag{A.272}$$

Explaining each contribution, one gets:

$$\begin{aligned}
(H)_{i,j}(T, \rho_i) = (H_{\text{ig}})_{i,j}(T, \rho_i) + (H_{\text{hs}})_{i,j}(T, \rho_i) + (H_{\text{chain}})_{i,j}(T, \rho_i) \\
+ (H_{\text{assoc}})_{i,j}(T, \rho_i) + (H_{\text{disp}})_{i,j}(T, \rho_i)
\end{aligned} \tag{A.273}$$

The ideal gas term is easily calculated:

$$(H_{\text{ig}})_{i,j}(T, \rho_i) = \frac{RT}{\rho_i} \delta_{i,j} \tag{A.274}$$

The hard sphere term is given by Xu et al.[19]:

$$(H_{\text{hs}})_{i,j}(T, \rho_i) = \frac{\zeta_j}{D(1 - \xi)^2} \left(3B_i C \xi + 3BC_i \xi - 3 \frac{C^2 C_i}{D} + 2 \frac{C^3 D_i}{D^2} \right)$$

$$
\begin{aligned}
&+ \frac{1}{D(1-\xi)}\left(3B_iC_j\xi + 3B_jC_i\xi - 6\frac{CC_iC_j}{D}\right.\\
&\left.+ 6\frac{C^2C_iD_j}{D^2} + 6\frac{C^2C_jD_i}{D^2} - 6\frac{C^3D_iD_j}{D^3}\right)\\
&+ 2\frac{\zeta_i\zeta_j}{(1-\xi)^3}\left(3\frac{BC\xi}{D} - \frac{C^3}{D^2}\right) + 2\frac{\zeta_j}{D^2(1-\xi)^3}\left(3C^2C_i - 2\frac{C^3D_i}{D}\right)\\
&+ \frac{\zeta_i}{D(1-\xi)^2}\left(3B_jC\xi + 3BC_j\xi - 3\frac{C^2C_j}{D} + 2\frac{C^3D_j}{D^2}\right)\\
&+ \frac{1}{D^2(1-\xi)^2}\left(6CC_iC_j - 6\frac{C^2C_iD_j}{D} - 6\frac{C^2C_jD_i}{D} + 6\frac{C^3D_iD_j}{D^2}\right)\\
&+ 6\frac{\zeta_i\zeta_jC^3}{D^2(1-\xi)^4} + 6\frac{C^2C_j\zeta_i}{D^2(1-\xi)^3} - 4\frac{C^3\zeta_iD_j}{D^3(1-\xi)^3}\\
&- \frac{\zeta_j}{1-\xi}\left(3\frac{C^2C_i}{D^2} - 2\frac{C^3D_i}{D^3} - A_i\right)\\
&+ \frac{\ln(1-\xi)}{D^2}\left(6CC_iC_j - 6\frac{C^2C_iD_j}{D} - 6\frac{C^2C_jD_i}{D} + 6\frac{C^3D_iD_j}{D^2}\right)\\
&- \frac{\zeta_i\zeta_j}{(1-\xi)^2}\left(\frac{C^3}{D^2} - A\right) - \frac{\zeta_i}{1-\xi}\left(3\frac{C^2C_j}{D^2} - 2\frac{C^3D_j}{D^3} - A_j\right)
\end{aligned}
\tag{A.275}
$$

The chain term is given by Xu et al.[19]:

$$
(H_{\text{chain}})_{i,j}(T,\rho_i) = (1-m_i)\frac{\partial g_{ii}}{\partial \rho_j}\bigg|_{T,\rho_{k\neq j}} + (1-m_j)\frac{\partial g_{jj}}{\partial \rho_i}\bigg|_{T,\rho_{k\neq i}} + \sum_k \rho_k(1-m_k)\frac{\partial^2 \ln(g_{kk})}{\partial \rho_i \partial \rho_j}\bigg|_{T,\rho_{l\neq i,j}}
\tag{A.276}
$$

And the following second order derivative is required to in order to calculate the previous equation:

$$
\begin{aligned}
\frac{\partial^2 g_{ij}}{\partial \rho_k \partial \rho_l}\bigg|_{T,\rho_{m\neq k,l}} &= \left(\frac{\pi N_a}{6}\right)^2 \frac{2m_km_l(\sigma_k\sigma_l)^2}{(1-\xi_3)^3}\left\{\sigma_k\sigma_l + 3\left(\frac{\sigma_i\sigma_j}{\sigma_i+\sigma_j}\right)\left[\sigma_k + \sigma_l + 3\frac{\xi_2\sigma_k\sigma_l}{1-\xi_3}\right]\right.\\
&\left.+ 2\left(\frac{\sigma_i\sigma_j}{\sigma_i+\sigma_j}\right)^2\left[1 + 3\frac{\sigma_k\xi_2}{1-\xi_3} + 3\frac{\sigma_l\xi_2}{1-\xi_3} + 6\frac{\sigma_k\sigma_l\xi_2^2}{(1-\xi_3)^2}\right]\right\}
\end{aligned}
\tag{A.277}
$$

The dispersion term is easily calculated:

$$
(H_{\text{disp}})_{i,j}(T,\rho_i) = -2N_a\frac{\pi N_a}{6}m_im_j\sigma_{ij}^3\varepsilon_{ij}
\tag{A.278}
$$

The association term is given by Xu et al.[19]:

$$
\begin{aligned}
(H_{\text{assoc}})_{i,j}(T,\rho_i) &= \sum_{A_i}\frac{\partial x_{A_i}}{\partial \rho_j}\bigg|_{T,\rho_{k\neq j}}\left(\frac{1}{x_{A_i}} - \frac{1}{2}\right) + \sum_{A_j}\frac{\partial x_{A_j}}{\partial \rho_i}\bigg|_{T,\rho_{k\neq i}}\left(\frac{1}{x_{A_j}} - \frac{1}{2}\right)\\
&+ \sum_k \rho_k\left\{\sum_{A_k}\left[\frac{\partial x_{A_k}}{\partial \rho_i \partial \rho_j}\bigg|_{T,\rho_{l\neq i,j}}\left(\frac{1}{x_{A_k}} - \frac{1}{2}\right) - \frac{1}{x_{A_k}^2}\frac{\partial x_{A_k}}{\partial \rho_i}\bigg|_{T,\rho_{l\neq i}}\frac{\partial x_{A_k}}{\partial \rho_j}\bigg|_{T,\rho_{l\neq j}}\right]\right\}
\end{aligned}
\tag{A.279}
$$

As before, the second order partial derivative in the previous equation can be calculated by solving the following system of linear equations:

$$Qy_{kl} = c_{kl} \tag{A.280}$$

Where Q is the same matrix as above, y_{kl} is the solution vector $\left(\dfrac{\partial x_{A_i}}{\partial \rho_k \partial \rho_l}_{|T, \rho_{j \neq k, l}} \right)_{A_i}$ and c_{kl} is given by Xu et al.[19]

$$c_{kl} = r_{kl} + s_{kl} + t_{kl} \tag{A.281}$$

Where:

$$(r_{kl})_{A_i} = \frac{2}{x_{A_i}} \frac{\partial x_{A_i}}{\partial \rho_k}_{|T, \rho_{j \neq k}} \frac{\partial x_{A_i}}{\partial \rho_l}_{|T, \rho_{j \neq l}} \tag{A.282}$$

$$
(s_{kl})_{A_i} = -N_a \rho x_{A_i}^2 \left\{ \sum_j \sum_{B_j} x_j \left(x_{B_j} \frac{\partial \Delta_{A_i B_j}}{\partial \rho_k \partial \rho_l}_{|T, \rho_{m \neq k, l}} + \frac{\partial x_{B_j}}{\partial \rho_k}_{|T, \rho_{m \neq k}} \frac{\partial \Delta_{A_i B_j}}{\partial \rho_l}_{|T, \rho_{m \neq l}} \right. \right.
$$
$$
\left. \left. + \frac{\partial x_{B_j}}{\partial \rho_l}_{|T, \rho_{m \neq l}} \frac{\partial \Delta_{A_i B_j}}{\partial \rho_k}_{|T, \rho_{m \neq k}} \right) \right\} \tag{A.283}
$$

$$
(t_{kl})_{A_i} = -N_a \rho x_{A_i}^2 \left\{ \sum_{B_k} \left(x_{B_k} \frac{\partial \Delta_{A_i B_k}}{\partial \rho_l}_{|T, \rho_{j \neq l}} + \frac{\partial x_{B_k}}{\partial \rho_l}_{|T, \rho_{j \neq l}} \Delta_{A_i B_k} \right) \right.
$$
$$
\left. + \sum_{B_l} \left(x_{B_l} \frac{\partial \Delta_{A_i B_l}}{\partial \rho_k}_{|T, \rho_{j \neq k}} + \frac{\partial x_{B_l}}{\partial \rho_k}_{|T, \rho_{j \neq k}} \Delta_{A_i B_l} \right) \right\} \tag{A.284}
$$

Again, there is a small mistake in the expression of t_{kl} provided by Xu et al.[19]. The second order derivatives of $\Delta_{A_i B_j}$ can be calculated using equation (A.277).

References

[1] Chapman, W. G.; Gubbins, K. E.; Jackson, G.; Radosz, M. New reference equation of state for associating liquids. *Industrial & Engineering Chemistry Research* **1990**, *29*, 1709–1721.

[2] Davidson, N. *Statistical Mechanics*; Dover Publications, 2003.

[3] Wertheim, M. S. Fluids with highly directional attractive forces. I. Statistical Thermodynamics. *Journal of Statistical Physics* **1984**, *35*, 19–34.

[4] Wertheim, M. S. Fluids with highly directional attractive forces. II. Thermodynamic perturbation theory and integral equations. *Journal of Statistical Physics* **1984**, *35*, 35–47.

[5] Wertheim, M. S. Fluids with highly directional attractive forces. IV. Equilibrium polymerization. *Journal of Statistical Physics* **1986**, *42*, 477–492.

[6] Wertheim, M. S. Fluids with highly directional attractive forces. III. Multiple attraction sites. *Journal of Statistical Physics* **1986**, *42*, 459–476.

[7] Morita, T.; Hiroike, K. A New Approach to the Theory of Classical Fluids. III. *Progress of Theoretical Physics* **1961**, *25*, 537–578.

[8] Stell, G. The Equilibrium Theory of Classical Fluids. *HL Frisch and JL Lebowitz* **1964**, 171–261.

[9] Chapman, W. G. Theory and simulation of associating liquid mixtures. Ph.D. thesis, Cornell University, 1988.

[10] Zmpitas, W.; Gross, J. Detailed pedagogical review and analysis of Wertheim's thermodynamic perturbation theory. *Fluid Phase Equilibria* **2016**, *428*, 121–152.

[11] Rushbrooke, G. S.; Silbert, M. On triplet potentials in the theory of classical fluids. *Molecular Physics* **1967**, *12*, 505–511.

[12] Mansoori, G. A.; Carnahan, N. F.; Starling, K. E.; Leland, T. W. Equilibrium Thermodynamic Properties of the Mixture of Hard Spheres. *The Journal of Chemical Physics* **1971**, *54*, 1523–1525.

[13] Boublík, T. Hard-Sphere Equation of State. *The Journal of Chemical Physics* **1970**, *53*, 471–472.

[14] Lockett, A. M. A theory of homogeneous condensation from small nuclei. I. Modified Mayer theory of physical clusters. *The Journal of Chemical Physics* **1980**, *72*, 4822.

[15] Chapman, W. G.; Jackson, G.; Gubbins, K. E. Phase equilibria of associating fluids. *Molecular Physics* **1988**, *65*, 1057–1079.

[16] Chapman, W. G.; Jackson, G.; Gubbins, K. E. Phase equilibria of associating fluids. *Molecular Physics* **1988**, *65*, 1–31.

[17] Peters, C. J.; Goodwin, A. R. H.; Sengers, J. V. *SAFT Associating Fluids and Fluid Mixtures*; Applied Thermodynamics of Fluids; Royal Society of Chemistry, 2010; p 1.

[18] Wertheim, M. S. Fluids of dimerizing hard spheres, and fluid mixtures of hard spheres and dispheres. *The Journal of Chemical Physics* **1986**, *85*, 2929–2936.

[19] Xu, G.; Brennecke, J. F.; Stadtherr, M. A. *Reliable Computation of Phase Stability and Equilibrium from the SAFT Equation of State*; 2001.

A2: MATLAB Code

In this part, a MATLAB code that creates phase diagrams using SAFT HS is presented. It is organized into three main parts. First all the equations to calculate the Helmholtz energy, chemical potentials, pressure and the Hessian are implemented. Then different subroutines are implemented to generate different data (phase diagram, tie lines, critical points...). Finally the main script gather all these subroutines and all the required parameters in order to generate different graphs (binary and ternary phase diagrams, Pressure/density diagrams...).

Names for parameters

```
kb = 1.38064852 * 10^(-23);%Boltzmann constant
nav = 6.022140857 * 10^23;%Avogadro number
R = kb * nav;%Ideal gas constant

%   Components are always written with the following order: (solvent, polymer,
%nanoparticle)
%   rho: molar density (mol/Angstrom^3)
%   eta: reduced density (i.e. packing fraction)
%   rho_i: molar component density vector (mol/Angstrom^3)
%   x: mole fraction vector
%   w: mass fraction vector
%   P: pressure imposed to the system (Pa)
%   T: temperature of the system (K)
%   sigma_i: sphere diameters vector (Angstrom)
%   m: mass (of one particle) vector of all the components in the system
%   (kg)
%   m_i: chain length vector
%   e_i: dispersion energy vector (J)
%   k_ij: binary interaction parameters as an array
%   e_AiBj: associating energy given as a 4 dimensions array (first and
%   third indexes give different association sites and the others different
%   molecules)
%   n_Ai: array of numbers of identical site A (row) on molecule i (column)
%   k_AiBj: associating volume given as a 4 dimensions array (first and
%   third indexes give different association sites and the others different
%   molecules)
%   error_assoc: error on the final result for the association contribution
%   rc: reciprocal condition number for the matrix associated to the linear system
%that has to be solved in order to calculate the association contribution to chemical
%potential
%
%Four input arguments are related to the way the equation P(rho) - P*=0 is solved in
%thermos_properties_p:
%   [eta_start_a,eta_start_b]: starting interval
%   max_counter: maximum number of loops done in the while loop
%   max_n_roots: the while loop stops if more roots than this parameter
%   have been found
```

Helmholtz free energy

```matlab
function [a] =
helmholtz(rho,x,T,sigma_i,m,m_i,e_i,k_ij,e_AiBj,n_Ai,k_AiBj,error_assoc)
%HELMHOLTZ gives the helmholtz energy for mixtures

aideal = a_ideal( rho,x,T,m );
ahs = a_hs( rho,x,T,sigma_i,m_i );
achain = a_chain( rho,x,T,m_i,sigma_i );
adisp = a_disp( rho,x,sigma_i,m_i,e_i,k_ij );
if ~isempty(e_AiBj)
    aassoc = a_assoc( rho,x,T,sigma_i,m_i,e_AiBj,n_Ai,k_AiBj,error_assoc );
else
    aassoc = 0;
end
a = aideal+ahs+achain+adisp+aassoc;

end

function [ a ] = a_ideal( rho,x,T,m )
%A_IDEAL gives the ideal gas contribution to the molar Helmholtz energy a
%of a mixture

kb = 1.38064852 * 10^(-23);%Boltzmann constant
nav = 6.022140857 * 10^23;%Avogadro number
R = kb * nav;%Ideal gas constant

nn = length(x);

a = 0;
for i = 1:nn
    if x(i)~=0
        a = a + R*T*x(i)*(log(x(i)*nav*rho*10^30*(broglie(i,T,m))^3)-1);
    end
end

end

function [ l ] = broglie( i,T,m )
%BROGLIE gives the Thermal de Broglie wavelength l of a component i

kb = 1.38064852 * 10^(-23);%Boltzmann constant
h = 6.626070040 * 10^(-34);%Planck constant

l = h/(2*pi*m(i)*kb*T)^(1/2);

end


function [ a ] = a_ideal2( rho,x,T )
%A_IDEAL2 gives the classical ideal gas contribution to the molar Helmholtz energy a
%of a mixture

kb = 1.38064852 * 10^(-23);%Boltzmann constant
nav = 6.022140857 * 10^23;%Avogadro number
R = kb * nav;%Ideal gas constant
```

131

```matlab
nn = length(x);

a = R*T*log(R*T*rho);
for i = 1:nn
    if x(i)~=0
        a = a + R*T*x(i)*log(x(i));
    end
end

end

function [ a ] = a_hs( rho,x,T,sigma_i,m_i )
%A_HS gives the hard sphere contribution to the molar Helmholtz energy a of
%a mixture

kb = 1.38064852 * 10^(-23);%Boltzmann constant
nav = 6.022140857 * 10^23;%Avogadro number
R = kb * nav;%Ideal gas constant

%Auxiliary parameters
A = rho.*sum(x.*m_i.*sigma_i.^0);
B = rho.*sum(x.*m_i.*sigma_i.^1);
C = rho.*sum(x.*m_i.*sigma_i.^2);
D = rho.*sum(x.*m_i.*sigma_i.^3);
cc = (pi/6)*nav.*D;

%Helmholtz energy
a = (R*T./rho).*((3.*B.*C.*cc./D)./(1-cc)+(cc.*C.^3./(D.^2))./((1-cc).^2)+...
    log(1-cc).*(C.^3./(D.^2)-A));

end

function [ a ] = a_chain( rho,x,T,m_i,sigma_i )
%A_CHAIN gives the chain formation contribution to the molar Helmholtz
%energy a of a mixture

kb = 1.38064852 * 10^(-23);%Boltzmann constant
nav = 6.022140857 * 10^23;%Avogadro number
R = kb * nav;%Ideal gas constant

nn = length(x);

a = 0;
for i = 1:nn
    g = mixraddist(rho,x,i,i,sigma_i,m_i);
    a = a + R*T*x(i)*(1-m_i(i))*log(g);
end

end

function [ g ] = mixraddist( rho,x,i,j,sigma_i,m_i )
%MIXRADDIST gives the radial distribution function g for components i and j
%in a mixture

nav = 6.022140857 * 10^23;%Avogadro number

%Auxiliary parameters
c2 = (pi/6)*nav.*rho.*sum(x.*m_i.*sigma_i.^2);
c3 = (pi/6)*nav.*rho.*sum(x.*m_i.*sigma_i.^3);

%Radial distribution function for mixtures of hard spheres
g = 1./(1-c3) ...
```

132

```matlab
    + (3.*sigma_i(i).*sigma_i(j))./(sigma_i(i)+sigma_i(j)).*(c2./(1-c3).^2) ...
    + 2.*((sigma_i(i).*sigma_i(j))./(sigma_i(i)+sigma_i(j))).^2.*(c2.^2)./((1-c3).^3);

end

function [ a ] = a_assoc( rho,x,T,sigma_i,m_i,e_AiBj,n_Ai,k_AiBj,error_assoc )
%A_ASSOC gives the association contribution to the molar Helmholtz energy a
%of a mixture

kb = 1.38064852 * 10^(-23);%Boltzmann constant
nav = 6.022140857 * 10^23;%Avogadro number
R = kb * nav;%Ideal gas constant

d = deltaAiBj( rho,x,T,sigma_i,m_i,e_AiBj,k_AiBj );
Xa = XA( rho,x,T,sigma_i,m_i,e_AiBj,k_AiBj,error_assoc );

siz = size(d);
n = siz(1);
p = siz(2);

a = 0;
for i = 1:p
    s1 = 0;
    for j = 1:n
        s1 = s1 + n_Ai(j,i)*(log(Xa{j,i})-Xa{j,i}/2+1/2);
    end
    a = a + R*T*x(i)*s1;
end

end

function [ y ] = XA( rho,x,T,sigma_i,m_i,e_AiBj,k_AiBj,error_assoc )
%XA gives y the cell array of fractions of not bonded association sites of a
%mixture

deltaaibj = deltaAiBj( rho,x,T,sigma_i,m_i,e_AiBj,k_AiBj );
a = size(deltaaibj);
n = a(1);%maximum number of association sites
p = a(2);%number of different molecules

%Initialization
X = cell(n,p);%matrix of mole fractions of molecules i not bonded at site A
X(:,:) = {0.5};
y = cell(n,p);%identical as X but one more step in the iterative process
y(:,:) = {0.5};
for i = 1:n
    for j = 1:p
        y{i,j}=iteration(i,j,rho,x,X,T,sigma_i,m_i,e_AiBj,k_AiBj);
    end
end

%Stop condition initialization
nor = cell2mat(X)-cell2mat(y);

%Iteration
while norm(nor)>error_assoc

    X = y;
    for i = 1:n
        for j = 1:p
            y{i,j}=iteration(i,j,rho,x,y,T,sigma_i,m_i,e_AiBj,k_AiBj);
        end
    end
```

133

```matlab
    %Test for end condition
    nor = cell2mat(X)-cell2mat(y);

end

end

function [ y ] = iteration( A,i,rho,x,X,T,sigma_i,m_i,e_AiBj,k_AiBj )
%ITERATION gives f_Ai(X) where X is the array of fractions of not bonded
%association sites and f_Ai the function given by SAFT for molecule i and
%site A
%   X: cell array of fractions of not bonded association sites (rows
%   represent different association sites and columns different molecules)

nav = 6.022140857 * 10^23;%Avogadro number

deltaaibj = deltaAiBj( rho,x,T,sigma_i,m_i,e_AiBj,k_AiBj );

a = size(deltaaibj);
n = a(1); %maximum number of association site
p = a(2); %number of different molecules
d = deltaaibj;

s2 = 0;
for l = 1:p %sum on molecules
    s1 = 0;
    for j = 1:n %sum on association sites for a given molecule
        s1 = s1 + d{A,i,j,l}.*X{j,l};
    end
    s2 = s2 + x(l)*s1;
end

y = 1./(1+nav.*rho.*s2);

end

function [ y ] = deltaAiBj( rho,x,T,sigma_i,m_i,e_AiBj,k_AiBj )
%DELTAAIBJ gives the delta quantity (noted here as y) required for the
%association contribution to the molar Helmholtz energy

kb = 1.38064852 * 10^(-23);%Boltzmann constant

siz = size(e_AiBj);
D = zeros(siz);
G = cell(siz);
y = cell(siz);
for i = 1:siz(1)
    for j = 1:siz(2)
        for k = 1:siz(1)
            for l = 1:siz(2)
                D(i,j,k,l) = (sigma_i(j)+sigma_i(l))/2;
                G{i,j,k,l} = mixraddist(rho,x,j,l,sigma_i,m_i);
                y{i,j,k,l} = ...
G{i,j,k,l}.*D(i,j,k,l)^3*k_AiBj(i,j,k,l)*(exp(e_AiBj(i,j,k,l)/(kb*T))-1);
            end
        end
    end
end

end

function [ a ] = a_disp( rho,x,sigma_i,m_i,e_i,k_ij )
```

134

```
%A_DISP gives the dispersion contribution to the molar Helmholtz energy a
%of a mixture

nav = 6.022140857 * 10^23;%Avogadro number

nn = length(x);

%diameters and energies of mixing
sig = zeros(nn);
eps = zeros(nn);
for i = 1:nn
    for j = 1:nn
        sig(i,j) = (sigma_i(i)+sigma_i(j))/2;
        eps(i,j) = (1-k_ij(i,j)) * (e_i(i)*e_i(j))^(1/2);
    end
end

%matrix x_im_ix_jm_j
xmxm = (transpose(x.*m_i)*(x.*m_i));

%Helmholtz energy
a = -nav*(pi*nav.*rho/6).*sum(sum(sig.^3.*eps.*xmxm));

end
```

Published with MATLAB® R2017b

Chemical potential

```
function [mu,rc] = chempot(
rho,x,T,sigma_i,m,m_i,e_i,k_ij,e_AiBj,n_Ai,k_AiBj,error_assoc )
%CHEMPOT gives the chemical potential for mixtures

nn = length(x);

mu = cell(1,nn);
for i = 1:nn
    muideal = mu_ideal( rho,x,i,T,m );
    muhs = mu_hs( rho,x,i,T,sigma_i,m_i );
    muchain = mu_chain( rho,x,i,T,sigma_i,m_i );
    mudisp = mu_disp( rho,x,i,sigma_i,m_i,e_i,k_ij );
    if ~isempty(e_AiBj)
        [muassoc,rc] = mu_assoc( rho,x,i,T,sigma_i,m_i,e_AiBj,n_Ai,k_AiBj,error_assoc
);
    else
        muassoc = 0;
        rc = 0;
    end
    mu{i} = muideal+muhs+muchain+mudisp+muassoc;
end

end
```

```matlab
function [ mu ] = mu_ideal( rho,x,i,T,m )
%MU_IDEAL gives the ideal gas contribution to the chemical potential mu of
%component i in a mixture

kb = 1.38064852 * 10^(-23);%Boltzmann constant
nav = 6.022140857 * 10^23;%Avogadro number
R = kb * nav;%Ideal gas constant

if x(i) == 0
    mu = 0;%in order to avoid -InF*0 issues when calculating Gibbs energy
else
    mu = R*T*log(x(i)*nav*rho*10^30*(broglie(i,T,m))^3);
end

end

function [ mu ] = mu_ideal2( rho,x,i,T )
%MU_IDEAL gives the classical ideal gas contribution to the chemical potential mu of
%component i in a mixture

kb = 1.38064852 * 10^(-23);%Boltzmann constant
nav = 6.022140857 * 10^23;%Avogadro number
R = kb * nav;%Ideal gas constant

if x(i) == 0
    mu = 0;%in order to avoid -InF*0 issues when calculating Gibbs energy
else
    mu = R*T*(log(R*T*x(i)*rho)+1);
end

end

function [ mu ] = mu_hs( rho,x,i,T,sigma_i,m_i )
%MU_HS gives the hard sphere contribution to the chemical potential mu of
%component i in a mixture

kb = 1.38064852 * 10^(-23);
nav = 6.022140857 * 10^23;
R = kb * nav;

%Auxiliary parameters
A = rho.*sum(x.*m_i.*sigma_i.^0);
B = rho.*sum(x.*m_i.*sigma_i.^1);
C = rho.*sum(x.*m_i.*sigma_i.^2);
D = rho.*sum(x.*m_i.*sigma_i.^3);
cc = (pi/6)*nav.*D;
Ai =m_i(i)*sigma_i(i)^0;
Bi =m_i(i)*sigma_i(i)^1;
Ci =m_i(i)*sigma_i(i)^2;
Di =m_i(i)*sigma_i(i)^3;
cci = (pi/6)*nav*Di;

%Chemical potential

mu = R*T*(...
    1./(1-cc).*...
    (3.*Bi.*C.*cc./D+3.*B.*Ci.*cc./D-C.^3.*cci./D.^2+A.*cci)...
    +1./(1-cc).^2.*...
    (3.*B.*C.*cc.*cci./D+3.*C.^2.*Ci.*cc./D.^2-C.^3.*cci./D.^2) ...
    +1./(1-cc).^3.*...
    (2.*C.^3.*cc.*cci./D.^2) ...
    +log(1-cc).*...
    (3.*C.^2.*Ci./D.^2-2.*C.^3.*Di./D.^3-Ai)...
```

```matlab
    );

end

function [ mu ] = mu_chain( rho,x,i,T,sigma_i,m_i )
%MU_CHAIN gives the chain formation contribution to the chemical potential
%mu of component i in a mixture

kb = 1.38064852 * 10^(-23);%Boltzmann constant
nav = 6.022140857 * 10^23;%Avogadro number
R = kb * nav;%Ideal gas constant

nn = length(x);
g = mixraddist(rho,x,i,i,sigma_i,m_i);
mu = R*T*(1-m_i(i))*log(g);
for j = 1:nn
    dlg = d_ln_raddist(rho,x,i,j,sigma_i,m_i);
    mu = mu + R*T*(x(j)*rho.*(1-m_i(j)).*dlg);
end

end

function [ dlg ] = d_ln_raddist( rho,x,i,j,sigma_i,m_i )
%D_LN_RADDIST gives the derivative dlg of the ln of the radial distribution
%function for component j with respect to the molar density of component i
%in a mixture

gg = mixraddist(rho,x,j,j,sigma_i,m_i);
dg = d_raddist(rho,x,i,j,j,sigma_i,m_i);
dlg = dg./gg;

end

function [ dg ] = d_raddist( rho,x,i,j,k,sigma_i,m_i )
%D_RADDIST gives the derivative dg of the radial distribution function
%between components j and k with respect to the molar density of component
%i in a mixture

nav = 6.022140857 * 10^23;%Avogadro number

%Auxiliary parameters
c2 = (pi*nav/6).*rho.*sum(x.*m_i.*sigma_i.^2);
c3 = (pi*nav/6).*rho.*sum(x.*m_i.*sigma_i.^3);

%Derivative  wrt component i of the radial distribution function of
%mixtures of hard spheres
dg = (pi/6).*nav.*m_i(i).*(sigma_i(i).^3./((1-c3).^2)+...
    3.*sigma_i(j).*sigma_i(k)./(sigma_i(j)+sigma_i(k)).*(sigma_i(i).^2./((1-
c3).^2)+...
    2.*sigma_i(i).^3.*c2./((1-c3).^3))+...

2.*(sigma_i(j).*sigma_i(k)./(sigma_i(j)+sigma_i(k))).^2.*(2.*sigma_i(i).^2.*c2./((1-
c3).^3)+...
    3.*sigma_i(i).^3.*c2.^2./((1-c3).^4)));

end

function [ mu,rc ] = mu_assoc( rho,x,i,T,sigma_i,m_i,e_AiBj,n_Ai,k_AiBj,error_assoc )
%MU_ASSOC gives the association contribution to the chemical potential mu
%of component i in a mixture

kb = 1.38064852 * 10^(-23);%Boltzmann constant
nav = 6.022140857 * 10^23;%Avogadro number
```

137

```matlab
R = kb * nav;%Ideal gas constant

a = size(e_AiBj);
n = a(1); %maximum number of association site
p = a(2); %number of different molecules

Xa = XA( rho,x,T,sigma_i,m_i,e_AiBj,k_AiBj,error_assoc );
[dXa,rc] = dXA(rho,x,Xa,i,T,sigma_i,m_i,e_AiBj,k_AiBj);

s1 = 0;
for j = 1:n
    s1 = s1 + n_Ai(j,i)*(log(Xa{j,i}) - Xa{j,i}/2 + 1/2);
end

s2 = 0;
for k = 1:p
    s3 = 0;
    for j = 1:n
        s3 = s3 + n_Ai(j,k)*(dXa{j,k}.*(1./Xa{j,k}-1/2));
    end
    s2 = s2 + x(k)*s3;
end

mu = R*T*(s1 + rho.*s2);

end

function [dxa,rc] = dXA(rho,x,Xa,q,T,sigma_i,m_i,e_AiBj,k_AiBj)
%dXA gives dxa the derivative with respect to the molar density of component q
%of the cell array of fractions of not bonded association sites for a
%system with the following properties:
%   Xa: cell array of fractions of not bonded association sites

nav = 6.022140857 * 10^23;%Avogadro constant

d = deltaAiBj( rho,x,T,sigma_i,m_i,e_AiBj,k_AiBj );
dd = d_deltaAiBj( rho,x,q,T,sigma_i,m_i,e_AiBj,k_AiBj );

siz = size(d);
n_assoc = siz(1)*siz(2);%total number of association sites (some can be "0")

%Creation of a matrix used to convert a matrix to a vector and back
conv = zeros(siz(1),siz(2));
for i = 1:siz(1)
    for j = 1:siz(2)
        conv(i,j)=j+(i-1)*siz(2);
    end
end

%Creation of Q and c
Q = zeros(n_assoc,n_assoc);
c = zeros(n_assoc,1);

for i = 1:siz(1)
    for j = 1:siz(2)

        %c
        s1 = 0;
        for k = 1:siz(1)
            s1 = s1 + Xa{k,q}.*d{i,j,k,q};
        end

        s2 = 0;
```

```matlab
        for l = 1:siz(2)
            s3 = 0;
            for k = 1:siz(1)
                s3 = s3 + Xa{k,l}.*dd{i,j,k,l};
            end
            s2 = s2 + x(l)*s3;
        end

        c(conv(i,j)) = -nav*Xa{i,j}.^2.*(s1 + rho.*s2);

        %Q
        for k = 1:siz(1)
            for l = 1:siz(2)
                Q(conv(i,j),conv(k,l)) = eq(conv(i,j),conv(k,l)) +
Xa{i,j}.^2.*nav.*rho.*x(l).*d{i,j,k,l};
            end
        end

    end
end

%Solve linear system
dxa = cell(siz(1),siz(2));%final solution as a matrix (cell)
rc = rcond(Q);
y = Q\c;%solution as a vector

%Convert vectors back to matrices
for i = 1:siz(1)
    for j = 1:siz(2)
        dxa{i,j} = y(conv(i,j));
    end
end

end

function [ y ] = d_deltaAiBj( rho,x,q,T,sigma_i,m_i,e_AiBj,k_AiBj )
%D_DELTAAIBJ gives the derivative with respect to the molar density of
%component q of the delta quantity (noted here as y) required for the
%association contribution to the molar Helmholtz energy

kb = 1.38064852 * 10^(-23);%Boltzmann constant

siz = size(e_AiBj);
D = zeros(siz);
G = cell(siz);
y = cell(siz);
for i = 1:siz(1)
    for j = 1:siz(2)
        for k = 1:siz(1)
            for l = 1:siz(2)
                D(i,j,k,l) = (sigma_i(j)+sigma_i(l))/2;
                G{i,j,k,l} = d_raddist(rho,x,q,j,l,sigma_i,m_i);
                y{i,j,k,l} =
G{i,j,k,l}.*D(i,j,k,l)^3*k_AiBj(i,j,k,l)*(exp(e_AiBj(i,j,k,l)/(kb*T))-1);
            end
        end
    end
end

end

function [ mu ] = mu_disp( rho,x,i,sigma_i,m_i,e_i,k_ij )
%MU_CHAIN gives the chain formation contribution to the chemical potential
```

```matlab
%mu of component i in a mixture

nav = 6.022140857 * 10^23;%Avogadro number

nn = length(x);

%diameters and energies of mixing
sig = zeros(nn);
eps = zeros(nn);
for k = 1:nn
    for j = 1:nn
        sig(k,j) = (sigma_i(k)+sigma_i(j))/2;
        eps(k,j) = (1-k_ij(k,j)) * (e_i(k)*e_i(j))^(1/2);
    end
end

mu = -nav*(pi*nav.*rho/6)*m_i(i)*2.*sum(x.*m_i.*(sig(i,:).^3).*eps(i,:));

end
```

Pressure

```matlab
function [p] = pressure( rho,x,T,sigma_i,m_i,e_i,k_ij,e_AiBj,n_Ai,k_AiBj,error_assoc )
%PRESSURE gives the pressure (directly derivated from Helmholtz energy) for
%mixtures

pideal = p_ideal(rho,T);
phs = p_hs(rho,x,T,sigma_i,m_i);
pchain = p_chain(rho,x,T,m_i,sigma_i);
if ~isempty(e_AiBj)
    passoc = p_assoc(rho,x,T,sigma_i,m_i,e_AiBj,n_Ai,k_AiBj,error_assoc);
else
    passoc = 0;
end
pdisp = p_disp(rho,x,sigma_i,m_i,e_i,k_ij);
p = pideal+phs+pchain+passoc+pdisp;

end

function [p] = p_ideal(rho,T)
%P_IDEAL gives the ideal contribution to the pressure p of a system

kb = 1.38064852 * 10^(-23);%Boltzmann constant
nav = 6.022140857 * 10^23;%Avogadro number
R = kb * nav;%Ideal gas constant

p = rho * 1e30 * R * T;
end

function [p] = p_hs( rho,x,T,sigma_i,m_i )
%P_HS gives the hard sphere contribution to the pressure p of a system

kb = 1.38064852 * 10^(-23);%Boltzmann constant
```

140

```matlab
nav = 6.022140857 * 10^23;%Avogadro number
R = kb * nav;%Ideal gas constant

%Auxiliary parameters
c0 = (pi/6)*nav.*rho.*sum(x.*m_i.*sigma_i.^0);
c1 = (pi/6)*nav.*rho.*sum(x.*m_i.*sigma_i.^1);
c2 = (pi/6)*nav.*rho.*sum(x.*m_i.*sigma_i.^2);
c3 = (pi/6)*nav.*rho.*sum(x.*m_i.*sigma_i.^3);
m = sum(x.*m_i);

%Pressure
p = m*R*T*rho*1e30*(1/(1-c3) + 3*c1*c2/(c0*(1-c3)^2)+(3*c2^3-c2^3*c3)/(c0*(1-c3)^3)-
1);

end

function [p] = p_chain( rho,x,T,m_i,sigma_i )
%P_CHAIN gives the chain formation contribution to the pressure p of a
%mixture

kb = 1.38064852 * 10^(-23);%Boltzmann constant
nav = 6.022140857 * 10^23;%Avogadro number
R = kb * nav;%Ideal gas constant

nn = length(x);

p = 0;
for i = 1:nn
    dlg = d_ln_raddist_rho(rho,x,i,sigma_i,m_i);
    p = p +R*T*rho*1e30*x(i)*(1-m_i(i))*dlg;
end

end

function [dlg] = d_ln_raddist_rho(rho,x,i,sigma_i,m_i)
%D_LN_RADDIST_RHO gives the derivative dlg of the ln of the radial distribution
%function for component i with respect to the overall molar density (times the molar
%density) in a mixture

nav = 6.022140857 * 10^23;%Avogadro number

%Auxiliary parameters
c2 = (pi*nav/6).*rho.*sum(x.*m_i.*sigma_i.^2);
c3 = (pi*nav/6).*rho.*sum(x.*m_i.*sigma_i.^3);

%Derivative  wrt component i of the radial distribution function of
%mixtures of hard spheres

g = mixraddist( rho,x,i,i,sigma_i,m_i );
dlg = 1/g*(c3/(1-c3)^2+3/2*(sigma_i(i)*c2)/((1-c3)^2)...
    +(3*sigma_i(i)*c2*c3)/((1-c3)^3)+(sigma_i(i)^2*c2^2)/((1-c3)^3)...
    +3/2*(sigma_i(i)^2*c2^2*c3)/((1-c3)^4));

end

function [ dg ] = d_raddist_rho( rho,x,i,j,sigma_i,m_i )
%D_RADDIST_rho gives the derivative dg of the radial distribution function
%between components i and j with respect to the overall molar density
%in a mixture

nav = 6.022140857 * 10^23;%Avogadro number

%Auxiliary parameters
```

```matlab
c2 = (pi*nav/6).*rho.*sum(x.*m_i.*sigma_i.^2);
c3 = (pi*nav/6).*rho.*sum(x.*m_i.*sigma_i.^3);

%Derivative  wrt component i of the radial distribution function of
%mixtures of hard spheres
dg = 1/rho*(...
    c3/((1-c3).^2)+...
    3.*sigma_i(i).*sigma_i(j)./(sigma_i(i)+sigma_i(j)).*(c2/((1-c3).^2)+...
    2.*c3.*c2./((1-c3).^3))+...
    2.*(sigma_i(i).*sigma_i(j)./(sigma_i(i)+sigma_i(j))).^2.*(2.*c2.^2./((1-
c3).^3)+...
    3.*c3.*c2.^2./((1-c3).^4))...
    );

end

function [p] = p_assoc( rho,x,T,sigma_i,m_i,e_AiBj,n_Ai,k_AiBj,error_assoc )
%P_ASSOC gives the association contribution to the pressure p
%of a mixture

kb = 1.38064852 * 10^(-23);%Boltzmann constant
nav = 6.022140857 * 10^23;%Avogadro number
R = kb * nav;%Ideal gas constant

a = size(e_AiBj);
n = a(1); %maximum number of association site
p = a(2); %number of different molecules

Xa = XA( rho,x,T,sigma_i,m_i,e_AiBj,k_AiBj,error_assoc );
dXa = dXA_rho(rho,x,Xa,T,sigma_i,m_i,e_AiBj,k_AiBj);

s2 = 0;
for k = 1:p
    s3 = 0;
    for j = 1:n
        s3 = s3 + n_Ai(j,k)*(dXa{j,k}.*(1./Xa{j,k}-1/2));
    end
    s2 = s2 + x(k)*s3;
end

p = R*T*rho*1e30*(rho.*s2);

end

function dxa = dXA_rho(rho,x,Xa,T,sigma_i,m_i,e_AiBj,k_AiBj)
%XA gives dxa the derivative with respect to the overall molar density
%of the cell array of fractions of not bonded association sites for a
%system
%   Xa: cell array of fractions of not bonded association sites

nav = 6.022140857 * 10^23;%Avogadro constant

d = deltaAiBj( rho,x,T,sigma_i,m_i,e_AiBj,k_AiBj );
dd = d_deltaAiBj_rho( rho,x,T,sigma_i,m_i,e_AiBj,k_AiBj );

siz = size(d);
n_assoc = siz(1)*siz(2);%total number of association sites (some can be "0")

%Creation of a matrix used to convert a matrix to a vector and back
conv = zeros(siz(1),siz(2));
for i = 1:siz(1)
    for j = 1:siz(2)
        conv(i,j)=j+(i-1)*siz(2);
```

142

```matlab
        end
    end

%Creation of Q and c
Q = zeros(n_assoc,n_assoc);
c = zeros(n_assoc,1);

for i = 1:siz(1)
    for j = 1:siz(2)

        %c
        s1 = 0;
        for l = 1:siz(2)
            s2 = 0;
            for k = 1:siz(1)
                s2 = s2 + Xa{k,l}.*(d{i,j,k,l} + rho.*dd{i,j,k,l});
            end
            s1 = s1 + x(l).*s2;
        end

        c(conv(i,j)) = -nav*Xa{i,j}.^2.*s1;

        %Q
        for k = 1:siz(1)
            for l = 1:siz(2)
                Q(conv(i,j),conv(k,l)) = eq(conv(i,j),conv(k,l)) +
Xa{i,j}.^2.*nav.*rho.*x(l).*d{i,j,k,l};
            end
        end

    end
end

%Solve linear system
dxa = cell(siz(1),siz(2));%final solution as a matrix (cell)
y = Q\c;%solution as a vector

%Convert vectors back to matrices
for i = 1:siz(1)
    for j = 1:siz(2)
        dxa{i,j} = y(conv(i,j));
    end
end

end

function [ y ] = d_deltaAiBj_rho( rho,x,T,sigma_i,m_i,e_AiBj,k_AiBj )
%D_DELTAAIBJ gives the derivative with respect to the overall molar density
%of the delta quantity (noted here as y) required for the
%association contribution to the molar Helmholtz energy

kb = 1.38064852 * 10^(-23);%Boltzmann constant

siz = size(e_AiBj);
D = zeros(siz);
G = cell(siz);
y = cell(siz);
for i = 1:siz(1)
    for j = 1:siz(2)
        for k = 1:siz(1)
            for l = 1:siz(2)
                D(i,j,k,l) = (sigma_i(j)+sigma_i(l))/2;
                G{i,j,k,l} = d_raddist_rho(rho,x,j,l,sigma_i,m_i);
```

```matlab
                y{i,j,k,l} =
G{i,j,k,l}.*D(i,j,k,l)^3*k_AiBj(i,j,k,l)*(exp(e_AiBj(i,j,k,l)/(kb*T))-1);
            end
        end
    end
end

end

function [p] = p_disp( rho,x,sigma_i,m_i,e_i,k_ij )
%A_DISP gives the dispersion contribution to the pressure p
%of a mixture

nav = 6.022140857 * 10^23;%Avogadro number

nn = length(x);

%diameters and energies of mixing
sig = zeros(nn);
eps = zeros(nn);
for i = 1:nn
    for j = 1:nn
        sig(i,j) = (sigma_i(i)+sigma_i(j))/2;
        eps(i,j) = (1-k_ij(i,j)) * (e_i(i)*e_i(j))^(1/2);
    end
end

%matrix x_im_ix_jm_j
xmxm = (transpose(x.*m_i)*(x.*m_i));

%Pressure
p = -nav*(pi*nav.*rho^2/6).*sum(sum(sig.^3.*eps.*xmxm))*1e30;

end
```

Hessian

```matlab
function [h] = hessian(
rho,rho_i,T,sigma_i,m_i,e_i,k_ij,e_AiBj,n_Ai,k_AiBj,error_assoc )
%HESSIAN gives the Hessian (wrt molar component densities) of the Helmholtz
%energy density for mixtures
nn = length(rho_i);

h = zeros(nn);
for i = 1:nn
    for j =1:nn
        hideal = h_ideal(rho_i,T,i,j);
        hhs = h_hs(rho,rho_i,T,m_i,sigma_i,i,j);
        hchain = h_chain(rho,rho_i,T,m_i,sigma_i,i,j);
        hdisp = h_disp(sigma_i,m_i,e_i,k_ij,i,j);
        if ~isempty(e_AiBj)
            hassoc =
h_assoc(rho,rho_i,T,sigma_i,m_i,e_AiBj,n_Ai,k_AiBj,error_assoc,i,j);
```

144

```matlab
        else
            hassoc = 0;
        end
        h(i,j) = hideal+hhs+hchain+hdisp+hassoc;
    end
end

end

function [h] = h_ideal(rho_i,T,i,j)
%H_IDEAL gives the ideal contribution to the (i,j) coefficient of the
%Hessian of the Helmholtz energy density in a mixture

kb = 1.38064852 * 10^(-23);%Boltzmann constant
nav = 6.022140857 * 10^23;%Avogadro number
R = kb * nav;%Ideal gas constant

h=0;
if i == j
    h = R*T/(rho_i(i));
end

end

function [h] = h_hs( rho,rho_i,T,m_i,sigma_i,i,j )
%H_HS gives the hard sphere contribution to the (i,j) coefficient of the
%Hessian of the Helmholtz energy density of a mixture

kb = 1.38064852 * 10^(-23);%Boltzmann constant
nav = 6.022140857 * 10^23;%Avogadro number
R = kb * nav;%Ideal gas constant
x = rho_i/rho;

%Auxiliary parameters
A = rho.*sum(x.*m_i.*sigma_i.^0);
B = rho.*sum(x.*m_i.*sigma_i.^1);
C = rho.*sum(x.*m_i.*sigma_i.^2);
D = rho.*sum(x.*m_i.*sigma_i.^3);
cc = (pi/6)*nav.*D;
Ai =m_i(i)*sigma_i(i)^0;
Bi =m_i(i)*sigma_i(i)^1;
Ci =m_i(i)*sigma_i(i)^2;
Di =m_i(i)*sigma_i(i)^3;
cci = (pi/6)*nav*Di;
Aj =m_i(j)*sigma_i(j)^0;
Bj =m_i(j)*sigma_i(j)^1;
Cj =m_i(j)*sigma_i(j)^2;
Dj =m_i(j)*sigma_i(j)^3;
ccj = (pi/6)*nav*Dj;

%Hessian
h = ccj/(D*(1-cc)^2) * (3*Bi*C*cc + 3*B*Ci*cc - 3*C^2*Ci/D + 2*C^3*Di/D^2)...
    + 1/(D*(1-cc)) * (3*Bi*Cj*cc + 3*Bj*Ci*cc - 6*C*Ci*Cj/D...
    + 6*C^2*Ci*Dj/D^2 + 6*C^2*Cj*Di/D^2 - 6*C^3*Di*Dj/D^3)...
    + 2*cci*ccj/(1-cc)^3 * (3*B*C*cc/D-C^3/D^2) + 2*ccj/(D^2*(1-cc)^3)*(3*C^2*Ci-
2*C^3*Di/D)...
    + cci/(D*(1-cc)^2) * (3*Bj*C*cc + 3*B*Cj*cc - 3*C^2*Cj/D + 2*C^3*Dj/D^2)...
    + 1/(D^2*(1-cc)^2) * (6*C*Ci*Cj - 6*C^2*Ci*Dj/D - 6*C^2*Cj*Di/D +
6*C^3*Di*Dj/D^2)...
    + 6*cci*ccj*C^3/(D^2*(1-cc)^4) + 6*C^2*Cj*cci/(D^2*(1-cc)^3) -
4*C^3*cci*Dj/(D^3*(1-cc)^3)...
    - ccj/(1-cc) * (3*C^2*Ci/D^2 - 2*C^3*Di/D^3 - Ai)...
    + log(1-cc)/D^2 * (6*C*Ci*Cj - 6*C^2*Ci*Dj/D - 6*C^2*Cj*Di/D + 6*C^3*Di*Dj/D^2)...
```

```matlab
        - cci*ccj/(1-cc)^2*(C^3/D^2-A) - cci/(1-cc) * (3*C^2*Cj/D^2 - 2*C^3*Dj/D^3 - Aj);

h = R*T*h;

end

function [h] = h_chain( rho,rho_i,T,m_i,sigma_i,i,j )
%H_CHAIN gives the chain contribution to the (i,j) coefficient of the
%Hessian of the Helmholtz energy density of a mixture

kb = 1.38064852 * 10^(-23);%Boltzmann constant
nav = 6.022140857 * 10^23;%Avogadro number
R = kb * nav;%Ideal gas constant

x = rho_i/rho;%mole fraction vector
nn = length(x);

dli = d_ln_raddist( rho,x,j,i,sigma_i,m_i );
dlj = d_ln_raddist( rho,x,i,j,sigma_i,m_i );

h = R*T*((1-m_i(i))*dli+(1-m_i(j))*dlj);

for k = 1:nn
    d2lk = d2_ln_raddist( rho,x,k,i,j,sigma_i,m_i );
    h = h + R*T* rho_i(k)*(1-m_i(k))*d2lk;
end

end

function [dlg] = d2_ln_raddist( rho,x,k,i,j,sigma_i,m_i )
%D2_LN_RADDIST gives the derivative dlg of the ln of the radial distribution
%function for component k with respect to the molar density of components i
%and j in a mixture

g = mixraddist(rho,x,k,k,sigma_i,m_i);
dgi = d_raddist(rho,x,i,k,k,sigma_i,m_i);
dgj = d_raddist(rho,x,j,k,k,sigma_i,m_i);
ddg = d2_raddist( rho,x,i,j,k,k,sigma_i,m_i );

dlg = ddg/g-dgi*dgj/g^2;

end

function [dg] = d2_raddist( rho,x,i,j,k,l,sigma_i,m_i )
%D2_RADDIST gives the second order derivative dg of the radial distribution function
%between components k and l with respect to the molar density of components
%i and j in a mixture

nav = 6.022140857 * 10^23;%Avogadro number

%Auxiliary parameters
c2 = (pi*nav/6).*rho.*sum(x.*m_i.*sigma_i.^2);
c3 = (pi*nav/6).*rho.*sum(x.*m_i.*sigma_i.^3);

%Derivative
dg = (pi*nav/6)^2*(2*m_i(i)*m_i(j)*(sigma_i(i)*sigma_i(j))^2)/(1-c3)^3*(...
    sigma_i(i)*sigma_i(j) + 3*(sigma_i(k)*sigma_i(l)/(sigma_i(k)+sigma_i(l)))...
    *(sigma_i(i)+sigma_i(j) + (3*c2*sigma_i(i)*sigma_i(j))/(1-c3))...
    +2*(sigma_i(k)*sigma_i(l)/(sigma_i(k)+sigma_i(l)))^2*...
    (1+3*sigma_i(i)*c2/(1-c3)+3*sigma_i(j)*c2/(1-c3)...
    +6*c2^2*sigma_i(i)*sigma_i(j)/(1-c3)^2)...
    );
```

```matlab
    end

function [h] = h_assoc( rho,rho_i,T,sigma_i,m_i,e_AiBj,n_Ai,k_AiBj,error_assoc,i,j )
%H_ASSOC gives the association contribution to the (i,j) coefficient of the
%Hessian of the Helmholtz energy density of a mixture

kb = 1.38064852 * 10^(-23);%Boltzmann constant
nav = 6.022140857 * 10^23;%Avogadro number
R = kb * nav;%Ideal gas constant

a = size(e_AiBj);
n = a(1); %maximum number of association site
p = a(2); %number of different molecules

x = rho_i/rho;

Xa = XA( rho,x,T,sigma_i,m_i,e_AiBj,k_AiBj,error_assoc );
dXai = dXA(rho,x,Xa,i,T,sigma_i,m_i,e_AiBj,k_AiBj);
dXaj = dXA(rho,x,Xa,j,T,sigma_i,m_i,e_AiBj,k_AiBj);
dXaij = d2XA(rho,x,Xa,dXai,dXaj,i,j,T,sigma_i,m_i,e_AiBj,k_AiBj);

s1 = 0;
for k = 1:n
    s1 = s1 + n_Ai(k,i)*(1/Xa{k,i} - 1/2) * dXaj{k,i};
end

s2 = 0;
for k = 1:n
    s2 = s2 + n_Ai(k,j)*(1/Xa{k,j} - 1/2) * dXai{k,j};
end

s3 = 0;
for l = 1:p
    s4 = 0;
    for k = 1:n
        s4 = s4 + n_Ai(k,l)*(1/Xa{k,l}-1/2)*dXaij{k,l} -
n_Ai(k,l)*dXai{k,l}*dXaj{k,l}/(Xa{k,l})^2;
    end
    s3 = s3 + rho_i(l)*s4;
end

%Hessian
h = R*T*(s1+s2+s3);

end

function dxa = d2XA(rho,x,Xa,dXap,dXaq,p,q,T,sigma_i,m_i,e_AiBj,k_AiBj)
%D2XA gives dxa the derivative with respect to the molar density of components p
%and q of the cell array of fractions of not bonded association sites for a
%system
%   Xa: cell array of fractions of not bonded association sites
%   dXap: cell array of  derivative wrt p of fractions of not bonded association sites
%   dXaq: cell array of  derivative wrt q of fractions of not bonded association sites

nav = 6.022140857 * 10^23;%Avogadro constant

d = deltaAiBj( rho,x,T,sigma_i,m_i,e_AiBj,k_AiBj );
ddp = d_deltaAiBj( rho,x,p,T,sigma_i,m_i,e_AiBj,k_AiBj );
ddq = d_deltaAiBj( rho,x,q,T,sigma_i,m_i,e_AiBj,k_AiBj );
d2d = d2_deltaAiBj( rho,x,p,q,T,sigma_i,m_i,e_AiBj,k_AiBj );

siz = size(d);
n_assoc = siz(1)*siz(2);%total number of association sites (some can be "0")
```

147

```matlab
%Creation of a matrix used to convert a matrix to a vector and back
conv = zeros(siz(1),siz(2));
for i = 1:siz(1)
    for j = 1:siz(2)
        conv(i,j)=j+(i-1)*siz(2);
    end
end

%Creation of Q and c
Q = zeros(n_assoc,n_assoc);
c = zeros(n_assoc,1);

for i = 1:siz(1)
    for j = 1:siz(2)

        %r
        r = 2*dXap{i,j}*dXaq{i,j}/Xa{i,j};

        %s
        s1 = 0;
        for l = 1:siz(2)
            s2 = 0;
            for k = 1:siz(1)
                s2 = s2 + Xa{k,l}*d2d{i,j,k,l} + dXap{k,l} * ddq{i,j,k,l} +
dXaq{k,l}*ddp{i,j,k,l};
            end
            s1 = s1 + x(l)*s2;
        end
        s = -nav*rho*(Xa{i,j}^2) * s1;

        %t
        s1 = 0;
        for k = 1:siz(1)
            s1 = s1 + ddq{i,j,k,p}*Xa{k,p} + d{i,j,k,p}*dXaq{k,p};
        end
        s2 = 0;
        for k = 1:siz(1)
            s2 = s2 + ddp{i,j,k,q}*Xa{k,q} + d{i,j,k,q}*dXap{k,q};
        end
        t = -nav*(Xa{i,j}^2) * (s1+s2);

        %c
        c(conv(i,j)) = r+s+t;

        %Q
        for k = 1:siz(1)
            for l = 1:siz(2)
                Q(conv(i,j),conv(k,l)) = eq(conv(i,j),conv(k,l)) +
Xa{i,j}.^2.*nav.*rho.*x(l).*d{i,j,k,l};
            end
        end

    end
end

%Solve linear system
dxa = cell(siz(1),siz(2));%final solution as a matrix (cell)
y = Q\c;%solution as a vector

%Convert vectors back to matrices
for i = 1:siz(1)
    for j = 1:siz(2)
```

148

```matlab
            dxa{i,j} = y(conv(i,j));
        end
    end

end

function [ y ] = d2_deltaAiBj( rho,x,p,q,T,sigma_i,m_i,e_AiBj,k_AiBj )
%D_DELTAAIBJ gives the derivative with respect to the molar density of
%components p and q of the delta quantity (noted here as y) required for the
%association contribution to the molar Helmholtz energy

kb = 1.38064852 * 10^(-23);%Boltzmann constant

siz = size(e_AiBj);
D = zeros(siz);
G = cell(siz);
y = cell(siz);
for i = 1:siz(1)
    for j = 1:siz(2)
        for k = 1:siz(1)
            for l = 1:siz(2)
                D(i,j,k,l) = (sigma_i(j)+sigma_i(l))/2;
                G{i,j,k,l} = d2_raddist( rho,x,p,q,j,l,sigma_i,m_i );
                y{i,j,k,l} =
G{i,j,k,l}.*D(i,j,k,l)^3*k_AiBj(i,j,k,l)*(exp(e_AiBj(i,j,k,l)/(kb*T))-1);
            end
        end
    end
end

end

function [h] = h_disp( sigma_i,m_i,e_i,k_ij,i,j )
%H_DISP gives the dispersion contribution to the (i,j) coefficient of the
%Hessian of the Helmholtz energy density of a mixture

nav = 6.022140857 * 10^23;%Avogadro number

nn = length(sigma_i);

%diameters and energies of mixing
sig = zeros(nn);
eps = zeros(nn);
for k = 1:nn
    for l = 1:nn
        sig(k,l) = (sigma_i(k)+sigma_i(l))/2;
        eps(k,l) = (1-k_ij(k,l)) * (e_i(k)*e_i(l))^(1/2);
    end
end

%Hessian
h = -nav*pi*nav/6*m_i(i)*m_i(j)*2*sig(i,j)^3*eps(i,j);

end
```

149

Subroutines

In this section, parameters for each solver must be adjusted depending on the system, starting points, etc. Some values are given as examples.

```matlab
function [f] =
critical_functions(rho_i,T,sigma_i,m,m_i,e_i,k_ij,e_AiBj,n_Ai,k_AiBj,error_assoc)
%CRITICAL_FUNCTIONS gives the critical functions i.e. the two functions to minimize in
order to find critical points (on top of the pressure difference)

rho = sum(rho_i);

%First critical function
h = hessian(rho, rho_i, T, sigma_i, m_i, e_i, k_ij, e_AiBj, n_Ai, k_AiBj,
error_assoc);
[u,e] = eig(h);
f1 = min(diag(e));

%Second critical function
[~,col] = find(diag(e)==f1);
u1 = u(:,col).';
if sum(u1)<0
    u1 = -u1;
end
d = norm(rho_i)*1e-3;%1e-3
rhoc = rho_i;
rhol = rho_i - d*u1;
rhor = rho_i + d*u1;

gradc = gradient(rhoc,T,sigma_i,m,m_i,e_i,k_ij,e_AiBj,n_Ai,k_AiBj,error_assoc);
gradc = gradc(2:end);
gradl = gradient(rhol,T,sigma_i,m,m_i,e_i,k_ij,e_AiBj,n_Ai,k_AiBj,error_assoc);
gradl = gradl(2:end);
gradr = gradient(rhor,T,sigma_i,m,m_i,e_i,k_ij,e_AiBj,n_Ai,k_AiBj,error_assoc);
gradr = gradr(2:end);

f2 = sum(rho_i)*(sum(gradr.*u1) - 2*sum(gradc.*u1) + sum(gradl.*u1))/(d^2);
f = [f1 f2];

end

function [f] =
critical_obj_binary(rhoT,P,sigma_i,m,m_i,e_i,k_ij,e_AiBj,n_Ai,k_AiBj,error_assoc)
%CRITICAL_OBJ gives an objective function to find critical points in
%binary systems
%   rhoT = [rho_i T]
rho_i = rhoT(1:end-1)*1e-26;
T = rhoT(end)*1e2;
rho = sum(rho_i);
x = rho_i/rho;

c = critical_functions(rho_i,T,sigma_i,m,m_i,e_i,k_ij,e_AiBj,n_Ai,k_AiBj,error_assoc);
p = pressure(rho,x,T,sigma_i,m_i,e_i,k_ij,e_AiBj,n_Ai,k_AiBj,error_assoc);

f = horzcat(c*1e-30,(P-p)/P);

end
```

```matlab
function [f] =
critical_obj_ternary(rho_i,T,P,sigma_i,m,m_i,e_i,k_ij,e_AiBj,n_Ai,k_AiBj,error_assoc)
%CRITICAL_OBJ gives an objective function to find critical points in
%ternary systems

rho_i = rho_i*1e-26;%multiply by a scaling factor to improve minimization
rho = sum(rho_i);
x = rho_i/rho;

c = critical_functions(rho_i,T,sigma_i,m,m_i,e_i,k_ij,e_AiBj,n_Ai,k_AiBj,error_assoc);
p = pressure(rho,x,T,sigma_i,m_i,e_i,k_ij,e_AiBj,n_Ai,k_AiBj,error_assoc);

f = horzcat(c*1e-30,(P-p)/P);

end

function [rhoc] =
critical_point_binary(rho_start,P,sigma_i,m,m_i,e_i,k_ij,e_AiBj,n_Ai,k_AiBj,error_asso
c)
%CRITICAL_POINT finds a critical point (in a binary system) close to the
%starting configuration rho_start (molar densities vector (mole/Angstrom^3)
%and temperature). The final molar densities are multiplied by 1e26 due to previous
%scaling
%   rho_start: starting point in the form [molar density vector, Temperature]

nn = length(rho_start);

rho_start(1:nn-1) = rho_start(1:nn-1)*1e26;
rho_start(nn) = rho_start(nn)*1e-2;

fun =
@(rhoT)critical_obj_binary(rhoT,P,sigma_i,m,m_i,e_i,k_ij,e_AiBj,n_Ai,k_AiBj,error_asso
c);

options = optimoptions('lsqnonlin','MaxFunctionEvaluations',(nn+1)*500,...
    'Display','iter','StepTolerance',1e-10,'FunctionTolerance',1e-
18,'OptimalityTolerance',1e-17,...
    'UseParallel',true,'TypicalX',rho_start);
problem.options = options;
problem.solver = 'lsqnonlin';
problem.objective = fun;
problem.lb = 0.8*rho_start;
problem.ub = 1.2*rho_start;
problem.x0 = rho_start;
rhoc = lsqnonlin(problem);

rhoc(nn) = rhoc(nn)*1e2;

end

function [rhoc] =
critical_point_ternary(rho_start,T,P,sigma_i,m,m_i,e_i,k_ij,e_AiBj,n_Ai,k_AiBj,error_a
ssoc)
%CRITICAL_POINT finds a critical point (in a ternary system) close to the
%starting configuration rho_start (molar densities vector (mole/Angstrom^3)
%). Some scaling factor are used.
%   rho_start: starting molar density vector

nn = length(rho_start);

rho_start = rho_start*1e26;
```

```matlab
fun =
@(rho_i)critical_obj_ternary(rho_i,T,P,sigma_i,m,m_i,e_i,k_ij,e_AiBj,n_Ai,k_AiBj,error
_assoc);

options = optimoptions('lsqnonlin','MaxFunctionEvaluations',(nn+1)*500,...
    'Display','iter','StepTolerance',1e-16,'FunctionTolerance',1e-
24,'OptimalityTolerance',1e-16,...
    'UseParallel',true,'TypicalX',rho_start);
problem.options = options;
problem.solver = 'lsqnonlin';
problem.objective = fun;
problem.lb = 0.8*rho_start;
problem.ub = 1.2*rho_start;
problem.x0 = rho_start;
rhoc = lsqnonlin(problem);

end

function [ rho ] = density( eta,x,sigma_i,m_i )
%DENSITY gives the molar density rho of a mixture for a reduced density (or packing
%fraction) eta

nav = 6.022140857 * 10^23;%Avogadro number

rho = 6*eta/(pi * nav * sum(x.*m_i.*sigma_i.^3));

end

function [dsup] =
Dsup(Tc0,rhoc0,rhot,sigma_i,m,m_i,e_i,k_ij,e_AiBj,n_Ai,k_AiBj,error_assoc)
%DSUP gives the support function around critical points defined by their
%temperature Tc0 and molar density vector rhoc0. rhot is the total density
%perturbation and it is taken along the direction of the eigenvector of the
%hessian whose eigenvalue is the smallest.

rho = sum(rhoc0);
xc0 = rhoc0/rho;
n = length(rhot);
dsup = zeros(1,n);
nn = length(rhoc0);

%Find eigenvector at the critical point
h = hessian(rho, rhoc0, Tc0, sigma_i, m_i, e_i, k_ij, e_AiBj, n_Ai, k_AiBj,
error_assoc);
[u,e] = eig(h);
f1 = min(diag(e));

[~,col] = find(diag(e)==f1);
u1 = u(:,col).';

%Pressure and chemical potential at the critical point
pc = pressure( rho,xc0,Tc0,sigma_i,m_i,e_i,k_ij,e_AiBj,n_Ai,k_AiBj,error_assoc );
muc = chempot( rho,xc0,Tc0,sigma_i,m,m_i,e_i,k_ij,e_AiBj,n_Ai,k_AiBj,error_assoc );

%dsup
for i = 1:n
    i
    rhoi = rhoc0+rhot(i)*u1;
    x = rhoi/sum(rhoi);
    p = pressure( sum(rhoi),x,Tc0,sigma_i,m_i,e_i,k_ij,e_AiBj,n_Ai,k_AiBj,error_assoc
);
    mu = chempot(
sum(rhoi),x,Tc0,sigma_i,m,m_i,e_i,k_ij,e_AiBj,n_Ai,k_AiBj,error_assoc );
```

152

```matlab
        dsup(i) = -(p-pc)/(sum(rhoi)*1e30);
        for j = 1:nn
            dsup(i) = dsup(i)+ x(j) * (mu{j}-muc{j});
        end
    end

end

function [f] =
equi_cond(rho_ab,rhob3,scale,P,T,sigma_i,m,m_i,e_i,k_ij,e_AiBj,n_Ai,k_AiBj,error_assoc
)
%EQUI_COND gives the equilibrium equations to be solved in order to find
%tie lines in the Helmholtz energy representation.
%If rho_a is the molar density vector of phase "a" and rho_b is the molar
%density vector of phase "b", then rho_ab=[rho_a(1) rho_a(2) rho_a(3)
%rho_b(1) rho_b(2)]. rhob3 = rho_b(3) (fixed);
%scale is a vector to scale densities. It is used to improve minimization

kb = 1.38064852 * 10^(-23);%Boltzmann constant
nav = 6.022140857 * 10^23;%Avogadro number
R = kb * nav;%Ideal gas constant

f = zeros(5,1);

%Scale molar density vector
rho_a = rho_ab(1:3);
rho_b = horzcat(rho_ab(4:5),rhob3);
rho_a = rho_a./scale;
rho_b = rho_b./scale;

xa = rho_a/sum(rho_a);
xb = rho_b/sum(rho_b);

mua = chempot(sum(rho_a),xa,T,sigma_i,m,m_i,e_i,k_ij,e_AiBj,n_Ai,k_AiBj,error_assoc);
mub = chempot(sum(rho_b),xb,T,sigma_i,m,m_i,e_i,k_ij,e_AiBj,n_Ai,k_AiBj,error_assoc);
Pa = pressure(sum(rho_a),xa,T,sigma_i,m_i,e_i,k_ij,e_AiBj,n_Ai,k_AiBj,error_assoc);
Pb = pressure(sum(rho_b),xb,T,sigma_i,m_i,e_i,k_ij,e_AiBj,n_Ai,k_AiBj,error_assoc);

%Chemical potential has to be the same in each phase
for i = 1:3
    f(i) = (mua{i}-mub{i})/(R*T);
end

%Pressure is the same in each phase
f(4) = (Pa-P)/P;
f(5) = (Pb-P)/P;

end

function [f] =
equi_pot_b(x_I,P,T,sigma_i,m,m_i,e_i,k_ij,e_AiBj,n_Ai,k_AiBj,error_assoc,eta_start_a,e
ta_start_b,max_counter,max_n_roots)
%EQUI_POT_B gives the equations to solve to find tie lines in the Gibbs free energy
%approach in binary mixtures i.e. equality of chemical potentials in each phase
%x_I is a vector which describes the composition of the system:[x_I(1) 1-x_I(1)] is
%the composition (mole fraction) of the first phase and [x_I(2) 1-x_I(2)] is the
%composition of the second phase

f = zeros(2,1);

muI = thermo_properties_p([x_I(1) 1-
x_I(1)],P,T,sigma_i,m,m_i,e_i,k_ij,e_AiBj,n_Ai,k_AiBj,error_assoc,eta_start_a,eta_star
t_b,max_counter,max_n_roots);
```

```matlab
muII = thermo_properties_p([x_I(2) 1-
x_I(2)],P,T,sigma_i,m,m_i,e_i,k_ij,e_AiBj,n_Ai,k_AiBj,error_assoc,eta_start_a,eta_star
t_b,max_counter,max_n_roots);

%Chemical potential has to be the same in each phase
for i = 1:2
    f(i) = (muI{i}-muII{i})/muII{i};
end


end

function [f] =
equi_pot_t(w_I,mw,P,T,sigma_i,m,m_i,e_i,k_ij,e_AiBj,n_Ai,k_AiBj,error_assoc,eta_start_
a,eta_start_b,max_counter,max_n_roots)
%EQUI_POT_T gives the equations to solve to find tie lines in the Gibbs free energy
%approach in ternary mixtures i.e. equality of chemical potentials in each phase
%plus mole balance (the mole fraction of each phase is set to 0.5).
%This function is made to get tie lines with mass fractions.
%w_I is an vector which describes the composition of the system:[1-w_I(1)-w_I(3)
%w_I(1) w_I(3)] is the composition of the first phase and [1-w_I(2)-w_I(4) w_I(2)
%w_I(4)] is the composition of the second phase (as mass fractions).

f = zeros(4,1);

%Transform mass fractions into mole fractions
x_I = zeros(2,3);
W1 = sum([1-w_I(1)-w_I(3) w_I(1) w_I(3)] ./mw);
W2 = sum([1-w_I(2)-w_I(4) w_I(2) w_I(4)] ./mw);
x_I(1,2) = (w_I(1)/mw(2))/W1;
x_I(1,3) = (w_I(3)/mw(3))/W1;
x_I(1,1) = 1-x_I(1,2)-x_I(1,3);
x_I(2,2) = (w_I(2)/mw(2))/W2;
x_I(2,3) = (w_I(4)/mw(3))/W2;
x_I(2,1) = 1-x_I(2,2)-x_I(2,3);

muI =
thermo_properties_p(x_I(1,:),P,T,sigma_i,m,m_i,e_i,k_ij,e_AiBj,n_Ai,k_AiBj,error_assoc
,eta_start_a,eta_start_b,max_counter,max_n_roots);
muII =
thermo_properties_p(x_I(2,:),P,T,sigma_i,m,m_i,e_i,k_ij,e_AiBj,n_Ai,k_AiBj,error_assoc
,eta_start_a,eta_start_b,max_counter,max_n_roots);

%Chemical potential has to be the same in each phase
for i = 1:3
    f(i) = 1000*(muI{i}-muII{i})/muII{i};
end

%Mole balance
xi = (x_I(1,:)+x_I(2,:))/2;
a = 0.5;
f(4) = (xi(1) - a*x_I(1) - (1-a)*x_I(2));

end

function [grad] =
gradient(rho_i,T,sigma_i,m,m_i,e_i,k_ij,e_AiBj,n_Ai,k_AiBj,error_assoc)
%GRADIENT gives the gradient of the Helmholtz energy density with respect to the molar
density of each component

rho = sum(rho_i);
x = rho_i/rho;
muu = chempot( rho,x,T,sigma_i,m,m_i,e_i,k_ij,e_AiBj,n_Ai,k_AiBj,error_assoc );
```

154

```matlab
p = pressure(rho, x, T, sigma_i, m_i, e_i, k_ij, e_AiBj, n_Ai, k_AiBj, error_assoc);

nn = length(muu);
mu = zeros(1,nn);

for i = 1:nn
    mu(i) = muu{i};
end

grad = horzcat(-p,mu);

end

function [ k ] = kappa( dsite,rc,d )
%KAPPA gives the bonding volume parameter k_AiBj for one site in a pure component
%system
%d: hard sphere diameter
%dsite: distance between a site and the center of the segment
%rc: diameter of the site
a = (d^2)*(log((rc+2*dsite)/d)*(6*(rc^3)+18*(rc^2)*dsite-24*(dsite^3))+ (rc+2*dsite-
d)*(22 * (dsite^2)-5*rc*dsite-7*dsite*d-8*(rc^2)+rc*d+(d^2)))/(72*(dsite^2));
k = (4*pi)*a/(d^3);
end

function [fval,Mins] =
min_TPD(xi,iter,P,T,sigma_i,m,m_i,e_i,k_ij,e_AiBj,n_Ai,k_AiBj,error_assoc,eta_start_a,
eta_start_b,max_counter,max_n_roots)
%MIN_TPD finds all minima of the tangent plane distance at xi, provided that iter
%is big enough
%xi is the mole composition where the tangent plane distance is calculated from
%iter is the number of random starting points to find minima

nn = length(xi);

%Define the tangent plane distance function
muxi = thermo_properties_p(
xi,P,T,sigma_i,m,m_i,e_i,k_ij,e_AiBj,n_Ai,k_AiBj,error_assoc,eta_start_a,eta_start_b,m
ax_counter,max_n_roots );
tpd_fun = @(x)TPD(
x,xi,muxi,P,T,sigma_i,m,m_i,e_i,k_ij,e_AiBj,n_Ai,k_AiBj,error_assoc,eta_start_a,eta_st
art_b,max_counter,max_n_roots );

%Define the solver to find all minima for the previous function
options = optimoptions('fmincon','Algorithm','interior-
point','Display','off','OptimalityTolerance',1e-10,'StepTolerance',1e-
10,'FunctionTolerance',1e-10,'UseParallel',false);
problem.options = options;
problem.solver = 'fmincon';
problem.objective = tpd_fun;
problem.x0 = zeros(1,nn);
problem.Aeq = ones(1,nn);
problem.beq = 1;%sum(xi) = 1
problem.lb = zeros(1,nn);%xi>=0
problem.ub = ones(1,nn);%xi=<1

%Create a MultiStart object for the global minimization
ms = MultiStart('StartPointsToRun','bounds','FunctionTolerance',1e-
6,'Display','iter','UseParallel',true);

%number of iterations for the global minimization
iterations = iter;

%Find minima with MATLAB Global Optimization Toolbox
```

```matlab
[~,fval,~,~,Mins] = run(ms,problem,iterations);

end

function [ obj_p ] = obj_pressure(
eta,x,P,T,sigma_i,m_i,e_i,k_ij,e_AiBj,n_Ai,k_AiBj,error_assoc )
%OBJ_PRESSURE defines the objective function related to the equation P*=P(eta) which
%is solved in thermo_properties_p

rho = density( eta,x,sigma_i,m_i );
p = pressure(rho,x,T,sigma_i,m_i,e_i,k_ij,e_AiBj,n_Ai,k_AiBj,error_assoc);
obj_p = (P-p)/P;

end

function [x_I] =
phase_split_b(Mins,P,T,sigma_i,m,m_i,e_i,k_ij,e_AiBj,n_Ai,k_AiBj,error_assoc,eta_start
_a,eta_start_b,max_counter,max_n_roots)
%PHASE_SPLIT_B finds tie lines in the Gibbs free energy approach for binary mixtures.
%Mins is a 1x2 cell whose elements are starting points obtained with min_TPD
%x_I is given as a 2x2 matrix whose rows are mole composition vectors for each phase

%Create starting points
x_I0 = zeros(1,2);
min1 = Mins{1};
min2 = Mins{2};
x_I0(1) = min1(1);
x_I0(2) = min2(1);

%Define the objective function
fun_equi_pot =
@(x_I)equi_pot_b(x_I,P,T,sigma_i,m,m_i,e_i,k_ij,e_AiBj,n_Ai,k_AiBj,error_assoc,eta_sta
rt_a,eta_start_b,max_counter,max_n_roots);

%Minimize the objective function
options = optimoptions('lsqnonlin','MaxFunctionEvaluations',3*300,...
    'Display','iter','StepTolerance',1e-10,'FunctionTolerance',1e-
17,'OptimalityTolerance',1e-17,...
    'UseParallel',true);
problem.options = options;
problem.solver = 'lsqnonlin';
problem.objective = fun_equi_pot;
problem.x0 = x_I0;
problem.lb = zeros(1,2);%xi>=0
problem.ub = ones(1,2);%xi=<1
x_I = lsqnonlin(problem);

end

function [w_I] =
phase_split_t(mw,Mins,P,T,sigma_i,m,m_i,e_i,k_ij,e_AiBj,n_Ai,k_AiBj,error_assoc,eta_st
art_a,eta_start_b,max_counter,max_n_roots)
%PHASE_SPLIT_T finds tie lines in the Gibbs free energy approach for ternary mixtures.
%Mins is a 1x2 cell whose elements are starting points obtained with min_TPD
%w_I is given as a 2x3 matrix whose rows are mass fraction vectors for each phase

%create starting points
w_I0 = zeros(1,4);
min1 = Mins{1};
min2 = Mins{2};
w_I0(1) = min1(2);
w_I0(2) = min2(2);
w_I0(3) = min1(3);
```

```matlab
w_I0(4) = min2(3);

%Define the objective function
fun_equi_pot =
@(w_I)equi_pot_t(w_I,mw,P,T,sigma_i,m,m_i,e_i,k_ij,e_AiBj,n_Ai,k_AiBj,error_assoc,eta_
start_a,eta_start_b,max_counter,max_n_roots);

%Minimize the objective function
options = optimoptions('lsqnonlin','MaxFunctionEvaluations',4*150000,...
    'Display','iter','StepTolerance',1e-8,'FunctionTolerance',1e-
17,'OptimalityTolerance',1e-17,...
    'UseParallel',true,'FiniteDifferenceType','central','MaxIterations',200000);
problem.options = options;
problem.solver = 'lsqnonlin';
problem.objective = fun_equi_pot;
problem.x0 = w_I0;
problem.lb = zeros(1,4);%wi>=0
problem.ub = ones(1,4);%wi=<1
w_I = lsqnonlin(problem);

w_I = [1-w_I(1)-w_I(3) w_I(1) w_I(3);1-w_I(2)-w_I(4) w_I(2) w_I(4)];

end

function [up,ep,um,em,rhop,rhom] = pre_tielines(
nc,rhoc1,rhoc2,T,sigma_i,m_i,e_i,k_ij,e_AiBj,n_Ai,k_AiBj,error_assoc )
%PRE_TIELINES gives various quantities used to find starting point for tie lines in
%the Helmholtz free energy approach.
%rhoc1 and rhoc2 are the molar density vectors at two critical points or at the middle
%of some previously calculated tie lines.
%rhop and rhom are the molar density vectors of two points away from rhoc1 in a
%direction perpendicular to u_1 (eigenvector corresponding to the minimum eigenvalue
%of the Helmholtz free energy Hessian at rhoc1).
%up and um are the eigenvectors at rhop and rhom. They correspond to the minimum
%eigenvalues ep and em of the Helmholtz free energy Hessian at rhop and rhom.
%nc characterizes the proximity between rhoc1 and rhop (and rhom)

%Define the distance away from rhoc1 and rhoc2
DL = norm(rhoc1 - rhoc2)/nc;
UL = (rhoc2-rhoc1)/norm(rhoc1 - rhoc2);

%Create rhom and rhop
hc1 = hessian( sum(rhoc1),rhoc1,T,sigma_i,m_i,e_i,k_ij,e_AiBj,n_Ai,k_AiBj,error_assoc
);
[uc1,ec1] = eig(hc1);
e1 = min(diag(ec1));
[~,col] = find(diag(ec1)==e1);
uc1(:,col) = [];
u2 = uc1(:,1).';
u3 = uc1(:,2).';
VL = dot(UL,u2)*u2+dot(UL,u3)*u3;
Uv = VL/norm(VL);
rhop = rhoc1 + DL*Uv;
rhom = rhoc1 - DL*Uv;

%Eigenvalues and eigenvectors at rhop and rhom
hp = hessian( sum(rhop),rhop,T,sigma_i,m_i,e_i,k_ij,e_AiBj,n_Ai,k_AiBj,error_assoc );
[ucp,ecp] = eig(hp);
ep = min(diag(ecp));
[~,col] = find(diag(ecp)==ep);
up = ucp(:,col).';

hm = hessian( sum(rhom),rhom,T,sigma_i,m_i,e_i,k_ij,e_AiBj,n_Ai,k_AiBj,error_assoc );
```

```matlab
[ucm,ecm] = eig(hm);
em = min(diag(ecm));
[~,col] = find(diag(ecm)==em);
um = ucm(:,col).';

end

function [ phase ] = Stability ( mu,xi,thresh )
%STABILITY gives a vector phase. phase(i) is 1 if one phase is stable at
%composition xi(i) and 2 otherwise.
%mu: chemical potential grid corresponding to a molar composition grid xi

n = length(xi);
phase = zeros(1,n);

xi0 = xi;
mu0 = mu;

parfor p = 1:n
    x0 = xi0{p};
    mux0 = mu0{p};
    phase(p) = TPD_x0(xi,x0,mu,mux0,thresh)
end

end

function [ mu,rho,g,p,rc,n_roots,eta_f,x0,eta_all ] = thermo_properties_p(
x,P,T,sigma_i,m,m_i,e_i,k_ij,e_AiBj,n_Ai,k_AiBj,error_assoc,eta_start_a,eta_start_b,ma
x_counter,max_n_roots )
%THERMO_PROPERTIES_P gives thermodynamic quantities at constant
%pressure P for a given molar composition x by solving P=p(eta). These
%quantities are:
%   mu: chemical potential (J/mol) (as a cell vector)
%   rho: molar density (mol/Angstrom^3)
%   g: Gibbs energy (J)
%   p: pressure (Pa)
%   eta_f: reduced density corresponding to rho
%rc: reciprocal condition number related to the matrix inverted in
%the calculation of the association contribution to the chemical potential
%n_root: number of roots of P(rho)=P*
%x0: vector of all the starting points created

%Solver initial parameters
x0 = [eta_start_a eta_start_b];
x0_next = x0;
n_roots = 0;
counter = 0;

%Define the objective function
fun = @(eta) obj_pressure(
eta,x,P,T,sigma_i,m,m_i,e_i,k_ij,e_AiBj,n_Ai,k_AiBj,error_assoc );
eta_f = zeros(1,max_n_roots);

%Find all roots of P(rho)=P*
while counter<=max_counter && n_roots<max_n_roots
    cut = 0;%number of bissections done during one "for" loop
    counter = counter + 1;
    for i = 1:(length(x0)-1)
        x0i = [x0(i)+10*eps x0(i+1)-10*eps];
        if x0i(2)-x0i(1)>10*eps%to avoid finding the same root multiple times
            if fun(x0i(1))*fun(x0i(2))<=0
                n_roots = n_roots + 1;
                options = optimset('TolX',eps);
```

```matlab
                sol = fzero(fun,x0i,options);
                eta_f(n_roots) = sol;
                x0_next = [x0_next(1:i+cut) sol x0_next(i+1+cut:end)];
                cut = cut + 1;
%                 if n_roots == max_n_roots cannot have "break" in a parfor loop
%                     break
%                 end
            else
                x0_next = [x0_next(1:i+cut) (x0(i)+x0(i+1))/2 x0_next(i+1+cut:end)];
                cut = cut + 1;
            end
        end
    end
    x0 = x0_next;
end

%Number of roots
eta_f = nonzeros(eta_f);
eta_all = eta_f;
n_eta = length(eta_f);
n_roots = n_eta;

%Find the root corresponding to the minimum Gibbs free energy
rho_f = density( eta_f,x,sigma_i,m_i );
g_f = zeros(1,n_eta);
for i = 1:n_eta
    [~,~,g_f(i),~] = thermo_properties_rho(
rho_f(i),x,T,sigma_i,m,m_i,e_i,k_ij,e_AiBj,n_Ai,k_AiBj,error_assoc );
end
gmin = min(g_f);
index = g_f == gmin;
eta = eta_f(index);
eta_f = eta;

%Final wanted quantities
rho = density( eta,x,sigma_i,m_i );
rho = rho(1);%in order to make sure that there is exactly one root in rho
[~,mu,g,p,rc] = thermo_properties_rho(
rho,x,T,sigma_i,m,m_i,e_i,k_ij,e_AiBj,n_Ai,k_AiBj,error_assoc );

end

function [ a,mu,g,p,rc ] = thermo_properties_rho(
rho,x,T,sigma_i,m,m_i,e_i,k_ij,e_AiBj,n_Ai,k_AiBj,error_assoc )
%THERMO_PROPERTIES_RHO gives thermodynamic quantities at constant molar
%density rho for a given molar composition x. These quantities are:
%   a: Helmholtz energy
%   mu: chemical potential (as a cell vector)
%   g: Gibbs energy
%   p: pressure (Pa)
%rc: reciprocal condition number related to the matrix inverted in
%the calculation of the association contribution to the chemical potential

nn = length(x);

%Helmhotz energy
aideal = a_ideal( rho,x,T,m );
ahs = a_hs( rho,x,T,sigma_i,m_i );
achain = a_chain( rho,x,T,m_i,sigma_i );
adisp = a_disp( rho,x,sigma_i,m_i,e_i,k_ij );
if ~isempty(e_AiBj)
    aassoc = a_assoc( rho,x,T,sigma_i,m_i,e_AiBj,n_Ai,k_AiBj,error_assoc );
else
```

```matlab
        aassoc = 0;
    end
    a = aideal+ahs+0*achain+adisp+aassoc;

    %Chemical potential and Gibbs energy
    mu = cell(1,nn);
    g = 0;%g has same size and type than rho
    for i = 1:nn
        muideal = mu_ideal( rho,x,i,T,m );
        muhs = mu_hs( rho,x,i,T,sigma_i,m_i );
        muchain = mu_chain( rho,x,i,T,sigma_i,m_i );
        mudisp = mu_disp( rho,x,i,sigma_i,m_i,e_i,k_ij );
        if ~isempty(e_AiBj)
            [muassoc,rc] = mu_assoc( rho,x,i,T,sigma_i,m_i,e_AiBj,n_Ai,k_AiBj,error_assoc
);
        else
            muassoc = 0;
            rc = 0;
        end
        mu{i} = muideal+muhs+0*muchain+mudisp+muassoc;
        g = g + x(i)*mu{i};
    end

    %Pressure
    p = rho.*(g-a).*10.^30;%in order to have p in Pa (because we use angstrom as the main
distance unit)

end

function [rho_ab] =
tie_line_A(rho_ab_start,rhob3,scale,P,T,sigma_i,m,m_i,e_i,k_ij,e_AiBj,n_Ai,k_AiBj,erro
r_assoc)
%TIE_LINE_A gives the molar density vectors of each phase if the system
%splits into two phases, using the Helmholtz free energy approach.
%If rho_a is the molar density vector of phase "a" and rho_b is the molar
%density vector of phase "b", then rho_ab=[rho_a(1) rho_a(2) rho_a(3)
%rho_b(1) rho_b(2)]. rhob3 = rho_b(3) (fixed);
%scale is a vector to scale densities

%Scale molar density vector
rho_a = rho_ab_start(1:3);
rho_b = horzcat(rho_ab_start(4:5),rhob3);
rho_a = rho_a.*scale;
rho_b = rho_b.*scale;
rho_ab_start = horzcat(rho_a,rho_b(1:2));
rhob3 = rho_b(3);

%Define the objective function
fun_equi_cond =
@(rho_ab)equi_cond(rho_ab,rhob3,scale,P,T,sigma_i,m,m_i,e_i,k_ij,e_AiBj,n_Ai,k_AiBj,er
ror_assoc);

%Minimize the objective function
options = optimoptions('lsqnonlin','MaxFunctionEvaluations',5*1000,...
    'Display','iter','StepTolerance',1e-17,'FunctionTolerance',1e-
17,'OptimalityTolerance',1e-17,...
    'UseParallel',true,'FiniteDifferenceType','central','MaxIterations',25);
problem.options = options;
problem.solver = 'lsqnonlin';
problem.objective = fun_equi_cond;
problem.lb = 0.99*rho_ab_start;
problem.ub = 1.01*rho_ab_start;
problem.x0 = rho_ab_start;
```

```matlab
rho_ab = lsqnonlin(problem);

rho_ab = vertcat(rho_ab(1:3),horzcat(rho_ab(4:5),rhob3));

end

function [ tpd ] = TPD (
x,x0,mux0,P,T,sigma_i,m,m_i,e_i,k_ij,e_AiBj,n_Ai,k_AiBj,error_assoc,eta_start_a,eta_st
art_b,max_counter,max_n_roots )
%TPD gives the tangent plane distance tpd at x0. It is evaluated at the molar
%composition x.
%mux0 is the chemical potential at x0.

nn = length(x);

tpd = 0;
mux = thermo_properties_p(
x,P,T,sigma_i,m,m_i,e_i,k_ij,e_AiBj,n_Ai,k_AiBj,error_assoc,eta_start_a,eta_start_b,ma
x_counter,max_n_roots );

for i = 1:nn
    if x(i)~=0 && x0(i) ~=0
        tpd = tpd + x(i).*(mux{i}-mux0{i});
    end
end

for i = 1:nn
   if x0(i) == 0 && x(i) ~= 0
        tpd = 0;
   end
end

end

function [ tpd ] = TPD_fast ( x,x0,mux,mux0 )
%TPD gives the tangent plane distance tpd with x0. It is
%evaluated at the composition x. mux and mux0 are the chemical potentials
%at compositions x and x0 respectively

nn = length(x);

tpd = 0;

for i = 1:nn
    if x(i)~=0 && x0(i) ~=0
        tpd = tpd + x(i).*(mux{i}-mux0{i});
    end
end

for i = 1:nn
   if x0(i) == 0 && x(i) ~= 0
        tpd = 0;
   end
end

end

function [phase] = TPD_x0(xi,x0,mu,mux0,thresh)
%TPD_X0 gives phase=1 if one phase in the system is stable at the molar
%composition x0 and phase=2 otherwise.
%xi: vector (grid) of all molar composition tested for the tangent plane criterion
%mu: vector of chemical potential for compositions given by xi
%mux0: chemical potential at x0
```

161

```matlab
%thresh: numerical noise threshold

n = length(xi);

phase = 1;

for q = 1:n
    x = xi{q};
    mux = mu{q};
    tpd = TPD_fast(x,x0,mux,mux0);
    if abs(tpd) < thresh
        tpd = 0;
    end
    if tpd < 0
        phase=2;
    end
end

end

function [tpd] = TPDA_u1(
rhoz,s,T,sigma_i,m,m_i,e_i,k_ij,e_AiBj,n_Ai,k_AiBj,error_assoc )
%TPDA_PLOT gives a vector for tangent plane distance values in the
%Helmholtz energy representation along a direction defined by u1. u1 is the
%eigenvector of the hessian at molar density vector rhoz whose eigenvalue
%is the smallest. sum(rhoz)+s is the vector of the corresponding overall
%molar densities.

rho = sum(rhoz);
xz = rhoz/rho;
n = length(s);
tpd = zeros(1,n);
nn = length(rhoz);

%Find eigenvector at rhoz
h = hessian(rho, rhoz, T, sigma_i, m_i, e_i, k_ij, e_AiBj, n_Ai, k_AiBj, error_assoc);
[u,e] = eig(h);
f1 = min(diag(e));

[~,col] = find(diag(e)==f1);
u1 = u(:,col).';

%Pressure and chemical potential at rhoz
pz = pressure( rho,xz,T,sigma_i,m_i,e_i,k_ij,e_AiBj,n_Ai,k_AiBj,error_assoc );
muz = chempot( rho,xz,T,sigma_i,m,m_i,e_i,k_ij,e_AiBj,n_Ai,k_AiBj,error_assoc );

%Tangent plane distance
for i = 1:n
    i
    rhoa = rhoz+s(i)*u1;
    x = rhoa/sum(rhoa);
    p = pressure( sum(rhoa),x,T,sigma_i,m_i,e_i,k_ij,e_AiBj,n_Ai,k_AiBj,error_assoc );
    mu = chempot( sum(rhoa),x,T,sigma_i,m,m_i,e_i,k_ij,e_AiBj,n_Ai,k_AiBj,error_assoc
);
    tpd(i) = -(p-pz)/(sum(rhoa)*1e30);
    for j = 1:nn
        tpd(i) = tpd(i)+ x(j) * (mu{j}-muz{j});
    end
end

end
```

162

Main Script

```matlab
format long

addpath('Intermediary functions')
addpath('Helmholtz energy')
addpath('Chemical potential')
addpath('Pressure')
addpath('Hessian')

coresenv=str2num(getenv('SLURM_CPUS_PER_TASK'))
c = parcluster('local');
c.NumWorkers = coresenv;
parpool(c, c.NumWorkers);

%Parameters

T = 300;
P = 10^5;
kb = 1.38064852 * 10^(-23);
nav = 6.022140857 * 10^23;
sigma_i = [3.165 4.1071 70];
mw_sol = 84.162;
mw_pol = 2.37e5;
mw_nan = (4/3)*pi*(sigma_i(3)/2)^3*2.3*10^(-24)*nav;
mw = [mw_sol mw_pol mw_nan];
m = [mw_sol mw_pol mw_nan]*10^(-3)/nav;
m_i = [3.970 mw_pol/104.152 1];
threshold = 1e-14;
nn = length(m);

e_i = kb * [3100 970 10000];
k23 = 0;
k13 = 0;
k_ij = [0 0 k13;0 0 k23;k13 k23 0];

%Identical association sites are counted as one here
e1 = kb * 0;%1800 (sol assoc + pol2)
e12 = kb * 500;
e13 = kb * 0;
e2 = kb*230;
e3 = kb*0;
e_AiBj(:,:,1,1) = 0*[e1 e12 e13];
e_AiBj(:,:,1,2) = 0*[e12 e2 0];
e_AiBj(:,:,1,3) = 0*[e13 0 e3];

%Number of identical association sites
n_Ai = [2 2*m_i(2) 0];

%Multiply each k by the number of identical association site
k1 = kappa(sigma_i(1)*0.5,sigma_i(1)*0.5,sigma_i(1));
k12 = k1;
k2 = k1;
k13 = kappa(sigma_i(3)/2, 2.75, sigma_i(3));
k3 = kappa(sigma_i(3)/2, 2.75, sigma_i(3));

k_AiBj(:,:,1,1) = n_Ai.*[k1 k12 k13];
k_AiBj(:,:,1,2) = n_Ai.*[k12 k2 0];
k_AiBj(:,:,1,3) = n_Ai.*[k13 0 k3];

error_assoc = 10^(-15);
```

164

```matlab
%Parameters to solve P(rho) = P*
eta_start_a = 0.1;
eta_start_b = 0.95;
max_n_roots = 1;%5
max_counter = 1;%6

%Resolution of the phase diagram
n = 600;
za=1;
zb=1;

%Pure components study

%Solvent density
[~,rho_sol] =
thermo_properties_p([1,0,0],P,T,sigma_i,m,m_i,e_i,k_ij,e_AiBj,n_Ai,k_AiBj,error_assoc,
eta_start_a,eta_start_b,max_counter,max_n_roots );
rho_sol_gl = sum(rho_sol*[1,0,0].*mw/1000)*1e30;%g/L

%Polymer density
[~,rho_pol] =
thermo_properties_p([0,1,0],P,T,sigma_i,m,m_i,e_i,k_ij,e_AiBj,n_Ai,k_AiBj,error_assoc,
eta_start_a,eta_start_b,max_counter,max_n_roots );
rho_pol_gl = sum(rho_pol*[0,1,0].*mw/1000)*1e30;%g/L

%Nanoparticle density
[~,rho_nan] =
thermo_properties_p([0,0,1],P,T,sigma_i,m,m_i,e_i,k_ij,e_AiBj,n_Ai,k_AiBj,error_assoc,
eta_start_a,eta_start_b,max_counter,max_n_roots );
rho_nan_gl = sum(rho_nan*[0,0,1].*mw/1000)*1e30;%g/L

%Ternary mixture initial property

%Mass fraction grid
wi_grid = cell(n+1);%cell (n+1,n+1) of (1,3) vectors = mass fraction of
%(solvent,polymer,nanoparticle)
conv = zeros(n+1);
np = 0;
for i = 1:n+1
    a = (i-1)*za/n;
    for j = 1:n+1
        b = (j-1)*zb/n;
        if n-za*(i-1)-zb*(j-1)>=0
            wi_grid{i,j} = [(1-a-b) a b];
            np = np+1;
            conv(i,j) = np;
        else
            wi_grid{i,j} = [0 0 0];
        end
        if i+j == n+2 && za+zb==2
            wi_grid{i,j}(1) = 0;%in order to avoid round off problems
        end
    end
end

%Corresponding mole fraction grid
xi_grid = cell(n+1);
for i = 1:n+1
    for j = 1:n+1
        w = wi_grid{i,j};
        if norm(w)~=0
            x = w./mw;
            xi_grid{i,j} = x/sum(x);
```

165

```matlab
            end
        end
    end

    %Mole fraction grid transformed into a vector in order to generalize
    %functions and use parallel computing
    xi = cell(1,np);%vector version of xi_square
    p = 0;
    for i = 1:n+1
        for j = 1:n+1
            if norm(xi_grid{i,j})~=0
                p = p+1;
                xi{p} = xi_grid{i,j};
            end
        end
    end

    %Definition of the quantities to study
    g = zeros(1,np);
    mu = cell(1,np);
    eta = zeros(1,np);
    rho = zeros(1,np);
    n_roots = zeros(1,np);
    h = zeros(1,np);

    %Calcul Gibbs curve and chemical potentials
    parfor p = 1:np
        [mu{p},rho(p),g(p),~,~,n_roots(p),eta(p)] = thermo_properties_p(
    xi{p},P,T,sigma_i,m,m_i,e_i,k_ij,e_AiBj,n_Ai,k_AiBj,error_assoc,eta_start_a,eta_start_
    b,max_counter,max_n_roots );
        rho(p) = sum(rho(p)*xi{p}.*mw/1000)*1e30;%g/L
    end

    x_nan = NaN(1,np);
    x_pol = NaN(1,np);

    for p = 1:np
        x_pol(p) = xi{p}(2);
        x_nan(p) = xi{p}(3);
    end

    figure
    stem3(x_nan,x_pol,g,'LineStyle','none','Marker','.')
    title('Gibbs curve')
    xlabel('nanoparticle mole fraction')
    ylabel('polymer mole fraction')

    %Phase stability
    stability = Stability(mu,xi,threshold);

    xphase1 = NaN(1,np);
    yphase1 = NaN(1,np);
    xphase2 = NaN(1,np);
    yphase2 = NaN(1,np);

    for p = 1:np
        x = xi{p}(2);
        y = xi{p}(3);
        if stability(p) == 1
            xphase1(p) = x;
            yphase1(p) = y;
        else
            xphase2(p) = x;
```

```matlab
        yphase2(p) = y;
    end
end

figure
hold on
stem(yphase1,xphase1,'Color','blue','LineStyle','none','Marker','.')
stem(yphase2,xphase2,'Color','red','LineStyle','none','Marker','.')
title('Phase diagram')
xlabel('nan mole fraction')
ylabel('pol mole fraction')
hold off
toc

%Mass fraction phase diagram
w_nan1 = NaN(1,np);
w_pol1 = NaN(1,np);
w_nan2 = NaN(1,np);
w_pol2 = NaN(1,np);

for p = 1:np
    w_pol = mw(2)*xi{p}(2)/sum(mw.*xi{p});
    w_nan = mw(3)*xi{p}(3)/sum(mw.*xi{p});
    if stability(p) == 1
        w_pol1(p) = w_pol;
        w_nan1(p) = w_nan;
    else
        w_pol2(p) = w_pol;
        w_nan2(p) = w_nan;
    end
end

figure
hold on
stem(w_nan1,w_pol1,'Color','blue','LineStyle','none','Marker','.')
stem(w_nan2,w_pol2,'Color','red','LineStyle','none','Marker','.')
title('Phase diagram')
xlabel('nanoparticle mass fraction')
ylabel('polymer mass fraction')
hold off

%Smallest eigenvalue of the Hessian
parfor p = 1:np
    r = rho(p)/sum(xi{p}.*mw/1000)*1e-30;
    hes = hessian( r,r*xi{p},T,sigma_i,m_i,e_i,k_ij,e_AiBj,n_Ai,k_AiBj,error_assoc );
    x = xi{p};
    l = 1:1:nn;
    for i = 1:nn
        if x(i) == 0
            t = find(l==i);
            l(t)=[];
        end
    end
    hes = hes(l,l);
    ev = min(eig(hes));
    h(p) = ev;
end

xphase1 = NaN(1,np);
yphase1 = NaN(1,np);
xphase2 = NaN(1,np);
yphase2 = NaN(1,np);
```

167

```matlab
for p = 1:np
    w_pol = mw(2)*xi{p}(2)/sum(mw.*xi{p});
    w_nan = mw(3)*xi{p}(3)/sum(mw.*xi{p});
    if h(p) > 0 || abs(h(p)) < threshold
        xphase1(p) = w_pol;
        yphase1(p) = w_nan;
    else
        xphase2(p) = w_pol;
        yphase2(p) = w_nan;
    end
end

figure
hold on
stem(yphase1,xphase1,'Color','blue','LineStyle','none','Marker','.')
stem(yphase2,xphase2,'Color','red','LineStyle','none','Marker','.')
title('Instability Phase diagram')
xlabel('polymer mole fraction')
ylabel('nanoparticle mole fraction')
hold off

%Contours: plots the binodal and the spinodal
bxs = [];
bys = [];
bxins = [];
byins = [];

for p = 1:np
    if ~isnan(w_pol2(p)) && w_pol2(p)+w_nan2(p)<0.8 && w_pol2(p)+w_nan2(p)~=0
        bxs = [bxs w_pol2(p)]; %#ok<AGROW>
        bys = [bys w_nan2(p)]; %#ok<AGROW>
    end
    if ~isnan(xphase2(p)) && xphase2(p)+yphase2(p)<0.8 && xphase2(p)+yphase2(p)~=0
        bxins = [bxins xphase2(p)]; %#ok<AGROW>
        byins = [byins yphase2(p)]; %#ok<AGROW>
    end
end

bxs = bxs.';
bys = bys.';
bxins = bxins.';
byins = byins.';
s = boundary(bys,bxs,0.4);%use shrink factor if the two phase region is not convex
ins = boundary(byins,bxins,0.4);

figure
hold on
plot(bys(s),bxs(s),'blue')%,'LineWidth',2)
plot(byins(ins),bxins(ins),'--r')%,'LineWidth',2)
title('T = 307K')
xlabel('Nanoparticle mass fraction')
ylabel('Polystyrene mass fraction')
set(gca, 'Layer', 'Top');
set(gcf,'color','w');
hold off

%Critical points
wc = [1-0.06433-0.001983 0.06433 0.001983];%starting point
xc = (wc./mw)/sum(wc./mw);

%Find the corresponding molar density and molar density vectors
```

```matlab
[~,rho_start] = thermo_properties_p(
xc,P,T,sigma_i,m,m_i,e_i,k_ij,e_AiBj,n_Ai,k_AiBj,error_assoc,eta_start_a,eta_start_b,m
ax_counter,max_n_roots );
rho_start = rho_start*xc;

%Solve critical points equations
rhoc0 =
critical_point_ternary(rho_start,T,P,sigma_i,m,m_i,e_i,k_ij,e_AiBj,n_Ai,k_AiBj,error_a
ssoc);
xc = rhoc0/sum(rhoc0);
wc = xc.*mw/sum(xc.*mw);

%Support function at the critical point
[~,rhotest] = thermo_properties_p(
xc,P,T,sigma_i,m,m_i,e_i,k_ij,e_AiBj,n_Ai,k_AiBj,error_assoc,eta_start_a,eta_start_b,m
ax_counter,max_n_roots );
rhot = linspace(-0.001*rhotest,0.001*rhotest,1000);
rhotest = rhotest*xc;
dsup = Dsup(T,rhotest,rhot,sigma_i,m,m_i,e_i,k_ij,e_AiBj,n_Ai,k_AiBj,error_assoc);

figure
plot(rhot,dsup)
title('Support function')
xlabel('Molar density')
ylabel('Support function value')

%Calculate tie lines in the Helmhotz free energy approach

%Initial guess for tie lines from two given points; start with critical points
%then use middle of tie lines

%Molar density vector at CP1 or middle of a tie line
w1 = (wa+wb)/2;
xc1 = w1./mw/sum(w1./mw);
[~,rhoc] = thermo_properties_p(
xc1,P,T,sigma_i,m,m_i,e_i,k_ij,e_AiBj,n_Ai,k_AiBj,error_assoc,eta_start_a,eta_start_b,
max_counter,max_n_roots );
rhoc1 = rhoc*xc1;

%Molar density vector at CP2 or middle of a tie line
w2 = wc1;
xc2 = w2./mw/sum(w2./mw);
[~,rhoc] = thermo_properties_p(
xc2,P,T,sigma_i,m,m_i,e_i,k_ij,e_AiBj,n_Ai,k_AiBj,error_assoc,eta_start_a,eta_start_b,
max_counter,max_n_roots );
rhoc2 = rhoc*xc2;

%Find rhop (or rhom), a molar density vector close to CP1 and inside the
%two phase region. up (or um) gives the corresponding direction of interest
%in the composition space
[up,ep,um,em,rhop,rhom] = pre_tielines(
50000,rhoc1,rhoc2,T,sigma_i,m_i,e_i,k_ij,e_AiBj,n_Ai,k_AiBj,error_assoc );

%Calculate the tangent plane distance in Helmholtz energy representation around the
%new molar density vector
xp = rhop/sum(rhop);
[~,rhoz] = thermo_properties_p(
xp,P,T,sigma_i,m,m_i,e_i,k_ij,e_AiBj,n_Ai,k_AiBj,error_assoc,eta_start_a,eta_start_b,m
ax_counter,max_n_roots );
ss = linspace(-0.01*rhoz,0.01*rhoz,1000);
rhoz = rhoz*xp;
tpd = TPDA_u1( rhoz,ss,T,sigma_i,m,m_i,e_i,k_ij,e_AiBj,n_Ai,k_AiBj,error_assoc );
```

169

```matlab
%Plots the tangent plane distance in order find two starting points
figure
plot(ss,tpd)
title('Support function')
xlabel('Molar density')
ylabel('Support function value')

%Minima of the previous plot
%Phase "b" contains more nanoparticles
sa = 6.163*1e-29;
sb = -5.849*1e-29;

%Corresponding molar density vectors
rho_a = rhop + up*sa;
rho_b = rhop + up*sb;
rho_ab_start = horzcat(rho_a,rho_b(1:2));
rhob3 = rho_b(3);

%Find a tie line
scale = 1e16;%scaling factor to improve minimization of the objective function
rho_ab =
tie_line_A(rho_ab_start,rhob3,scale,P,T,sigma_i,m,m_i,e_i,k_ij,e_AiBj,n_Ai,k_AiBj,erro
r_assoc);
rho_ab = rho_ab./scale;

rho_ab_start = horzcat(rho_ab(1,:),rho_ab(2,1:2));
rhob3 = rho_ab(2,3);
equi_cond(rho_ab_start,rhob3,1,P,T,sigma_i,m,m_i,e_i,k_ij,e_AiBj,n_Ai,k_AiBj,error_ass
oc);%test

%Transform into mass fraction
xa = rho_ab(1,:)/sum(rho_ab(1,:));
wa = xa.*mw/sum(xa.*mw);
xb = rho_ab(2,:)/sum(rho_ab(2,:));
wb = xb.*mw/sum(xb.*mw);
wab = vertcat(wa,wb);

%Calculate tie lines in the Gibbs free energy approach

%Global minimization of the tangent plane distance to find stationary points
w0 = [1-0.0455 0.042 0.0035];
x0 = (w0./mw)/sum(w0./mw);
[fval,Mins] =
min_TPD(x0,30,P,T,sigma_i,m,m_i,e_i,k_ij,e_AiBj,n_Ai,k_AiBj,error_assoc,eta_start_a,et
a_start_b,max_counter,max_n_roots);

%Choose stationary points

%Transform mole fractions into mass fractions
w0 = mw.*x0/sum(mw.*x0);
nm = length(Mins);
mins = cell(1,nm);
for i = 1:nm
    minn = Mins(i).X;
    mins{i} = mw.*minn/sum(mw.*minn);
end

figure
hold on
plot(bys(s),bxs(s),'blue')
plot(byins(ins),bxins(ins),'--r')
title('Phase diagram')
xlabel('nan mass fraction')
```

```matlab
ylabel('pol mass fraction')
for i = 1:nm
    m = mins{i};
    plot(m(3),m(2),'+','Color','green')
end
plot(w0(3),w0(2),'+','Color','black')

%Find a tie line
Min = {mins{1},mins{3}};%use previous points

[w_I,resnorm] =
phase_split_t(mw,Min,P,T,sigma_i,m,m_i,e_i,k_ij,e_AiBj,n_Ai,k_AiBj,error_assoc,eta_sta
rt_a,eta_start_b,max_counter,max_n_roots);

Min={w_I(1,:),w_I(2,:)};%redefine if needed to restart the solver with a better
%starting point

%Final Phase Diagram
figure
hold on
plot(bys(s),bxs(s),'blue')
plot(byins(ins),bxins(ins),'--r')
title('T=307')
xlabel('Nanoparticle mass fraction')
ylabel('Polystyrene mass fraction')
set(gca, 'Layer', 'Top');
set(gcf,'color','w');
plot(wc1(3),wc1(2),'^','MarkerSize',6,'MarkerEdgeColor','black','MarkerFaceColor','bla
ck')%need to define wc1 first
plot(wc2(3),wc2(2),'^','MarkerSize',6,'MarkerEdgeColor','black','MarkerFaceColor','bla
ck')%need to define wc2 first
plot([w_I(1,3) w_I(2,3)],[w_I(1,2) w_I(2,2)],'Color','black')
plot([w_I(1,3) w_I(2,3)],[w_I(1,2) w_I(2,2)],'s','Color','black')%can be repeated to
plot more tie lines
```

Published with MATLAB® R2017b

171

A3: Parametric study

Other ternary phase diagrams with different set of parameters are presented here. When not specified, the parameters are provided by table 4.1, 4.2 and 4.3 with k_{ij} values set to 0. Dispersion energy values are adjusted to match liquid densities of cyclohexane and polystyrene and a pure silica nanoparticle packing fraction of 0.6.
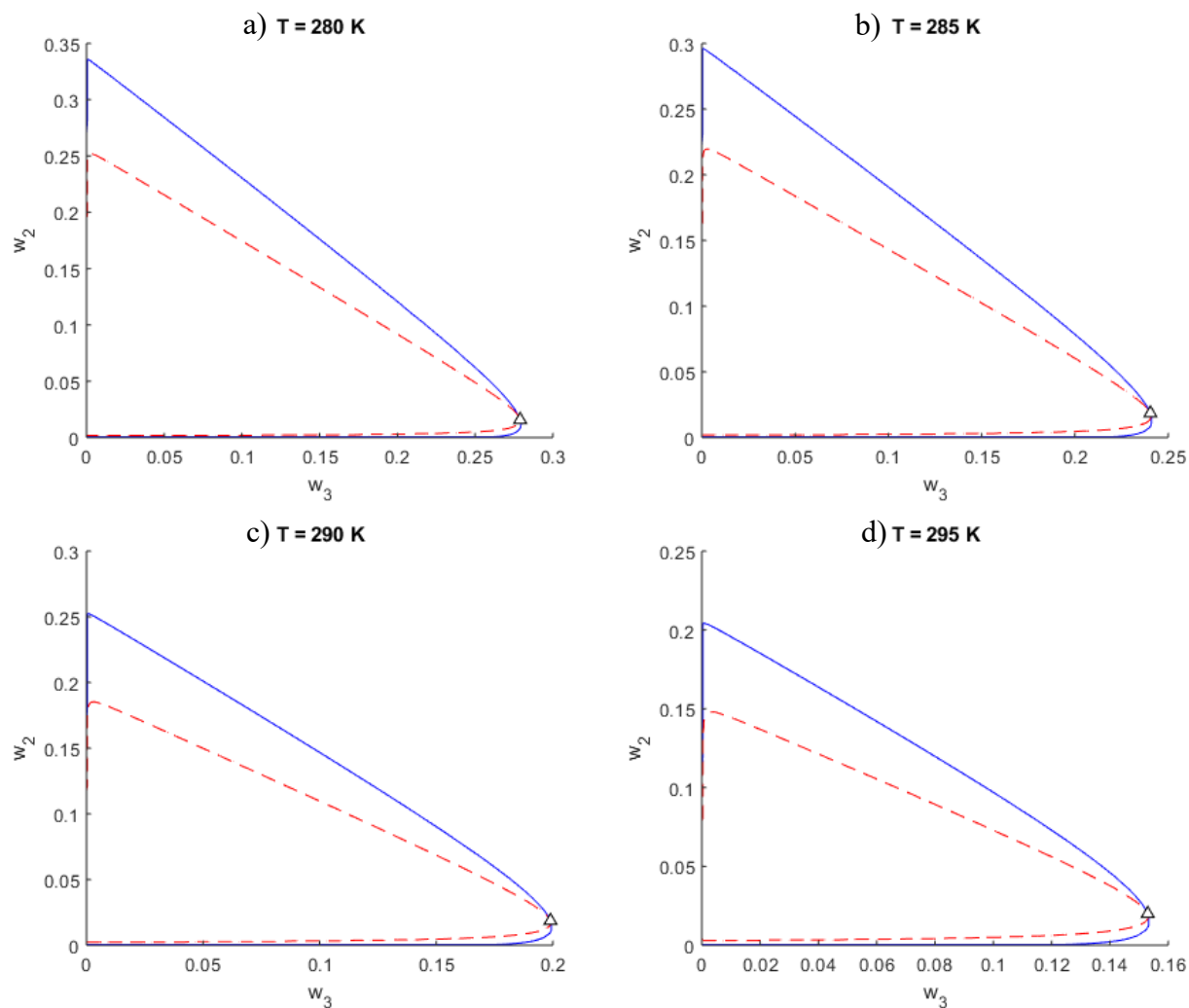

Figure A3.1 Ternary phase diagrams for cyclohexane + polystyrene + silica nanoparticles mixtures for $\varepsilon_3 = k_B\ 20000$ J and different temperatures. The blue solid line is the binodal and the red dashed line is the spinodal. Open triangles represent critical points for which the graphic test failed. a) T=280K, b) T=285K, c) T=290K, d) T=295K.
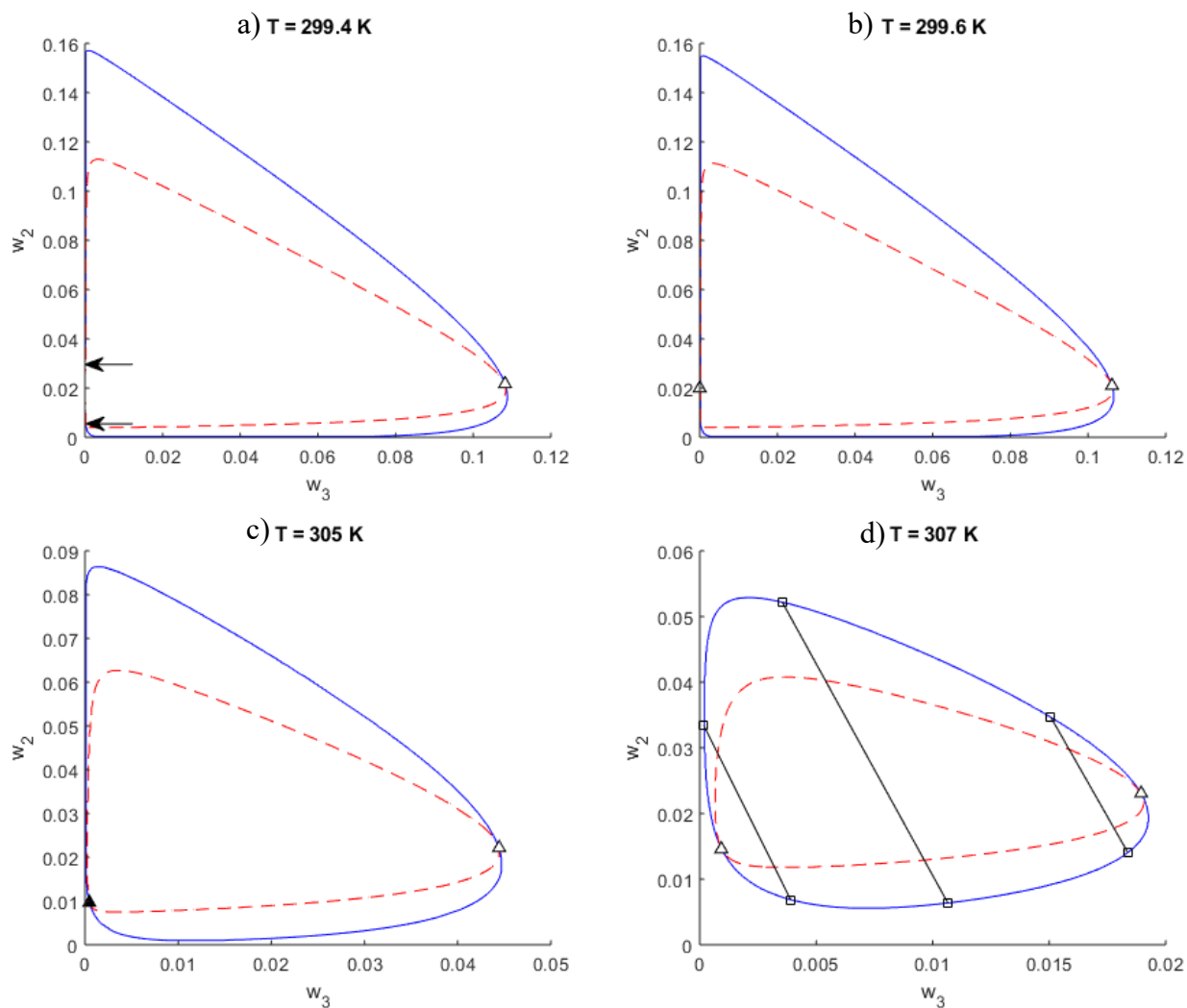
Figure A3.2 Ternary phase diagrams for cyclohexane + polystyrene + silica nanoparticles mixtures for $\varepsilon_3 = k_B$ 20000 J and different temperatures. The blue solid line is the binodal and the red dashed line is the spinodal. Solid triangles represent the critical points calculated with "critical_point_ternary". Open squares and lines joining them represent tie lines. Open triangles represent critical points for which the graphic test failed. a) T=299.4K, b) T=299.6K, c) T=305K, d) T=307K.
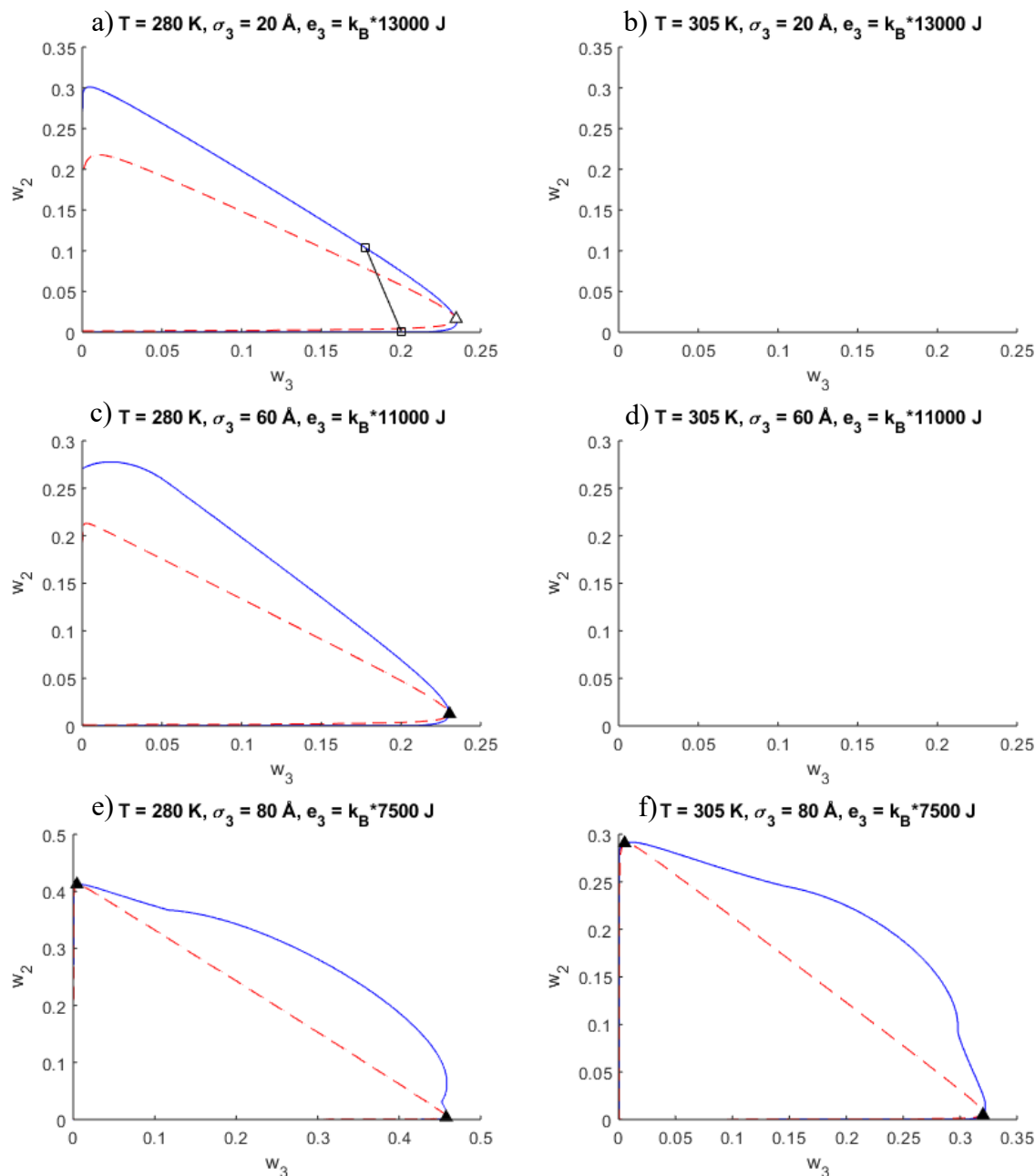
Figure A3.3 Ternary phase diagrams for cyclohexane + polystyrene + silica nanoparticles mixtures for different nanoparticle diameters and different temperatures. The blue solid line is the binodal and the red dashed line is the spinodal. Solid triangles represent the critical points calculated with "critical_point_ternary". Open squares and lines joining them represent tie lines. Open triangles represent critical points for which the graphic test failed. a) T=280K, $\sigma_3 = 20$Å, b) T=305K, $\sigma_3 = 20$Å, c) T=280K, $\sigma_3 = 60$Å, d) T=305K, $\sigma_3 = 60$Å, e) T=280K, $\sigma_3 = 80$Å, f) T=305K, $\sigma_3 = 80$Å.
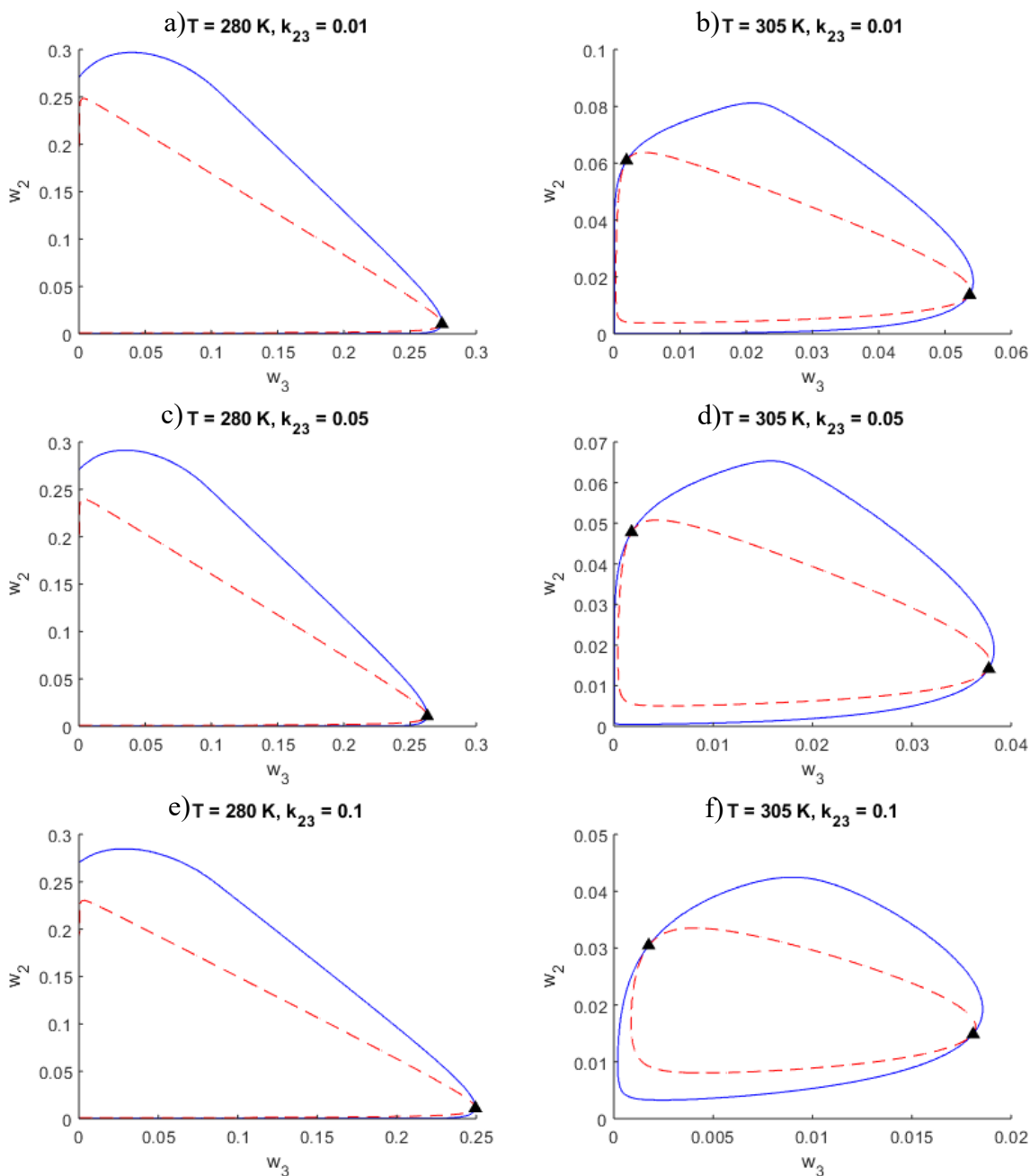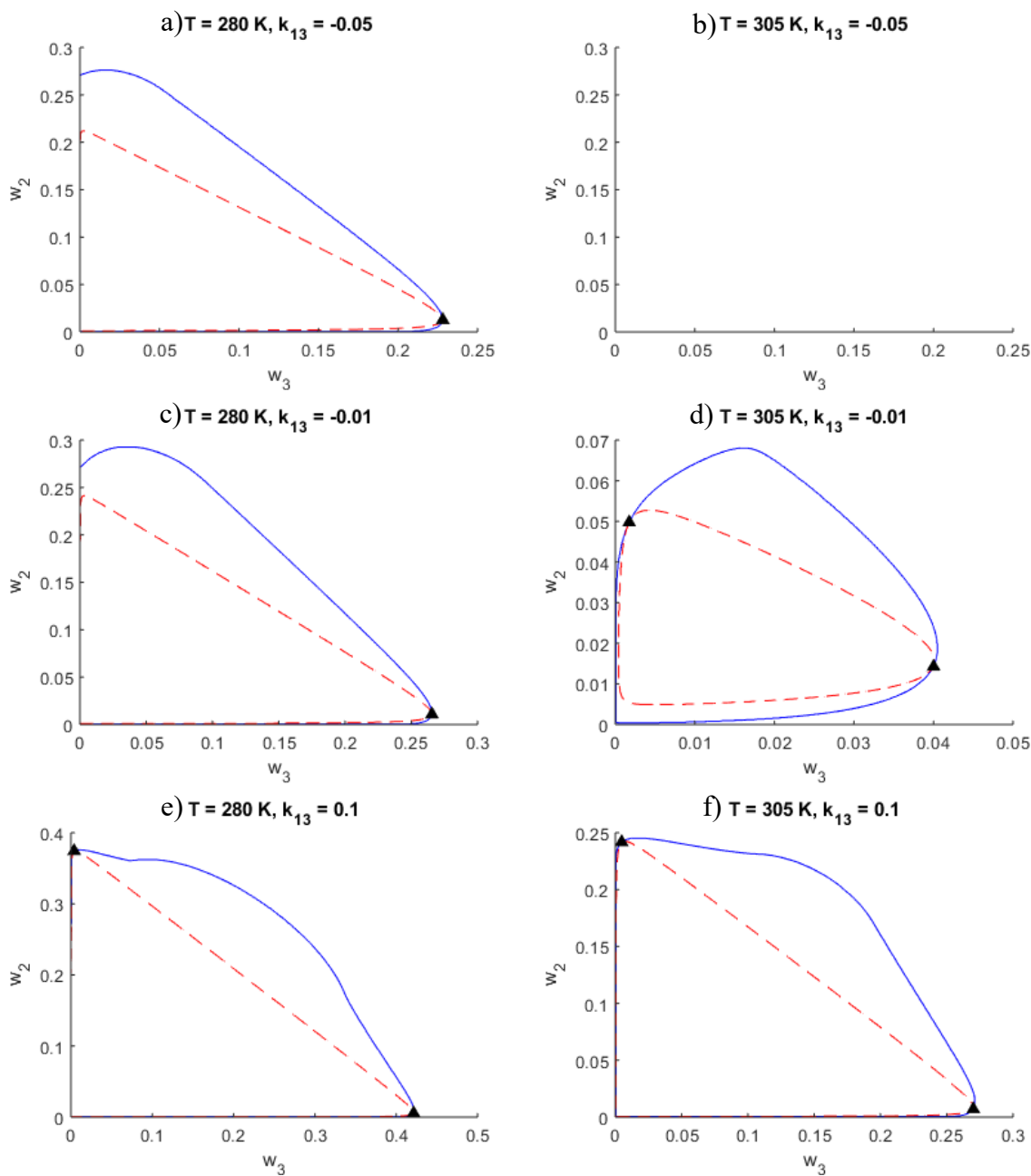
Figure A3.4 Ternary phase diagrams for cyclohexane + polystyrene + silica nanoparticles mixtures for different values of k_{23}. The blue solid line is the binodal and the red dashed line is the spinodal. Solid triangles represent the critical points calculated with "critical_point_ternary". a) T=280K, $k_{23} = 0.01$, b) T=305K, $k_{23} = 0.01$, c) T=280K, $k_{23} = 0.05$, d) T=305K, $k_{23} = 0.05$, e) T=280K, $k_{23} = 0.1$, f) T=305K, $k_{23} = 0.1$.

Figure A3.5 Ternary phase diagrams for cyclohexane + polystyrene + silica nanoparticles mixtures for different values of k_{13}. The blue solid line is the binodal and the red dashed line is the spinodal. Solid triangles represent the critical points calculated with "critical_point_ternary". a) T=280K, k_{13} = -0.015, b) T=305K, k_{13}= -0.05, c) T=280K, k_{13} = -0.01, d) T=305K, k_{13} = -0.01, e) T=280K, k_{13} = 0.1, f) T=305K, k_{13} = 0.1.
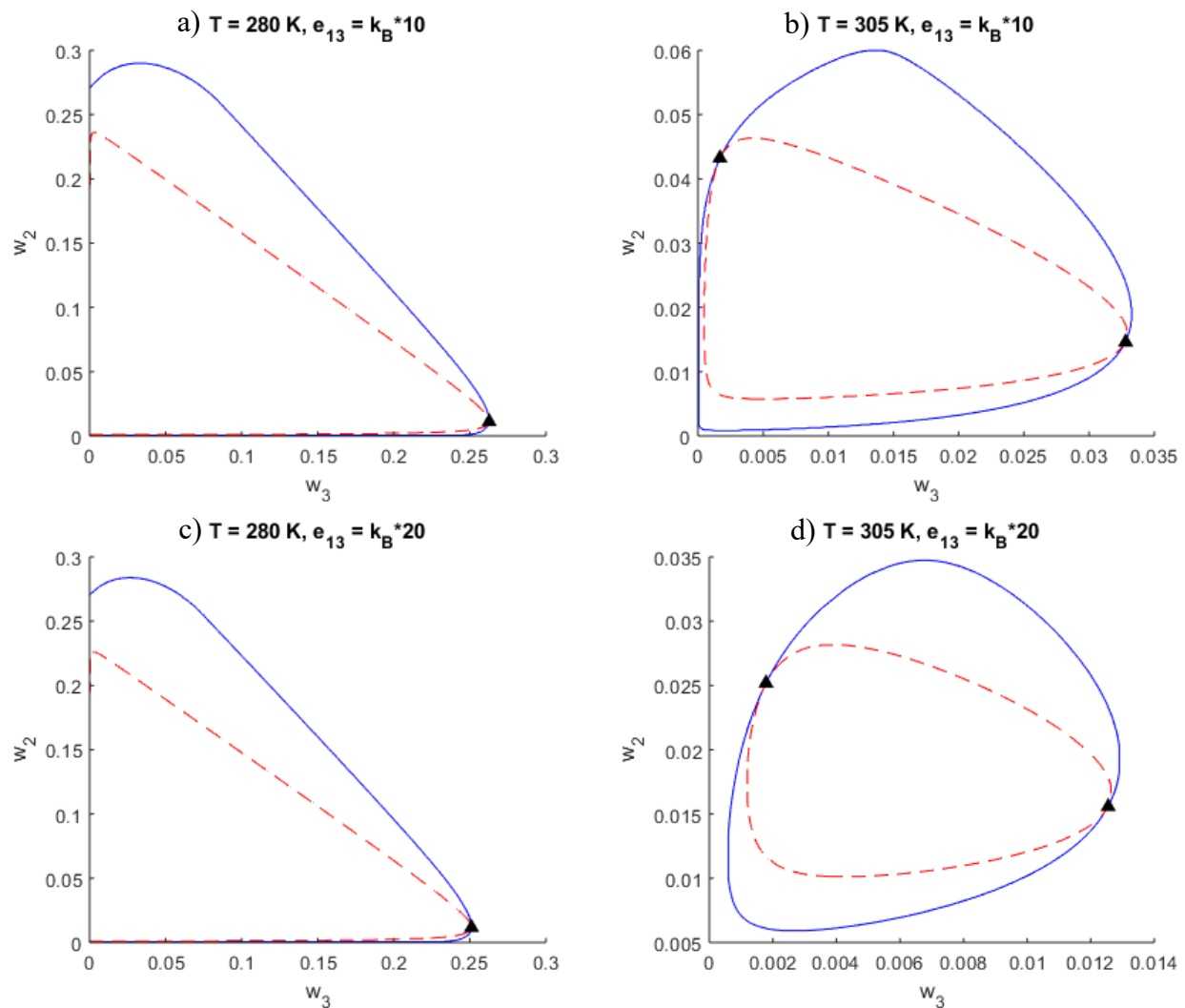
Figure A3.6 Ternary phase diagrams for cyclohexane + polystyrene + silica nanoparticles mixtures for different values of the association energy ε_{13} between cyclohexane and silica nanoparticles as explained in section 4.3. The blue solid line is the binodal and the red dashed line is the spinodal. Solid triangles represent the critical points calculated with "critical_point_ternary". a) T=280K, $\varepsilon_{13} = k_B 10$ J, b) T=305K, $\varepsilon_{13} = k_B 10$ J, c) T=280K, $\varepsilon_{13} = k_B 20$ J, d) T=305K, $\varepsilon_{13} = k_B 20$ J.